AD-A080 519 AIR FORCE INST OF TECH WRIGHT-PATTERSON AFB OH SCHOO--ETC F/G 5/8
ANALYSIS OF THE EFFECTS OF HIGHER ORDER CONTROL SYSTEMS ON AIRC--ETC(U)
DEC 79 M A PASHA

UNCLASSIFIED AFIT/GE/EE/79-27 NL

1 OF 3
AD A080519

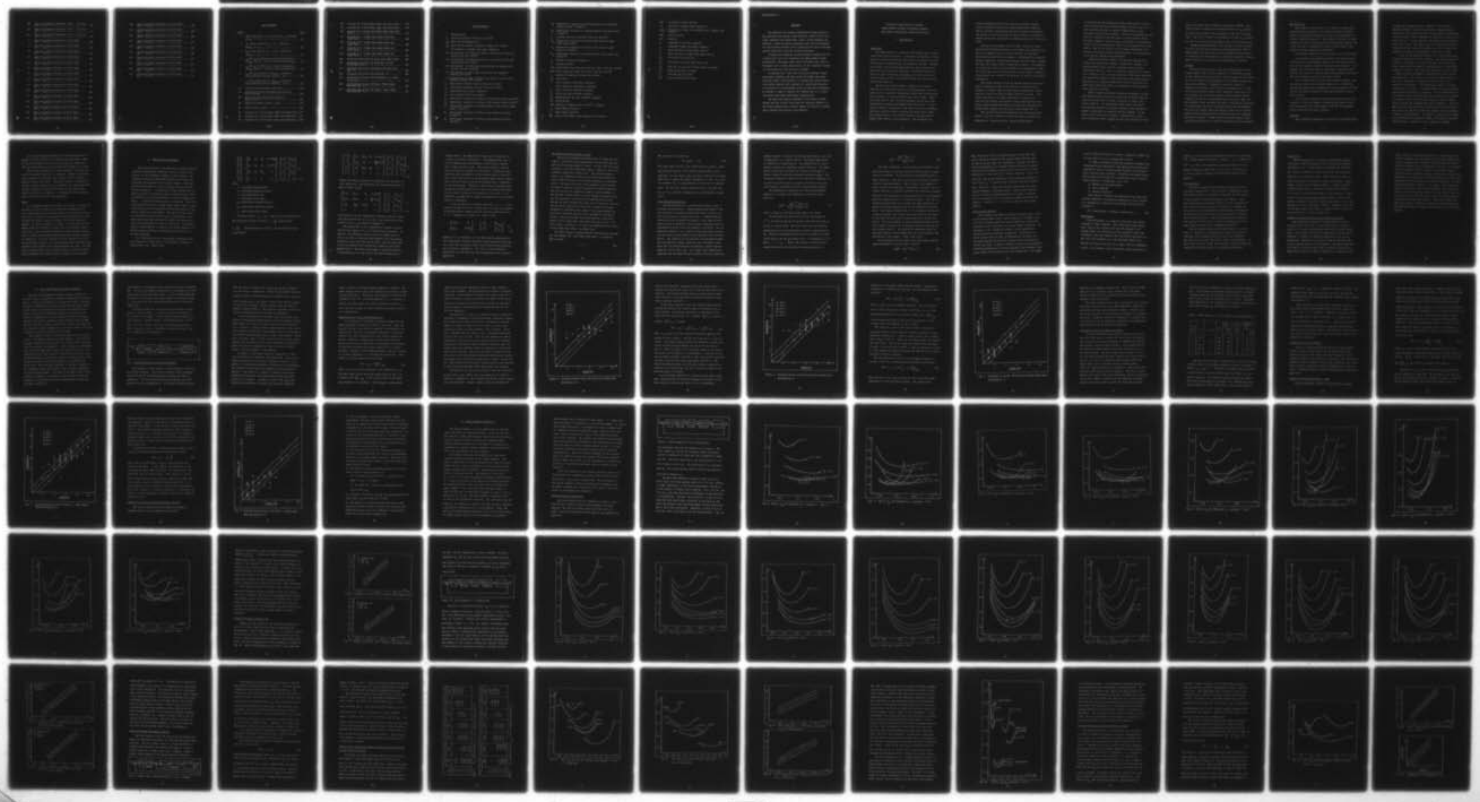

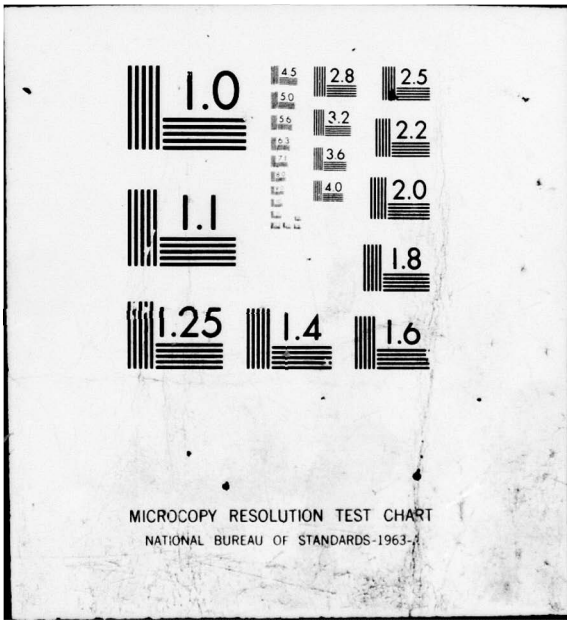
1.0
1.1
1.25
1.4
1.6
1.8
2.0
2.2
2.5
2.8
3.2
3.6
4.0
4.5
5.0
5.6
6.3
MICROCOPY RESOLUTION TEST CHART
NATIONAL BUREAU OF STANDARDS-1963-A

UNITED STATES AIR FORCE

AIR UNIVERSITY

AIR FORCE INSTITUTE OF TECHNOLOGY

Wright-Patterson Air Force Base, Ohio

AFIT/GE/EE/79-27

ANALYSIS OF THE EFFECTS OF HIGHER ORDER CONTROL SYSTEMS ON AIRCRAFT APPROACH AND LANDING LONGITUDINAL HANDLING QUALITIES

THESIS

AFIT/GE/EE/79-27 Muhammad A Pasha
Sqn/Ldr PAF

Approved for public release; distribution unlimited

(14) AFIT/GE/EE/79-27

(6) # ANALYSIS OF THE EFFECTS OF HIGHER ORDER CONTROL SYSTEMS ON AIRCRAFT APPROACH AND LANDING LONGITUDINAL HANDLING QUALITIES.

Presented to the Faculty of the School of Engineering
of the Air Force Institute of Technology
Air University
In Partial Fulfillment of the
Requirements for the Degree of
Master of Science

(12) 236

(9) Master's thesis,

by Anwar

(10) Muhammad [illegible] Pasha
Sqn/Ldr PAF

Graduate Electrical Engineering

(11) December 1979

012 225

Preface

This study is an attempt to present analytical techniques which may be used to evaluate handling qualities of an aircraft during the landing and approach phases of flight regime in terms of pilot opinion, and to identify the landing approach as a closed-loop tracking task. Three analytical techniques: open-loop frequency response analysis, closed-loop analog simulation, and open-loop impulse response analysis are presented and the results thus obtained are described. It is my hope that this analytical study may be of some help to future investigators.

I wish to express my indebtedness to Ronald O. Anderson for his sponsorship, expert assistance, and timely guidance in all phases of this study. I would like to give special thanks to my thesis advisors Professor John J. D'Azzo and Captain James T. Silverthorn for their continuous encouragement, enthusiasm, many hours of useful discussion and advice, and above all unlimited patience throughout the course of this study. My sincere appreciations are due to Major J.G.Reid for his continued interest and providing publications in the field of pilot modelling.

Finally I would like to thank D. Lamont for typing the manuscript.

Table of Contents

List of Figures

List Of Tables

List Of Symbols

ζ	Damping ratio
ω_n	Natural frequency (radians per second)
ζ_{SP}	Short Period damping ratio
ω_{SP}	Short Period natural frequency (radians per second)
γ	Perturbation in flight path angle (degrees)
$u, \dot{u}$	Perturbation in forward air speed, acceleration (feet per second, feet per second^2)
$w, \dot{w}$	Perturbation in downward velocity, acceleration (feet per second, feet per second^2)
$q, \dot{q}$	Perturbation in pitch rate and acceleration (degrees per second, feet per second^2)
$\theta, \dot{\theta}$	Perturbation in pitch angle and pitch rate (degrees, degrees per second
$\alpha, \dot{\alpha}$	Perturbation in angle of attack and angle of attack rate (degrees, degrees per second)
u_o	Equalibrium forward velocity (feet per second)
W_o	Equilibrium downward velocity (feet per second)
θ_o	Equilibrium pitch angle (degrees)
V_T	True airspeed (feet per second)
X_u	Dimensional variation of X-force with forward speed (second^{-1})
Z_u	Dimensional variation of Z-force with forward speed (second^{-1})
M_u	Dimensional variation of pitching moment with forward speed (feet^{-1} second^{-1})
X_w	Dimensional variation of X-force with downward velocity (second^{-1})
Z_w	Dimensional variation of Z-force with downward velocity (second^{-1})

M_w Dimensional variation of pitching moment with downward velocity (feet^{-1} second^{-1})

M_q Dimensional variation of pitching moment with pitch rate (second^{-1})

g Acceleration due to gravity (feet per second^2)

X_{δ_e} Dimensional variation of X-force with elevator angle (feet per second^2)

Z_{δ_e} Dimensional variation of Z-force with elevator angle (feet per second^2)

M_{δ_e} Dimensional variation of pitching moment with pitch rate (second^{-2})

δ_e Elevator deflection (degrees)

s Laplace operator

$h, \dot{h}$ Perturbation altitude and sink rate (feet, feet per second)

$R, \dot{R}$ slant range and range rate (feet, feet per second)

ω_c Crossover frequency (radians per second)

K_p Pilot gain

τ' Pilot reaction time delay (seconds)

τ Pilot effective time delay (seconds)

T_L Pilot Lead time constant (seconds)

T_I Pilot Lag time constant (seconds)

T_N Neuromuscular lag time constant (seconds)

PR Pilot Rating

ISE Integral of Squared Error (Volts^2 - seconds)

ϕ_M Phase Margin (Degrees)

ϕ Phase Angle (Degrees)

$\frac{\delta\phi}{\delta\omega}$ Slope of the phase curve (degrees per rad/sec)

ΔPR	Deviation in Pilot Rating
$\Delta\phi$	Deviation in Phase Angle (Degrees)
$\Delta \frac{\delta\phi}{\delta\omega}$	Deviation in slope of the phase curve (degrees per rad/sec)
C/S	Control System
A/C	Aircraft
θ_c	Commanded Pitch Angle (Degrees)
γ_c	Commanded Flight Path Angle (Degrees)
e_θ	Error Voltage in Pitch Angle (Volts)
e_γ	Error Voltage in Flight Path Angle (Volts)
K_{p_θ}	Pilot gain in pitch loop
K_{p_γ}	Pilot gain in flight path angle loop
T_{10}	Time for ten percent of final value (seconds)
T_D	Duplicating Time (seconds)
T_s	Settling Time (seconds)
PIO	Pilot Induced Oscillations

Abstract

The approach and landing longitudinal flying qualities data generated by Calspan using variable stability NT-33 aircraft combined with significant control system dynamics was analyzed. Three different approaches were used to determine the relationship between pilot ratings and the pilot workload, system sensitivity, and the system performance.

An open-loop frequency response analysis showed that for a particular cross over frequency and phase margin (fixed performance), the phase angle (pilot workload) and slope of the phase curve (system sensitivity) at the crossover frequency correlated well with the pilot ratings.

An optimum pilot lead time for pitch tracking, flight path angle tracking, and both pitch and flight path angle tracking tasks is determined by a closed-loop analog simulation using integral error squared as a performance measure. A correlation is found between pilot ratings and performance. An attempt is made to explain the landing task as a closed-loop pitch and flight path angle tracking task.

The open-loop impulse response of the pitch attitude showed that the initial delay and the transient behavior of the pitch response have a direct impact on the pilot ratings, pilot induced oscillations, and comments.

ANALYSIS OF THE EFFECTS OF HIGHER ORDER CONTROL SYSTEMS ON AIRCRAFT APPROACH AND LANDING LONGITUDINAL HANDLING QUALITIES

I Introduction

Background

The human being is a necessary and integral part of many closed-loop control systems. In the past two decades, a large amount of research effort has been done to determine the role and response of human beings in man-machine systems. Mathematical models representing human behavior while performing a particular task have been developed. The United States Air Force has made significant contribution in this area of research because of the relationship between the pilot and the aircraft he controls.

The Air Force Flight Dynamics Laboratory at Wright-Patterson Air Force Base has been conducting studies and contracting for research in developing a model that would predict pilot response in various closed-loop control tasks. Models for tasks such as roll and pitch attitude control have been successfully developed and demonstrated (Refs 4,5). Of particular interest at present is the study of aircraft handling qualities and pilot behavior during the glide slope, flare, and landing phases of the flight regime in the presence of higher order control system dynamics. The evaluation of

aircraft handling qualities by the pilot during in-flight tests can provide a means for understanding pilot behavior, and for properly interpreting the pilot ratings and comments. The results of such an evaluation may be used as a guideline in making qualitative assessments of handling qualities of any aircraft.

During the development and in-flight testing of recent sophisticated fighter aircraft it has become more apparent that the final landing task is critical and must be considered during design and flight test phases. The demand for increased fighter capability, coupled with present day electronic systems, has made the flight control systems more complex. The addition of significant control system dynamics can considerably change the flying qualities of the aircraft, and may require extensive concentration and workload by the pilot to achieve the desired performance.

The Flight Research Branch of Calspan Advanced Technology Center conducted a study of the effects of control system dynamics on fighter approach and landing longitudinal flying qualities using an NT-33A variable stability aircraft. This study consisted of in-flight simulations to generate an approach and landing longitudinal flying qualities data base using a highly augmented fighter aircraft and contained documented pilot comments and ratings on each flight (Ref 2).

The aircraft short period damping ratio and natural frequency (ζ, ω_n) were varied to select five basic aircraft configurations. Fourteen control system configurations

(3 lead and 10 lag) ranging from first order lead to fourth order lag and the bare airframe dynamics (control systems = 1) were selected and used in various combinations to form aircraft-control system dynamics. The exact configurations are listed in appendix A and the details can be found in Ref 2. The pilot comments, pilot ratings, and summary of experimental results of each configuration flown is also documented in this report. One of the results of the Calspan study shows that the pitch attitude tracking task performance is representative of the actual landing task performance.

McDonnell Aircraft Company used the data generated by Calspan and applied the concept of equivalent systems, i.e. matching higher-order aircraft responses with low-order equivalents (Ref 3). Also, a regression analysis was carried out to develop a pilot rating expression. The study shows that the regression analysis of the equivalent lower-order system parameters gave adequate prediction of pilot rating and the equivalent system time delay is a definite correlating parameter with pilot rating.

Earlier studies conducted by McRuer and Ashkenas reveal that short-period control of attitude and altitude using the elevator can be seen as either a parallel or series loop closure (Ref 6). In the parallel loop closure the pitch and altitude channels are closed separately and combined together to generate the required elevator command. In the series loop closure the altitude is fed back as an outer loop to generate pitch command and the pitch attitude is fed

back as an inner loop to generate an elevator command. The series closure is found to be beneficial for low ω_{sp}, because an inner loop attitude lead is helpful in the outer altitude loop. The series closure is detrimental for high ω_{sp}, because the lag in the attitude loop degrades the outer altitude loop.

Anderson postulated that Pilot Rating is closely related to pilot workload and closed-loop system performance (Ref 4). Specifically, he associated the pilot workload as the amount of lead the pilot must generate to maintain reasonable response, and he defined r.m.s. error as the performance criterion.

Problem

During the glide slope, flare and landing phases of the flight regime, both the pilot behavior as a feed-back element in the closed-loop pilot-aircraft control system and the effects of aircraft-control system dynamics on the handling qualities are as yet undefined. Fundamental questions, based on Anderson's postulates, which need to be answered are: 1) What is the relationship between "pilot workload" required to control a given set of aircraft-control system dynamics during landing task and the corresponding pilot rating? 2) What are the aircraft output variables the pilot is primarily interested in controlling, and the relationship between the "performance" the pilot can achieve while operating a given set of aircraft-control system dynamics during landing task and the corresponding pilot ratings? 3) What specific aircraft dynamic behavior does the pilot like or dislike and reflect in his comments?

The Objectives

The purpose of this thesis is to carryout a qualitative and quantitative analysis of the data generated by Calspan aimed at determing the effects of control system dynamics on aircraft handling qualities. This analysis provides an understanding of pilot-aircraft interaction during the landing task in the presence of significant control system dynamics and answers the three questions stated above.

The specific objectives of this thesis are the following:

1) To analyze the different aircraft and control system combinations in the frequency domain and to find the correlation of the frequency response data with pilot ratings. It is thought that the phase angle at particular frequencies will indicate the amount of lead the pilot must generate (workload) and will therefore correlate with pilot rating.

2) To simulate the pilot-aircraft dynamics together with the control systems on an analog computer as a closed-loop pitch/flight path angle tracking task with the purpose of finding the correlation between closed-loop performance and the pilot ratings.

3) To analyze different aircraft and control system combinations in the time domain, by applying an impulse input, and interpreting the pitch response with the corresponding pilot ratings and the pilot comments.

Approach

Three different approaches are used for correlating pilot

ratings and interpreting pilot comments. In the first approach (Chapter 3) open-loop frequency response plots of pitch angle and flight path angle are generated for different aircraft-control system combinations which were flown and evaluated (Ref 2). A pilot reaction time delay of 0.3 seconds is used in all cases. The phase angle at 3 radians per second (rad/sec) and the slope of the phase curve at 3 rad/sec are tabulated to show the relationship with pilot ratings.

In the second approach (Chapter 4) a closed-loop analog computer simulation of pilot, aircraft, and control system is studied in two phases. In the first phase the closed-loop pitch response of one aircraft configuration to a step pitch command is studied. The pilot gain and lead time are varied to obtain the best performance for different control system configurations. The results are plotted to show changes in the pilot rating due to changes in control system, as a function of performance. The flight path angle (γ) loop is closed next for a step 'γ' command without any pitch feedback and the above procedure is repeated. In the second phase the closed-loop pitch and flight path angle responses are studied as in phase one for pilot-aircraft dynamics without adding control systems but changing the aircraft dynamics. The pilot gain and lead time are varied to obtain the best performance. The results are plotted to show the changes in pilot rating as a function of performance. In addition, using aircraft number one and different lag control systems, the effect of closing only the outer γ loop for a step γ command is studied.

In the third approach (Chapter 5) the open-loop time responses of pitch attitude to an impulse are generated. Some of the pilot comments and the pilot ratings are correlated with the pitch behavior in the initial few tenths of a second.

For the above analyses, aircraft equations of motion and a pilot describing function are required. Chapter II develops these equations and presents the concepts of pilot ratings applied towards this study. Anderson's concept is modified to include "system sensitivity" as a parameter in evaluating pilot ratings, measured in terms of the slope of the phase angle about the cross-over frequency. A description of the landing task as seen by a pilot is also presented.

Scope

It is emphasized that this thesis is neither an attempt to develop a new pilot model nor to develop an expression for pilot rating which can be readily used for any given situation. The study is limited to the anlysis of the Calspan data to demonstrate the effect on pilot ratings for the pilot-aircraft dynamics as control systems are varied. A "Lead only" form of McRuer model for the pilot is used with a 0.3 second reaction time delay. For the analog simulation a short period airframe model is used and the high frequency feel and actuator dynamics are neglected. The time integral of error squared is used as the performance measure. For the open loop pitch attitude time responses the aircraft short period dynamics are used. No wind gust or random inputs are considered and the aircraft forward speed throughout the landing task is assumed to be constant.

II. Theoretical Development

This chapter presents the theoretical concepts and the associated mathematical equations which are used for the analysis in the subsequent chapters of this report. The linearized aircraft longitudinal equations of motion are developed and expressed in the Laplace domain. The short period approximation is used to develop the short period aircraft equations. A description of the landing task, as seen by a pilot, is presented and the significance of dynamic behavior of the pitch attitude, θ, and the flight path angle, γ, during the landing task is discussed. The pilot describing function for a single input-single output closed-loop tracking task is described and the model used for the analog simulation is developed. The pilot rating concepts are enumerated and the factors such as performance, workload, and sensitivity which may be taken into account by a pilot while providing a rating are explained. The methods used for analysing the aircraft-control system dynamics for measuring the performance, workload, and sensitivity are briefly mentioned.

The linearized aircraft longitudinal equations of motion expressed in body axes, in the absence of external disturbances, are: (Ref 2:211)

$$\begin{bmatrix} \dot{u} \\ \dot{w} \\ \dot{q} \\ \dot{\theta} \end{bmatrix} = \begin{bmatrix} X_u & X_w & -W_o & -g\cos\theta_o \\ Z_u & Z_w & u_o & -g\sin\theta_o \\ M_u & M_w & M_q & 0 \\ 0 & 0 & 1 & 0 \end{bmatrix} \begin{bmatrix} u \\ w \\ q \\ \theta \end{bmatrix} + \begin{bmatrix} X_{\delta_e} \\ Z_{\delta_e} \\ M_{\delta_e} \\ 0 \end{bmatrix} \delta_e \qquad (1)$$

where:

u = perturbed forward speed

w = perturbed downward velocity

q = perturbed pitch rate

θ = perturbed pitch angle

u_o = Equilibrium forward velocity

W_o = Equilibrium downward velocity

θ_o = Equilibrium pitch angle

For small angles, $u_o \simeq V_T$, the true trim airspeed, and the perturbation angle of attack $\alpha \simeq \frac{w}{u_o}$ which implies $\dot{\alpha} \simeq \frac{\dot{w}}{u_o}$. Substituting for w and $\dot{w}$, the perturbation equations become:

$$\begin{bmatrix} \dot{u} \\ \dot{\alpha} \\ \dot{q} \\ \dot{\theta} \end{bmatrix} = \begin{bmatrix} X_u & X_w u_o & -W_o & -g\cos\theta_o \\ Z_u/u_o & Z_w & 1 & \frac{-g}{u_o}(\sin\theta_o) \\ M_u & M_w u_o & M_q & 0 \\ 0 & 0 & 1 & 0 \end{bmatrix} \begin{bmatrix} u \\ \alpha \\ q \\ \theta \end{bmatrix} + \begin{bmatrix} X_{\delta_e} \\ Z_{\delta_e}/u_o \\ M_{\delta_e} \\ 0 \end{bmatrix} \delta_e \qquad (2)$$

Taking the Laplace Transform of equations (2) with zero initial conditions, and expressing the resulting equations in Matrix format yields:

$$\begin{bmatrix} (S-X_u) & -X_w u_o & W_o & g\cos\theta_o \\ -Z_u/u_o & (S-Z_w) & -1 & \frac{+g}{u_o}\sin\theta_o \\ -M_u & -M_u u_o & (S-M_q) & 0 \\ 0 & 0 & -1 & S \end{bmatrix} \begin{bmatrix} u \\ \alpha \\ q \\ \theta \end{bmatrix} = \begin{bmatrix} X_{\delta_e} \\ Z_{\delta_e}/u_o \\ M_{\delta_e} \\ 0 \end{bmatrix} \delta_e \qquad (3)$$

From equation (3) the longitudinal transfer functions representing perturbations in u, α, q and θ can be derived for the elevator input, δ_e, as shown in appendix B.

The denominator of the longitudinal transfer function derived from equation (3) is a fourth order polynomial. In general, the polynomial factors into two complex pair of roots, one with a relatively high damping ratio and natural frequency called the short period poles, and the other with a very low damping ratio and natural frequency called the phugoid poles. The short period mode is primarily made up of perturbations in α and θ with very small variations in

forward speed. The phugoid mode consists of variations in θ and u with almost a constant α. The phugoid mode, due to its low damping and low frequency of oscillation, appears for a longer period of time. But pilots generally control these oscillations without any difficulty. During the landing task, the perturbation in the forward speed is controllable, either manually or by an automatic speed control system. Also, the time frame in which the landing task is completed, is relatively small. Therefore, neglecting the phugoid mode during the landing task will not cause any serious deviations in the overall results of the analysis of the task. It is, therefore, assumed that the small perturbations in the forward speed are negligible.

If the assumption of constant speed and $\theta_o \simeq o$, a reasonable assumption for the landing task, are made the u-degree of freedom becomes superfluous and, with the substitution of $q = \dot{\theta}$, equation (3) reduces to: (Ref 7:6-30)

$$\begin{bmatrix} (S-Z_w) & -S \\ -M_w u_o & S(S-M_q) \end{bmatrix} \begin{bmatrix} \alpha \\ \theta \end{bmatrix} = \begin{bmatrix} Z_{\delta_e/u_o} \\ M_{\delta_e} \end{bmatrix} \delta_e \qquad (4)$$

Equation (4) is refered to as the short period approximation. The longitudinal transfer functions representing perturbations in α and θ for an elevator input can be derived from equation (4) as shown in appendix B. The values of the stability derivatives for the five aircraft configurations are listed in appendix B.

The Landing Task As Seen By A Pilot

During the approach-to-landing phase of flight the aircraft is initially on the glide-slope and the pilot must decide on the minimum height to flare. At this time the pitch attitude, θ, and the flight path angle, γ, appear to be of considerable importance to the pilot. The minimum height to flare is an imaginary window on the glide slope which the pilot selects relative to the runway threshold or touchdown point. The pilot starts the flare maneuver in this window in order to achieve a smooth exponential landing trajectory. The selection of the imaginary window in space depends on the aircraft forward speed, aircraft dynamic characteristics, and the experience of the pilot in handling the aircraft. During the flare maneuver the sink rate, $\dot{h}$ (vertical velocity) and the slant range rate, $\dot{R}$ (the rate at which the runway threshold or touchdown point appears to be approaching) are the motion cues that the pilot gets through his peripheral vision. The pilot pitches up and establishes a desired $\dot{h}$ and/or $\dot{R}$ until touch down, where h,$\dot{h}$ and R go to zero. All three output variables, h, $\dot{h}$, and R are mathematically related to the flight path angle γ as shown below:

For small angles, assuming constant forward speed through out the landing task, the flight path angle γ is given by: (Ref 8:15,83)

$$\gamma = \theta - \alpha \qquad (5)$$

The sink rate h is given by:

$$\dot{h} = u_o \text{Sin } \gamma \simeq u_o \gamma \qquad (6)$$

The slant range rate $\dot{R}$ is the vector sum of u_o and $\dot{h}$. Since u_o is assumed constant, $\dot{R}$ is directly proportional to $\dot{h}$ or γ. Therefore, all the motion cues are direct functions of flight path angle γ. Hence the dynamic behavior of θ and γ for elevator commands (δ_e) is representative of the over all landing task. The aircraft transfer functions θ/δ_e, α/δ_e and γ/δ_e for all five aircraft configurations are developed in appendix B.

Pilot Describing Function

The determination of a suitable pilot model is not a straight forward process. Understanding human behavior and his reactions in a given situation has been a serious concern in the studies carried out so far. A human being perceives his task, evaluates it mentally, then takes certain action which is delayed to varying degree depending upon his psychophysiological state and firmness of decision. This is generally refered to as a reaction time delay which accounts for the delay from perception to the decision for corrective action. The execution of his decision is performed through the neuromuscular system, which not only contributes some delay but also high frequency attenuation, usually approximated by a first order lag. In a single loop compensatory tracking task the human being interfaces with the system and

adjusts himself to achieve the desired performance, just like a compensator in a control system. The human compensation is refered to as equalization. The equalization is represented in terms of a lead/lag transfer function. The human being is also able to adjust the overall system gain to select a desired operating frequency and phase margin. The operating frequency is known as the cross-over frequency, ω_c at which the overall gain is adjusted for Odb on the open loop frequency response plots for a desired phase margin.

The mathematical expression for the aforesaid human behavior in a single loop compensatory tracking task is given by:

$$Y_p(S) = \frac{K_p e^{-\tau' s} (T_L S + 1)}{(T_I S + 1)(T_N S + 1)} \qquad (7)$$

which is known as the McRuer model (Ref 1:29; 10:8).

In this model the pure time delay is represented by $e^{-\tau' s}$, the gain by K_p and the general lead and lag terms as T_L and T_I respectively. The first order lag time constant approximation of the neuromuscular system is represented by T_N. Often the neuromuscular lag term is treated as an additional delay, and the pure delay term, τ' is modified as $e^{-\tau s}$, where $\tau = \tau' + \tau_N$. Hence, the Laplace transform of the simplified version of the pilot describing function is:

$$Y_p(S) = \frac{K_p e^{-\tau S}(T_L S + 1)}{(T_I S + 1)} \qquad (8)$$

The model parameters τ, T_L, T_I and K_p are adjusted to produce both stability and good closed-loop performance without excessive workload. In particular by increasing K_p and T_L, while reducing τ, the pilot can achieve the desired level of stability and performance. This is done at the expense of pilot activity and workload. Furthermore, the pilot can introduce lag (T_I) to maintain desirable low frequency response. Obviously the adjustment of these parameters is very dependent upon the system the pilot is trying to control. One way of optimizing performance is to adjust the model parameters to minimize the mean squared error as the performance measurement. A performance measurement is an evaluation of how well a system operates, how closely the output follows the input, or how small the error can be maintained over a given time period. The time integral of error squared has been successfully used to evaluate the performance of pilot-aircraft control systems (Ref:9). The details of adjustment rules for the human operator's describing function can be found in the literature on the subject (Ref: 1:30; 10:9).

For the purpose of this thesis the pilot model used for analog simulation is of the form: (Ref 4)

$$Y_p(S) = K_p e^{-\tau S}(T_L S + 1) \qquad (9)$$

This "lead only" form is selected because of the fact that pilot lag may be neglected when higher order effects, such as control system lags, are considered. Besides, the short period approximation of aircraft dynamics provides a reasonably good low frequency response due to the "free s" in the denominator of the $\theta(s)/\delta_e(s)$ transfer function. Also it is only when the natural frequency of the controlled element is very large ($\omega_n > 6$ rad/sec) that the pilot lag may be desirable (Ref 4:4). Since the aircraft under study have short period frequencies varying between 1 rad/sec and 4 rad/sec, the form of pilot describing function as shown in equation (9) is considered to be a satisfactory model for analog simulation. A value of $\tau = 0.3$ sec is used for this study (Ref 2).

Pilot Rating Concepts

Pilot Ratings are based on numerical rating scales, such as the Cooper-Harper scale, which represent an attempt to relate pilot comments about the ease or difficulty with which airplanes can be controlled in certain flight situations. Unfortunately the ratings are ordinal scales subjectively applied and hence difficult to quantify. Predictions of pilot ratings could be made if mathematical relations were developed between the numerical rating scale and how hard a "pilot must work" to achieve "desired closed-loop performance". Developing mathematical relations appears to be extremely complex, though certain trends have been identified. For example

a pilot objects seriously if he has to generate "leads" (T_L) of more than 0.5 to 1.0 seconds (Ref 7:12-9).

In order to develop closed-loop analysis procedures for flying qualities assessments, some generalized criteria are required in terms of pilot-aircraft dynamics, task performance, and the pilot workload. Therefore the factors which may be taken into account by a skilled test pilot in providing an opinion or rating are: (Ref 1:35)

a) Measure of task performance

b) Pilot workload

c) System sensitivity

These factors obviously are affected by the particular aircraft dynamics, including any additional control systems. As a mathematical function, pilot ratings (PR) can be expressed as:

$$PR = f(\text{Performance, workload, sensitivity,... }) \qquad (10)$$

Performance

Task performance is a measure of how well the system responds to input commands. The closed-loop system quantities, such as the response time and the integral error squared (ISE), are indicative of the accuracy of the task. In general, both the response time and ISE are functions of the cross-over frequency (ω_c) and the phase margin (ϕ_m). Ratings are known to be poor if ω_c and/or ISE are inadequate. A pilot is an element in the closed-loop system and tries to

adjust ω_c and to maintain sufficient phase margin to minimize ISE. Pilots generally consider 1 rad/sec < ω_c < 5 rad/sec and $40^\circ < \phi_m < 60^\circ$ to be satisfactory operating regions for adequate performance (Ref 6:81; 7·12.4-12.6). The choice of ω_c and ϕ_m, however depends on the aircraft control system dynamics.

Pilot Workload

The pilot workoad can be divided into pilot activity and pilot equalization. Pilot activity is dependent on the pilot gain K_p and is an important component of Pilot Rating in the presence of gust disturbances and remnant. Since gust disturbances and remnant effects are not considered in this study, the pilot activity is neglected. Besides the pilot gain is also determined by the mechanical arrangement of the controls placed between the pilot and the elevator, like the gearing ratio. The data generated by Calspan had the facility for the pilot to select the gearing ratio for each flight evaluation of a configuration (Ref:2).

The pilot equalization can be represented in two ways (Ref 1). One way is to determine the slope of the pilot's amplitude ratio evaluated near the cross-over frequency. The other way is to use the pilot's "lead" time constant. In this study the pilot "lead" time constant is used to represent workload, as the pilot gain is an adjustable parameter.

Sensitivity

System sensitivity is a measure of performance degradation due to small deviations in the closed-loop operating frequency or ω_c. It may neither be possible nor desirable for a pilot to maintain a fixed ω_c all the time during the execution of a particular task. Small deviations about ω_c cause variations in the overall system phase angle or phase margin as seen in the frequency domain. A sharp variation of phase angle about ω_c (measured in degrees per rad/sec) will result in considerable change in ϕ_M, and hence a significant closed-loop performance degradation in terms of ISE, whereas a gradual variation of phase angle about ω_c will not degrade the system performance rapidly. Therefore, the slope of the phase angle curve about ω_c indicates the relative system sensitivity to small changes in ω_c.

Methods For Longitudinal Handling Qualities Analysis

The mathematical equations representing the aircraft characteristics are known, as the formulation of transfer functions is usually accomplished during the aircraft design phase. The transfer functions of additional control systems designed to enhance the aircraft capabilities can also be formulated. Therefore an open-loop frequency response plot of the complete system can be generated. The phase angle and the slope of the phase curve about a nominal cross-over frequency where pilots are known to operate is a measure of the

pilot workload and system sensitivity. Closed-loop pilot-aircraft dynamics can be simulated on an analog computer for a given tracking task, assuming a form for the pilot model. The pilot parameters can be adjusted to minimize the integral of error squared, which is used as a performance measure. The closed-loop operating frequency and the phase margin thus obtained is an indication of system performance, and the pilot parameters are an indication of estimated workload. An open-loop pitch attitude response to an impulse can be generated using the aircraft-control system dynamics. The system behavior in the initial few-tenths of a second reveals the overall system lag or delay and can be used to interpret the expected pilot ratings and comments. These three approaches: open-loop frequency response, closed-loop analog simulation, and open-loop impulse response are analyzed in the next three chapters.

III Open Loop Frequency Response Analysis

The open loop frequency response analysis provides an overall picture of magnitude and phase relationship of the output of a system with respect to a sinusoidal input. From the frequency response plots the gain margin and the phase margin of the system can be measured at any desired operating frequency. The gain and the phase margins are related to the effective damping ratio of the resulting closed loop system, and hence the overall system transient behavior (Ref 11:288). The gain and phase margins also provide a basis for selection of a suitable cascade compensator in order to achieve a desired closed-loop system performance (Ref 11:386).

This chapter presents a brief description of the overall system. The digital computer program "TOTAL" is used for the frequency response analysis (Ref 12) and the results obtained from the analysis are explained. Pilot ratings are correlated with the phase angle data using least square curve fit. The justification for this analysis is derived from the fact that the desired phase margin at the crossover frequency for a reasonable closed-loop system performance is achieved by the pilot lead. Hence the pilot workload is directly related to the resultant system phase angle at the crossover frequency in the frequency domain. The slope of the phase curve at the crossover frequency is a measure of the system sensitivity. Therefore a correlation can exist between pilot ratings and the phase angle data.

Two methods of correlating pilot rating expressions are presented. In the first method an expression is developed to fit the total pilot rating with phase angle. In the second method the deviation in the pilot rating with respect to the best rating is correlated with the corresponding deviations in the phase angle data.

The block diagram of the open-loop system under investigation is shown in Fig. 1. A pilot reaction time delay of 0.3 seconds is included. In the Laplace transform domain, a pure delay of τ seconds becomes a multiplying factor of $e^{-s\tau}$. Since $|e^{-j\omega\tau}|$ is unity, this does not affect the gain plot, but on the phase curve it introduces an additional phase lag of $\omega\tau$ radians at each frequency ω.

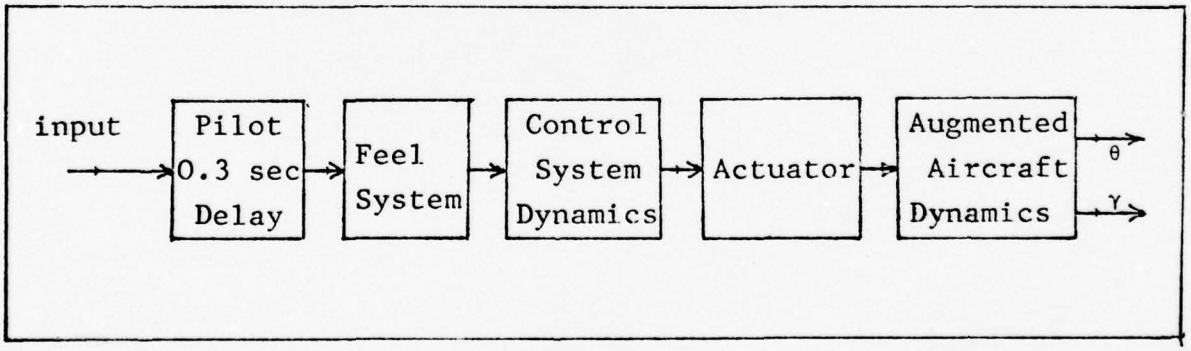

Fig 1 Overall Open-Loop System Block Diagram

The variables in the analysis are the elements of the control system dynamics. The aircraft-control system configuration used and the corresponding pilot ratings are shown in appendix A. The feel system and actuator dynamics are held constant for all configurations. The transfer functions used

for the control systems, feel system and actuator dynamics are also shown in appendix A. Using the $\frac{\theta}{\delta_e}$ transfer function and $\frac{\gamma}{\delta_e}$ transfer function developed in Appendix B for each aircraft configuration, the control systems were varied to generate open-loop frequency response curves using the digital computer program "TOTAL". The magnitude and phase curves for selected configurations are attached as Appendix E.

A close examination of the phase angle plots shows some distinct correlating trends between the pilot ratings, and the phase angle and slope of the phase curve in the vicinity of 1 to 4 rads/sec. Control systems generating more phase lag in this frequency region have a much higher rating as compared to the control systems generating less lag in this region. Therefore, the phase angles of each aircraft-control system configuration were measured at 1,2,3, and 4 rads/sec and tabulated. Tables E1 thru E 10 (Appendix E) show the values of phase angles ϕ and the change in ϕ per rad/sec.

In chapter II the pilot rating is explained as a function of performance, workload, and sensitivity. Since no information about any of the three variables is known, a frequency of 3 rad/sec(representing a fixed level of performance) was selected as the cross over frequency for the purpose of analysis. The choice of 3 rad/sec is based on the earlier finding that the pilots like performing closed-loop tasks around 3 to 4 rad/sec. In order to control the system for satisfactory operation, the pilot must generate sufficient

lead to achieve the required phase margin at 3 rad/sec. The phase margin and the cross over frequency are directly related to the performance. Therefore, this analysis is based on the assumption that, for a fixed performance, i.e., for given ω_c and ϕ_M, the phase angle and slope of the phase curve at ω_c are a relative measure of pilot workload and system sensitivity, respectively.

Determination of Pilot Rating Expression

It is possible to correlate the pilot ratings with the phase angle data recorded in tables E1 thru E10. Since the aircraft dynamics are varied to generate five different configurations, the data is analysed to determine a rating expression for each configuration as the control systems are varied. Anderson's concept (Ref 4) that pilot rating is based on some linear combination of performance and workload is modified to include the system sensitivity as a third variable. Therefore, for fixed performance, the pilot rating is a linear combination of workload and sensitivity. This leads to a rating expression of the form

$$PR = \alpha_1 \phi_3 + \alpha_2 \frac{\delta \phi}{\delta \omega} \Big|_{Avg} \qquad (11)$$

where α_1 and α_2 are some constants to be determined, ϕ_3 is the phase angle of the open-loop system shown in Fig. 1 at 3 rad/sec and $\frac{\delta \phi}{\delta \omega} \Big|_{Avg}$ is the average slope of the phase curve between 2 to 4 rad/sec. This average is obtained by

taking the mean phase difference between 2 and 3 rad/sec, and 3 and 4 rad/sec. The estimated pilot rating is represented by PR. The procedure of linear least square curve fit is used to evaluate α_1 and α_2 such that the square of the error between the estimated and actual Pilot Ratings is minimized. This procedure is discussed and the equations used are derived in Appendix C.

The values of α_1 and α_2 are obtained using the equations developed in Appendix C and the pitch angle frequency response data tabulated in Tables E1 thru E5. The data for aircraft number 3, listed in Table E3 is not used as it has a very significant slope variation between 3 and 4 rad/sec. Therefore, averaging the two slopes is not a reasonable approximation for this set of data. Also the data obtained by adding lead control systems to the five aircraft were not included because the lead control system improves the phase angle and slope, hence the expression shown in equation 11 would yield better pilot ratings. But the actual pilot ratings given by the pilot for all the aircraft flown with lead control systems are always worse than the aircraft with no control system added. This reverse trend in pilot ratings could not be explained at this point and therefore these data points were omitted.

The values of α_1 and α_2 for aircraft 1,2,4 and 5 obtained by the linear least square curve fit analysis are listed in Table E11, Appendix E. The estimated PR and the actual ratings are also tabulated. Figure 2 shows a plot of estimated PR

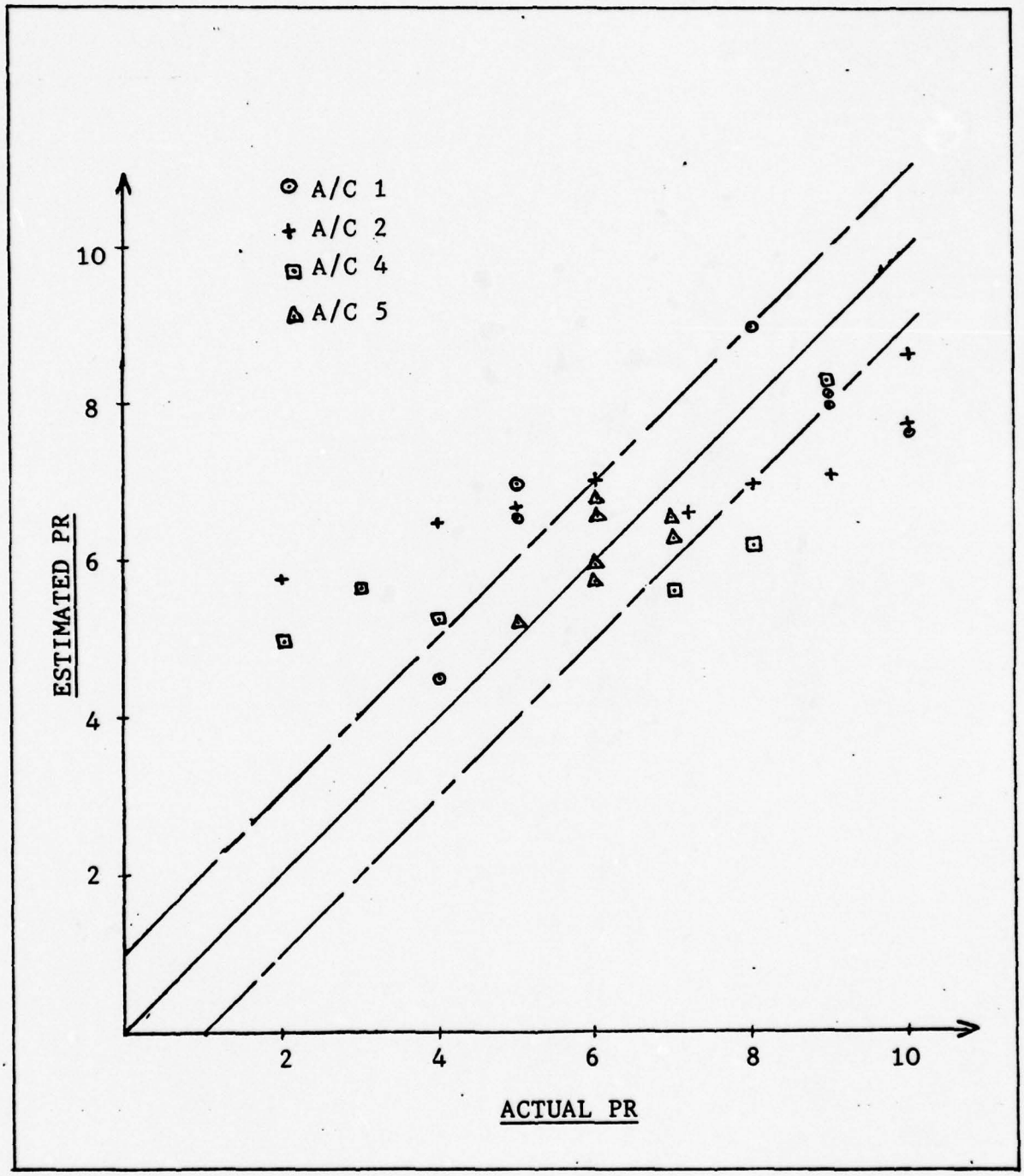

Figure 2. Estimated Verses Actual PR Using Pitch Phase Data And Equation 11.

versus the actual PR. Fourteen out of the thirty points plotted are outside the limits of ±1 from the best line of co-relation. Out of the fourteen points six data points represent aircraft 2, five data points represent aircraft 4, and three represent aircraft 1.

In the above analysis, since the average slope did not accurately represent the actual slope of the phase curve at three rad/sec, an alternate expression is developed to include both the slopes from 2 to 3 rad/sec $\frac{\delta\phi}{\delta\omega}\Big|_{2-3}$ and 3 to 4 rad/sec $\frac{\delta\phi}{\delta\omega}\Big|_{3-4}$ as shown:

$$PR = \alpha_1\phi_3 + \alpha_2 \frac{\delta\phi}{\delta\omega}\Big|_{2-3} + \alpha_3 \frac{\delta\phi}{\delta\omega}\Big|_{3-4} \qquad (12)$$

where α_1, α_2 and α_3 are the constants evaluated applying the method of least squares. The data for aircraft 3 is also included. The results thus obtained are tabulated in Table E12. A plot of the estimated against the actual PR is shown in Fig. 3. From the figure it is seen that eleven out of thirty five points are outside the ±1 PR boundary. Seven out of the eleven points represent aircraft 2, three data points represent aircraft 1 and one data point represents aircraft 4. The second PR expression (eqn. 12) did show a better corelation as compared to the first (eqn. 11), but of course it added an additional degree of freedom.

As an alternate approach for correlating the phase angle data, the deviations in the pilot ratings with respect to the best rating in the data was curve fit to corresponding

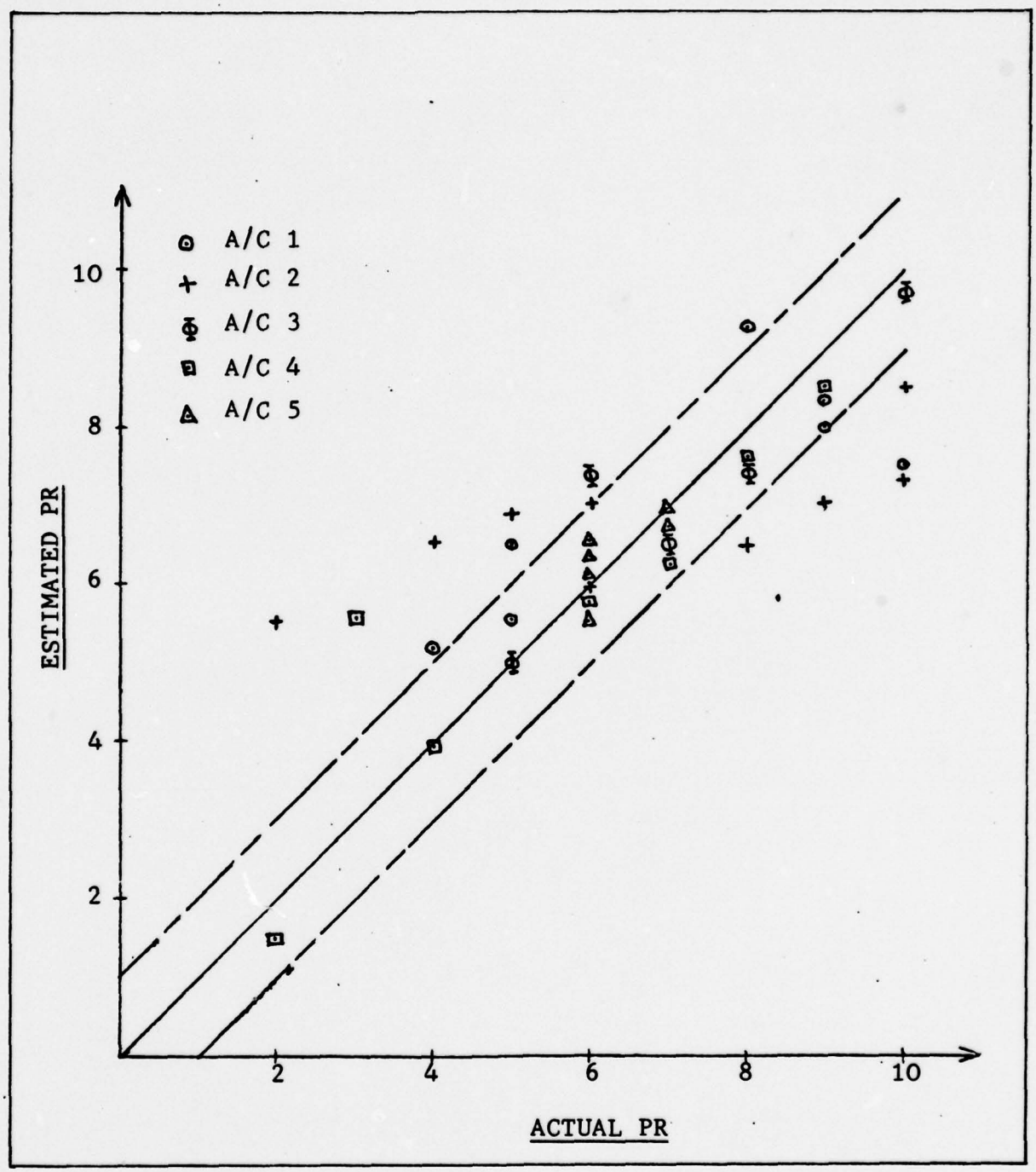

Figure 3. Estimated Verses Actual PR Using Pitch Phase Data And Equation 12.

deviations in the phase angles and the slopes. Once again a frequency of 3 rad/sec was selected. The PR expression thus used was:

$$\Delta PR = \alpha_1(\Delta\phi)\Big|_3 + \alpha_2\, \Delta\frac{\delta\phi}{\delta\omega}\Big|_{Avg} \qquad (13)$$

where α_1 and α_2 are the unknown constants, PR is the deviation in pilot rating with respect to the best PR, $\Delta\phi$ is the corresponding deviation in the phase angles, and $\Delta\frac{\delta\phi}{\delta\omega}\Big|_{Avg}$ is the average deviation in the slope with respect to the average slope corresponding to best rating.

The values of α_1 and α_2 for each aircraft, obtained by using the method of least squares, and the estimated PR are tabulated in Table E13. A plot of actual versus the estimated ΔPR is shown in Fig. 4. Eight out of thirty points are outside the $\pm$1PR region. Out of the eight data points four represent aircraft 2, two represent aircraft 1, and two represent aircraft 4. This analysis primarily indicates the effects of lag control systems on the pilot ratings.

The ΔPR expression of eqn. 13, was slightly modified to include a bias (α_o) as shown and the procedure was repeated.

$$\Delta PR = \alpha_o + \alpha_1(\Delta\phi)\Big|_3 + \alpha_2\, \Delta\frac{\delta\phi}{\delta\omega}\Big|_{Avg} \qquad (14)$$

Only aircraft 1 and 2 were analyzed to see if any noticeable improvement in the correlation exists. The results thus

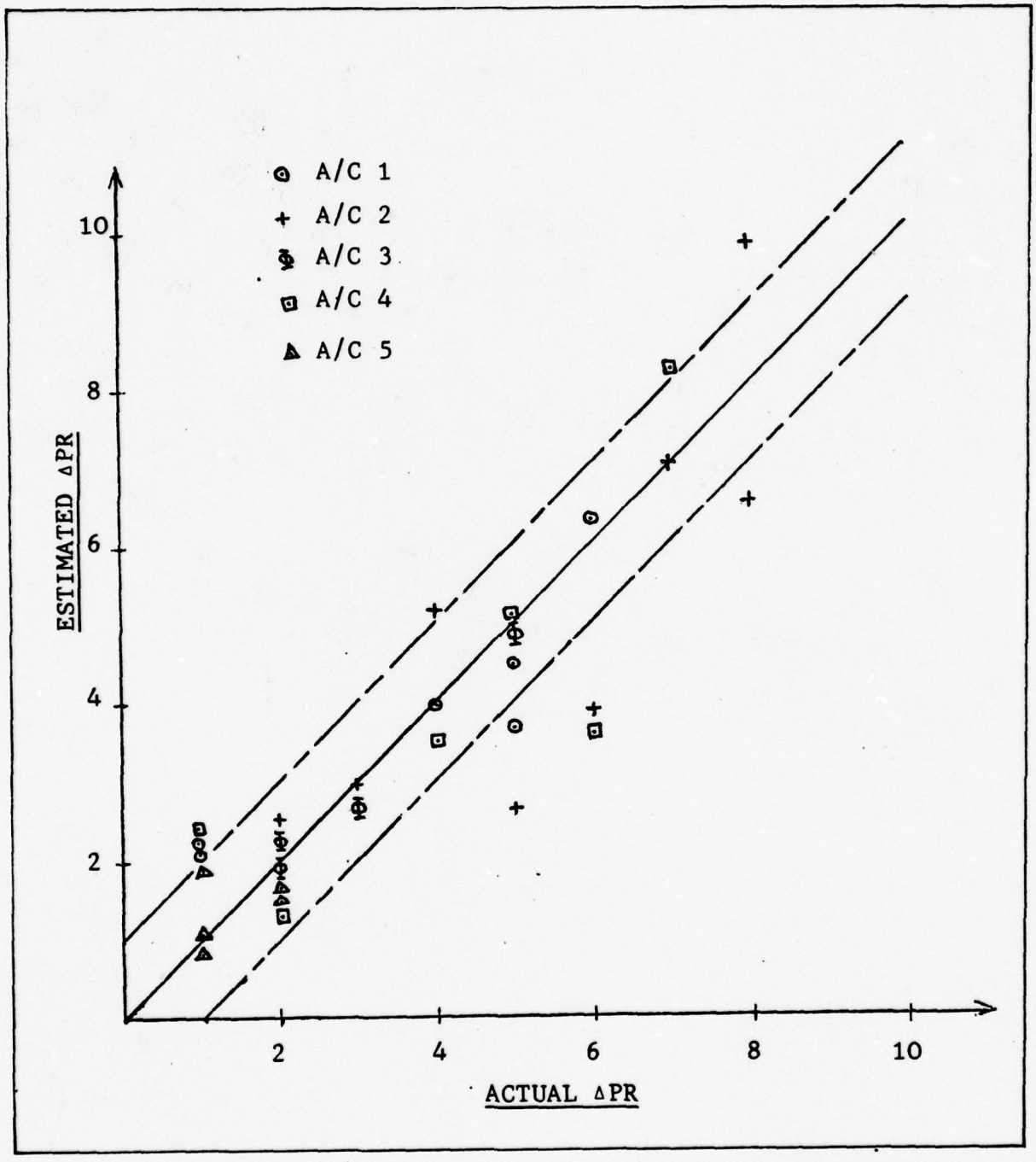

Fig. 4. Estimated Vs. Actual ΔPR Using Pitch Phase Angle Data And Equation 13

obtained are tabulated in Table E14. Five out of the eight data points of aircraft 2 were outside the ±1 PR range. Therefore addition of a constant bias did not result in any changes in the correlation.

The above analyses reveal that a trend does exist between the pilot rating and the pitch phase angle data obtained by generating the open-loop frequency response. However, the pilot may not desire to operate all the systems at 3 rad/sec. Therefore, fixing the cross-over frequency at 3 rad/sec may not necessarily be an appropriate assumption for performance representation and the workload evaluation.

Alternate Analysis For Data Correlation

It seems reasonable and practical that the pilot, does not close the loop at 3 rad/sec for every case, but adjusts for a suitable cross-over frequency by adding some lead and maintaining a desirable phase margin. Pilots generally do not object to adding leads of the order of 0.5 sec to 1.0 sec time constant. The phase angle data of Table 1 thru 5 for the pitch attitude show that addition of a pilot lead of 0.5 sec. to 1.0 sec. in general, would provide sufficient phase margin for all aircraft with no control system (C/S = 1) when evaluated at a frequency 1 rad/sec above the aircraft short period natural frequency. This fact is also shown by the closed loop analog simulation results, discussed in the next chapter. However with the addition of control systems, the pilot tends to adjust the lead time constant

and the cross-over frequency to obtain a desirable phase margin. As an example to elaborate this point, let us examine the phase angle of all aircraft with no control system and with a pilot lead time of either 0.5 or 1.0 sec. The phase angle generated at the frequencies of interest and the resultant phase margins, ϕ_M, are tabulated in Table 1.

Table 1 Phase Angle Due to Pilot Lead at ω_c and Range of ϕ_M.

Aircraft No.	ω_{SP}	$\omega_c \simeq \omega_{SP+1}$	ϕ^o at ω_c	For T_L=0.5 ϕ Lead at ω_c	For T_L=0.75 ϕ Lead at ω_c	Range of ϕ_M for $0.5 \leq T_L \leq 1.0$
1	1.026	2	-196	+45	+63	29 - 67
2	2.3	3.3	-205	+59	+73	34 - 48
3	2.19	3	-220	+56	+72	16 - 32
4	1.99	3	-188	+56	+72	48 - 54
5	3.9	5	-227	+63	+76	26 - 29

The data shown in Table 1 indicate that a sufficient range of phase margin is available and hence it may be reasonable to choose $\omega_c \simeq \omega_{SP} + 1$. The effect of adding control systems to the aircraft in terms of phase angle and slope at ω_c can then be measured. The overall concept of fixing the performance and correlating pilot ratings with workload and sensitivity remains the same, except that ω_c for each aircraft is

chosen to be $(\omega_{SP} + 1)$, instead of a fixed 3 rad/sec. The method of least squares is used to curve fit the data for correlating the pilot ratings with the respective phase angles and slopes at ω_c.

The analysis is not repeated for aircraft 3 and 4 as it has already been demonstrated earlier since for these aircraft $(\omega_{SP} + 1)$ is 3 rad/sec. Therefore, aircraft 1 and 2 are analyzed using 2 and 3.3 rad/sec as ω_c respectively, to test the validity of the choice of ω_c. Only the lag control systems were considered to draw a comparison between these results and the earlier results. The deviation in PR from the best ratings were correlated. The results thus obtained are tabulated in Table E15.

Comparison of the Two Methods

The pilot rating expressions obtained by both methods showed a similar trend between the ratings and the phase angle and slope at the chosen cross-over frequency. Unfortunately, there was no significant improvement when the second method was used. However it only seems appropriate and reasonable to select different cross-over frequencies for each aircraft. The same concept is used for analyzing the flight path angle data.

Analysis of Flight Path Angle, γ, Data

The data recorded in Tables E6 thru E10 for the phase

angle and slope of phase curve of 'γ' exhibit different characteristics than the pitch angle data. Since the $\frac{\gamma}{\delta_e}$ transfer function constitutes a non-minimum phase system, the system tends to be unstable much faster than the minimum phase $\frac{\theta}{\delta_e}$ transfer function. From the data it is seen that if the pilot closes the γ-loop at a frequency 1 to 1.5 octave below the ω_{SP}, he is able to operate the aircraft with no control system dynamics with a nominal 0.5 to 1.0 sec lead time constant. Therefore, instead of analyzing the data at a fixed ω_c, the phase angle and slope of the phase curve at a frequency 1 octave below ω_{SP} was analyzed to match a pilot rating expression of the form

$$PR = \alpha_1 \phi + \alpha_2 \left.\frac{\delta\phi}{\delta\omega}\right|_1 + \alpha_3 \left.\frac{\delta\phi}{\delta\omega}\right|_2 \qquad (15)$$

where α_1, α_2 and α_3 are constants evaluated for each aircraft individually using the method of least squares explained earlier. $\left.\frac{\delta\phi}{\delta\omega}\right|_1$ is the slope of the phase curve below ω_c and and $\left.\frac{\delta\phi}{\phi\omega}\right|_2$ is the slope of the phase curve above ω_c.

The values of α_1,α_2 and α_3 and the estimated and actual PR are tabulated in Table E16. For aircraft 1 and 5 the two slopes are averaged, since the variation is small. A plot of the estimated PR versus the actual PR is shown in Fig. 5.

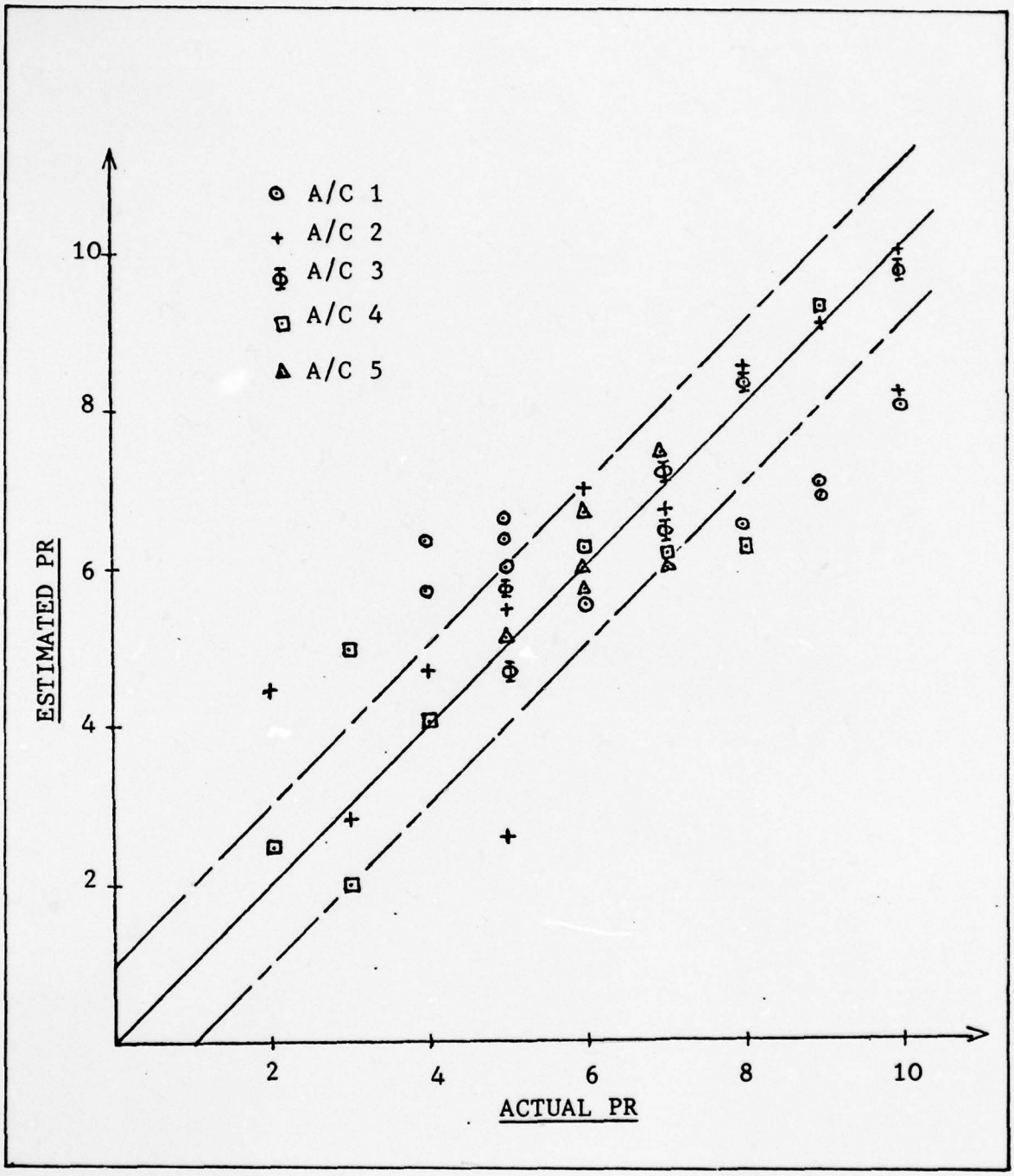

Fig. 5. Estimated Verses Actual PR Using 'γ' Phase Angle Data And Equation 15

The lead control system configurations were also included for this analysis. Out of 42 data points 13 data points are outside the ±1PR boundary. 8 out of the 13 points represent aircraft 1, and 3 points represent aircraft 2, and 2 points represent aircraft 4. If the data for aircraft 1 is removed from the figure, only 5 points out of 32 are outside the ±1PR boundary, which is a much better correlation compared to the pitch angle data.

To observe the effect of adding control systems on pilot rating an alternate expression was developed as shown:

$$\Delta PR = \alpha_1 \Delta\phi + \alpha_2 \Delta \frac{\delta\phi}{\delta\omega} \qquad (16)$$

where ΔPR is the deviation in pilot rating from the best rating in the data. $\Delta\phi$ and $\Delta \frac{\delta\phi}{\delta\omega}$ are the deviations in the corresponding phase angle and slope. Five expressions were developed, one for each aircraft. The values of α_1 and α_2 and the estimated and actual ΔPR are tabulated in Table E17. Fig. 6 shows a plot of estimated versus actual ΔPR. It is seen that 14 out of 37 points lie outside the ±1ΔPR boundary. Out of the 14 points, 5 represent aircraft 1, 5 represent aircraft 2, 2 points represent aircraft 4 and 2 points represent aircraft 3 and 5.

Summary of Open-Loop Frequency Response Analysis

The results obtained from the open-loop frequency response analysis can be summarized as follows:

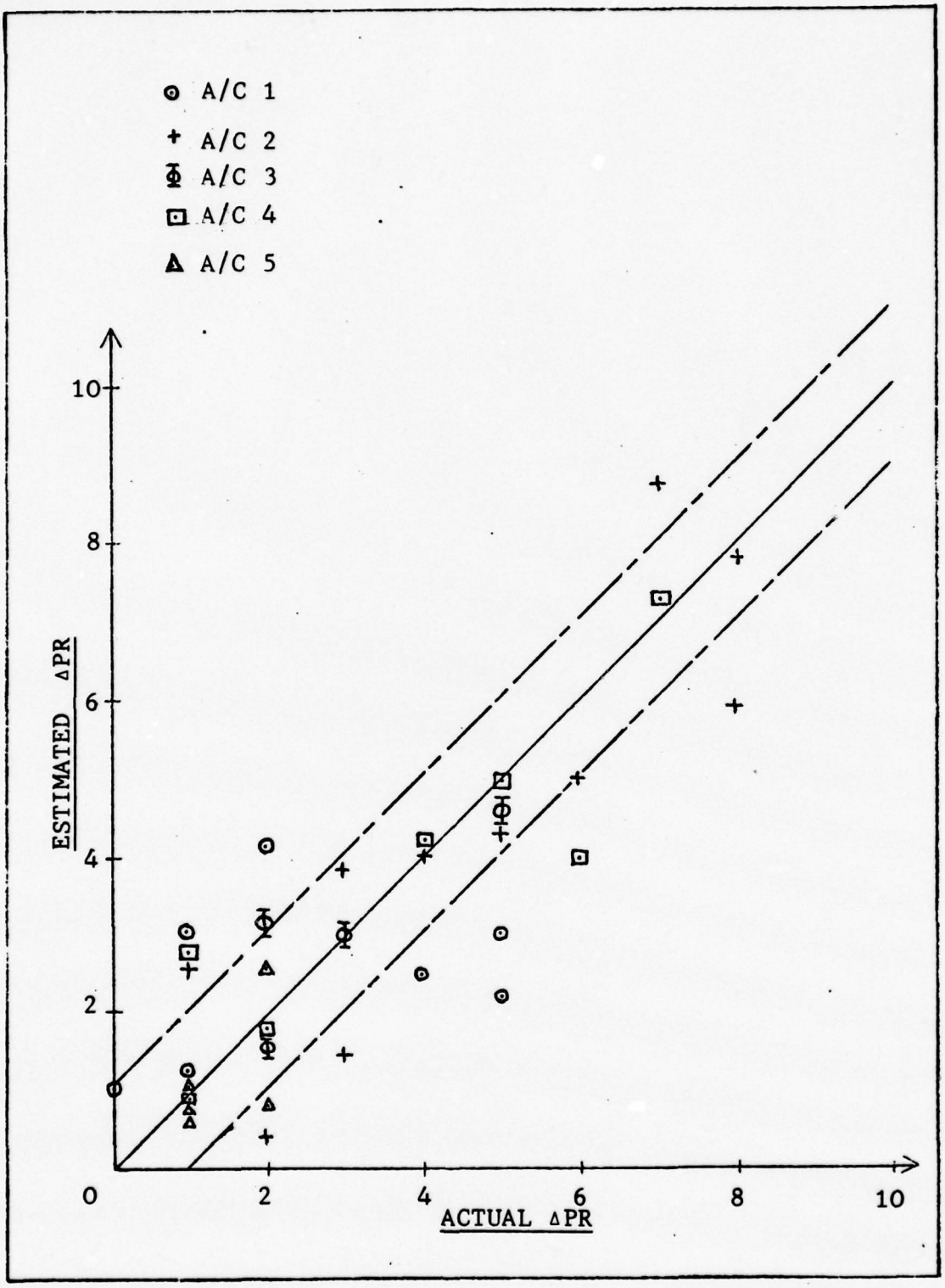

Fig. 6 Estimated Verses Actual ΔPR Using 'γ' Phase Angle Data And Equation 16

1) For a particular cross-over frequency (fixed performance) the phase angle (pilot workload) and the slope of the phase curve (system sensitivity) correlated reasonably well with the pilot rating. This was especially true for the flight path angle data (Figure 5). Inclusion of the system performance as a variable in the pilot rating expression may provide better correlation. An approach for accomplishing this is described in the recommendation section of this report.

2) The deviation in the pilot rating with respect to the best rating correlated well with the corresponding deviation in the phase angle and slope. This was true for both the pitch angle (Figure 4) and the flight path angle (Figure 6) data.

3) The pilot can obtain good phase margin for aircraft with no control system dynamics if,

   a) He closes the pitch loop at ω_c approximately equal to $(\omega_{SP} + 1)$ rad/sec.

   b) He closes the γ-loop at ω_c approximately one octave below ω_{SP}.

4) Aircraft with control systems introducing significant lags around ω_{SP} will have poor ratings.

5) The degree of correlation between the phase angle data and the pilot ratings indicate that the pitch and flight path angles seem to be important tracking parameters for pilots during landing task.

IV Analog Computer Simulation

The Analog computer is a tool which helps in the simulation and study of a physical system. It can be used for the analysis, design and testing of open-loop and closed-loop control systems in the time domain for standard inputs. Analog simulation studies are very handy for parameter adjustments in a control system to achieve a desired objective, vis-a-vis, performance and time response.

This chapter discusses the simulation of the pilot-aircraft closed-loop system on the analog computer. This study is undertaken to find an optimum pilot lead time which yields the best system performance for the aircraft-control system configurations simulated. The performance thus measured is correlated with PR. The objective is two fold:
1) To see if a correlation between performance and PR exists;
2) To see if the pilot could improve the system performance by choosing different forms of pitch angle and flight path angle feedback. The "Lead only" form of McRuer model is used for the pilot as explained in Chapter II with a reaction time delay of 0.3 sec. The ISE (integral of squared error) is used as the performance criterion. The pilot gain, K_p, and lead, T_L, are adjusted to minimize ISE when the pilot performs a particular tracking task for a step command. Using, the short period approximation dynamics of A/C 1, first the effects of adding control systems on the performance are studied.

The tracking task is analyzed in three phases: 1) Inner-loop pitch attitude (θ) tracking for a step pitch command; 2) outer-loop flight path angle (γ) tracking for a step γ-command; and 3) combined pitch and flight path angle tracking (inner and outer loop) to minimize the error in the flight path angle for a step γ-command. The results thus obtained are described. These three phases are repeated for the remaining four aircraft using the baseline control system (control system = 1) to observe the performance variations between the five aircraft configurations. Since the natural frequency of the elevator servo (75 rad/sec) and the feel system (26 rad/sec) dynamics are very high, their effect at the frequencies of interest are assumed to be negligible and hence are not included in the simulation.

Thus, the objective of the analog simulation study is to find optimum pilot parameters K_p and T_L which would minimize the ISE for a particular tracking task. The description of the analog computer circuits used during the simulation may be found in Appendix D. References 13,14, and 15, were very useful in programming the simulation.

Pitch Attitude Tracking Task

The block diagram used for simulation is shown in Fig. 7. Aircraft No. 1 with no control system dynamics was first analyzed. The control systems which were flown with aircraft 1 were then simulated and the analysis was repeated for each case.

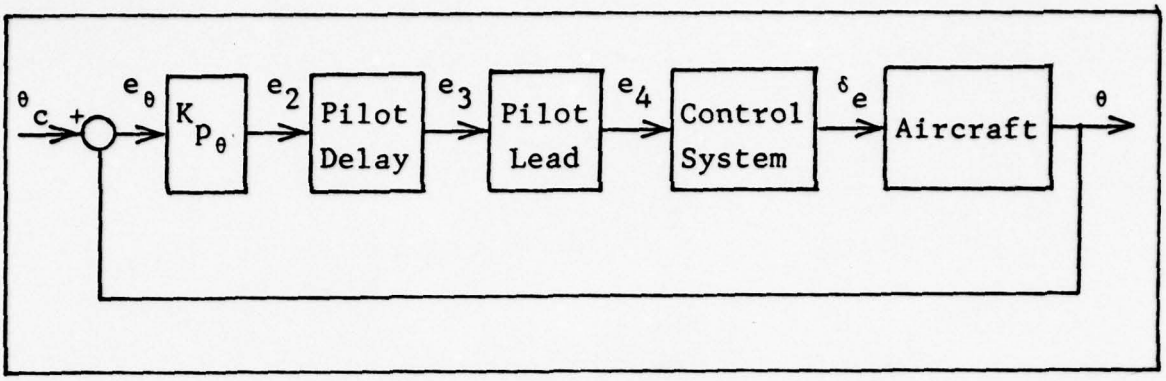

Figure 7 Block Diagram of Pitch Tracking Task

The proceedure used for the analysis is as follows. The error signal e_θ, was fed to a quarter-square multiplier circuit to generate e_θ^2, which was then integrated to generate ISE. The pilot lead time T_L was varied from 0 to 1.25 sec in steps of 0.25 sec. For each value of T_L, the pilot gain K_p was varied and the value of ISE was recorded for a step pitch command (θ_c).

The data thus generated is shown in Fig. 8 thru 16. While pilot lead times greater than 0.5 or 0.75 sec, produce a slight improvement in the system performance, they do so at the expense of greater pilot workload. For a 1.0 sec. and 1.25 sec. lead time the relative difference in the ISE value is insignificant. Besides, the curves for 1.0 and 1.25 sec. lead time show much larger variations in the value of ISE about the minimum, thus indicating higher system sensitivity due to pilot gain variations. Therefore, a value of 0.5 or 0.75 sec. pilot lead seems to be the optimum choice. Fig. 14

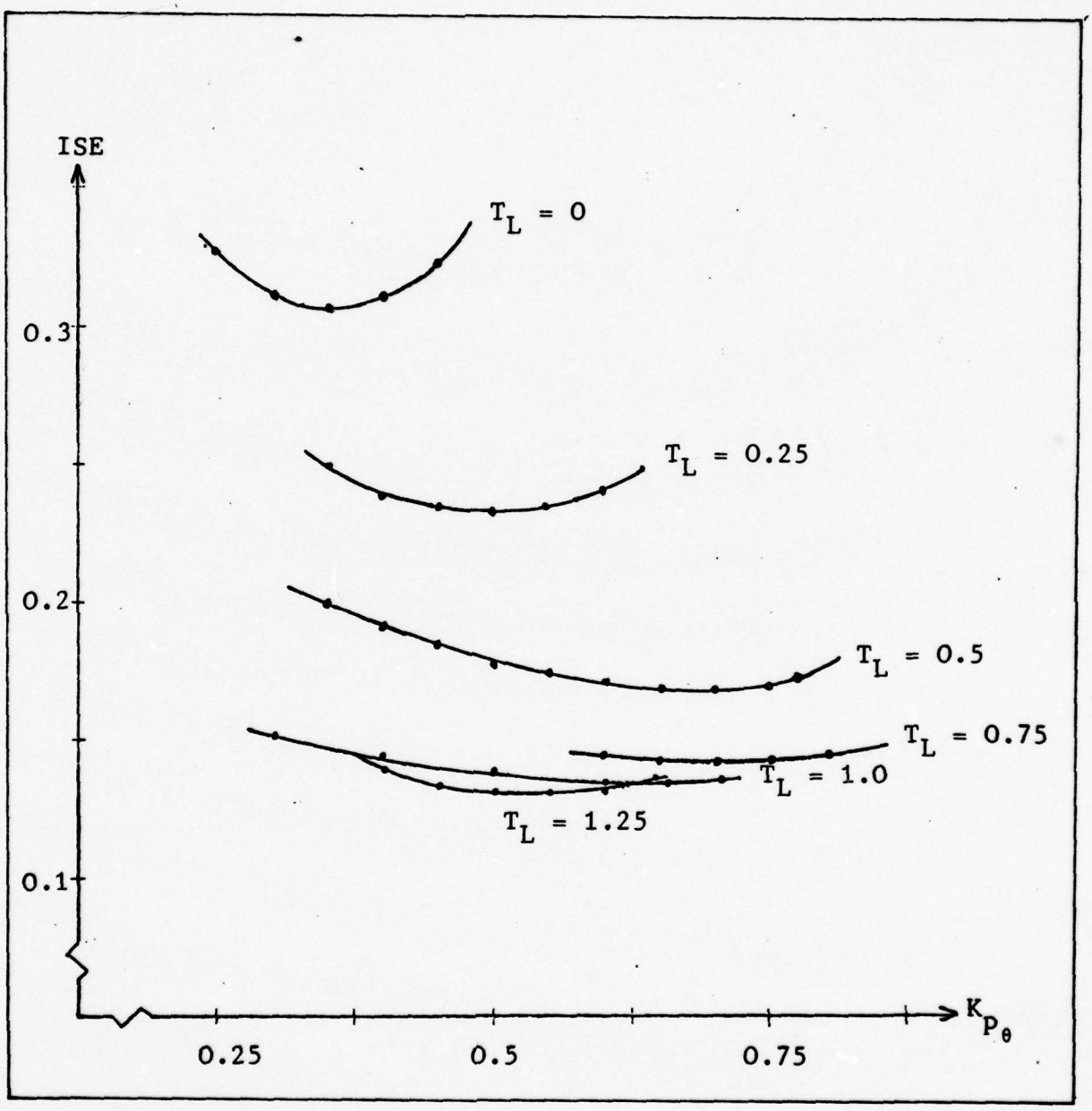

Fig. 8 ISE Vs. K_{P_θ} For Different T_L - Aircraft 1 C/S = 1

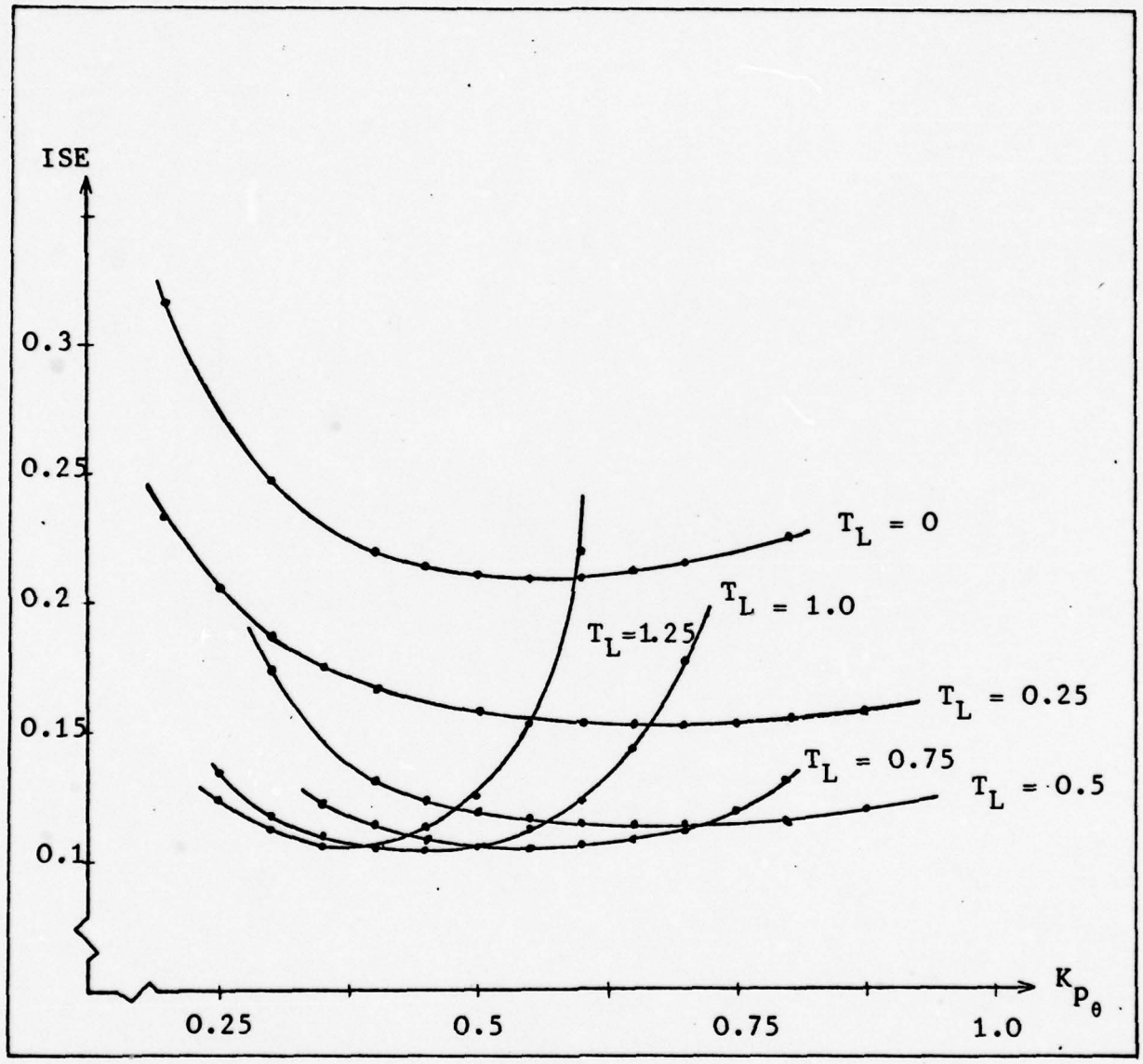

Fig. 9. ISE Vs. K_{P_θ} For Different T_L - Aircraft 1 C/S 1

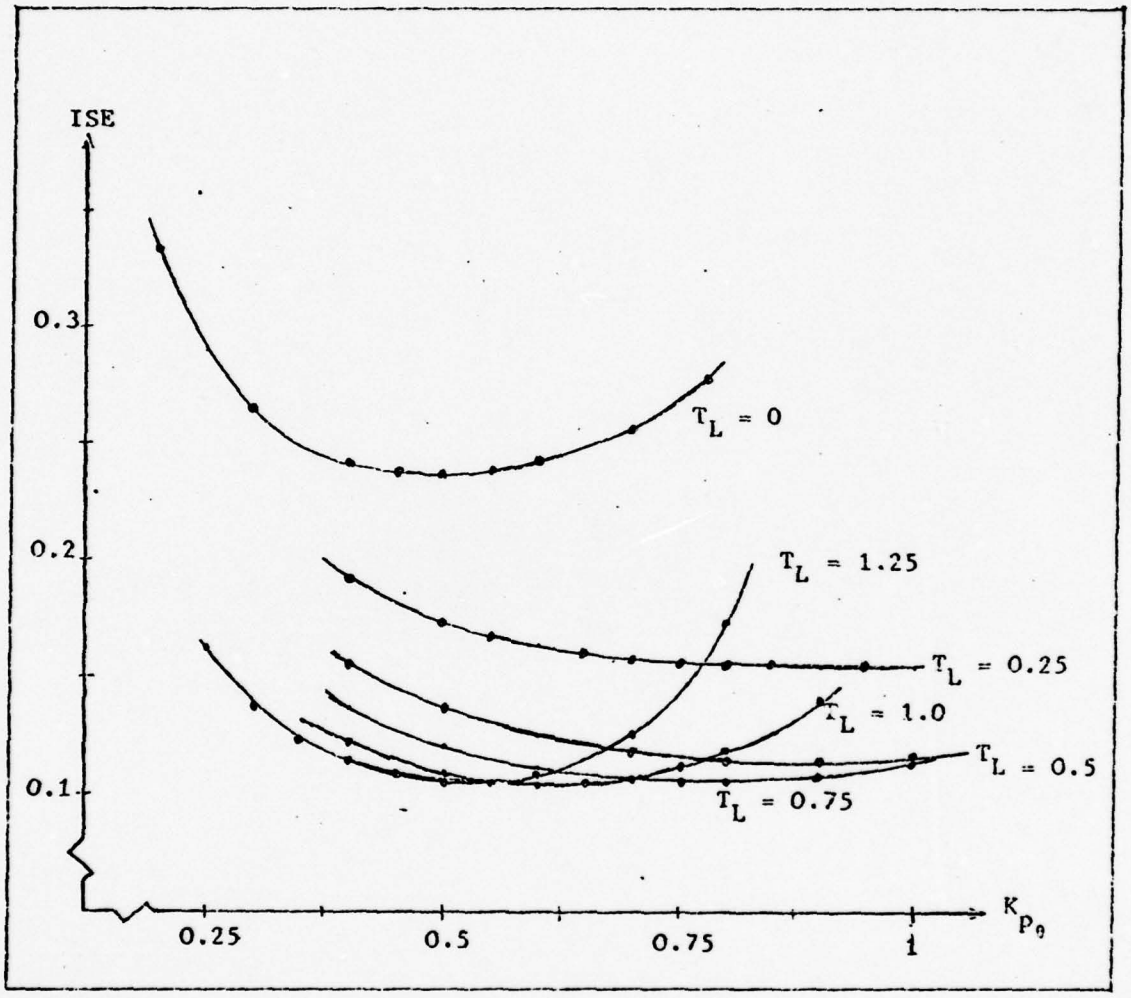

Fig. 10 ISE Vs. K_{P_0} For Different T_L -- Aircraft 1 C/S 2

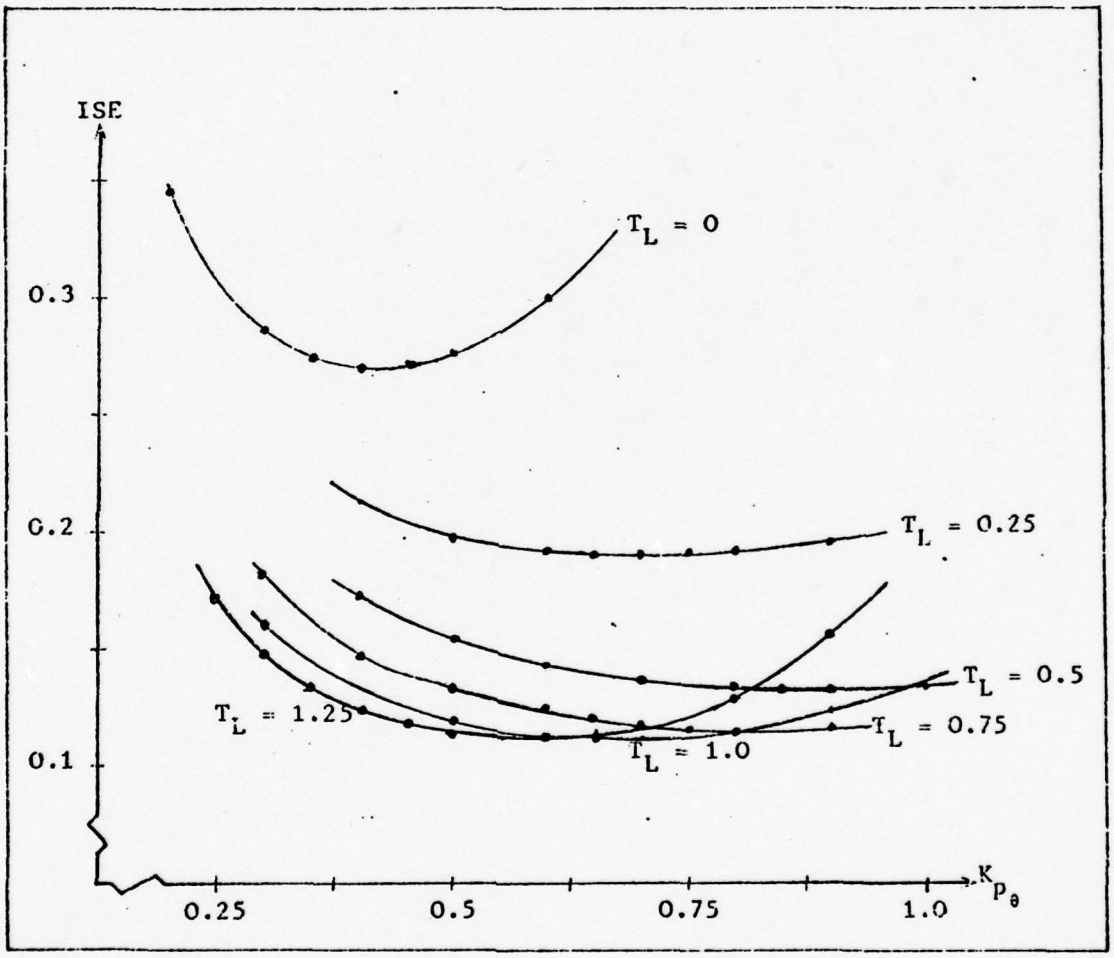

Fig. 11. ISE Vs. K_{p_θ} For Different T_L - Aircraft 1 C/S 3

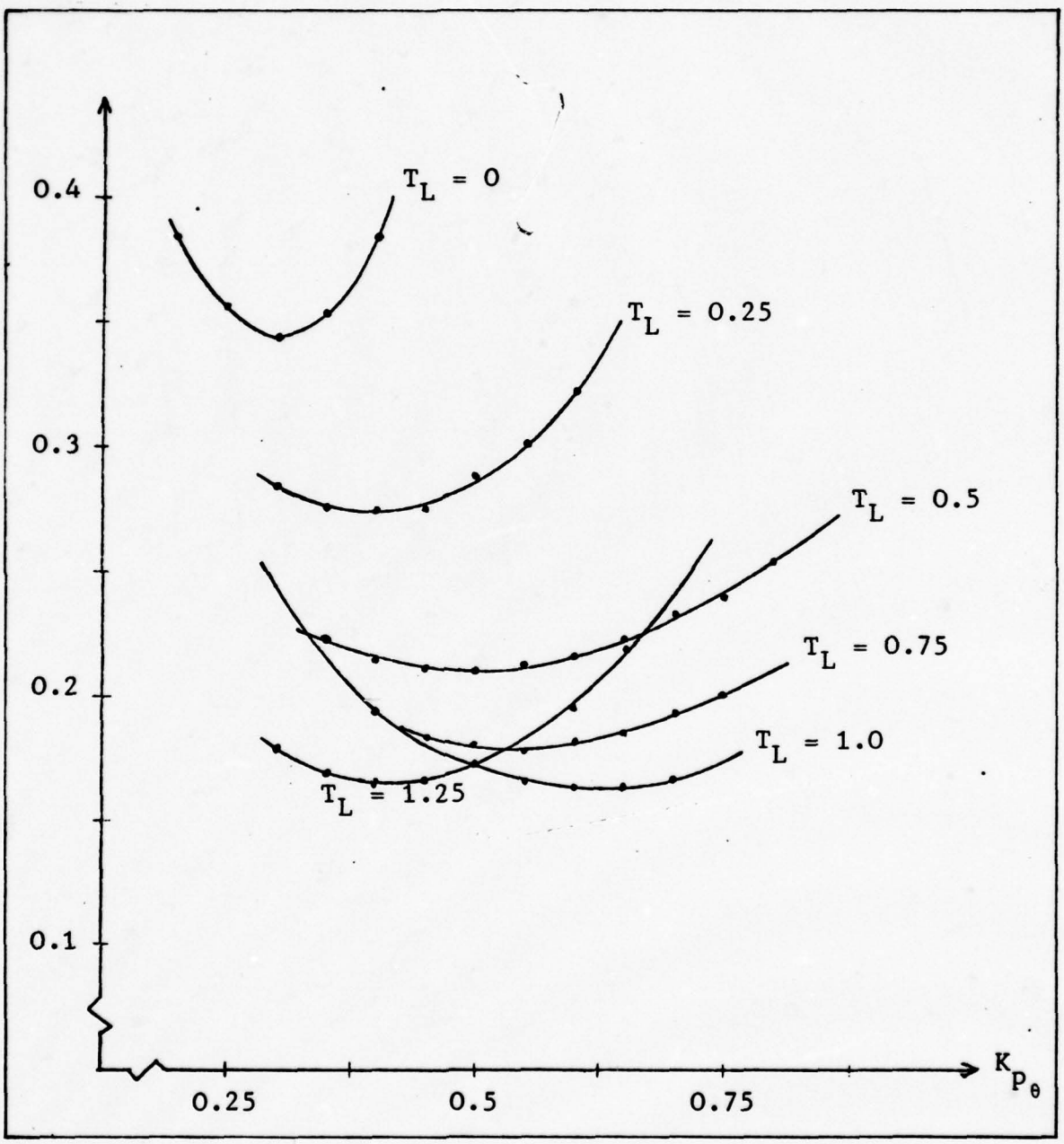

Fig. 12 ISE Vs. K_{p_θ} For Different T_L - Aircraft 1 C/S 4

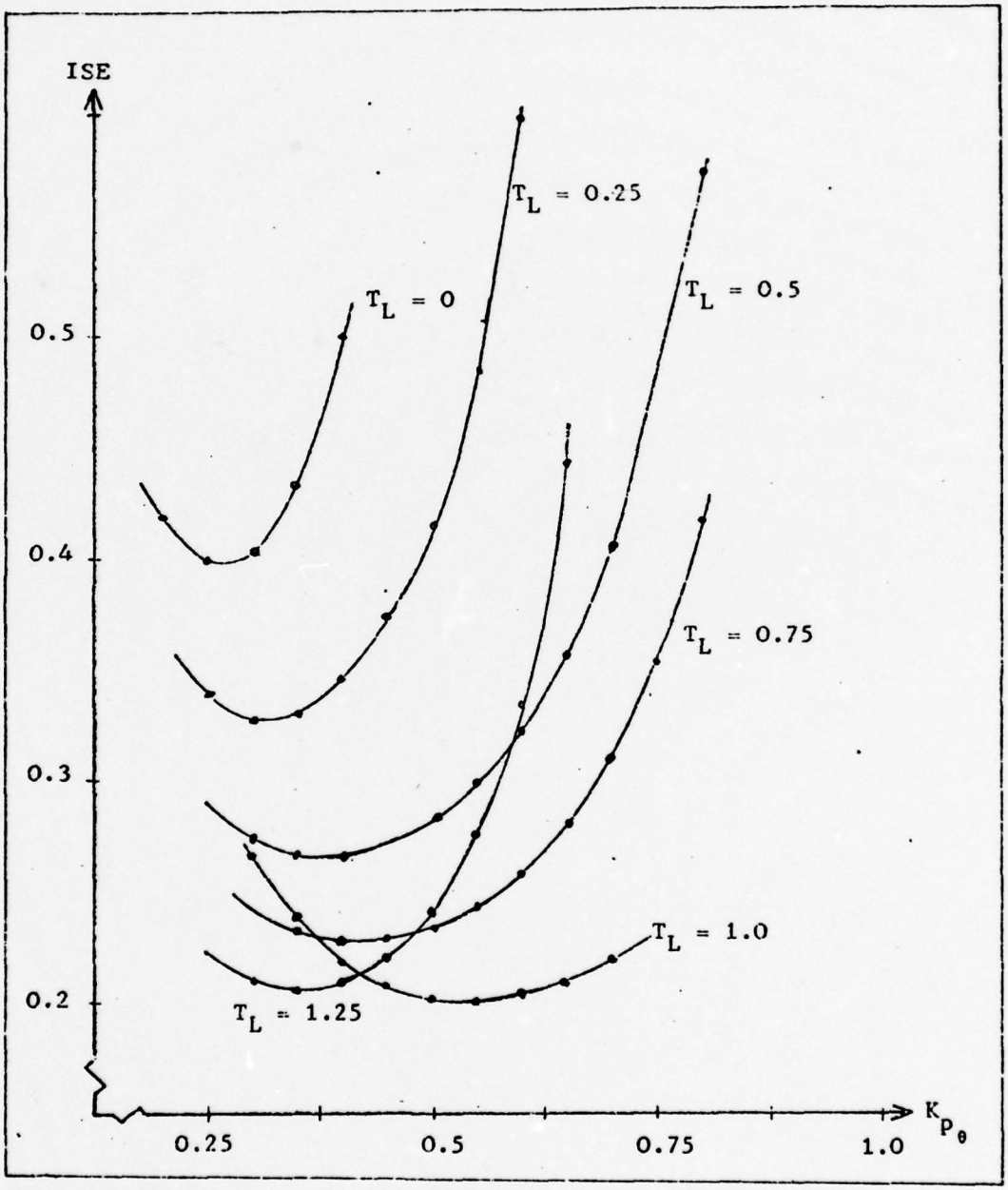

Fig. 13 ISE Vs. K_{p_θ} For Different T_L - Aircraft 1 C/S 5

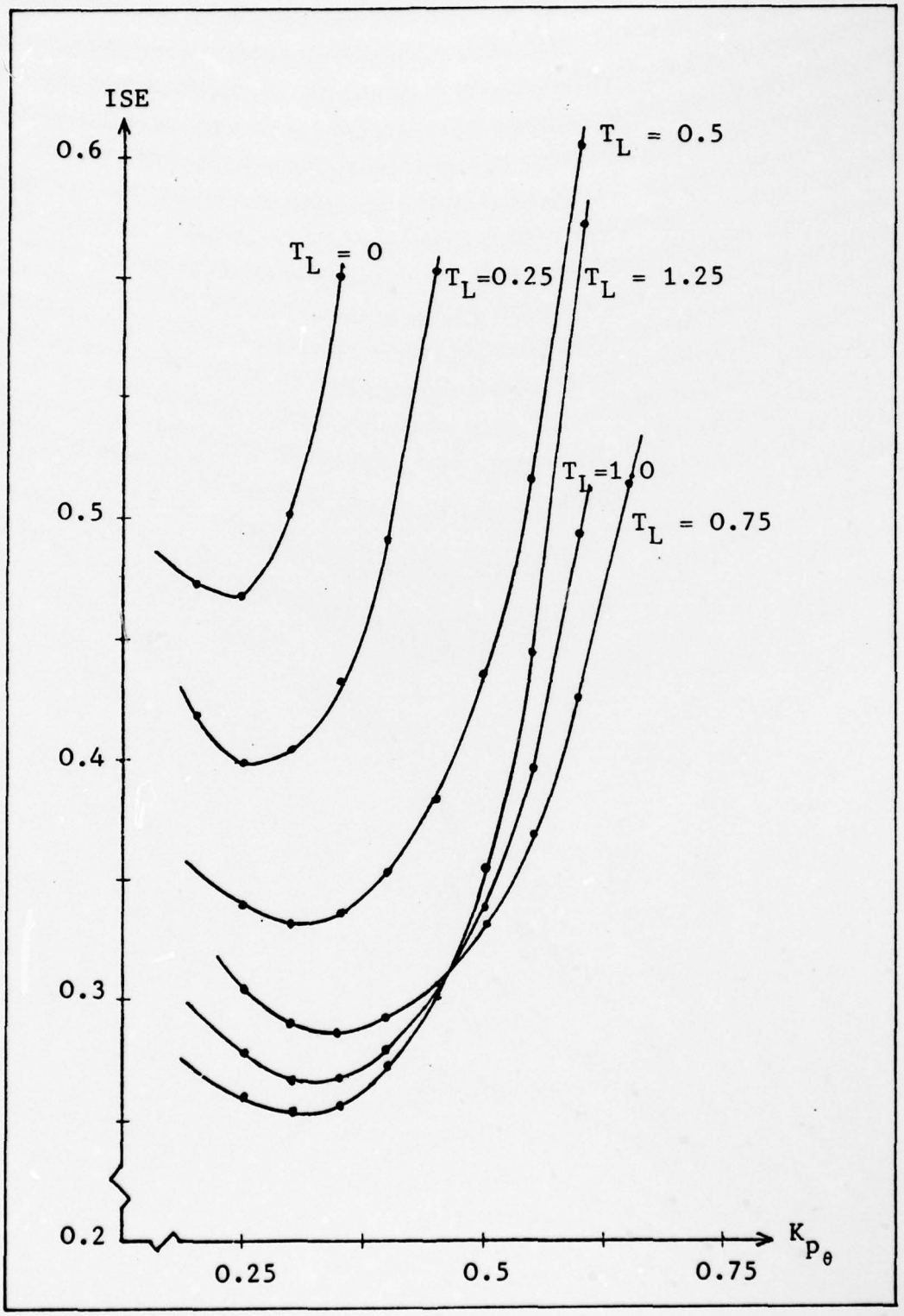

Fig. 14 ISE Vs. K_{p_θ} For Different T_L - Aircraft 1 C/S 6

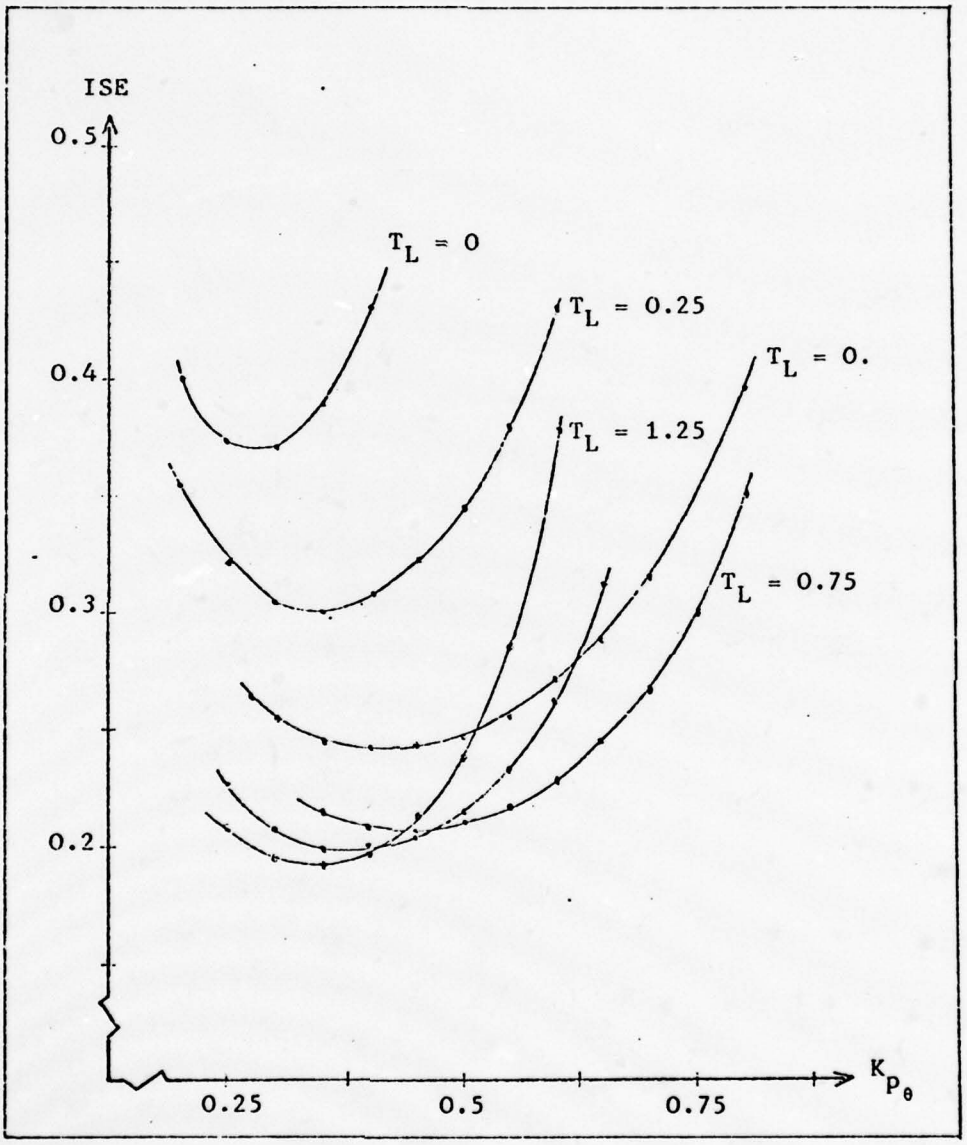

Fig. 15 ISE Vs. K_{p_θ} For Different T_L - Aircraft 1 C/S 10

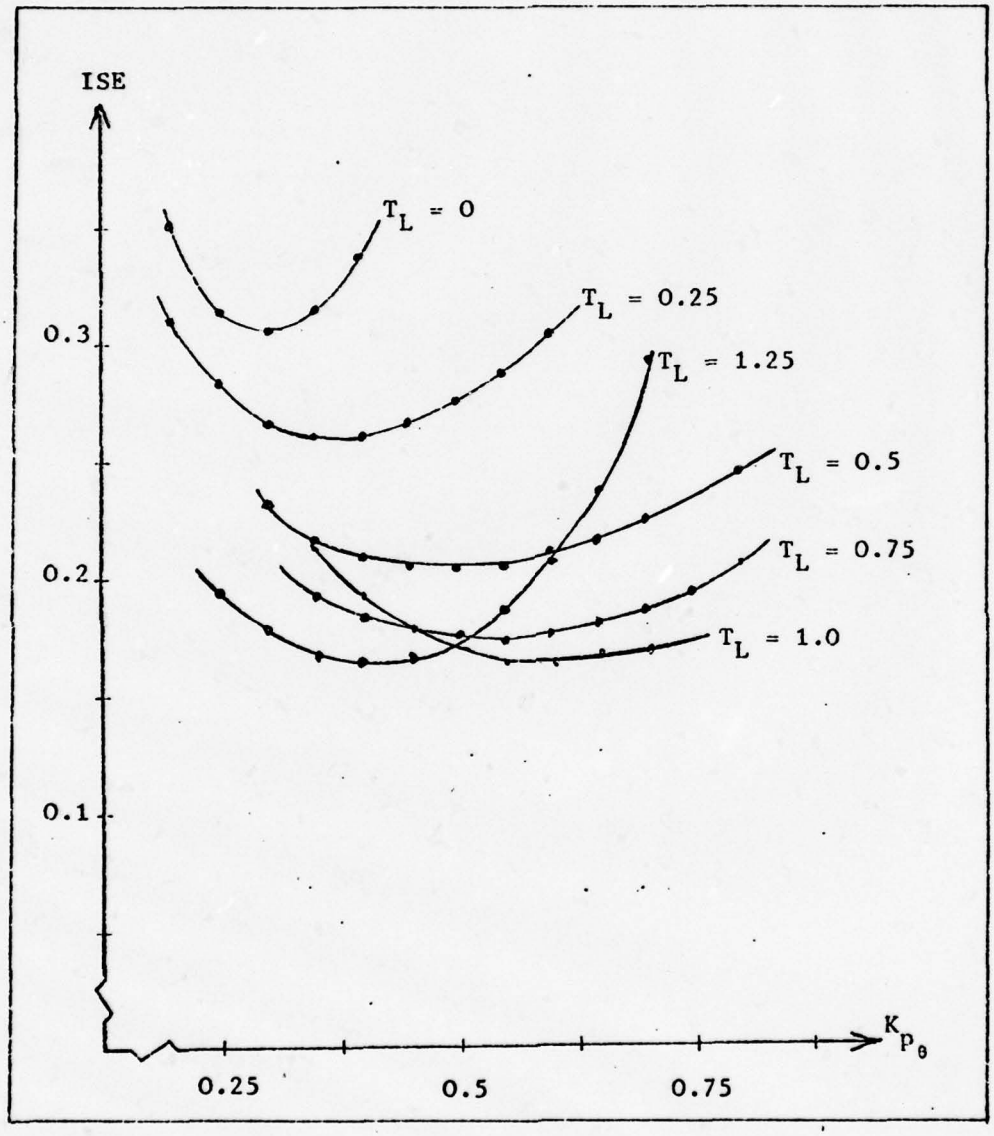

Fig. 16 ISE Vs. K_{p_θ} For Different T_L - Aircraft 1 C/S 12

shows the performance curve of aircraft 1 with control system dynamics $\frac{2}{(S + 2)}$. Since this control system introduces significant amount of lag near the short period natural frequency of the aircraft (1 rad/sec), the aircraft dynamic response is very sensitive to gain change. In other words, for good performance the pilot must hold the gain steady to avoid large variations in ω_c and ϕ_M. This in effect amounts to an additional workload in terms of pilot concentration and hence a degraded pilot opinion of the task. This corresponds to a very negative slope of the phase curve around ω_c in the open-loop frequency response analysis of the last chapter. The value of minimum ISE and the corresponding pilot ratings are plotted in Fig. 17 and 18 for a 0.5 and 0.75 sec. pilot lead, respectively. The rating degradation with poor performance for lag cases can be observed, but the reverse trend with the lead cases is again a puzzle which could not be explained.

Flight Path Angle Tracking Task

During the flare maneuver, the sink rate information is one of the visual cues the pilot uses in performing the landing task. Since flight path angle, γ , is directly related to the sink rate, it is logical to analyze the pilot in the γ-loop. This was done by first assuming no pitch angle feedback. The block diagram used for this simulation is shown in Fig. 19. Short period dynamics of aircraft 1 were used and

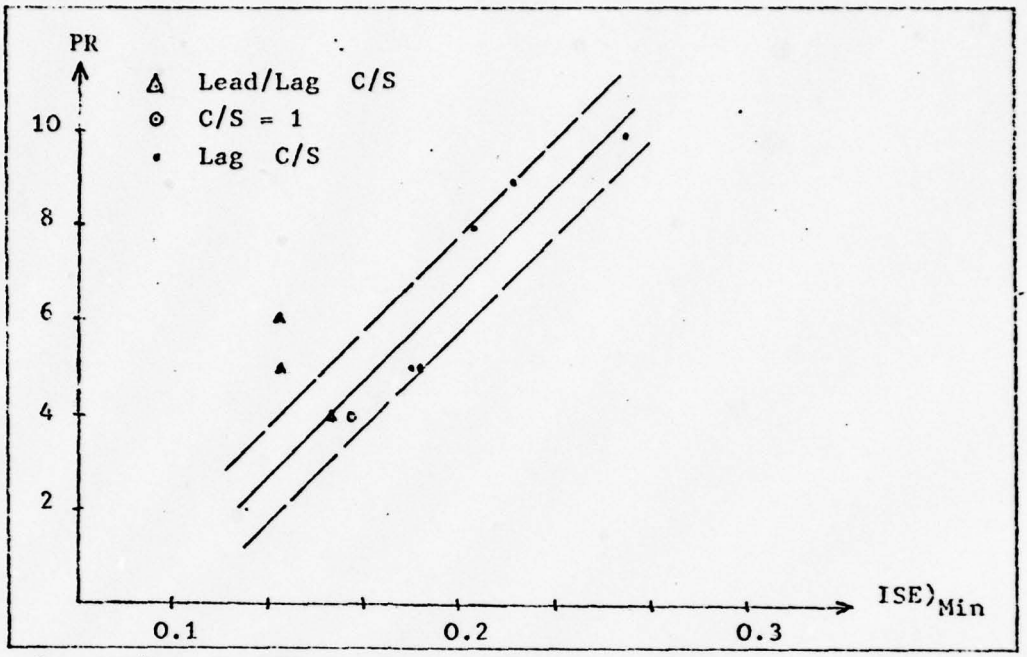

Fig. 18 $ISE)_{Min}$ Vs. PR For $T_L = 0.75$ - Aircraft 1 With Control System

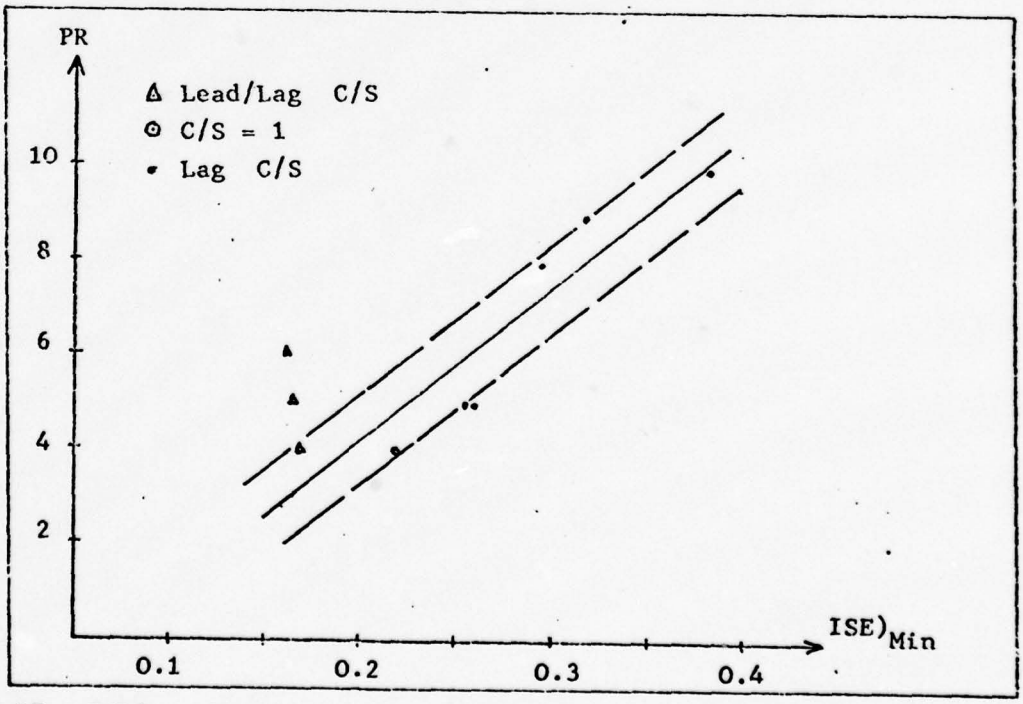

Fig. 17 $ISE)_{Min}$ Vs. PR For $T_L = 0.5$ - Aircraft 1 With Control Systems

the ISE (e_γ^2) was measured for a step γ-command. The pilot parameters K_{p_γ} and T_L were varied and the procedure used for the analysis of pitch loop was repeated, vis-a-vis, measuring the value of ISE until a minimum is reached, as K_{p_γ} and T_L were varied.

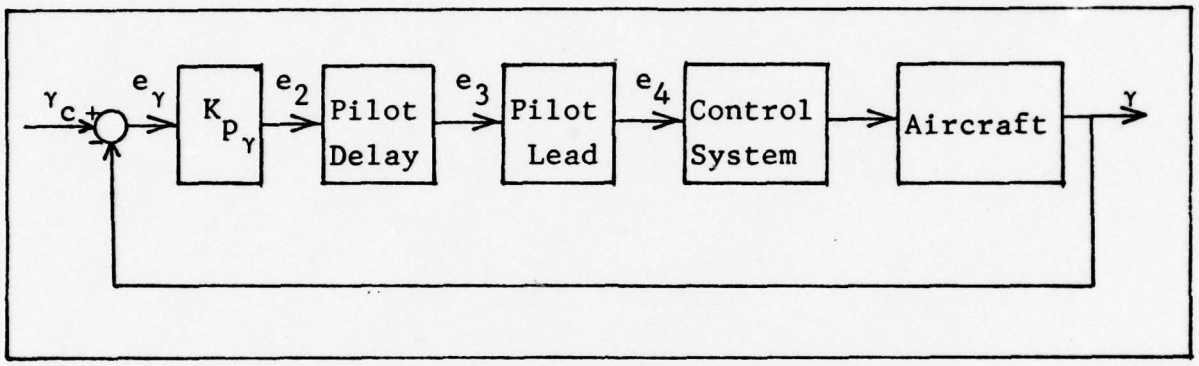

Figure 19 Block Diagram of γ Tracking Task

The plots of ISE versus the gain, K_{p_γ} as T_L is varied is shown in Figures 20 thru 28. From the plots it is seen that the γ-loop performance shows gradual improvement as pilot lead time, T_L, increases. However, the relative improvement in performance beyond $T_L = 0.75$ sec. shows a converging trend and indicates that additional pilot lead beyond this point does not result in proportional improvement in performance. Therefore a 0.75 sec. lead seems to be the optimum lead time constant for the closed-loop flight path angle tracking task. The tendency of the system to become more and more sensitive in the presence of lag control systems is evident from the

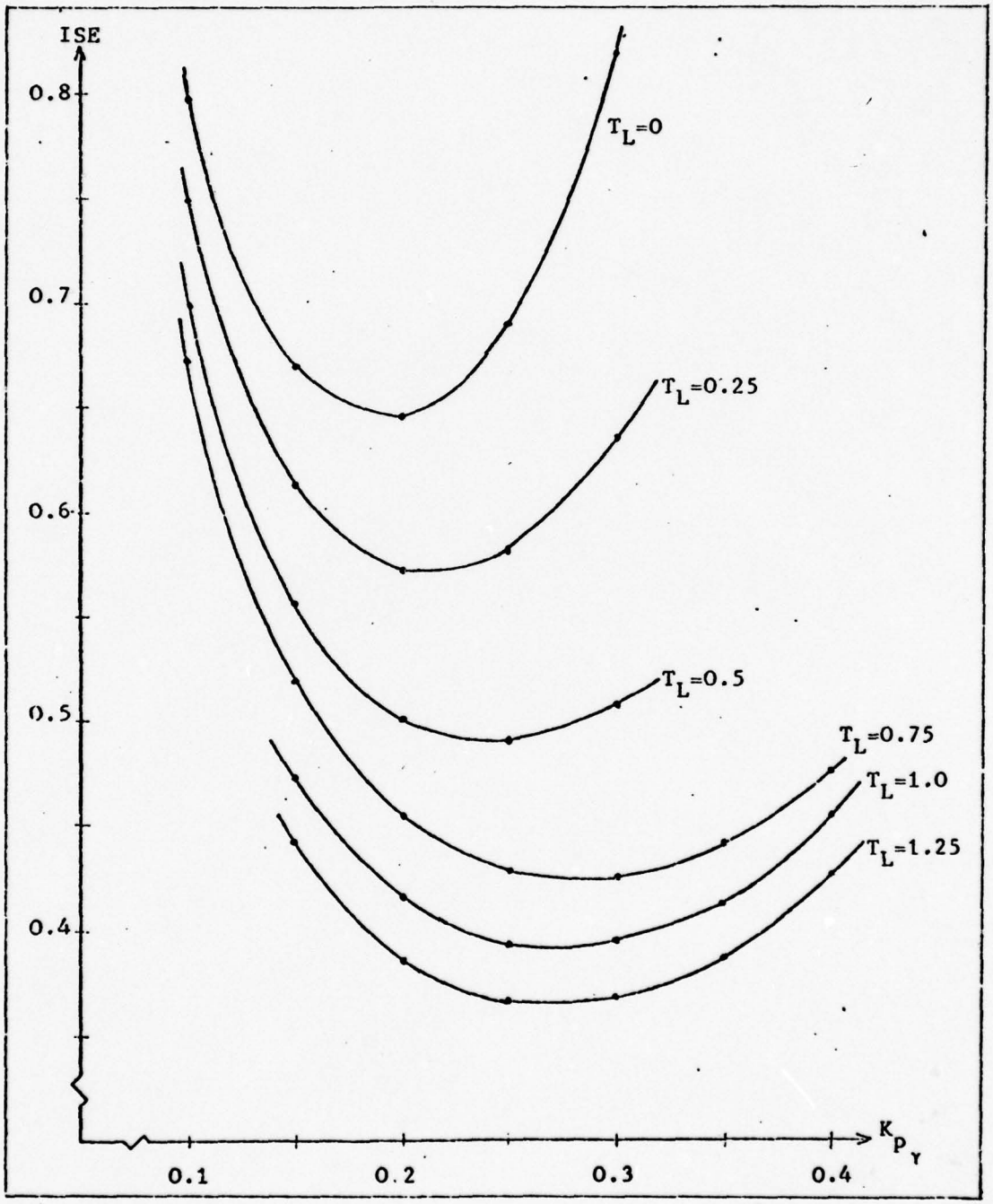

Fig. 20 ISE Vs. K_{p_Y} - Aircraft 1 C/S = 1

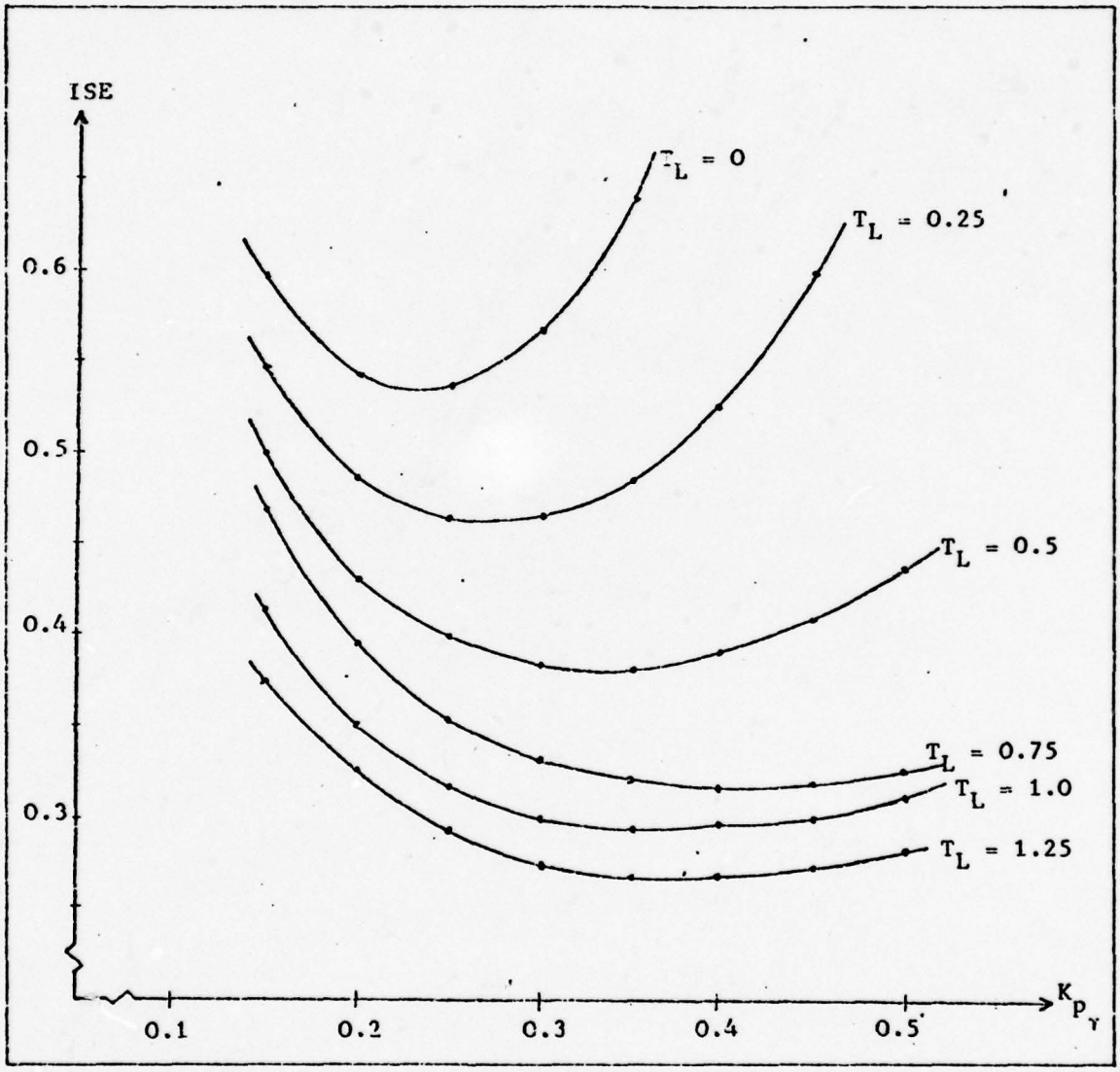

Fig. 21 ISE Vs. K_{p_Y} - Aircraft No. 1 C/S 1

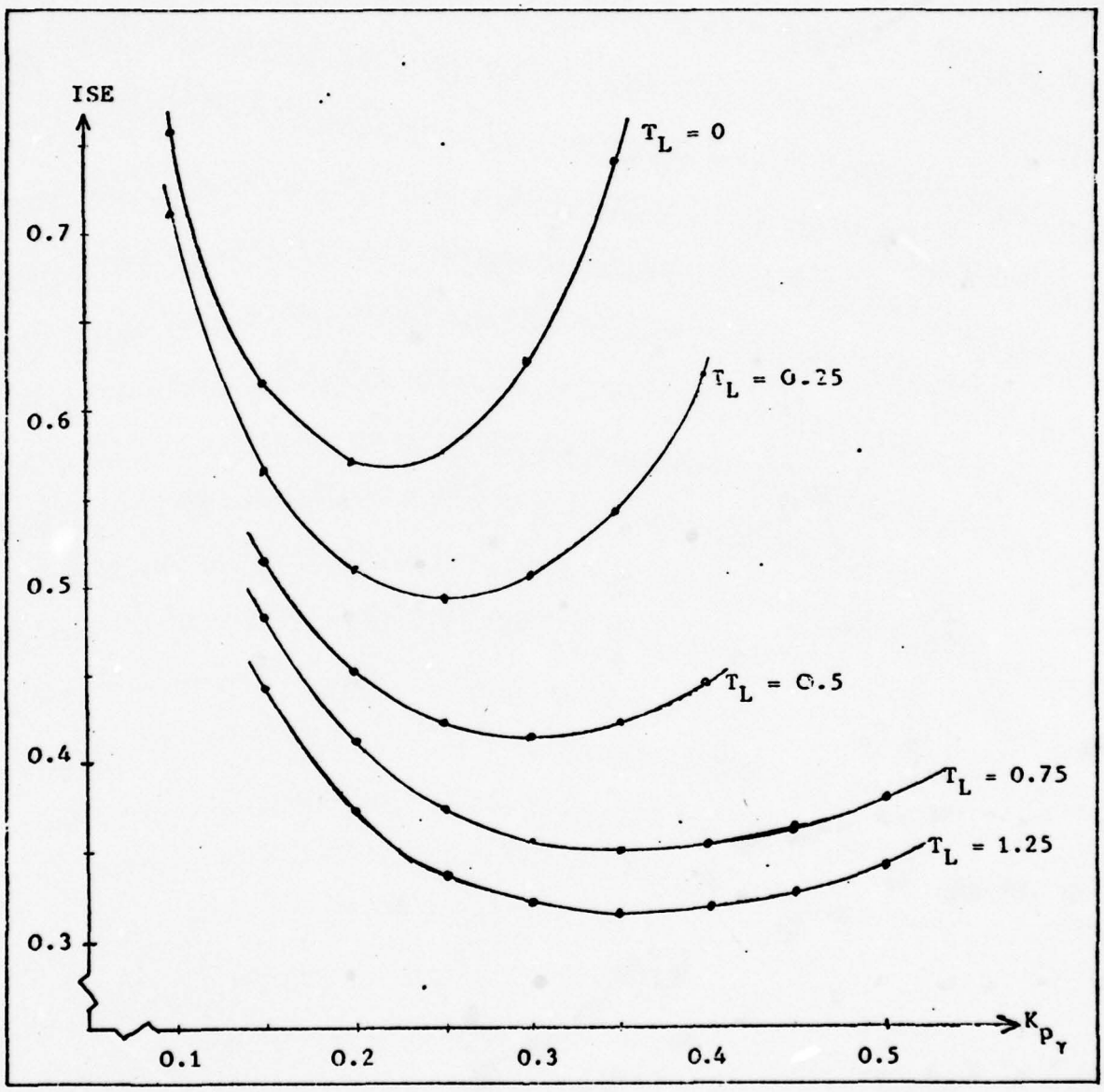

Fig. 22 . ISE Vs. K_{p_Y} Aircraft 1 C/S 2

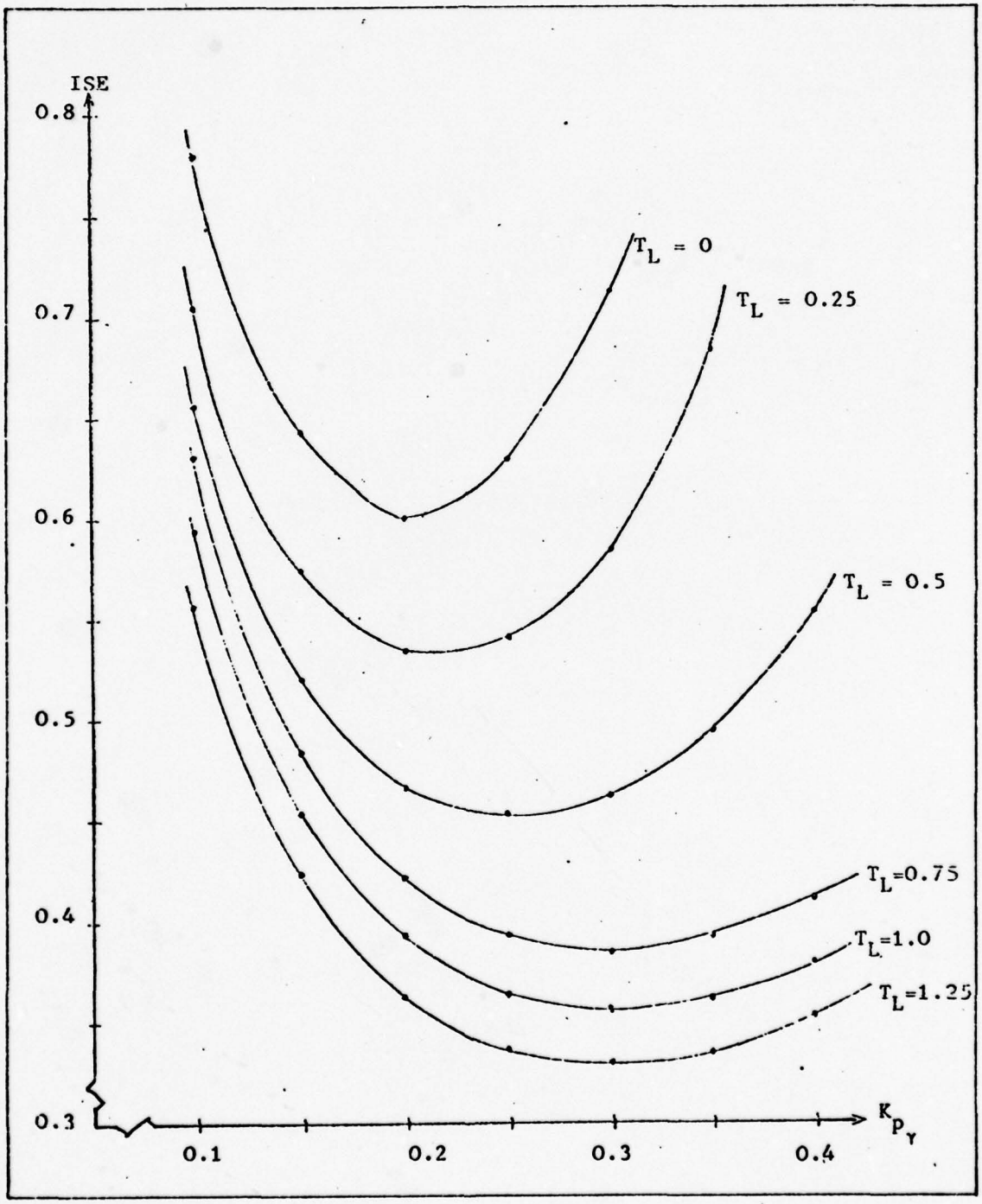

Fig. 23 ISE Vs. K_{p_Y} - Aircraft 1 C/S 3

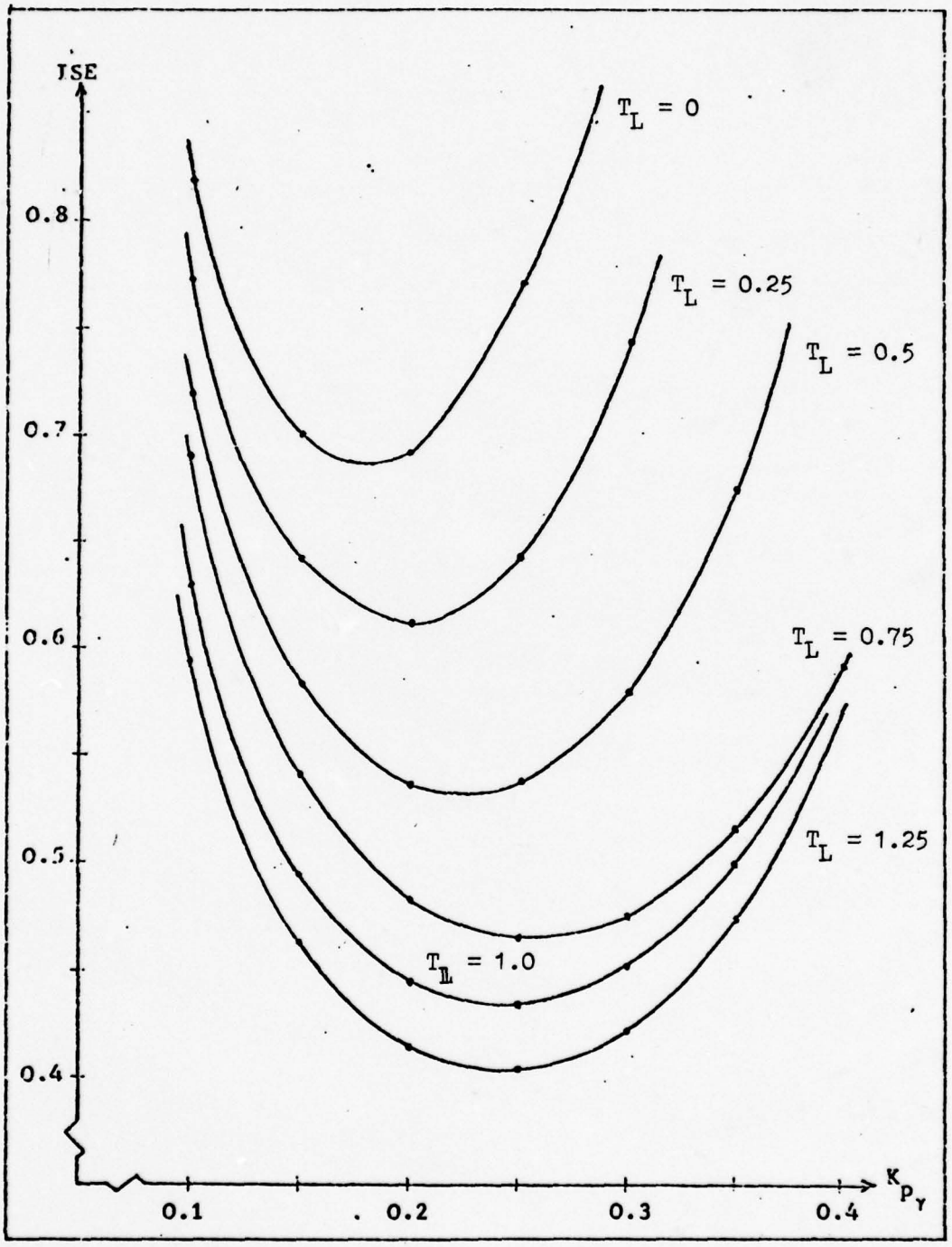

Fig. 24 ISE Vs. K_{P_Y} Aircraft 1 C/S 4

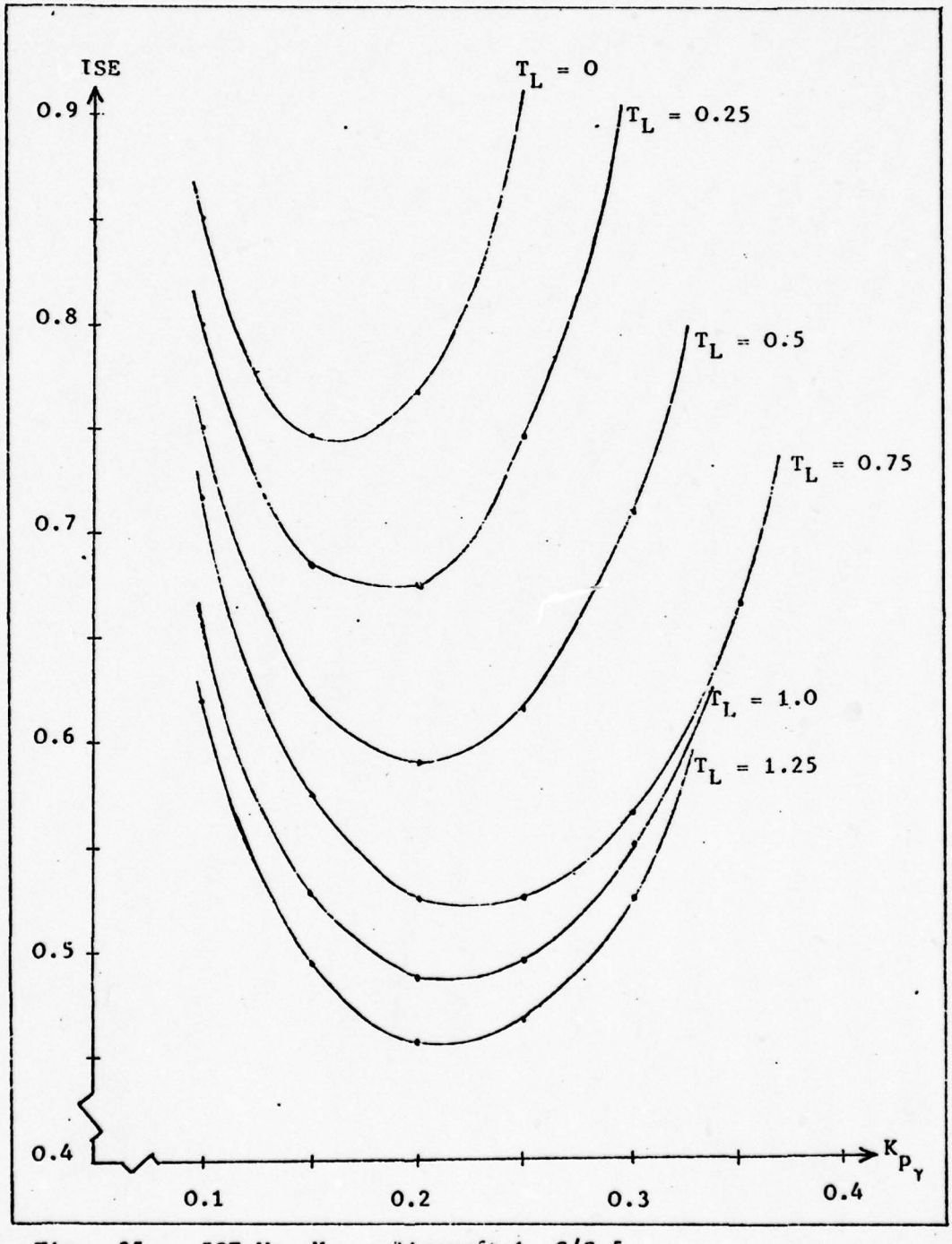

Fig. 25 ISE Vs. K_{p_Y} - Aircraft 1 C/S 5

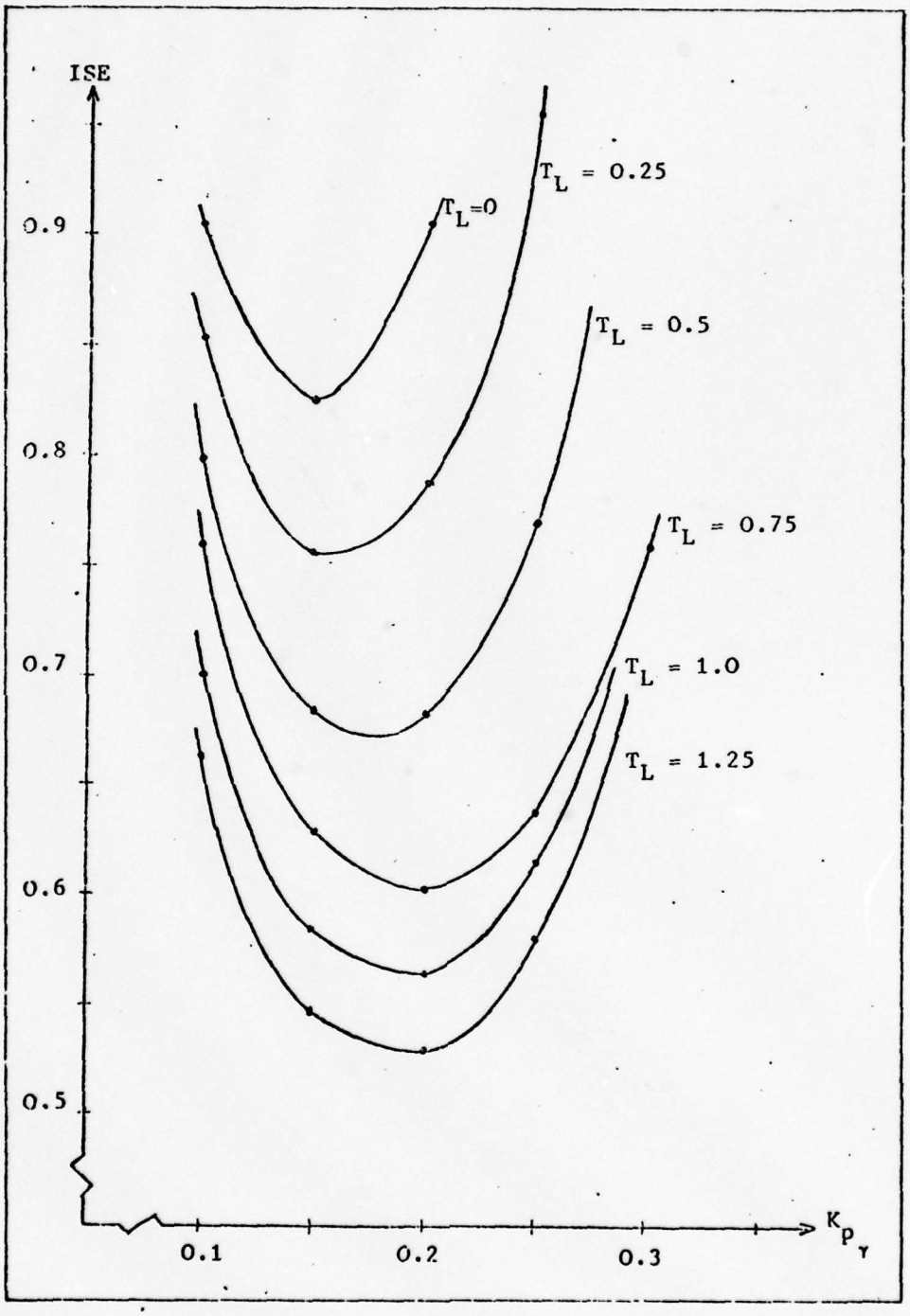

Fig. 26 ISE Vs. K_{p_γ} Aircraft 1 C/S 6

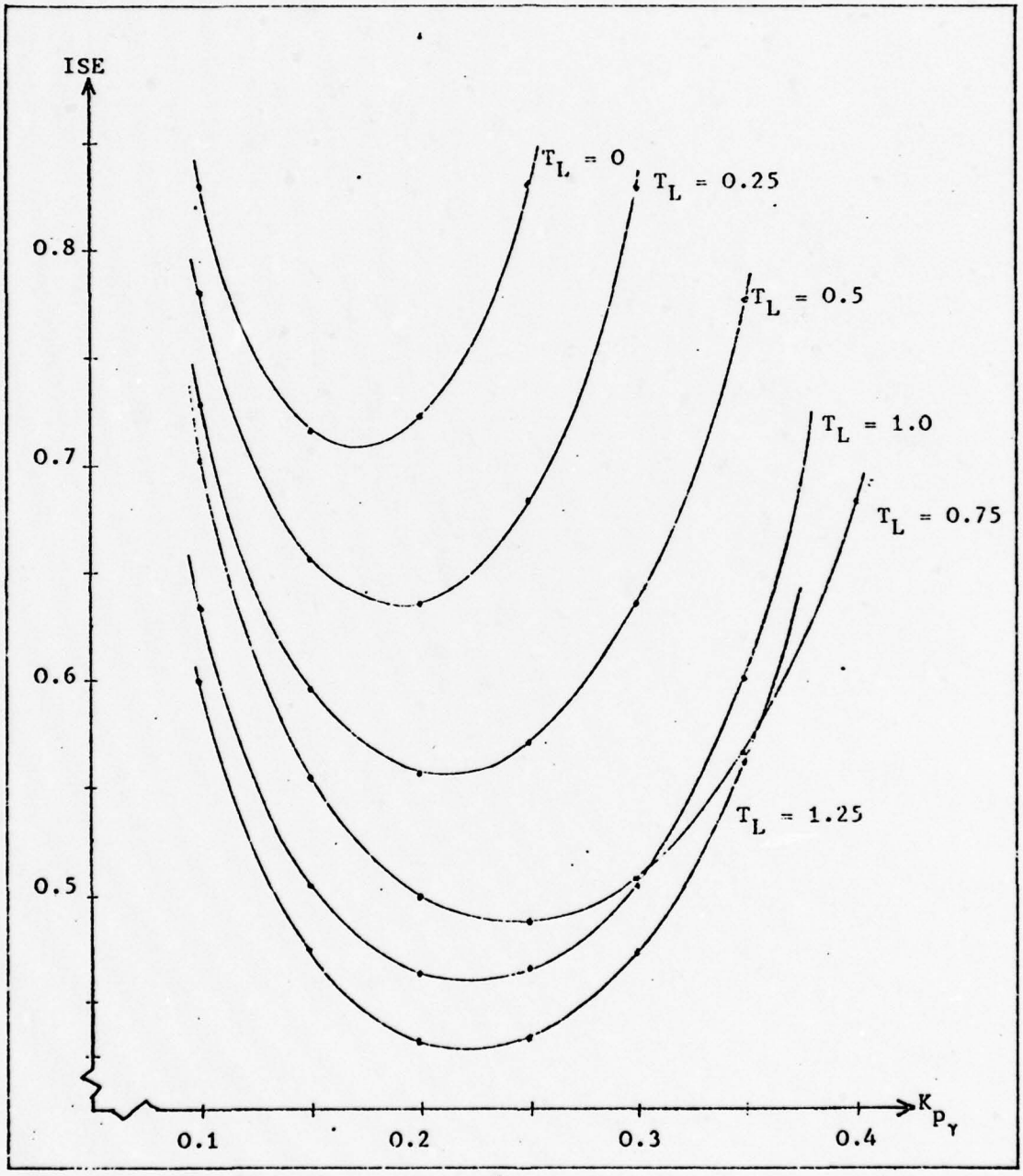

Fig. 27 ISE Vs. K_{p_γ} Aircraft 1 C/S 10

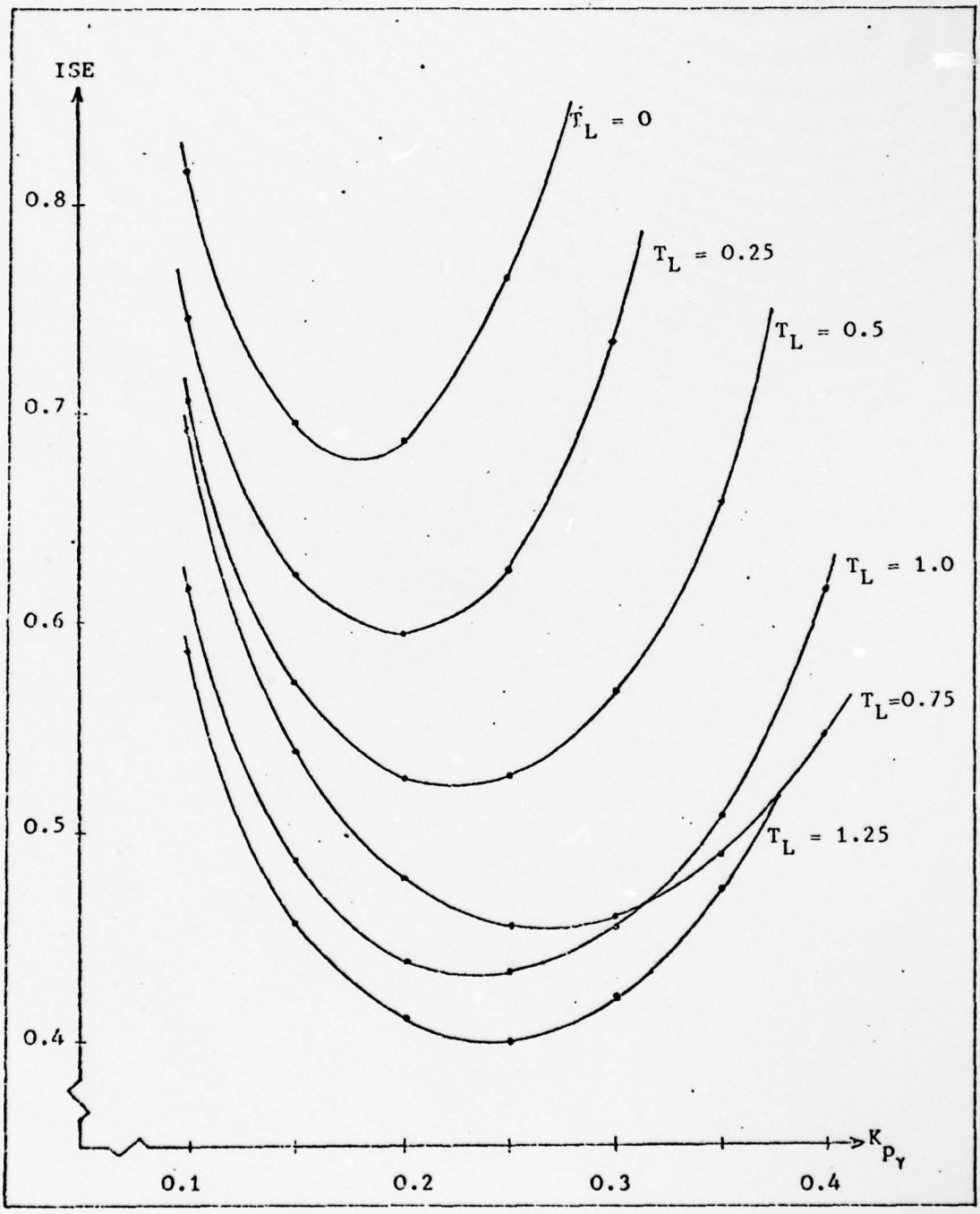

Fig. 28 ISE Vs. K_{p_Y} Aircraft 1 C/S 12

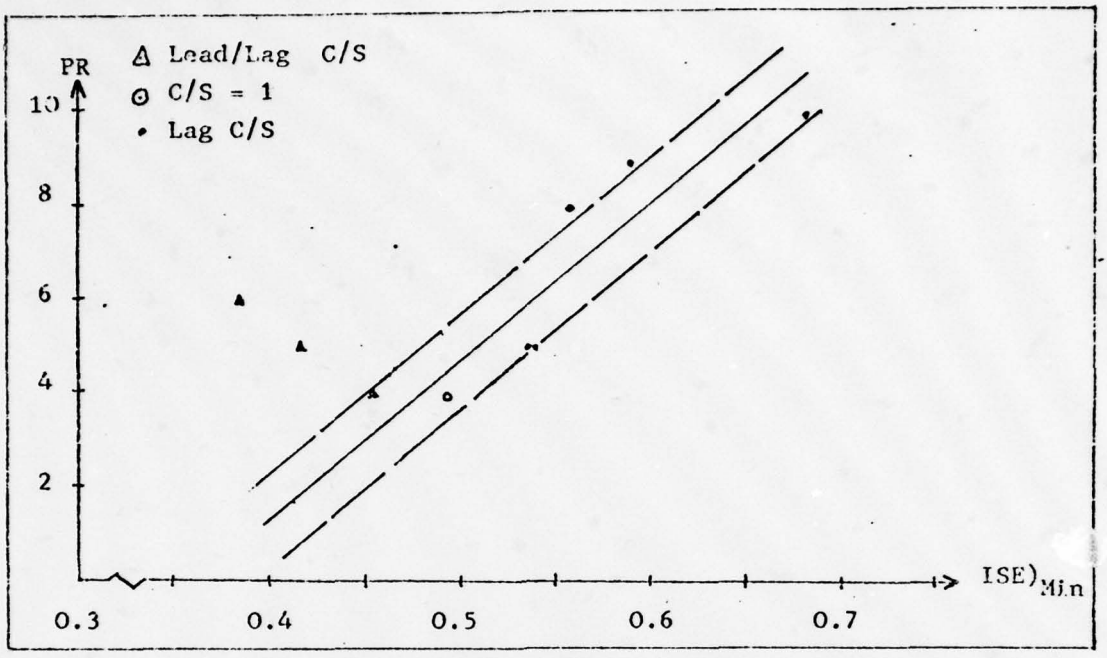

Fig. 29 $ISE)_{Min}$ Vs. PR - 'γ' Tracking Task For $T_L = 0.5$
A/C 1 With Control Systems

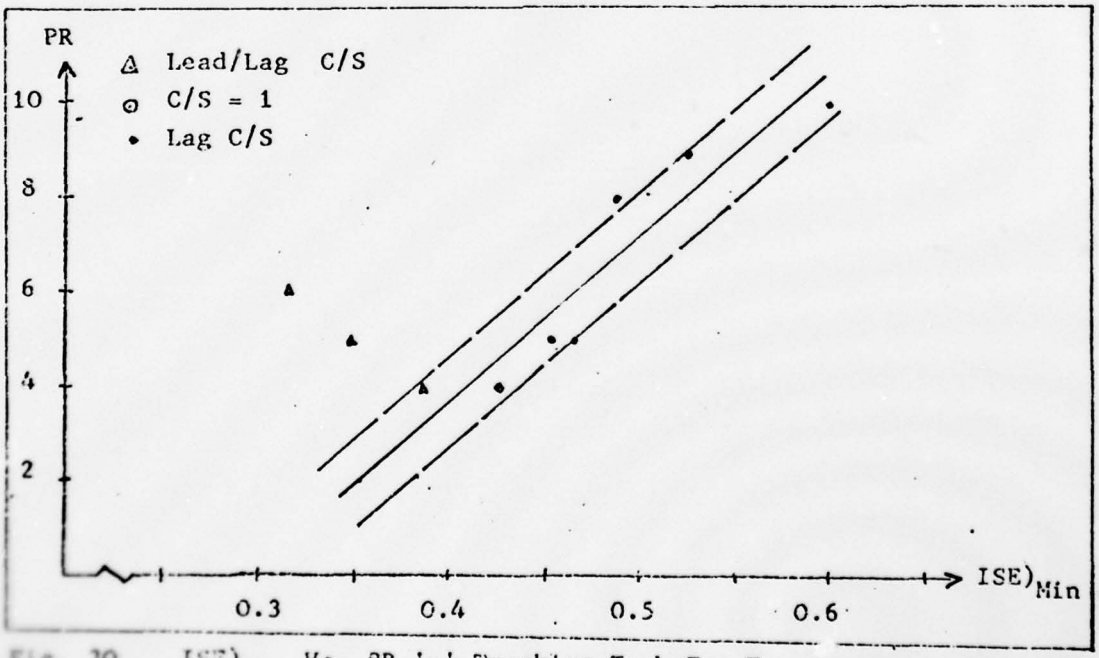

Fig. 30 $ISE)_{Min}$ Vs. PR 'γ' Tracking Task For $T_L = 0.75$
A/C 1 With Control Systems

plots when T_L exceeds 0.75 sec. The addition of lag control system dynamics also results in a system which is more sensitive to gain variations. In particular Fig. 26, the performance curve of aircraft 1 with control system 6, 2/S+2, depicts a very sensitive system. The achievable minimum ISE is also considerably greater than the minimum ISE for the aircraft with the other control systems. Similar results for this aircraft/control system combination were observed in the pitch tracking task and in the open-loop frequency response analysis of Chapter III. Figures 29 and 30 show a plot of minimum ISE versus the PR. The plots show an increase in rating as the performance degrades. The reverse trend for the lead control systems needs further investigation.

Pitch and Flight Path Angle Tracking

The above analyses show that both pitch and flight path angles are important parameters for the pilot during the landing task. The next logical step is to study the effect of feeding back both pitch and flight path angle as a multi-output system for a single input step γ-command. Figure 31 shows a block diagram of the system used for simulation.

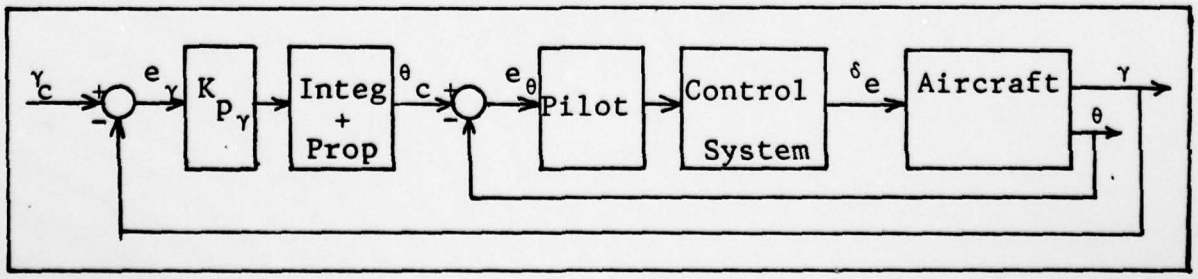

Fig. 31 Both θ and γ Tracking Task For A Step γ-Command

The analysis was restricted to only aircraft 1 and the lag control systems flown with aircraft 1. The short period configuration was used for the aircraft simulation. The 'lead only' form of pilot dynamics was used for the pilot in the pitch loop. Two values of T_L, 0.5 and 0.75 seconds, were used and the corresponding gains K_{P_θ} which minimized the ISE in the pitch tracking task were used. With the inner loop parameters fixed, the closed-loop pitch transfer function forms a type zero system. If only a pilot gain, K_{P_γ}, is used in the outer loop there will always be a steady-state error, e_γ, for a step γ-command input. Therefore, an integral plus proportional control system was used as shown in Figure 31.

It is assumed that the integral plus proportional control represents the pilot in the outer loop. A pilot reaction time delay was not included in the outer loop.

The transfer function used for integral and proportional control is of the form;

$$G(s) = 1 + \frac{a}{s} \qquad (17)$$

Determining the appropriate value of 'a' to be used for the task was the next logical step. Therefore, K_{P_γ} was varied to measure ISE $\int e_\gamma^2$ for a step γ-command while the value of 'a' was varied from 0.1 to 0.4 in steps of 0.05. This proceedure was used for both a T_L of 0.5 and 0.75 seconds for pilot lead in the pitch loop. The data thus generated is

shown in Tables 2 and 3. Since the change in the value of the ISE for 'a' greater than 0.25 was not significant, a value of a = 0.25 was selected and used for subsequent analysis.

The lag control systems flown with aircraft 1 were simulated to study the effect of performance degradation on pilot rating. The values for the variables K_{p_θ}, α, and T_L were discussed above. The outer loop pilot gain K_{p_γ} was varied and the ISE $\int e_\gamma^2$ was recorded for a step γ-command. Figures 32 and 33 show a plot of ISE $\int e_\gamma^2$ versus the K_{p_γ}. The effect of performance degradation on pilot rating can be clearly seen from these plots. Figures 34 and 35 show the plot of minimum ISE $\int e_\gamma^2$ versus the PR for aircraft 1 without the control system and with the lag control systems. These figures also indicate a relationship between PR and performance for a fixed pilot workload.

Comparison of Flight Path Angle Tracking Task With and Without the Inner Pitch Loop

The flight path angle tracking without the inner pitch loop yields a relatively higher value of ISE $\int e_\gamma^2$ as compared to the tracking with the pitch loop. However, the pilot model becomes more complicated for the two loop closure task, in that, in addition to the inner loop lead time and gain which is common to both the tasks, an outer loop gain and integral plus proportional control is required from the pilot.

K_{p_γ}	a = 0.1	a = 0.15	a = 0.2	a = 0.25	a = 0.3	a = 0.35	a = 0.6
	ISE	ISE	ISE	ISE	ISE	ISE	ISE
0.9	-	-	-	-	-	-	0.366
1.0	0.779	-	-	-	-	0.366	0.349
1.1	-	-	0.454	0.41	0.376	0.356	0.362
1.2	0.635	0.51	0.437	0.397	0.373	0.359	0.351
1.3	0.622	0.496	0.437	0.406	0.39	-	-
1.4	0.615	0.51	0.464	0.44	-	-	-
1.5	0.652	0.571	-	-	-	-	-

Table 2 K_{p_γ} Verses ISE For T_{L_θ} = 0.5 - Different Values Of "a"

K_{p_γ}	a = 0.1	a = 0.15	a = 0.2	a = 0.25	a = 0.3	a = 0.35	a = 0.4
	ISE	ISE	ISE	ISE	ISE	ISE	ISE
1.2	-	-	-	-	-	-	0.289
1.3	-	-	-	-	-	0.292	0.281
1.4	-	-	0.354	0.321	0.3	0.287	0.278
1.5	-	0.394	0.344	0.316	0.29	0.288	0.281
1.6	0.477	0.385	0.341	0.317	0.3	-	-
1.7	0.466	0.385	0.347	0.327	-	-	-
1.8	0.468	0.397	-	-	-	-	-

Table 3 K_{p_γ} Verses ISE For T_{L_θ} = 0.75 - Different Values Of "a"

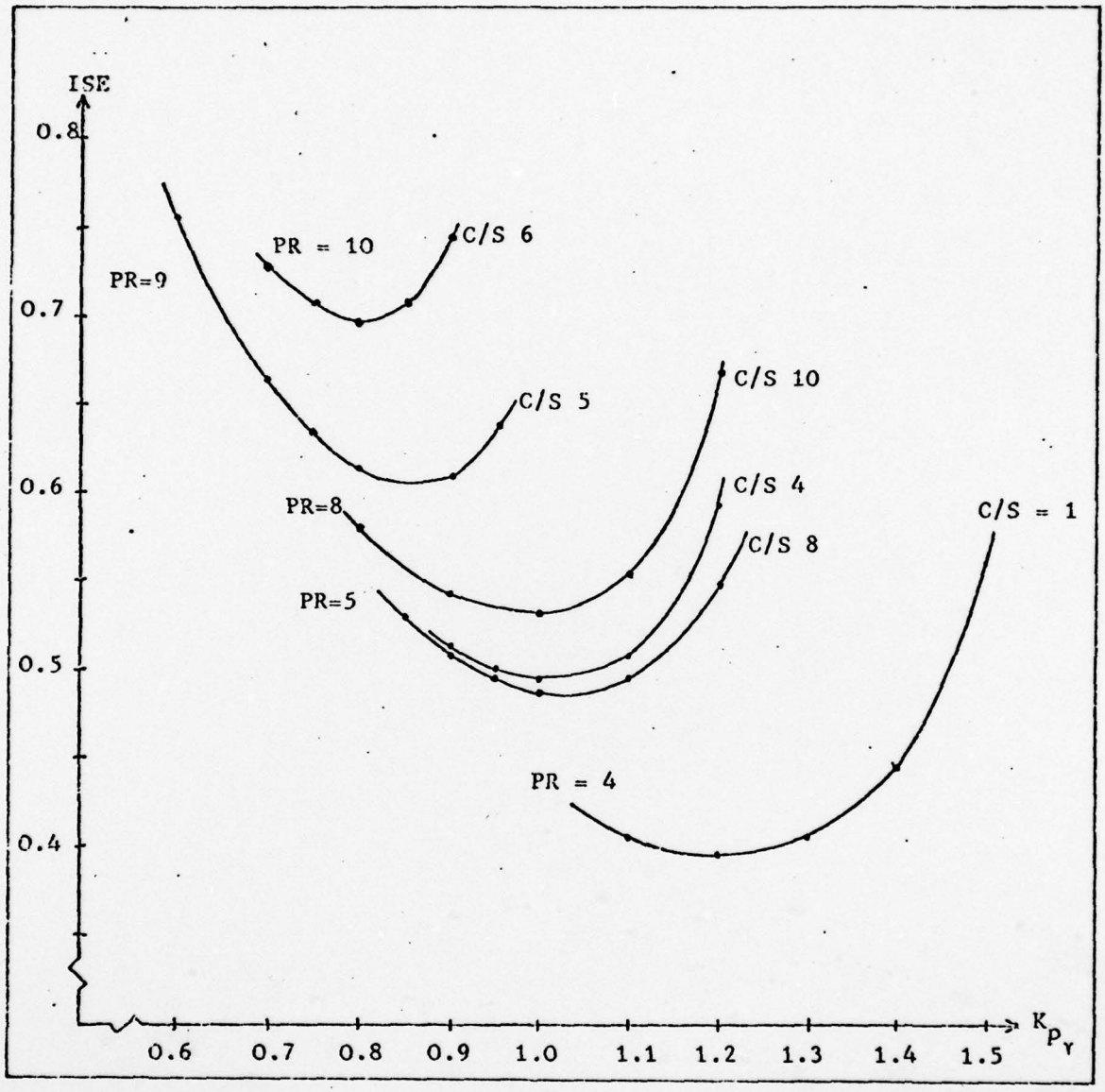

Fig. 32 ISE Vs. K_{p_γ} For T_L = 0.5 Aircraft 1 With Lag C/S - 'θ' And 'γ' Tracking Task

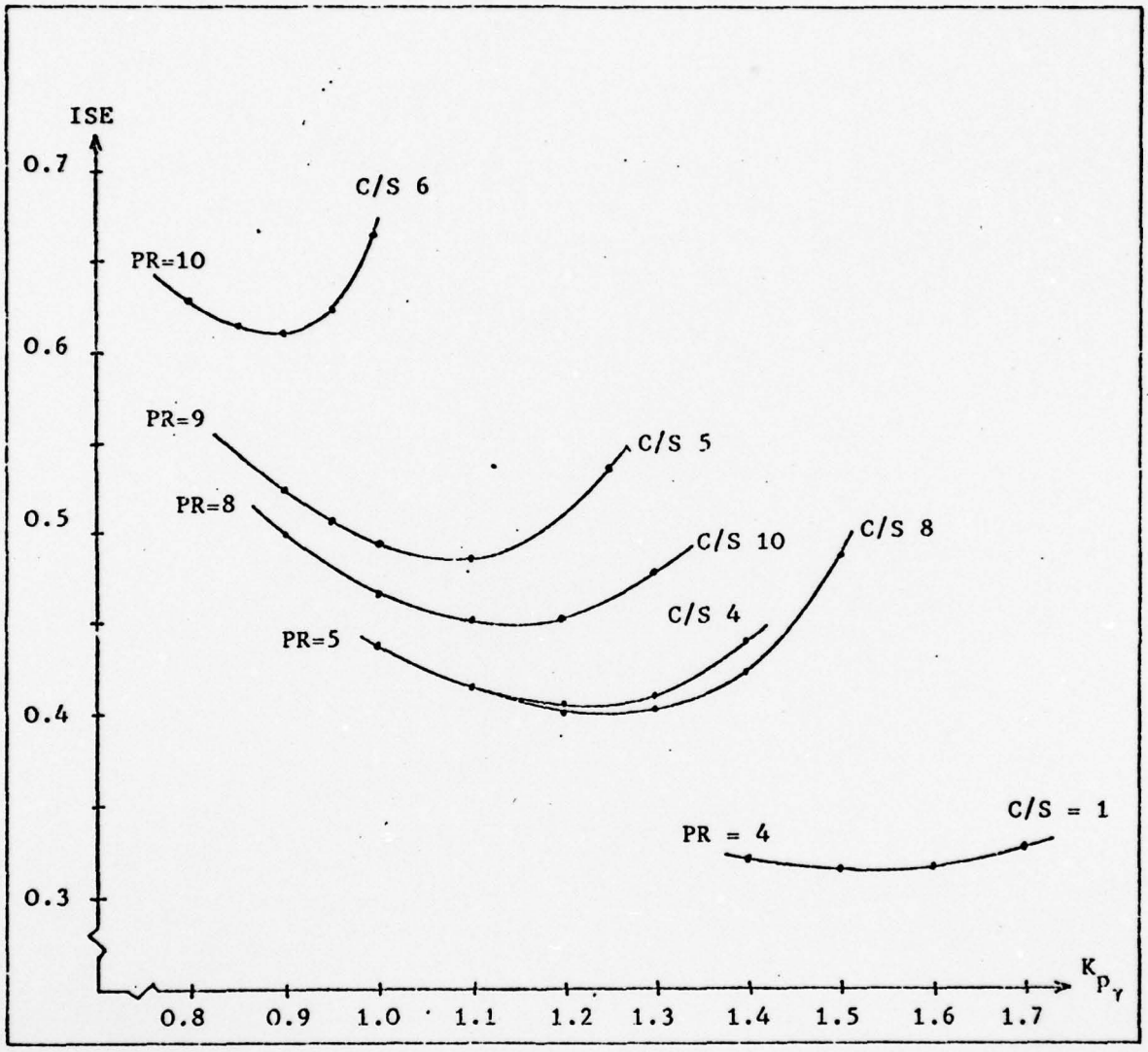

Fig. 33 ISE Vs K_{p_γ} For T_L = 0.75 Aircraft 1 And Lag C/S - 'θ' And 'γ' Tracking Task

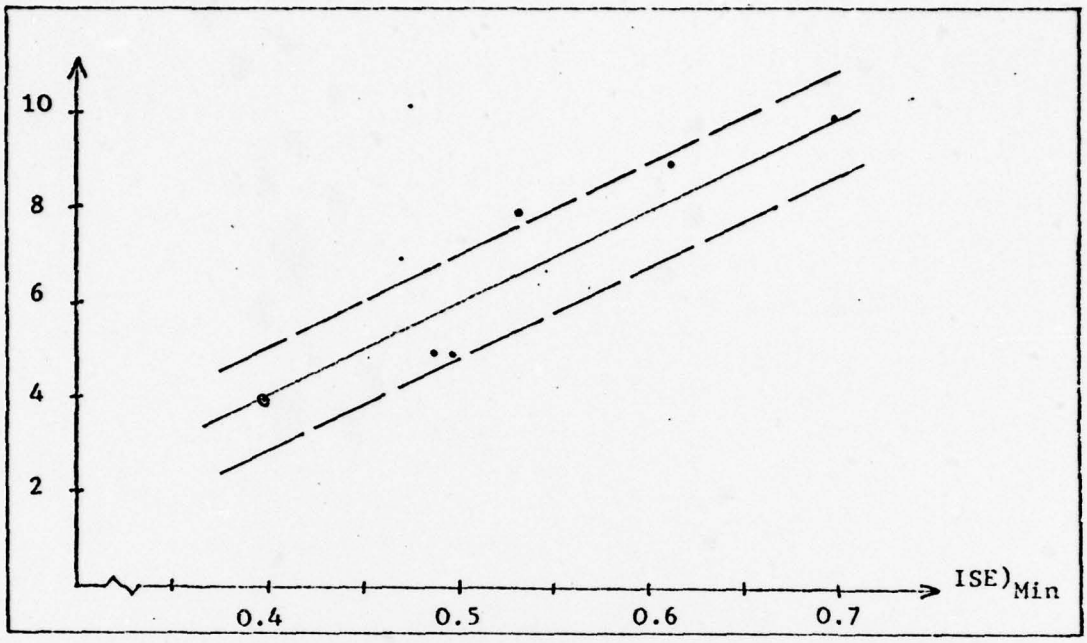

Fig. 34 PR Vs. $ISE)_{Min}$ For T_L = 0.5 Aircraft 1 And Lag C/S 'θ' And 'γ' Tracking Task

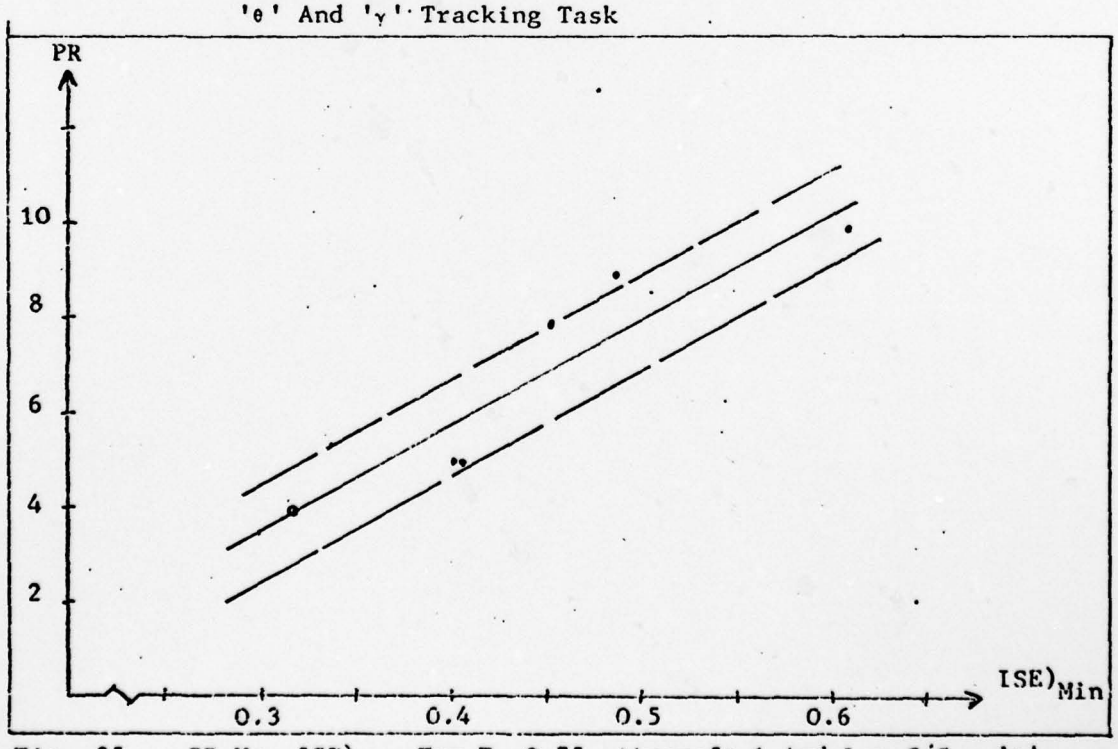

Fig. 35 PR Vs. $ISE)_{Min}$ For T_L=0.75 Aircraft 1 And Lag C/S - 'θ' And 'γ' Tracking Task

The task of integrating an error essentially means remembering the past errors and thus represents an increase in the pilot workload. Whether the pilot would like this kind of additional workload or if the additional workload is worth the improvement in the performance needs to be determined. Also, for a multi-output tracking task, such as the one described here, how the pilot would time share his control of the two outputs θ and γ, needs to be investigated. It may be possible that during the glide slope the pilot is flying the aircraft by tracking only the pitch angle, θ, up to a certain altitude where the rate of sink, $\dot{h}$ becomes important for him. This altitude may be about 100 feet, where the pilot may begin tracking both pitch angle and flight path angle until the flare maneuver. During flare, especially the last 50 feet, the pilot may switch over to tracking only the altitude, assuming that he has done his best to stabilize the θ-loop. A plot of ISE versus K_p is shown in Figure 36 for a pitch loop T_L of 0.5 and 0.75 seconds for the three tracking tasks using aircraft 1 without the control systems.

The above hypothesis, i.e., during approach the pilot is essentially tracking the pitch attitude and during flare and landing phase the pilot is tracking the flight path angle while holding a fixed optimum pitch loop performance may be verified by the following proceedure. The pilot, in a large number of flight configurations flown, evaluated the approach task, and the overall landing task separately and provided

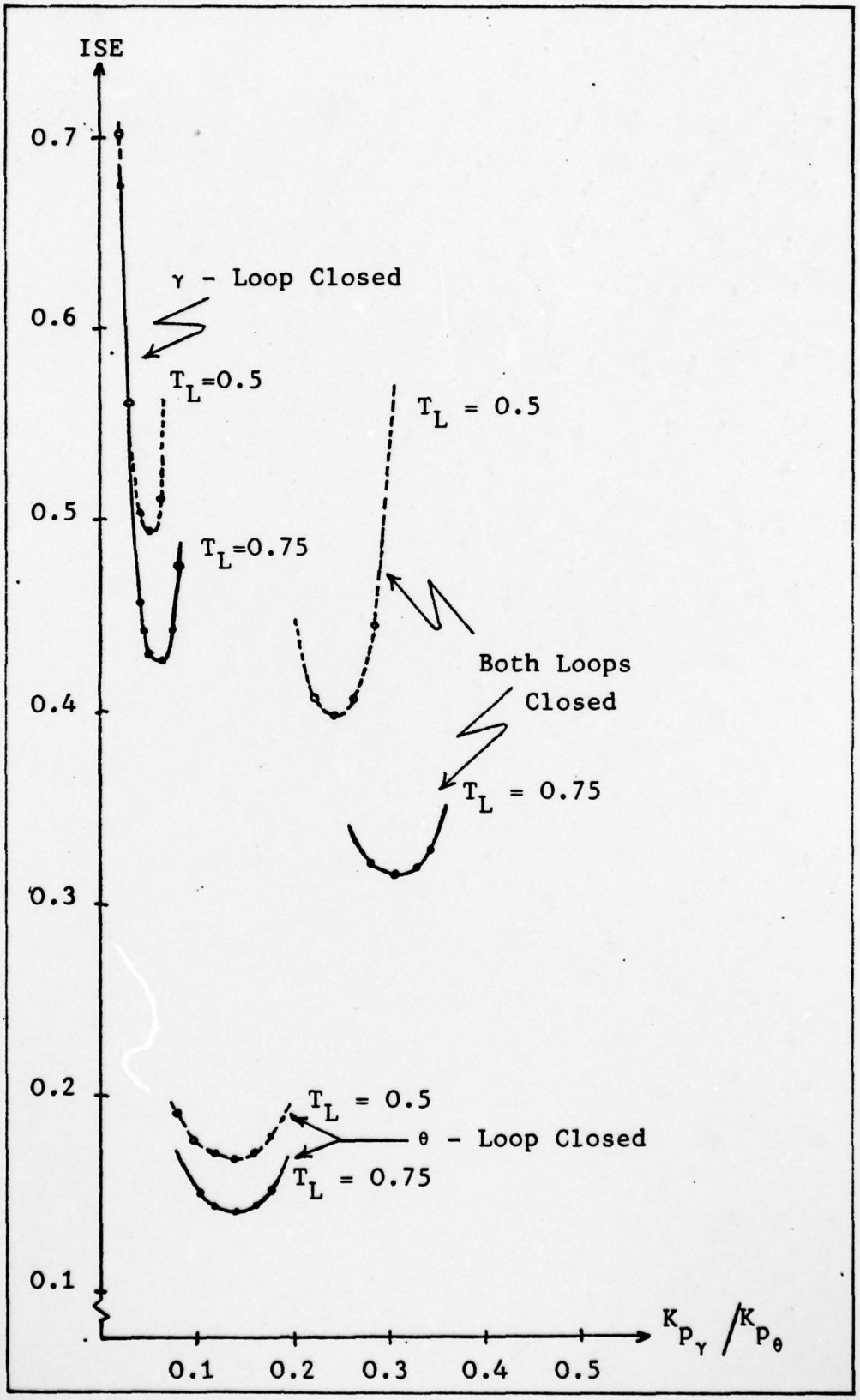

Fig. 36 ISE Vs. $K_{P_\gamma}/K_{P_\theta}$ Aircraft 1 C/S = 1

two different ratings. An optimum pilot workload and performance evaluation can be performed on analog computer. The proceedure described in this chapter and those flight configurations for which both ratings were provided may be used; first as a pitch tracking task, and then as a γ-loop tracking task with the pitch loop optimized as per the first analysis. The results thus obtained can be correlated with the corresponding approach and overall pilot ratings to validate the hypotheses. This analysis was not carried out due to lack of time. The data generated in this chapter is insufficient to draw any positive conclusions about this hypothesis.

Pitch Attitude Tracking For Different Aircraft

The previous analysis is restricted to only Aircraft 1. In order to extend the analysis to aircraft configurations 2,3,4, and 5, it is assumed that the effects of adding control systems will have similar trends as observed for aircraft 1. Therefore only the aircraft short period dynamics are simulated and analyzed without adding the control systems. The analysis is carried out in two phases; 1) closing the pitch loop alone for a step θ-command. 2) closing the γ-loop without closing the pitch loop for a step γ-command. A pilot lead time of 0.5 sec. and 0.75 sec. was selected and the pilot gain K_{p_θ} was varied for each T_L to measure ISE for a step θ-command. The choice of 0.5 sec. and 0.75 sec. lead time is based on the previous analysis of aircraft 1. The values of K_{p_θ} and ISE thus measured for each aircraft are

plotted. Figure 37 shows a plot of ISE versus the pilot gain for the five aircraft configurations with a lead time of 0.5 sec. The figure shows that aircraft 1,3 and 5 are relatively more sensitive to gain variations than aircraft 2 and 4. The values of ω_c and phase margin (ϕ_M) were determined from the Bode plot for the gain, K_{P_θ}, corresponding to the minimum value of ISE. Digital computer program TOTAL was used for this purpose. Table 4 shows the values of ω_c and ϕ_M for each aircraft configuration.

The values of minimum ISE for each aircraft configuration are plotted against PR (Figure 38). While the plot does not show a direct relationship between PR and performance (ISE), a rating expression of the form shown in Eqn. 18 indicates that a linear combination of $\frac{1}{\omega_c}$ and $\frac{1}{\phi_M}$ has a relationship with PR.

$$P.R. = \alpha_1 \frac{1}{\omega_c} + \alpha_2 \frac{1}{\phi_M} \qquad (18)$$

The values of α_1 and α_2 were determined using the method of least squares. the plot of actual versus estimated PR using Eqn. 18 is shown in Figure 39. The above proceedure was repeated for a 0.75 sec. lead time and the data thus generated is plotted. A plot of ISE versus K_{P_θ} is shown in Figure 40. From the figure it can be clearly seen that all aircraft are relatively more sensitive to gain variations as compared to

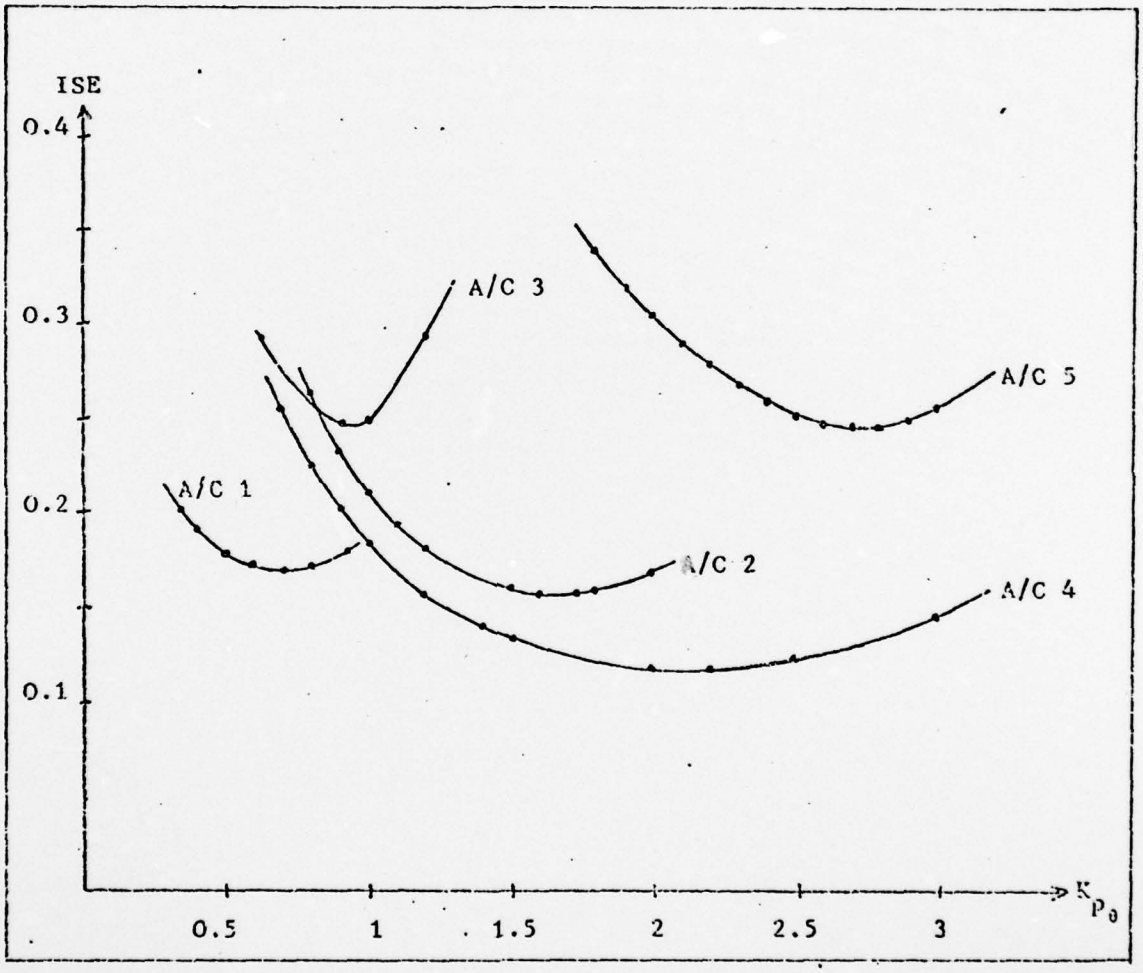

Fig. 37 ISE Vs. K_{p_θ} Pitch Tracking Task – Different Aircraft And C/S = 1 For T_L = 0.5

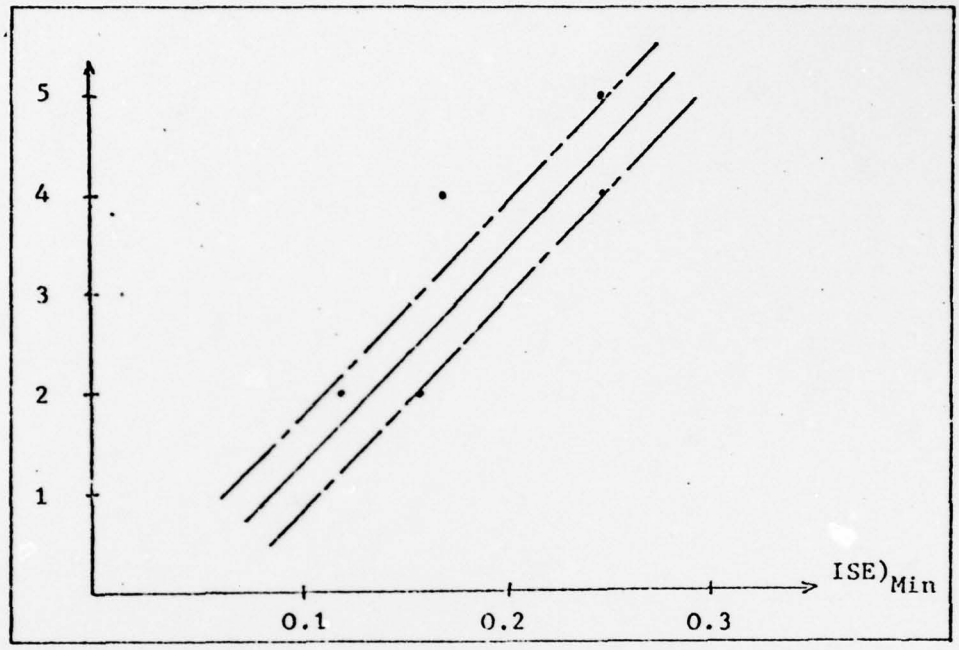

Fig. 38 PR Vs. $ISE)_{Min}$ Different Aircraft Pitch Tracking Task T_L = 0.5 sec.

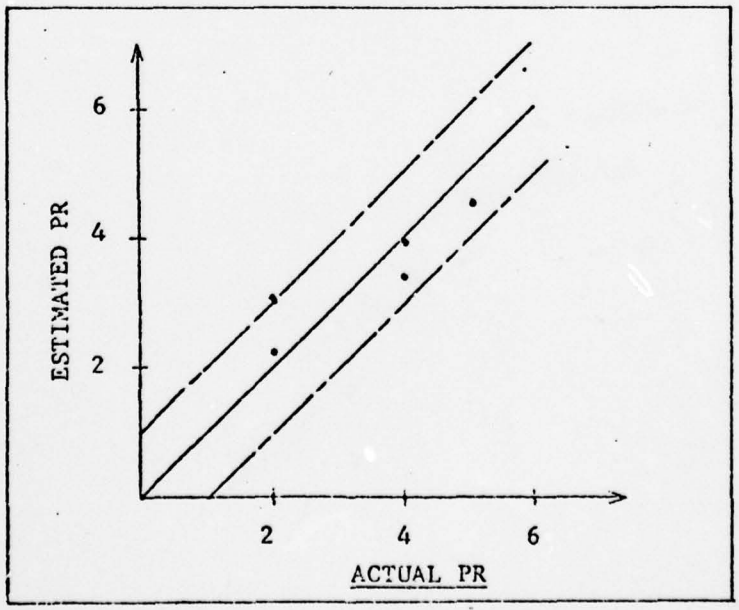

Fig. 39 Estimated Vs. Actual PR Using Eqn. 18 Different A/S 0- Tracking Task T_L = 0.5

AD-A080 519 AIR FORCE INST OF TECH WRIGHT-PATTERSON AFB OH SCHOO--ETC F/G 5/8
ANALYSIS OF THE EFFECTS OF HIGHER ORDER CONTROL SYSTEMS ON AIRC--ETC(U)
DEC 79 M A PASHA

UNCLASSIFIED AFIT/GE/EE/79-27

NL

2 OF 3
AD A080519

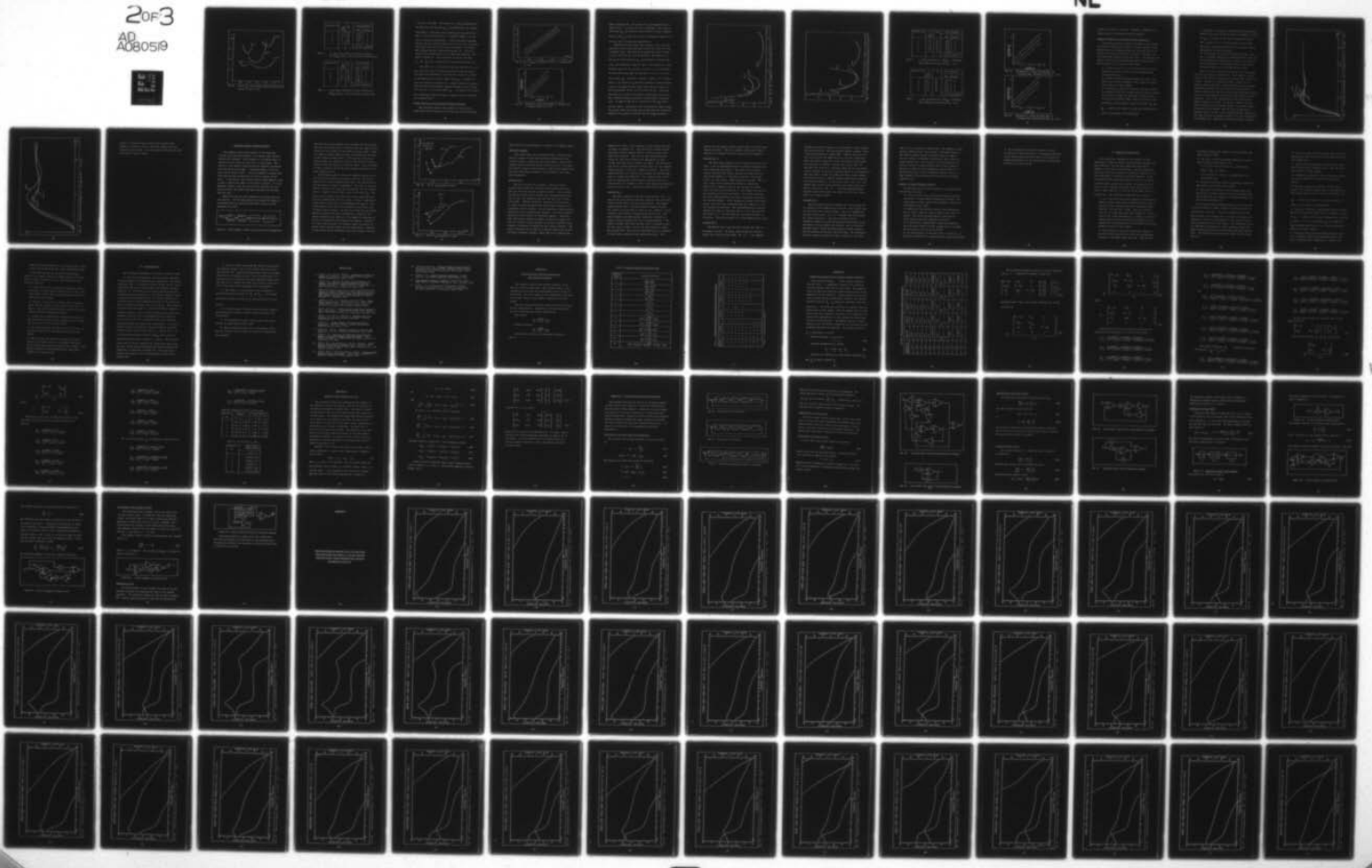

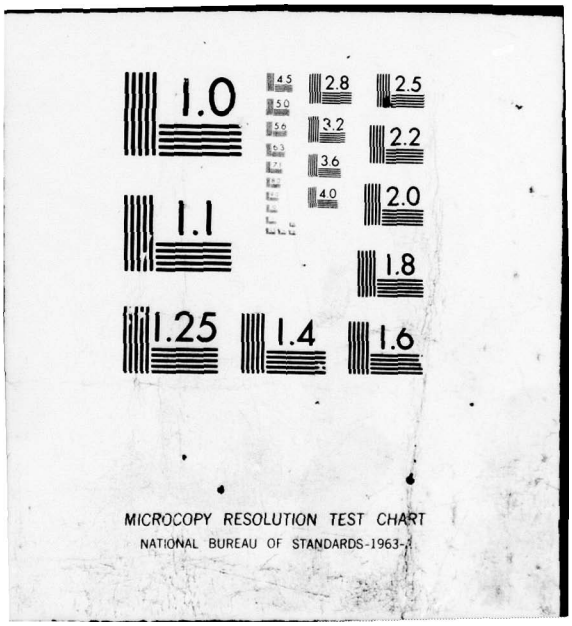
1.0
1.1
1.25
1.4
1.6
1.8
2.0
2.2
2.5
2.8
3.2
3.6
4.0
4.5
5.0
5.6
6.3
7.1
MICROCOPY RESOLUTION TEST CHART
NATIONAL BUREAU OF STANDARDS-1963-A

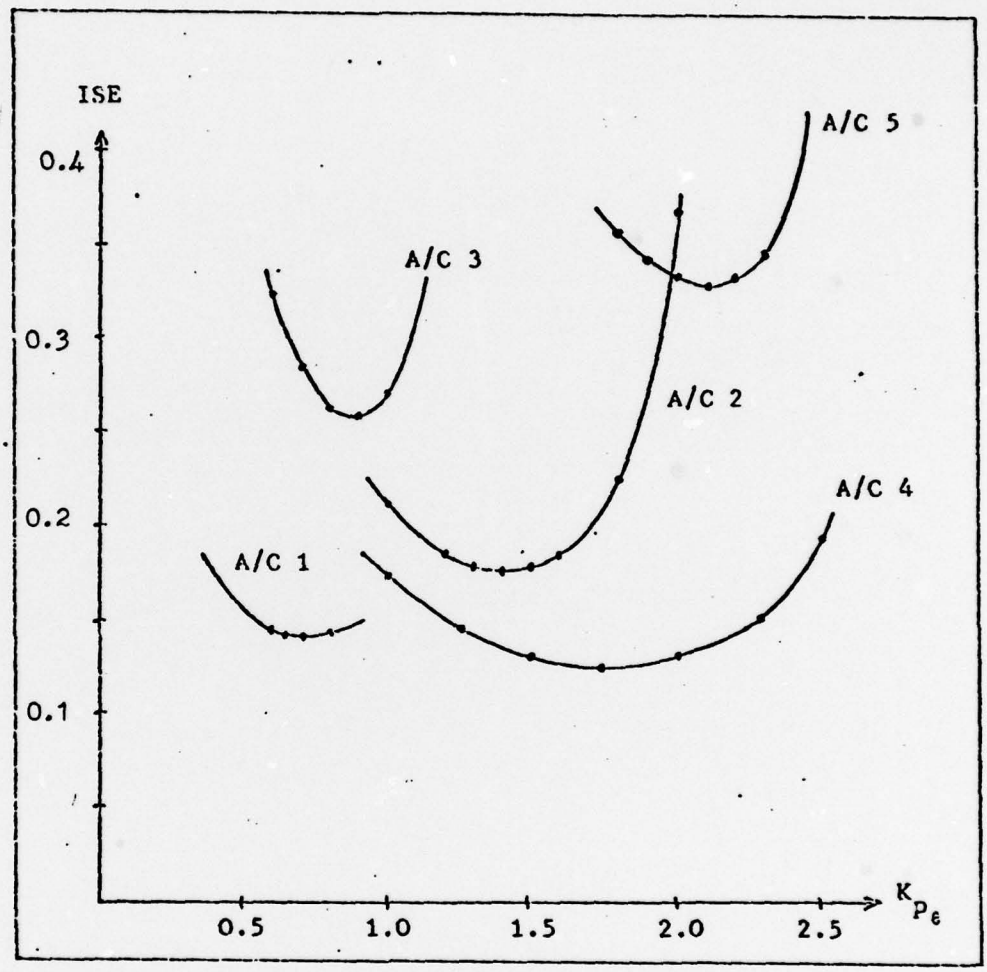

Fig. 40 ISE Vs. K_{P_θ} - Pitch Tracking Task Different Aircraft And C/S = 1 For T_L = 0.75

Aircraft No.	ω_c rad/ sec.	ϕ^o_M	Pilot Ratings	
			Est.	Actual
1	1.8	40	3.38	4
2	3.5	40	3.03	2
3	3	31	3.98	4
4	3	60	2.2	2
5	5.5	25	4.5	5
			α_1=1.29	α_2=106.4

Table 4 ω_c And ϕ_M For Different Aircraft Evaluated At ISE)$_{Min}$ And T_L = 0.5 For Pitch Tracking Task

Aircraft No.	ω_c rad/ sec.	ϕ^o_M	Pilot Ratings	
			Est.	Actual
1	2.1	45	3.46	4
2	4	37	3.1	2
3	3.3	30	3.78	4
4	3.4	60	2.38	2
5	6	20	4.68	5
			α_1=3.42	α_2=82.27

Table 5 ω_c And ϕ_M For Different Aircraft Evaluated At ISE)$_{Min}$ And T_L = 0.75 For Pitch Tracking Task

a 0.5 sec. lead time. The values of ω_c and ϕ_M obtained from the Bode plot for the gain K_{P_θ}, corresponding to the minimum ISE (Table 5), show that with a higher lead time the pilot is able to close the pitch loop at a slightly higher ω_c at the cost of increased sensitivity. A plot of PR versus minimum ISE for the five aircraft (Figure 41) for 0.75 sec. lead time shows that four out of five points are within ±1 PR limits. The estimated PR were evaluated using Eqn. 18. A plot of actual and estimated PR for a 0.75 lead time using Eqn. 18 is shown in Figure 42. From the figure it can be seen that $\frac{1}{\omega_c}$ and $\frac{1}{\phi_M}$ have a proportional relationship with the PR.

The values of ω_c obtained for the five aircraft for a 0.5 sec. lead time and for minimum ISE indicate that the pitch attitude task performance is optimum for a value of ω_c which is approximately one rad/sec higher than ω_{SP}. A similar result was obtained in Chapter III. Another conclusion revealed from the open-loop frequency response analysis is the closure of γ-loop at a ω_c an octave below ω_{SP}. To confirm this result, the closed-loop flight path angle tracking task was simulated as discussed below.

Flight Path Angle Tracking Task-Different Aircraft

The proceedure used for the analysis of closed-loop flight path angle tracking task was the same as for the pitch

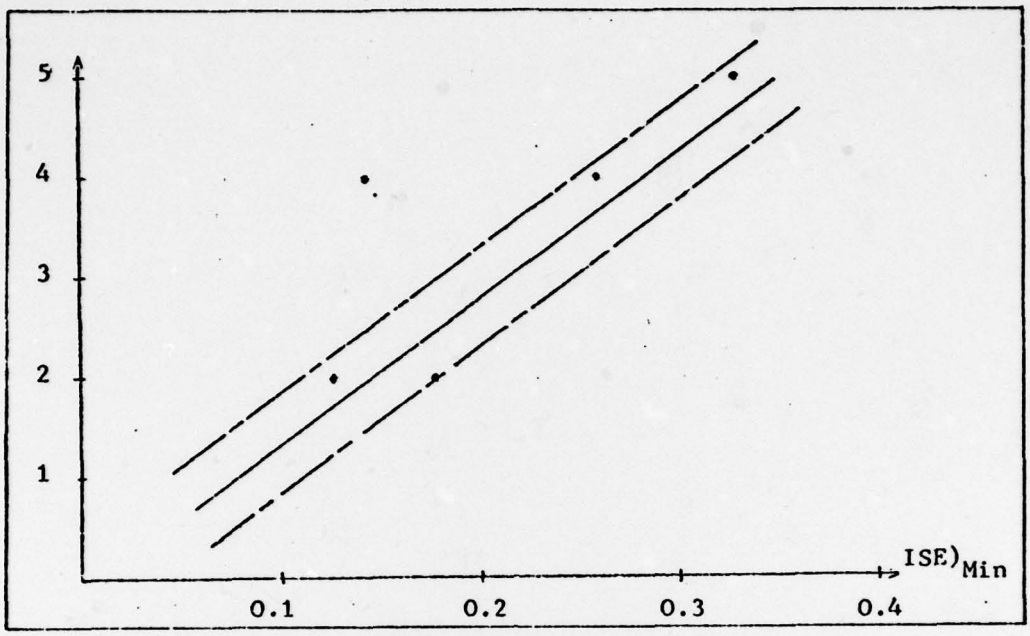

Fig. 41 PR Vs. $ISE)_{Min}$ For Different Aircraft - θ Tracking Task, $T_L = 0.75$

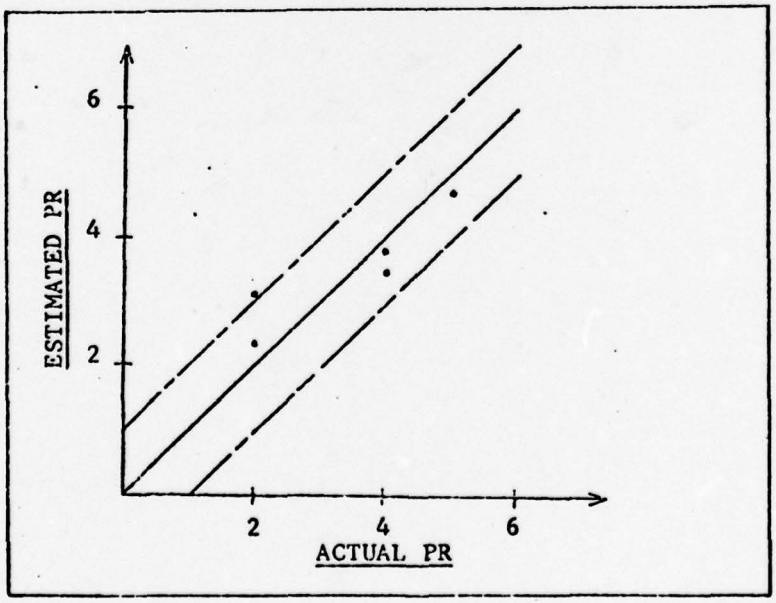

Fig. 42 Estimated Vs. Actual PR Using Eqn. 18 Different A/C θ - Tracking Task For $T_L = 0.75$

angle tracking task. The values of T_L were adjusted to 0.5 and 0.75 sec. to obtain two sets of readings. The value of pilot gain K_{p_γ} was varied to obtain ISE for a step γ-command. The plot of K_{p_γ} versus ISE is shown in Figures 43 and 44, for 0.5 sec. and 0.75 lead time respectively.

Figures 43 and 44 reveal that aircraft 1 and 3 are more sensitive to gain variation than aircraft 2,4, and 5 for the γ-tracking task. The increase in sensitivity with increase in pilot lead time can also be observed. The values of ω_c and ϕ_M were determined for K_{p_γ} corresponding to minimum ISE value and tabulated in Tables 6 and 7. The values of ω_c thus obtained show that for aircraft 1,2 and 4, ω_c is very nearly an octave below ω_{SP} while for aircraft 5, it is 1.5 to 2 octaves below ω_{SP}. Aircraft 3, however, yields ω_c of 2 rad/sec which is the value of ω_{SP} and thus contradicts this guideline. A plot of estimated versus actual PR is shown in Figures 45 and 46 using Eqn. 18 for T_L of 0.5 and 0.75 sec. The plots show that for aircraft 1,2,3 and 4 a correlation exists, but the estimated rating of aircraft 5 needs further investigation. It appears that PR is a function of only $\frac{1}{\phi_M}$ within certain limits. According to this relationship, higher values of ϕ_M will reduce the rating, but we know that the system performance for ϕ_M greater than 80° will be sluggish and the

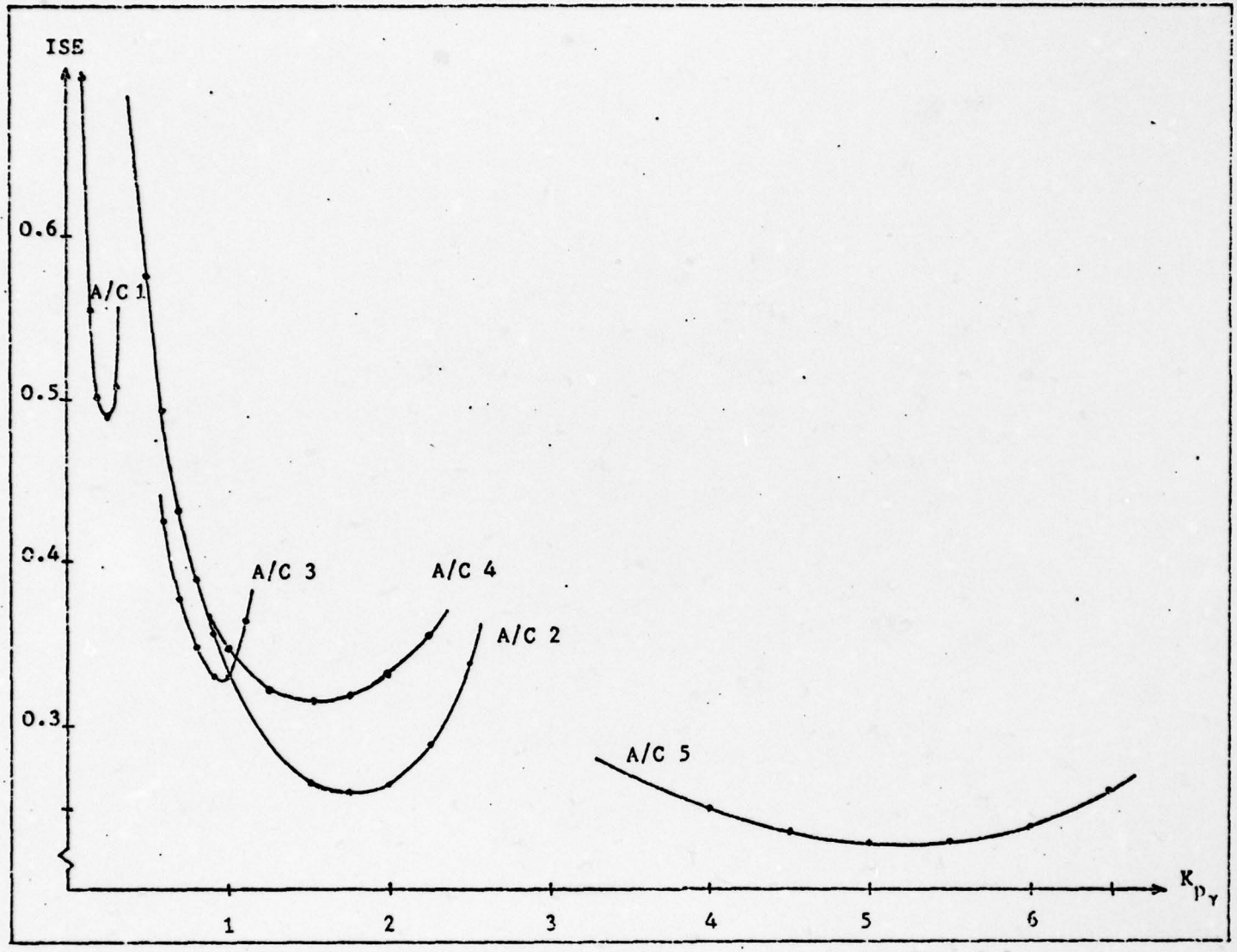

Fig. 43 K_{p_γ} Vs. ISE $_\gamma$- Tracking Task - Different Aircraft For T_L = 0.5

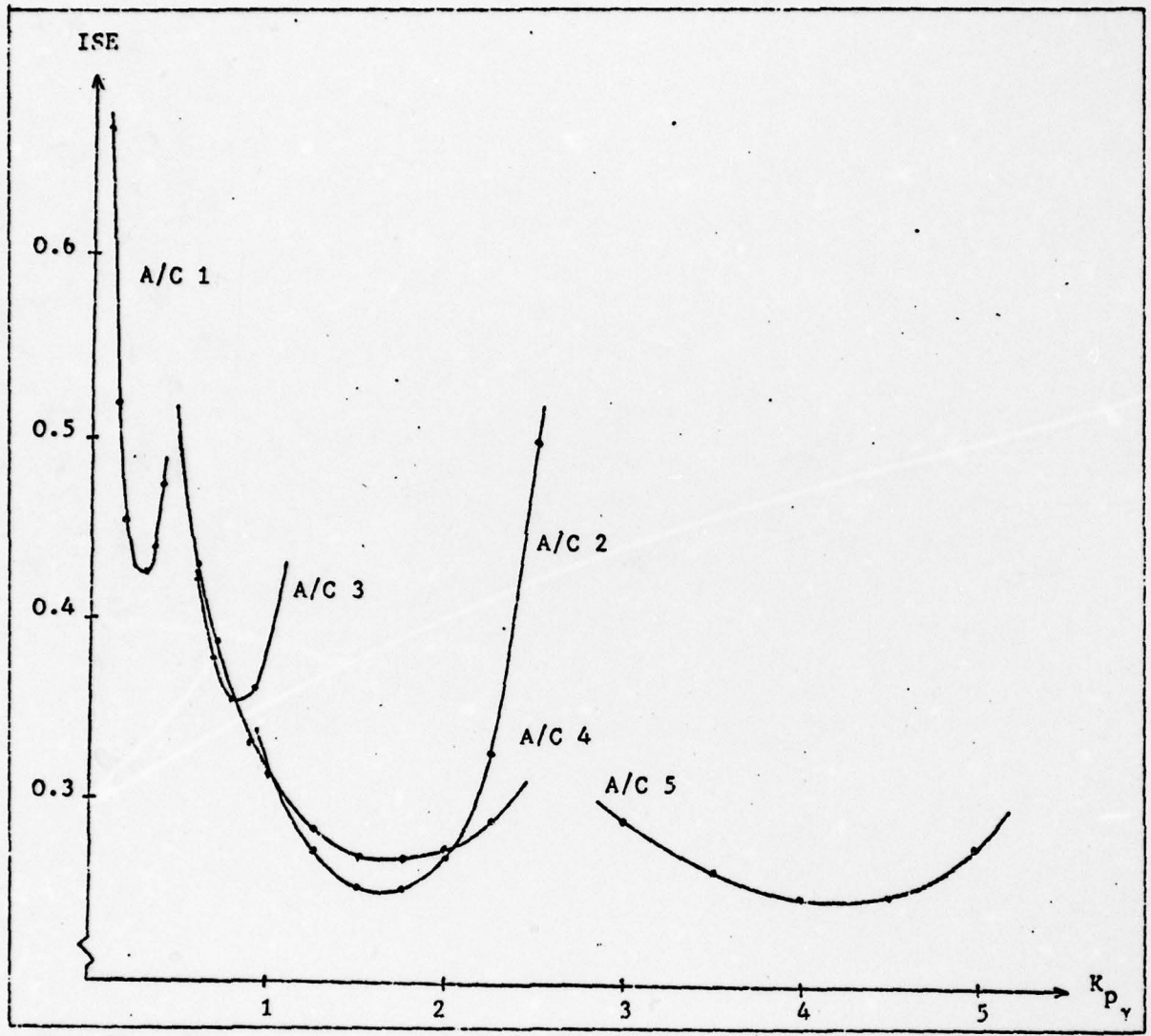

Fig. 44 ISE Vs. K_{p_γ} γ- Tracking Task Different Aircraft For T_L = 0.75

Aircraft No.	ω_c rad/ sec.	ϕ^o_M	Pilot Ratings	
			Est.	Actual
1	0.6	43	4.96	4
2	1.0	66	2.04	2
3	1.9	40	3.49	4
4	0.9	45	3.01	2
5	1.0	80	2.94	5
			α_1=2.6	α_2=26.71

Table 6 ω_c and ϕ_M Evaluated at ISE)$_{Min}$ γ-Tracking Task Different Aircraft With T_L = 0.5

Aircraft No.	ω_c rad/ sec.	ϕ^o_M	Pilot Ratings	
			Est.	Actual
1	0.7	43	4.24	4
2	1.3	66	2.6	2
3	2.0	42	3.34	4
4	1.1	47	3.46	2
5	1.6	80	2.1	5
			α_1=1.04	α_2=118.53

Table 7 ω_c And ϕ_M Evaluated at ISE)$_{Min}$ γ-Tracking Task Different Aircraft With T_L = 0.75

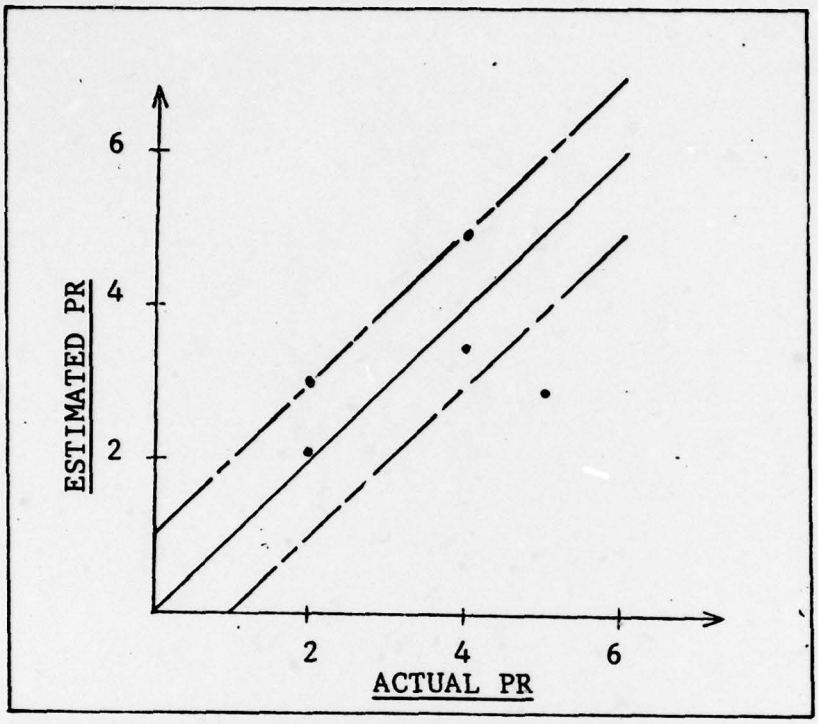

Fig. 45 Estimated Vs. Actual PR Using Eqn. 18
γ Tracking Task Different A/C For T_L = 0.5

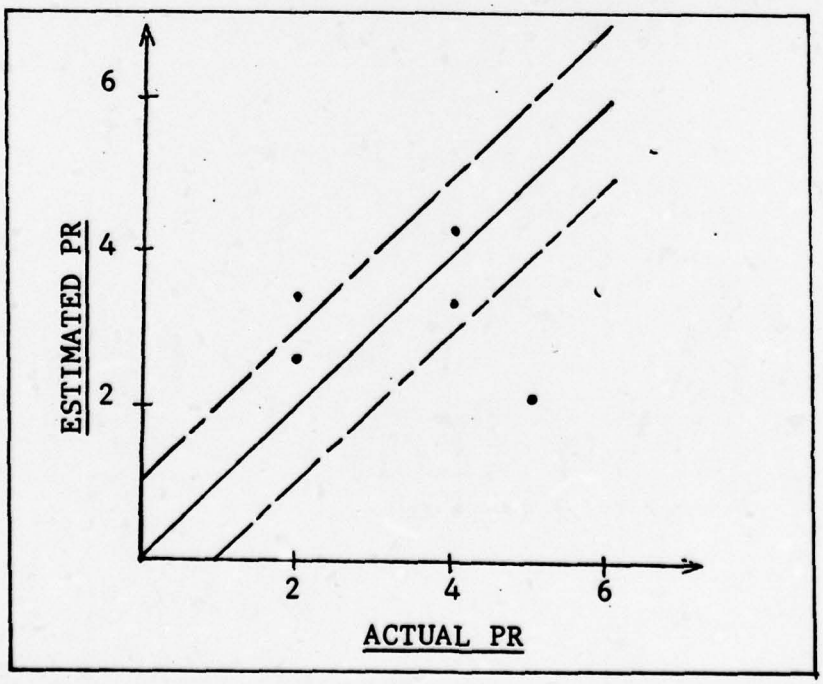

Fig. 46 Estimated Vs. Actual PR Using Eqn. 18
γ Tracking Task Different A/C For T_L = 0.75

ratings are likely to increase. Therfore, a boundary of ω_c and ϕ_M needs to be determined for this analysis.

Summary of Results of Closed-Loop Analog Simulation

The analog simulation studies described in this chapter were based on finding the effects of control systems on the performance, while adjusting the pilot workload (T_L) for an optimum value and then holding it constant. Different aircraft were then analyzed on the same lines. The analysis consisted of both pitch and flight path angle tracking tasks. The following are the results of the study:

1) A lead time of 0.5 to 0.75 seconds seems to be the optimum pilot lead for most of the aircraft-control system combinations.

2) Control systems generating significant lag at the short period natural frequency tend to make the system very sensitive to gain changes.

3) Performance, measured in terms of ISE, has a direct correlation with PR for aircraft with lag control systems.

4) The pilot ratings for different aircraft with no control system dynamics added, shows a correlation with performance measured both in terms of ISE and $\frac{1}{\omega_c}$ and $\frac{1}{\phi_M}$. However, the range of ω_c and ϕ_M in which this result is valid needs to be determined.

5) The pilot, in general, would achieve the best performance if he closes the pitch loop at a frequency ω_c equal to ω_{SP} + 1 rad/sec for the pitch tracking task alone and ω_c equal to 1 to 1.5 octave below ω_{SP} for flight path angle tracking task alone for all aircraft without the addition of control systems.

6) Closing both the pitch and flight path angle loops for a γ-command, improves the performance but at the cost of increased pilot compensation. However, the relative merits and demerits of closing only the γ-loop versus closing the pitch and γ-loop need further study.

Some of the conclusions drawn from this study do support the earlier analysis of Chapter III. Both chapters concentrate on the effects of performance and work load on the pilot ratings. However, no attempt was made in either of the analyses which would help in understanding the pilot comments associated with each aircraft control system flown (Ref 1). The only observation made during the closed-loop pitch tracking task is the noticeable initial delay in the closed-loop time histories. Some of the representative time histories are shown in Figures 47 and 48. The pilots' comments indicate that the initial pitch attitude response, oscillatory nature of aircraft pitch response, and the final (steady state) response seem to be some of the aircraft behavior characteristics that the pilot is paying attention to in the execution of the landing task. Therefore, an open-loop impulse response

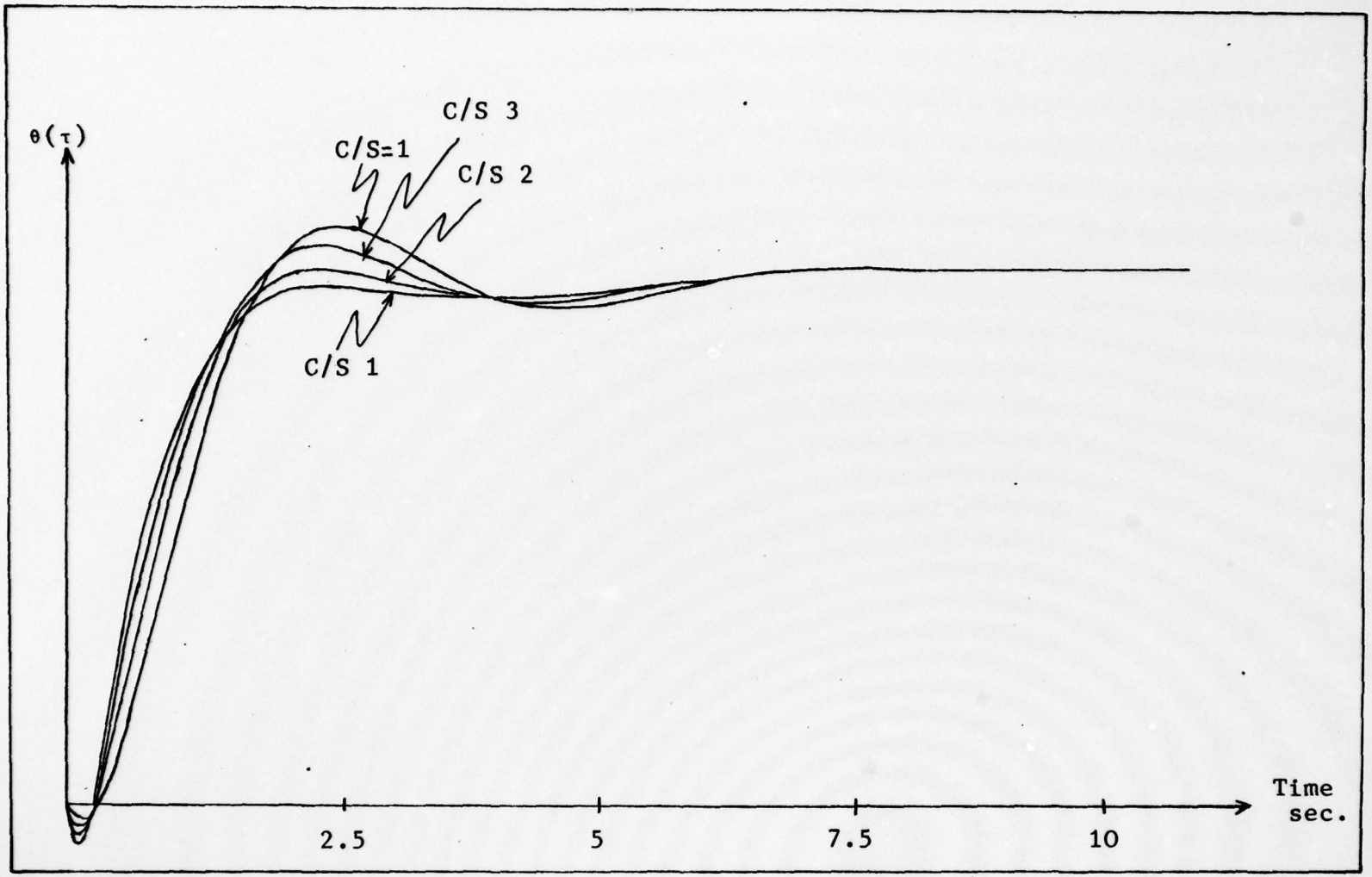

Fig. 47 Closed-Loop Pitch Response A/C 1 and Lead C/S For T_L = 0.5 and τ = 0.3

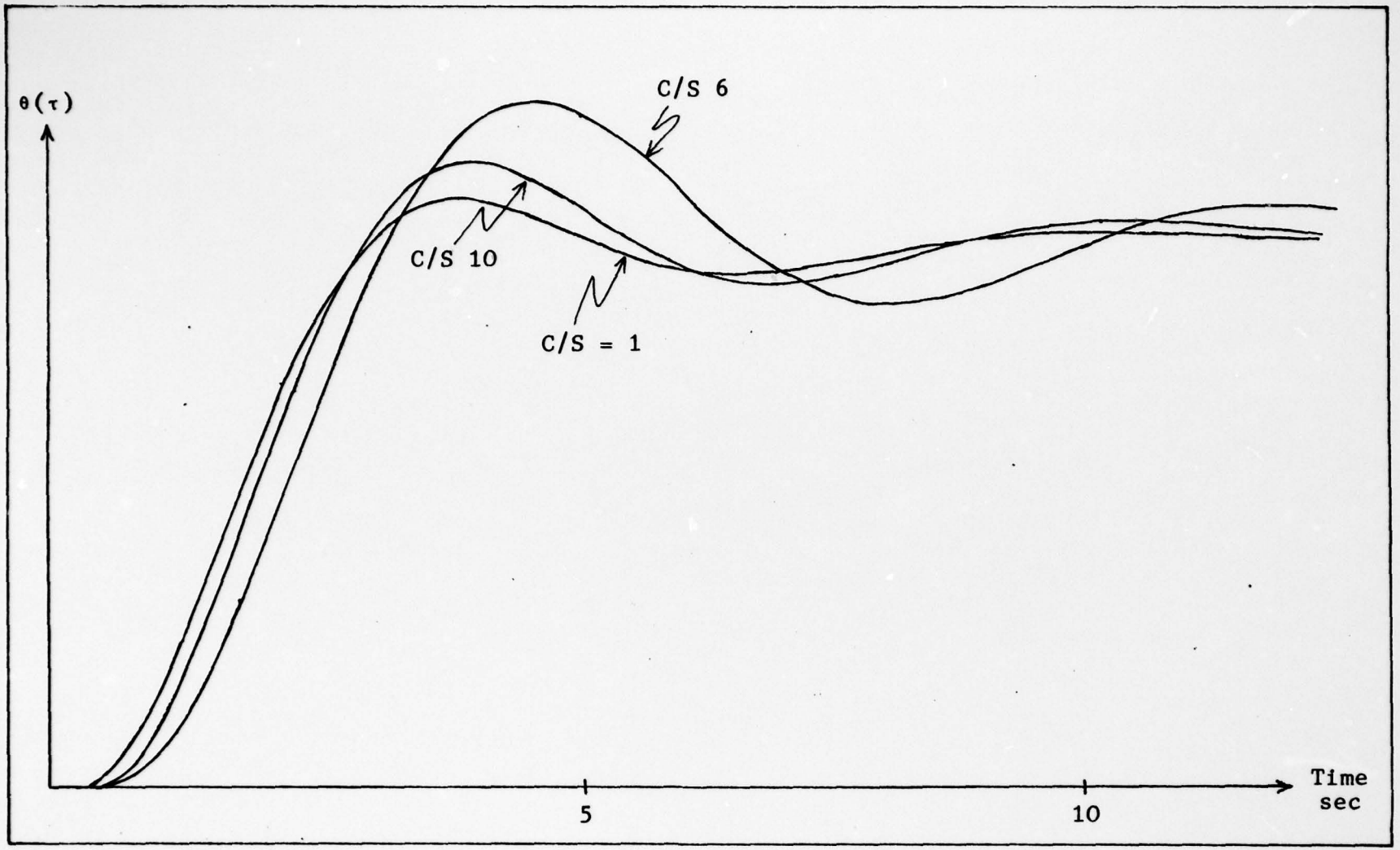

Fig. 48 Closed-Loop Pitch Response A/C 1 And Lag C/S For τ = 0.3 sec.

study is carried out using aircraft short period pitch dynamics to correlate some of the pilot comments with the aircraft pitch attitude. The next chapter describes the open-loop impulse response study.

V Open-Loop Impulse Response Analysis

This chapter presents the analysis of the open-loop aircraft pitch attitude response to an impulse input and the results thus obtained. Pitch response to an impulse input is identical to the study of pitch rate to a step input. This portion of the analysis resulted from the comments provided by the pilot after each flight. A detailed summary of the comments can be found in Ref 2. From the comments it appears that the pitch attitude response was one of the concerns of the pilot. In particular, the initial pitch attitude behavior seems to have a significant impact on the pilot's opinion. It is emphasized, however, that the initial pitch attitude will also directly affect the flight path angle and hence the altitude and sink rate.

Figure 49 shows the block diagram of the system used for the analysis. For the same reasons as discussed in Chapter II, the phugoid mode was ignored and the short period aircraft equations were used.

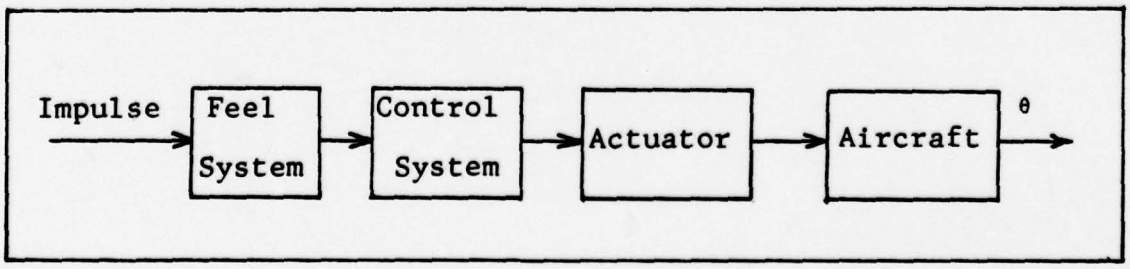

Figure 49 Block Diagram of Open Loop Aircraft C/S Configuration

The feel and actuator dynamics were included for this analysis while the pilot block was not included since the study was concerned with the behavior of the system to pilot inputs. Digital computer program TOTAL was used to both generate and analyze the impulse response plots. From the plots the initial pitch response was studied in terms of time taken for the sy-system to reach ten percent of the final value. Also an attempt is made to explain some of the pilot comments based on the impulse response plots.

The procedure used for the pitch response analysis was to plot the pitch attitude to an impulse input for all the aircraft-control system configurations flown. The selected plots thus generated are shown in Appendix F. The time to reach ten percent of final value (T_{10}) was recorded for all the configurations. Figures 50 and 51 show a plot of PR versus T_{10}. The plots clearly indicate that the pilots always liked the basic aircraft configuration (control system = 1) best. Addition of either lead or lag control system degraded his opinion. This trend indicates that the pilot anticipates a particular kind of initial pitch response. Any deviation from this anticipated behavior surprises the pilot causing him to adjust to the actual response he has observed. This degree of adjustment on his part is reflected in his opinion and comments. Addition of a lead control system, for instance, makes the initial response faster and more abrupt than his expectation. Addition of lag control system introduces significant amount of initial

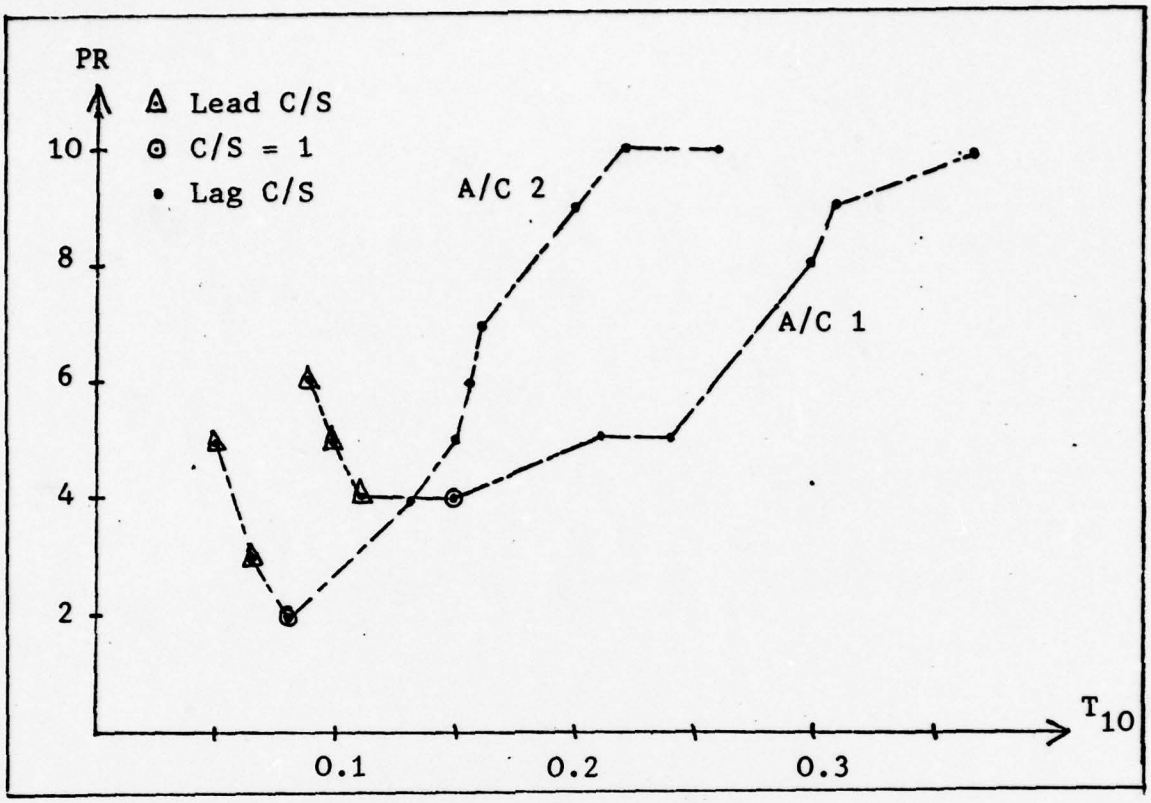

Fig. 50 PR Vs. T_{10} Aircraft 1 and 2

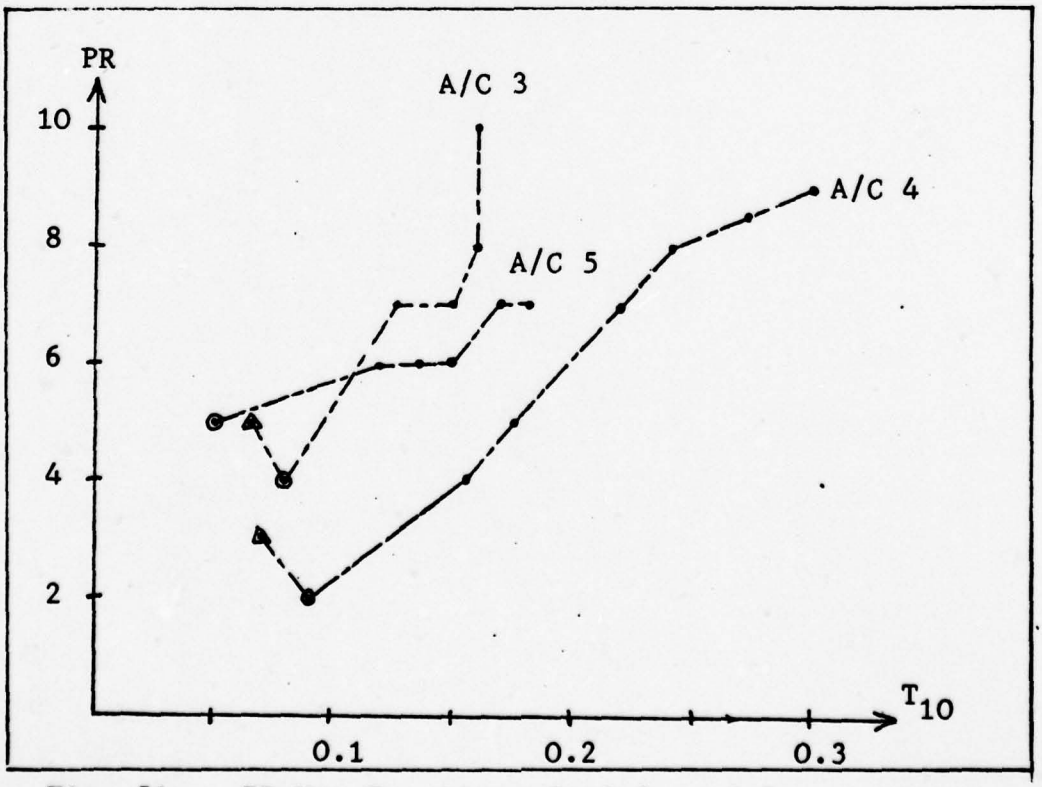

Fig. 51 PR Vs. T_{10} Aircraft 3,4, and 5

delay before the system begins to respond to the impulse input.

The Pilot Comments

After each flight test performed in Ref 2, the pilot was asked to comment on the initial and the steady-state pitch attitude response, especially the initial delay. Many of the comments made by the pilot can be clearly observed in the open-loop impulse response time histories. Some of the comments and the associated impulse responses are described in the subsequent paragraphs.

Aircraft No. 1

The pilot comments for aircraft 1 with lead control systems indicate that the "initial pitch response was reasonable, but the final response tended to drift". The corresponing impulse response plots indicate that the duplicating time (T_D) is about one second but the settling time (T_s) is about 4.8 seconds (Figures F1,F2,F3). The pilot has the ability to reduce the gain and adjust the initial fast response to an acceptable initial response. But the reduction in gain directly affects the final (steady-state) response. The pilot commented about this final response as "drifting tendency". Therefore, when lead control systems are added, if the pilot adjusts the gain for a better initial response, he notices a drifting final response, he observes an abrupt and fast initial response. The pilot, therefore, has to work for a balance between the initial and final acceptable response, which adds to his workload and

degrades his rating. This tendency is very clearly observed in Figure 47 (Chapter IV). The lead control systems providing faster initial response exhibit a reverse trend in the final pitch response. This was the only observation made during the study which explains the degradation in pilot ratings when lead control systems were added. The addition of lag control systems produces an initial delay in the response ranging from 0.1 to 0.15 sec (Figures F5,F6,F7). The pilot complained about the "initial slow response and unpredictable final or steady-state behavior." As a result of the initial lag and unpredictable final behavior, the pilot also complained about the "tendency to PIO" (Pilot Induced Oscillations). An initial delay, thus, causes poor predictability and PIO.

Aircraft No. 2

The pilot comments for the base line aircraft (c/s = 1) and aircraft with control system No.3 indicate that the "pilot enjoyed flying" these aircraft configurations. The impulse response plots show a very good response (Figures F9,F10). The response settling time is about 3.2 sec. However, a large overshoot exists which is being ignored by the pilot. The pilot comments concerning control system No.1 indicate an "abrupt initial response" and "lack of predictability." The impulse response shows that the peak value is reached in only 0.4 sec, while it takes 3.9 sec. for the response to settle down (Figure F8). This lack of predictability due to addition of lead control system has been explained earlier. The

addition of lag control systems clearly shows an initial delay (Figures F11,F12). The pilot comments reflect the "initial delayed pitch response" and the associated "PIO tendency."

Aircraft No. 3

The short period damping ratio of aircraft No.3 was 0.25. Since it was an underdamped system the impulse responses were slowly decaying oscillations. The pilot in his comments clearly indicated this dynamic behavior by saying "oscillatory pitch response" or "looseness in pitch." One of the pilots, for some reason, liked flying this aircraft (PR = 2) with a lead control system (No.3) which is surprising (Figure F13). However, this was one odd case, as another pilot rated the same aircraft as 5. All flights with lag control systems were rated 7 and above. For all the lag cases the pilot complained about the initial lag, poor predictability, and PIO tendency. After flying the aircraft with control system 5 the pilot even commented about his inability to control quickly and precisely. The corresponding pitch response (Figure F15) shows a large peak time (1.1 sec.) and settling time (8.87 sec.). He also noted the "aircraft bouncing" in turbulance. This was obviously due to poor damping ratio (ξ_{SP}).

Aircraft No. 4

The damping ratio (ξ_{SP}) for this aircraft was 1.06, an overdamped aircraft. The pilot liked flying this aircraft without any control systems added (PR = 2) . His comments

indicate good initial response, no PIO tendency, and no problem with predictability. The corresponding impulse response, shows a smooth pitch behavior (Figure F18). However, when lead control system (no.3) was added and flown, the pilot complained about the initial response as "fast and abrupt," which caused minor problems in landing. However, his rating (PR = 3) indicates that while he is concerned about the fast and abrupt initial response, he does not seriously object to it (Figure F17). When lag control systems were added and flown, he did comment about delayed initial response, reduced predictability and the resulting PIO tendency. In one of the cases (c/s = 12) his comment about initial pitch response read, "Felt like it was glued in concrete," (PR = 9) . The corresponding impulse response (Figure F20) shows that, there is a 0.15 sec. delay before the response begins.

Aircraft No. 5

The short period natural frequency for this aircraft was 3.9 rad/sec and the damping ratio was 0.54. This aircraft was not flown with lead control systems. The pilot comments for the base line aircraft (c/s = 1) indicate that the aircraft was "overly sensitive." The pilot noticed an initial "bobbling tendency" in pitch and expressed uncertainty in predictability of the steady-state response. One of the pilots observed "Quick, abrupt and objectionable" initial response and PIO tendency during flare and touch down. The corresponding pitch impulse response plot shows a 0.06 sec. rise time

and 2.7 sec. settling time (Figure F22). The addition of lag control systems did not seem to cause a noticeable delay in the initial response except for control system 13, where a 0.15 sec. delay is noticeable followed by a fast rising response (Figure F25). This tendency is also reported by the pilot as "initial response delayed, then a fast response." The pilot ratings for all configurations varied from 5 to 7 which indicate that it was a difficult aircraft to fly. A high frequency PIO was observed by the pilot in all flight configurations.

Summary of Impulse Response Analysis

The aircraft pitch attitude response to an impulse input revealed the following:

1) Pilots seem to like a particular transient response. Any faster or slower behavior degrades his rating. The exact nature of this initial pitch response could not be identified in this study.

2) Addition of lead control systems, while providing a faster initial response, cause a drift in the final response. This pitch attitude behavior increases the pilot workload and hence degrades his opinion.

3) Initial delay, unpredictable steady-state behavior, and oscillatory nature of pitch response due to low damping ratio seem to be the causes of PIO.

4) An initial delay, on the order of 0.1 to 0.15 sec. in the pitch response will in general yield a poor pilot rating.

5) The time taken for the pitch response to reach ten percent of the final value is a reasonable indication of the initial delay and may be used as an estimate in predicting deviations in the expected pilot rating with reference to a known rating.

VI Summary and Conclusions

The conclusions, supported by the analysis of data generated by using the aircraft-control system configurations from reference 2 and the three approaches described in Chapters III,IV and V are summarized. The three approaches did reveal that pilot ratings are certainly a function of system performance, sensitivity, and pilot workload. In the first approach the system performance in terms of ω_c and ϕ_M is held constant and the pilot opinion is analyzed with respect to pilot workload and system sensitivity measured in terms of phase angle at ω_c and slope of the phase curve at ω_c respectively. The conclusions drawn from this study are:

1) For a particular cross-over frequency (fixed performance) the phase angle (pilot workload) and the slope of the phase curve (system sensitivity) correlated reasonably well with the pilot rating. This was especially true for the flight path angle data (Figure 5). Inclusion of the system performance as a variable in the pilot rating expression may provide better correlation. An approach for accomplishing this is described in the recommendation section of this report.

2) The deviation in the pilot rating with respect to the best rating correlated well with the corresponding deviation in the phase angle and slope. This was true

for both the pitch angle (Figure 4) and the flight path angle (Figure 6) data.

3) The pilot can obtain good phase margin for aircraft with no control system dynamics if,

a) He closes the pitch loop at ω_c approximately equal to $(\omega_{SP} + 1)$ rad/sec.

b) He closes the γ-loop at ω_c approximately one octave below ω_{SP}.

4) Aircraft with control systems introducing significant lags around ω_{SP} will have poor ratings.

5) The degree of correlation between phase angle data and the pilot ratings indicate that the pitch and flight path angles seem to be important tracking parameters for pilots during landing task.

In the second approach optimum values of pilot lead time T_L were determined by analog simulation studies using ISE as a performance critierion. The pilot workload (T_L) was then held constant at the optimum value, and the pilot opinion was studied as a function of performance of the aircraft-control system configurations for step inputs. The closed-loop system was simulated and analyzed as a pitch tracking, flight path angle tracking, and both pitch and flight path angle tracking tasks. The conclusions drawn from the results of the simulation are:

1) A lead time of 0.5 to 0.75 seconds seems to be the optimum pilot lead for most of the aircraft-control system combinations.

2) Control systems generating significant lag at the short period natural frequency tend to make the system very sensitive to gain changes.

3) Performance, measured in terms of ISE, has a direct correlation with PR for aircraft with lag control systems.

4) The pilot ratings for different aircraft with no control system dynamics added, shows a correlation with performance measured both in terms of ISE and $\frac{1}{\omega_c}$ and $\frac{1}{\phi_M}$. However, the range of ω_c and ϕ_M in which this result is valid needs to be determined.

5) The pilot, in general, would achieve the best performance if he closes the pitch loop at a frequency ω_c equal to ω_{SP} + 1 rad/sec for the pitch tracking task alone and ω_c equal to 1 to 1.5 octave below ω_{SP} for flight path angle tracking task alone for all aircraft without the addition of control systems.

6) Closing both the pitch and flight path angle loops for a γ-command, improves the performance but at the cost of increased pilot compensation. However, the

relative merits and demerits of closing only the γ-loop versus closing the pitch and γ-loop need further study.

In the third approach the aircraft pitch attitude response to an impulse input was studied using the aircraft-control system combinations flown. The conclusions drawn from this study are:

1) Pilots seem to like a particular transient response. Any faster or slower behavior degrades his rating. The exact nature of this initial pitch response could not be identified in this study.

2) Addition of lead control systems, while providing a faster initial response, cause a drift in the final response. This pitch attitude behavior increases the pilot workload and hence degrades his opinion.

3) Initial delay, unpredictable steady-state behavior, and oscillatory nature of pitch response due to low damping ratio seem to be the causes of PIO.

4) An initial delay on the order of 0.1 to 0.15 sec. in the pitch response will in general yield a poor pilot rating.

5) The time taken for the pitch response to reach ten percent of the final value is a reasonable indication of the initial delay and may be used as an estimate in predicting deviations in the expected pilot rating with reference to a known rating.

VII Recommendations

The following recommendations are made for further study.

1) The first two approaches used for analysis assumed a fixed performance and fixed workload respectively. The results did reveal that A) correlation exists between PR and, system sensitivity and pilot workload (open-loop frequency response anslysis) B) correlation exists between PR and performance (closed-loop analog simulation). An alternate approach, which is essentially combining the two, is to first simulate each aircraft-control system configuration flown on the analog computer to determine optimum values of T_L and K_p. Then determine the phase angle and slope at ω_c from the open-loop frequency response analysis. Thus for each aircraft-control system configuration there will be a corresponding set of values for T_L, ω_c and ϕ_M, and $\delta\phi/\delta\omega$, representing the pilot workload, system performance and sensitivity respectively. A linear regression analysis may then be carried out between the pilot ratings and the sets of values for T_L, ω_c and ϕ_M, $\delta\phi/\delta\omega$. As an alternate the measured value of $ISE)_{Min}$ may be used for representing performance instead of ω_c and ϕ_M. The procedure may be used for pitch tracking task, flight path angle tracking task, and both pitch and flight path angle tracking task simulations as explained in Chapter IV. The results thus obtained may provide a better understanding of the overall landing task.

2) The pilot while evaluating the landing task provided two separate ratings: one for the overall task and one for the approach task. The data generated above may be correlated with each set of ratings to see if pitch tracking task is representative of the approach task and flight path angle tracking task with or without the pitch loop closed is representative of the overall task including flare and touchdown.

3) The range of ω_c and ϕ_M needs to be determined to measure performance in terms of $\frac{1}{\omega_c}$ and $\frac{1}{\phi_M}$. An alternate performance measure in terms of $\frac{1}{\omega_c}$ and ϕ_M may also be investigated.

4) The exact nature of initial pitch transient response and steady-state character liked by the pilots needs to be investigated.

5) The degradation in pilot ratings when lead control systems are added needs further study

6) While analyzing Aircraft No.5, introducing a pilot lag time constant (T_I) to reduce the crossover frequency may be considered.

Bibliography

1. McRuer, D.T. and E.S. Krendel. Mathematical Models Of Human Pilot Behavior. AGARD-AG-188: North Atlantic Treaty Organization, January 1976.

2. Smith, R.E. Effects Of Control System Dynamics On Fighter Approach And Landing Longitudinal Flying Qualities Volume 1. AFFDL-TR-78-122. WPAFB, Ohio: Air Force Flight Dynamics Laboratory, March 1978.

3. McDonnell Douglas Corporation. Report Number MDC A5596 Flying Qualities Analysis Of An In-Flight Simulation Of High Order Control System Effects On Fighter Approach And Landing. McDonnell Aircraft Company, St. Louis, Missouri. 22 December 1978.

4. Anderson, R.O., A.J. Conners, and J.D. Dillow. Paper Pilot Ponders Pitch. AFFDL/FGC-TM-70-1. WPAFB, Ohio: Flight Control Division, Air Force Flight Dynamics Laboratory, November 1970 (Revised January 1971).

5. Naylor, Flynoy R. Predicting Roll Task Flying Qualities With "Paper Pilot." AF1T Thesis GAM/MA/73-1. WPAFB, Ohio: Air Force Institute of Technology, September 1972.

6. McRuer, D.T. and I.L. Ashlcenas. Notebook For Pilot Dynamics And Aircraft Handling Qualities. Systems Technology, Inc.

7. Roskam, Jan. Flight Dynamics Of Rigid And Elastic Airplanes. Lawrence, Kansas: Roskam Aviation and Engineering Corporation, 1972.

8. Blakelock, John H. Automatic Control Of Aircraft And Missiles. New York: John Wiley and Sons, Inc., 1965.

9. Fisher, J.D. Extension Of Human Describing Function Models To Step Plus Random Appearing Inputs. AFIT Thesis GE/EE/69S-2. WPAFB, Ohio: Air Force Institute Of Technology, May 1969.

10. McRuer, D.T., Graham Dunstan, and E.S. Krendal. Manual Control Of Single-Loop Systems: Part I and Part II. Reprinted from Journal Of The Franklin Institute Vol. 283, January-February, 1967.

11. D'Azzo, John J. and Constantine H. Houpis. Linear Control System Analysis And Design: Conventional and Modern. New York: McGraw-Hill Book Company, 1975.

12. Larimer, Stanley R. "Digital Computer Program TOTAL" An Interactive Computer Aided Program For Discrete And Continuous Control System Analysis And Design. AFIT Thesis, March 1978.

13. Johnson, C.L. Analog Computer Techniques, Second Edition. New York: McGraw-Hill Book Company, 1963.

14. 231R Computer Reference Handbook, Publication Number L800 1003 OA, Electronic Associates, INC., October, 1966.

15. D'Azzo, J.J. Lecture notes distributed in EE6-41, Automatic Flight Control II. School of Engineering, Air Force Institute of Technology, WPAFB, 1979.

Appendix A

Aircraft-Control System Configurations And Transfer Functions

This appendix contains the transfer functions of the thirteen control systems used. The aircraft-control system configuration flown and the corresponding pilot ratings are also listed. The first number in the configuration represents the aircraft and the second number indicates the control system.

The feel system and actuator dynamics were held constant for all configurations. Approximate transfer functions for the feel system and the actuator dynamics are:

Feel system:

$$\frac{84.5}{S^2 + 31.2S + 676}$$

Elevator Actuator:

$$\frac{5625}{S^2 + 105S + 5625}$$

A description of these two sub-systems is given in Ref. 2.

Table: A1 Control System Transfer Functions

Control System No:	Transfer Function
1	$\frac{4(S + 2.5)}{(S + 10)}$
2	$\frac{3(S + 3.33)}{(S + 10)}$
3	$\frac{2(S + 5)}{(S + 10)}$
4	$\frac{10}{(S + 10)}$
5	$\frac{4}{(S + 4)}$
6	$\frac{2}{(S + 2)}$
7	$\frac{1}{(S + 1)}$
8	$\frac{256}{(S^2 + 22.4S + 256)}$
9	$\frac{144}{(S^2 + 16.8S + 144)}$
10	$\frac{81}{(S^2 + 12.6S + 81)}$
11	$\frac{36}{(S^2 + 8.4S + 36)}$
12	$\frac{16}{(S^2 + 5.6S + 16)}$
13	$\frac{512}{(S^2 + 29.76S + 256)(S^2 + 12.16S + 256)}$

Table A2 Aircraft-Control System Configuration Flown and Pilot Ratings

Configuration	P.R.	Configuration	P.R.	Configuration	P.R.	Configuration	P.R.	Configuration	P.R.
1 - 1	6	2 - 1	5	3 - 3	5	4 - 3	3	5 - 0	5
1 - 2	5	2 - 3	3	3 - 0	4	4 - 0	2	5 - 5	6
1 - 3	4	2 - 0	2	3 - 4	7	4 - 5	6	5 - 6	6
1 - 0	4	2 - 4	4	3 - 5	10	4 - 6	7	5 - 7	7
1 - 4	5	2 - 5	6	3 - 8	7	4 - 8	4	5 - 8	6
1 - 5	9	2 - 6	5	3 - 9	8	4 - 9	3	5 - 9	6
1 - 6	10	2 - 8	9			4 - 12	9	5 - 13	7
1 - 8	5	2 - 9	7			4 - 13	8		
1 - 10	8	2 - 11	10						
1 - 13	9	2 - 12	10						
		2 - 13	8						

Note: 0 - indicates control system = 1

Appendix B

Stability Derivatives and Aircraft Transfer Functions

Data from the Calspan, NT-33 variable stability aircraft (Ref 2), augmented to simulate five different aircraft dynamics, were used in this study. This appendix lists the equivalent body axis stability derivatives of the augmented aircraft (Table B1). These stability derivatives were estimated during a prior AFFDL contract. The aircraft transfer functions $\frac{\theta}{\delta_e}$, $\frac{\alpha}{\delta_e}$ and $\frac{\gamma}{\delta_e}$ are developed using these derivatives. The subscript used with the transfer functions denotes the aircraft number. Both the phugoid and the short period modes are included in the first set of equations. The short period approximation is then utilized for developing the short period equations. The phugoid and short period damping ratios and natural frequencies are evaluated from the resulting equations and tabulated. The transfer function $\frac{\gamma}{\delta_e}$ is developed as follows:

Flight path angle γ is given by:

$$\gamma = \theta - \alpha \tag{B1}$$

dividing throughout by δ_e yields,

$$\frac{\gamma}{\delta_e} = \frac{\theta - \alpha}{\delta_e} = \frac{\theta}{\delta_e} - \frac{\alpha}{\delta_e} \tag{B2}$$

Therefore the difference of the transfer functions $\frac{\theta}{\delta_e}$ and $\frac{\alpha}{\delta_e}$ is taken to obtain $\frac{\gamma}{\delta_e}$.

Table:B1 NT-33 Aircraft Dimensional Stability Derivatives

Stability Derivatives	Aircraft No. 1	Aircraft No. 2	Aircraft No. 3	Aircraft No. 4	Aircraft No. 5
X_u	-0.041	-0.041	-0.041	-0.041	-0.041
X_w	0.11	0.11	0.11	0.11	0.11
Z_u	-0.25	-0.26	-0.26	-0.26	-0.26
Z_w	-0.75	-0.8	-0.81	-0.76	-0.92
M_u	0.0	0.0	0.0	0.0	0.0
M_w	-0.0023213	-0.018745	-0.022392	-0.006632	-0.059341
M_q	-0.76	-1.83	-0.29	-3.49	-3.25
u_o	205	205	205	205	205
W_o	25	25	25	25	25
X_{δ_e}	0.0032	0.0032	0.0032	0.0032	0.0032
Z_{δ_e}	1.1	1.1	1.1	1.1	1.1
M_{δ_e}	0.33685	0.33685	0.33685	0.33685	0.33685
θ_o	4.5	4.5	4.5	4.5	4.5

The perturbation equations with zero initial conditions and $\theta_o \simeq o$, expressed in Laplace s-domain are:

$$\begin{bmatrix} (S - X_u) & -X_w u_o & W_o & g \\ -Z_u/u_o & (S - Z_w) & -1 & 0 \\ -M_u & -M_w u_o & (S - M_q) & 0 \\ 0 & 0 & -1 & S \end{bmatrix} \begin{bmatrix} u \\ \alpha \\ q \\ \theta \end{bmatrix} = \begin{bmatrix} X_{\delta_e} \\ Z_{\delta_e}/u_o \\ M_{\delta_e} \\ 0 \end{bmatrix} \delta_e \quad \text{(B3)}$$

Applying Cramer's Rule, the transfer functions $\frac{\alpha}{\delta_e}$ and $\frac{\theta}{\delta_e}$ are given by:

$$\frac{\alpha}{\delta_e} = \frac{\begin{vmatrix} (S - X_u) & X_{\delta_e} & w_o & g \\ -Z_u/u_o & Z_{\delta_e}/u_o & -1 & 0 \\ -M_u & M_{\delta_e} & (S - M_q) & 0 \\ 0 & 0 & -1 & S \end{vmatrix}}{\triangle} \quad \text{(B4)}$$

$$\frac{\theta}{\delta_e} = \frac{\begin{vmatrix} (S - X_u) & -X_w u_o & w_o & X_{\delta_e} \\ -Z_{u/u_o} & (S - Z_w) & -1 & Z_{\delta_e/u_o} \\ -M_u & -M_w \dot{u}_o & (S - M_q) & M_{\delta_e} \\ 0 & 0 & -1 & 0 \end{vmatrix}}{\triangle} \quad \text{(B5)}$$

where,

$$\triangle = \begin{vmatrix} (S - X_u) & -X_w U_o & W_o & g \\ -Z_u/U_o & (S - Z_w) & -1 & 0 \\ -M_u & -M_w U_o & (S - M_q) & 0 \\ 0 & 0 & -1 & S \end{vmatrix} \quad \text{(B6)}$$

Substituting the values of stability derivatives and evaluating the determinants for each aircraft yields:

$$\left.\frac{\theta}{\delta_e}\right|_1 = \frac{0.336847S^2 + 0.263892S + 0.0195185}{S^4 + 1.551S^3 + 1.1353S^2 + 0.072629S + 0.018372}$$

$$\left.\frac{\theta}{\delta_e}\right|_2 = \frac{0.336847S^2 + 0.262669S + 0.0198526}{S^4 + 2.671S^3 + 5.4431S^2 + 0.34444S + 0.15437}$$

$$\left.\frac{\theta}{\delta_e}\right|_3 = \frac{0.336847S^2 + 0.262025S + 0.0198292}{S^4 + 1.141S^3 + 4.8991S^2 + 0.29516S + 0.18441}$$

$$\left.\frac{\theta}{\delta_e}\right|_4 = \frac{0.336847S^2 + 0.262519S + 0.0198364}{S^4 + 4.211S^3 + 15.354S^2 + 0.95023S + 0.4887}$$

$$\left.\frac{\theta}{\delta_e}\right|_5 = \frac{0.336847S^2 + 0.258435S + 0.0197128}{S^4 + 4.211S^3 + 15.354S^2 + 0.95023S + 0.4887}$$

and

$$\left.\frac{\alpha}{\delta_e}\right|_1 = \frac{S^3 + 69.9339S^2 + 4.11992S + 2.666}{205(S^4 + 1.551S^3 + 1.1353S^2 + 0.072429S + 0.018372)}$$

$$\left.\frac{\alpha}{\delta_e}\right|_2 = \frac{1.1S^3 + 71.1108S^2 + 4.25147S + 2.77408}{205(S^4 + 2.671S^3 + 5.4431S + 0.3444S + 0.15437)}$$

$$\left.\frac{\alpha}{\delta_e}\right|_3 = \frac{1.1S^3 + 69.4168S^2 + 4.1833S + 2.77408}{205(S^4 + 1.141S^3 + 4.8991S^2 + 0.29516S + 0.18441)}$$

$$\left.\frac{\alpha}{\delta_e}\right|_4 = \frac{1.1S^3 + 69.4168S^2 + 4.32495S + 2.77408}{205(S^4 + 4.291S^3 + 4.2149S^2 + 0.29067S + 0.054619)}$$

$$\left.\frac{\alpha}{\delta_e}\right|_5 = \frac{1.1S^3 + 72.6728S^2 + 4.31433S + 2.77408}{205(S^4 + 4.211S^3 + 15.354S^2 + 0.95023S + 0.4887)}$$

The transfer fundtions, $\frac{\gamma}{\delta_e}$, obtained by using the relationship $\frac{\theta - \alpha}{\delta_e} = \frac{\gamma}{\delta_e}$ are:

$$\left.\frac{\gamma}{\delta_e}\right|_1 = \frac{-S^3 - 0.880265S^2 + 49.97794S + 1.335243}{205(S^4 + 1.551S^3 + 1.1353S^2 + 0.072429S + 0.018372)}$$

$$\left.\frac{\gamma}{\delta_e}\right|_2 = \frac{-1.1S^3 - 2.057165S^2 + 49.59568S + 1.2957}{205(S^4 + 2.671S^3 + 5.4431S^2 + 0.3444S + 0.15437)}$$

$$\left.\frac{\gamma}{\delta_e}\right|_3 = \frac{-1.1S^3 - 0.363165S^2 + 49.53183S + 1.291}{205(S^4 + 1.141S^3 + 4.899S^2 + 0.29516S + 0.18441)}$$

$$\left.\frac{\gamma}{\delta_e}\right|_4 = \frac{-1.1S^3 - 3.88317S^2 + 49.491445S + 1.2924}{205(S^4 + 4.291S^3 + 4.2149S^2 + 0.29067S + 0.05462)}$$

$$\left.\frac{\gamma}{\delta_e}\right|_5 = \frac{-1.1S^3 - 3.5192S^2 + 48.66485S + 1.267}{205(S^4 + 4.2115^3 + 15.354S^2 + 0.95023S + 0.4.887)}$$

The perturbation equations using the short period approximation are:

$$\begin{bmatrix} (S - Z_w) & -S \\ -M_w u_o & S(S - M_q) \end{bmatrix} \begin{bmatrix} \alpha \\ \theta \end{bmatrix} = \begin{bmatrix} Z_{\delta_e/u_o} \\ M_{\delta_e} \end{bmatrix} \delta_e \qquad \text{(B7)}$$

The transfer functions $\frac{\alpha}{\delta_e}$ and $\frac{\theta}{\delta_e}$ are given by:

$$\frac{\alpha}{\delta_e} = \frac{\begin{vmatrix} Z_{\delta_e/u_o} & -S \\ M_{\delta_e} & S(S - M_q) \end{vmatrix}}{\Delta_{S.P.}} \qquad \text{(B8)}$$

$$\frac{\theta}{\delta_e} = \frac{\begin{vmatrix} (S - Z_w) & Z_{\delta_e/u_o} \\ -M_w u_o & M_{\delta_e} \end{vmatrix}}{\Delta sp} \qquad \text{(B9)}$$

where,

$$\Delta sp = \begin{vmatrix} (S - Z_w) & -S \\ -M_w u_o & S(S - M_q) \end{vmatrix} \qquad \text{(B10)}$$

Substituting the values of stability derivatives the following aircraft short period transfer functions are obtained.

$$\left.\frac{\theta}{\delta_e}\right|_1 = \frac{0.33685S + 0.25}{S(S^2 + 1.51S + 1.04587)}$$

$$\left.\frac{\theta}{\delta_e}\right|_2 = \frac{0.33685S + 0.25}{S(S^2 + 2.63S + 5.30673)}$$

$$\left.\frac{\theta}{\delta_e}\right|_3 = \frac{0.33685S + 0.2482}{S(S^2 + 1.1S + 4.8253)}$$

$$\left.\frac{\theta}{\delta_e}\right|_4 = \frac{0.33685S + 0.2487}{S(S^2 + 4.25S + 4.012)}$$

$$\left.\frac{\theta}{\delta_e}\right|_5 = \frac{0.33685S + 0.24463}{S(S^2 + 4.17S + 15.155)}$$

$$\left.\frac{\alpha}{\delta_e}\right|_1 = \frac{0.00537S + 0.341}{(S^2 + 1.513S + 1.04587)}$$

$$\left.\frac{\alpha}{\delta_e}\right|_2 = \frac{0.00537S + 0.3467}{(S^2 + 2.63S + 5.3067)}$$

$$\left.\frac{\alpha}{\delta_e}\right|_3 = \frac{0.00537S + 0.3384}{(S^2 + 1.1S + 4.8253)}$$

$$\left.\frac{\alpha}{\delta_e}\right|_4 = \frac{0.00537S + 0.3556}{(S^2 + 4.25S + 4.012)}$$

$$\left.\frac{\alpha}{\delta_e}\right|_5 = \frac{0.00537S + 0.3543}{(S^2 + 4.17S + 15.155)}$$

The transfer functions $\frac{\gamma}{\delta_e}$ are obtained as shown earlier.

$$\left.\frac{\gamma}{\delta_e}\right|_1 = \frac{-0.00537S^2 - 0.0041S + 0.25}{S(S^2 + 1.51S + 1.04587)}$$

$$\left.\frac{\gamma}{\delta_e}\right|_2 = \frac{-0.00537S^2 - 0.00982S + 0.2489}{S(S^2 + 2.63S + 5.3067)}$$

$$\left.\frac{\gamma}{\delta_e}\right|_3 = \frac{-0.00537S^2 - 0.001556S + 0.258}{S(S^2 + 1.1S + 4.8253)}$$

$$\left.\frac{\gamma}{\delta_e}\right|_4 = \frac{-0.005373S^2 - 0.0187S + 0.2487}{S(S^2 + 4.25S + 4.012)}$$

$$\left.\frac{\gamma}{\delta_e}\right|_5 = \frac{-0.00537S^2 - 0.01744S + 0.245}{S(S^2 + 4.17S + 15.155)}$$

Table B2 Phugoid and Short Period ω_n and ξ

Aircraft No.	Phugoid		Short Period	
	ω_n	ξ	ω_n	ξ
1	0.132	0.166	1.026	0.735
2	0.171	0.148	2.298	0.57
3	0.196	0.135	2.19	0.248
4	0.118	0.25	1.988	1.064
5	0.18	0.15	3.886	0.535

Table B3 Short Period ω_n And ξ

Aircraft No.	Short Period Approximation	
	ω_n	ξ
1	1.023	0.738
2	2.304	0.571
3	2.197	0.25
4	2.003	1.061
5	3.89	0.536

Appendix C

Method of Least Squares Curve Fit

This appendix presents the mathematical development of the method of linear least squares, used for the analysis of the open-loop frequency response data. The method is useful in matching an arbitrary set of data points with a known set of data points. The mathematical phylosophy behind the method is to find a set of constants, such that the square of the error between a known set of data and a linear combination of an arbitrary set of data is minimized. The known set of data are the actual pilot ratings. The arbitrary set of data points are the phase angles and slopes of the phase angles. The method, therefore, is applied to find a pilot rating expression as a linear combination of the phase angle and the slope of the phase curve.

Consider a set of three data points u_i, x_i and y_i whose linear combination is equal to PR. Expressing it mathematically we get:

$$(PR)_i = \alpha_1 u_i + \alpha_2 x_i + \alpha_3 y_i \qquad (C1)$$

where α_1, α_2 and α_3 are constants. For our problem $(PR)_i$ are the estimated pilot ratings, u_i, the phase angles, and x_i, y_i are the slopes. If Z_i represents the actual pilot ratings, then the error in the rating expression E_i is given by

$$E_i = Z_i - (PR)_i \tag{C2}$$

Or

$$E_i = Z_i - (\alpha_1 u_i + \alpha_2 x_i + \alpha_3 y_i) \tag{C3}$$

and

$$\sum_{i=1}^{n} E_i^2 = \sum_{i=1}^{n} \left\{ Z_i - (\alpha_1 u_i + \alpha_2 x_i + \alpha_3 y_i) \right\}^2 = E \tag{C4}$$

To find $\alpha_1, \alpha_2, \alpha_3$ such that ΣE_i^2 is a minimum,

$$\frac{\partial E^2}{\partial \alpha_1} = \sum_{i=1}^{n} 2[Z_i - (\alpha_1 u_i + \alpha_2 x_i + \alpha_3 y_i)](-u_i) = 0 \tag{C5}$$

$$\frac{\partial E^2}{\partial \alpha_2} = \sum_{i=1}^{n} 2[Z_i - (\alpha_i u_i + \alpha_2 x_i + \alpha_3 y_i)](-x_i) = 0 \tag{C6}$$

$$\frac{\partial E^2}{\partial \alpha_3} = \sum_{i=1}^{n} 2[Z_i - (\alpha_i u_i + \alpha_2 x_i + \alpha_3 u_i)](-y_i) = 0 \tag{C7}$$

Dividing equations C5,C6,C7 by 2 and rearranging yields,

$$\Sigma Z_i u_i = (\Sigma u_i^2)\alpha_1 + (\Sigma u_i x_i)\alpha_2 + (\Sigma u_i y_i)\alpha_3 \tag{C8}$$

$$\Sigma Z_i x_i = (\Sigma u_i x_i)\alpha_1 + (\Sigma x_i^2)\alpha_2 + (\Sigma x_i y_i)\alpha_3 \tag{C9}$$

$$\Sigma Z_i y_i = (\Sigma u_i y_i)\alpha_1 + (\Sigma x_i y_i)\alpha_2 + (\Sigma y_i^2)\ 3 \tag{C10}$$

Equations C8, C9 and C10 are three linear algebraic equations in unknowns α_1, α_2 and α_3. Writing the equations in matrix format yields:

$$\begin{bmatrix} \Sigma u_i^2 & \Sigma u_i x_i & \Sigma u_i y_i \\ \Sigma u_i x_i & \Sigma x_i^2 & \Sigma x_i y_i \\ \Sigma u_i y_i & \Sigma x_i y_i & \Sigma y_i^2 \end{bmatrix} \begin{bmatrix} \alpha_1 \\ \alpha_2 \\ \alpha_3 \end{bmatrix} = \begin{bmatrix} \Sigma Z_i u_i \\ \Sigma Z_i x_i \\ \Sigma Z_i y_i \end{bmatrix} \quad (C11)$$

Solving for $\alpha_1, \alpha_2, \alpha_3$ yields:

$$\begin{bmatrix} \Sigma u_i^2 & \Sigma u_i x_i & \Sigma u_i y_i \\ \Sigma u_i x_i & \Sigma x_i^2 & \Sigma x_i y_i \\ \Sigma u_i y_i & \Sigma x_i y_i & \Sigma y_i^2 \end{bmatrix}^{-1} \begin{bmatrix} \Sigma Z_i u_i \\ \Sigma Z_i x_i \\ \Sigma Z_i y_i \end{bmatrix} = \begin{bmatrix} \alpha_1 \\ \alpha_2 \\ \alpha_3 \end{bmatrix} \quad (C12)$$

Equation C12 is used for the evaluation of α_1, α_2 and α_3 and to develop pilot rating expressions described in chapter III of the report. It can be modified for cases where there are only two unknown constants α_1 and α_2 by deleting the third row and column.

Appendix D Analog Computer Simulation Diagrams

This appendix contains the details of the analog computer circuitry used in the simulation of pilot-aircraft dynamics and the control system dynamics. Figure D1 is a block diagram description of the system simulated as a closed-loop pitch angle tracking task. Figures D2 and D3 are the block diagrams showing closed-loop flight path angle tracking task without the pitch feedback and with pitch feedback respectively. For simplicity, each block in the diagrams are discussed individually.

Simulation of Aircraft Short Period Dynamics

The aircraft short period equations of motion are given by:

$$\dot{\alpha} - Z_w\alpha - \dot{\theta} = \frac{Z_{\delta_e}}{u_o}\delta_e \qquad \text{(D1)}$$

$$-M_\omega u_o\alpha + \ddot{\theta} - M_q\dot{\theta} = M_{\delta_e}\delta_e \qquad \text{(D2)}$$

Rearranging these equations yields the following.

$$\dot{\alpha} = Z_w\alpha + \dot{\theta} + \frac{Z_{\delta_e}}{u_o}\delta_e \qquad \text{(D3)}$$

$$\ddot{\theta} = M_q\dot{\theta} + M_w u_o\alpha + M_{\delta_e}\delta_e \qquad \text{(D4)}$$

$$\gamma = \theta - \alpha \qquad \text{(D5)}$$

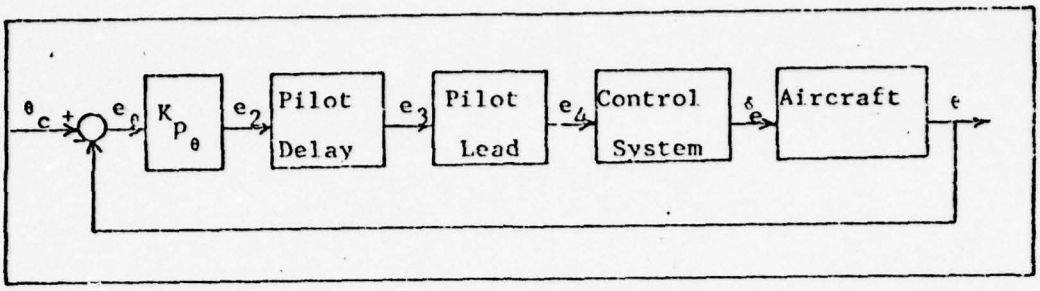

Fig. D1 Closed-Loop Pitch Tracking Task

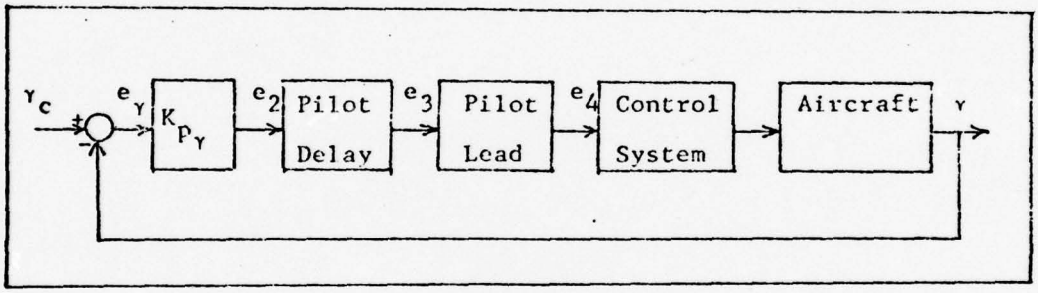

Fig. D2 Closed-Loop γ-Tracking Task

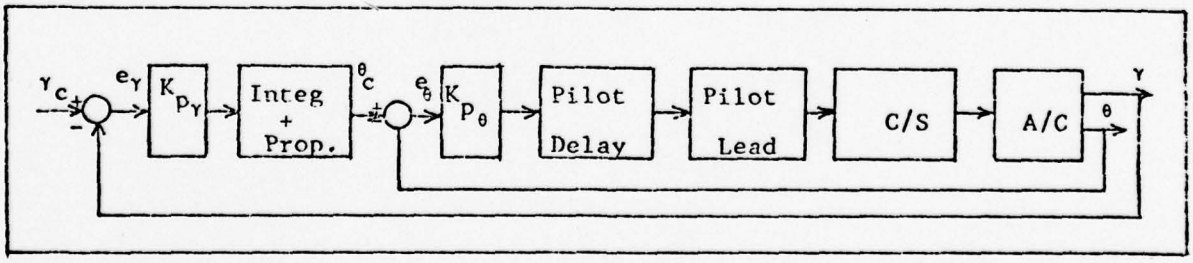

Fig. D3 Closed-Loop γ-Tracking Task With 'θ' Loop Closed

Eqns. D3, D4 and D5 are utilized for the simulation. By using appropriate values of the dimensional stability (Z_w, M_q, M_w) and control $\frac{Z_{\delta_e}}{u_o}$, M_{δ_e} derivatives, any one of the five aircraft configurations can be easily formed. The analog circuit diagram is shown in Figure D4.

Simulation of Control System

Since the control systems varied from a first order lead/lag to a first-order and second-order lag systems, three separate patching areas were used, one for each type of control system. The three categories are described separately. The fourth-order lag control system (c/S 13) was not simulated.

First-Order Lag Control System

A first order lag transfer function is given by

$$\frac{y(s)}{x(s)} = \frac{a}{s + a} \qquad \text{(D6)}$$

where x and y are the input and output. Rewriting equation in a differential equation form yields,

$$\dot{y} = -ay + ax \qquad \text{(D7)}$$

Equation D7 can be simulated as shown in Figure D5. The value of 'a' can be adjusted to simulate any desired first-order lag control system.

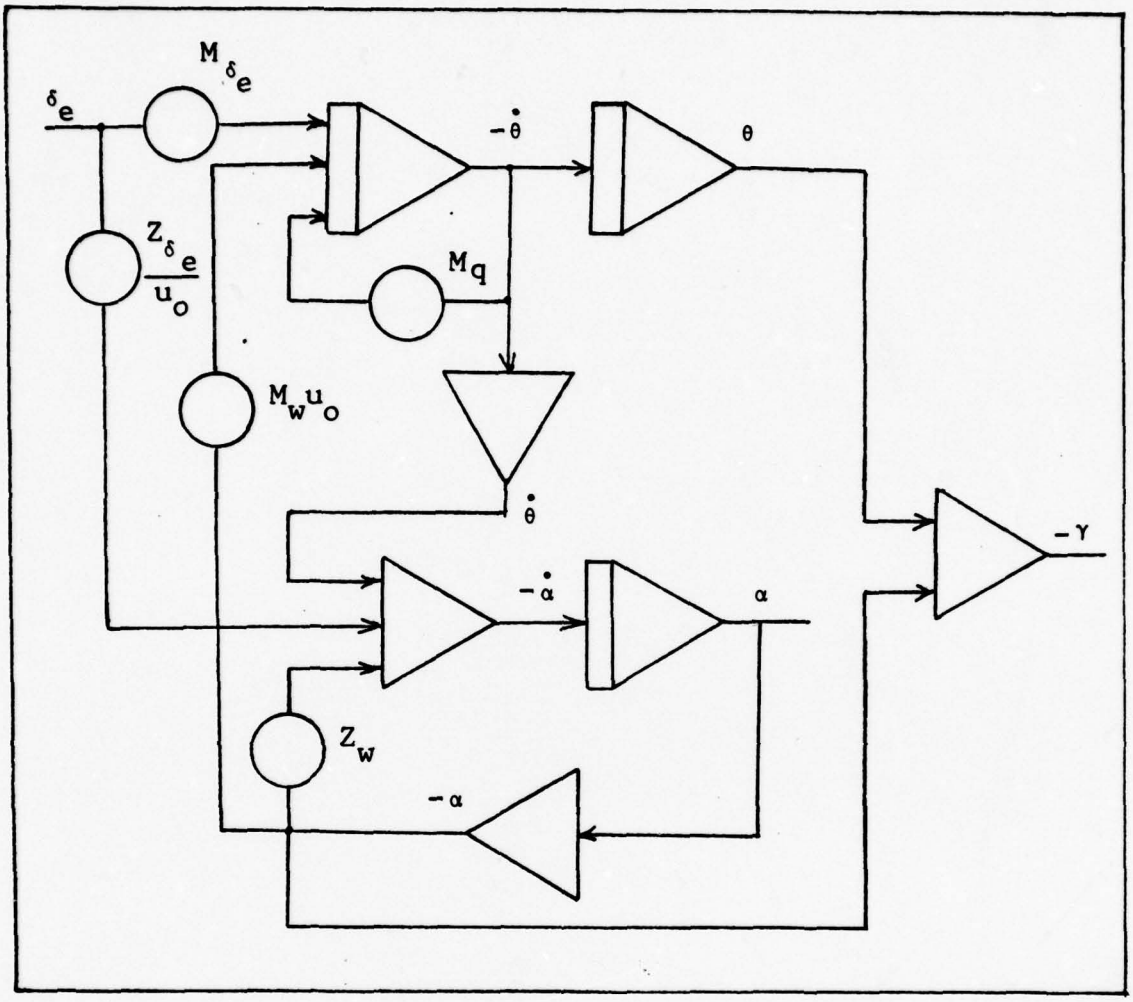

Fig. D4 Aircraft Short Period Analog Simulation Diagram

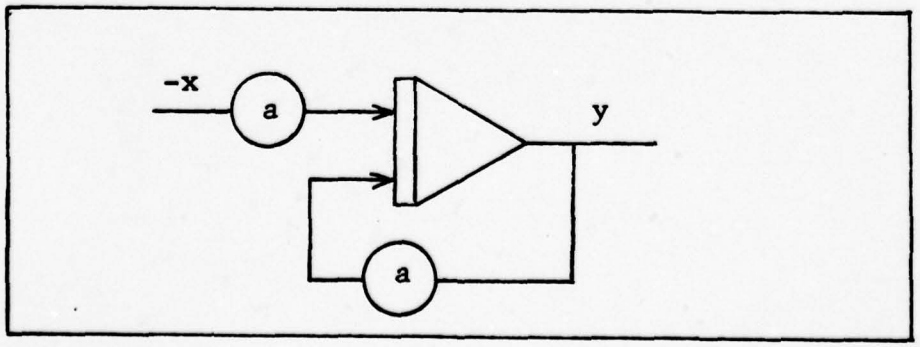

Fig. D5 First-Order Lag Control System Simulation Diagram

Second-Order lag Control System

A second-order lag transfer function is given by,

$$\frac{y(s)}{x(s)} = \frac{b}{S^2 + as + b} \tag{D8}$$

The above equation can be written as

$$ys^2 + ays + by = bx \tag{D9}$$

or

$$-y = \frac{ay}{s} + \frac{by}{s^2} - \frac{bx}{s^2} \tag{D10}$$

The simulation diagram of equation D10 is shown in Figure D6, where 'a' and 'b' can be set to any desired value to simulate the required second-order lag system.

Lead/Lag Control System

The transfer function of a lead/lag control system can be written as,

$$\frac{y(s)}{x(s)} = \frac{as + b}{s + b} \tag{D11}$$

Dividing the numerator by the denominator gives,

$$\frac{y(s)}{x(s)} = a - \frac{b(a - 1)}{(s + b)} \tag{D12}$$

Rearranging this equation yields

$$y(s) = ax(s) - \frac{b(a - 1)}{(s + b)}x(s) \tag{D13}$$

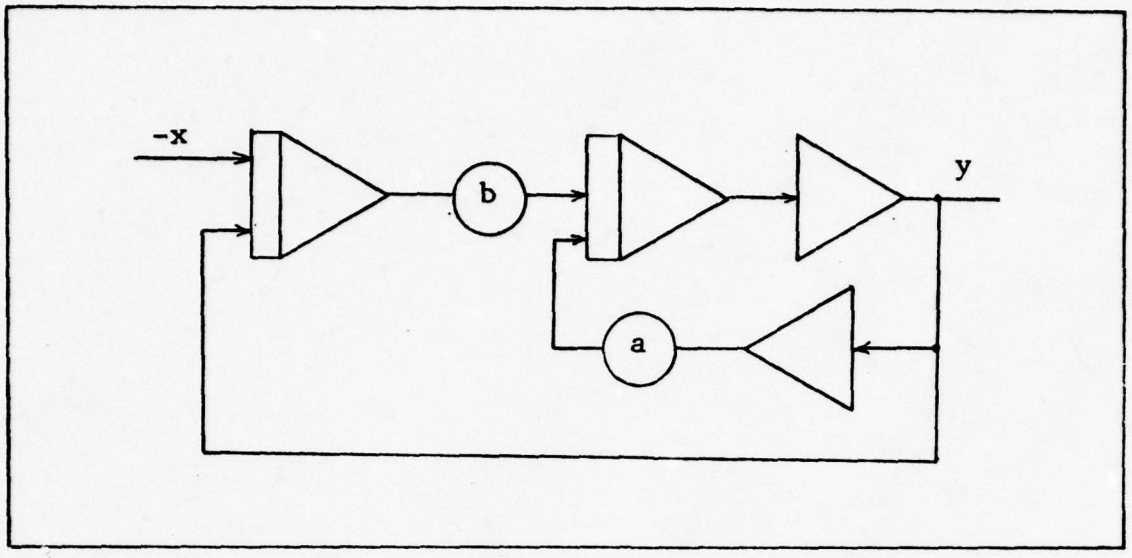

Fig. D6 Second Order Lag Control System Simulation Diagram

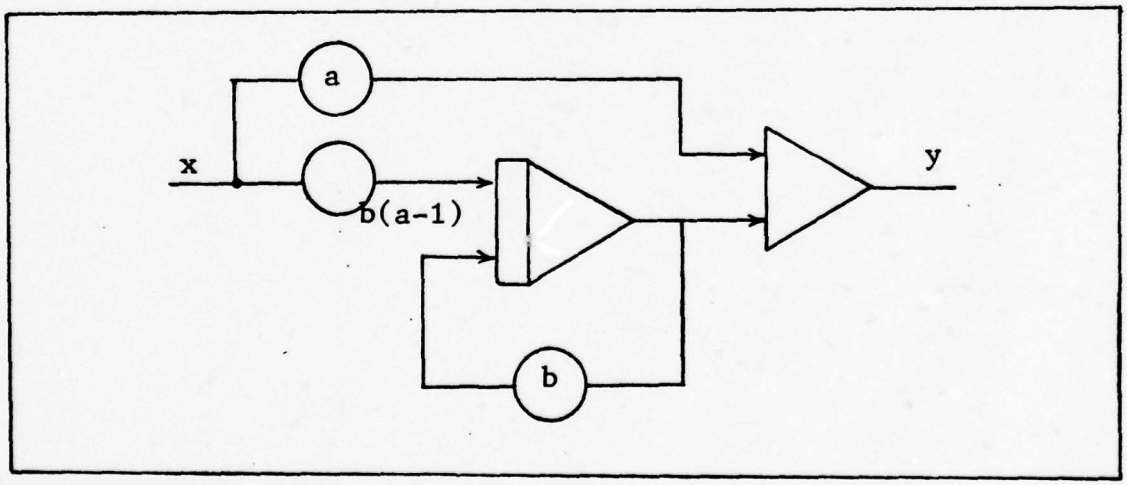

Fig. D7 Lead/Lag Control System Simulation Diagram

The simulation diagram of eqn. D13 is shown in Figure D7. Appropriate lead/lag control systems can be simulated by selecting the values of 'a' and 'b'.

Simulation of Pilot Model

The pilot model used for simulation has a 0.3 sec delay, a pilot gain K_p, and a fist-order lead circuit with pilot lead time constant T_L. A first order Padé approximation was used for the time delay in the model. The pilot transfer function thus reduces to

$$y_p(s) = K_p(T_L s + 1)e^{-\tau s} \simeq \frac{-K_p(T_L s + 1)(s - 2/\tau)}{(s + 2/\tau)} \qquad (D14)$$

For ease of programming, the pilot model is decomposed into the block diagram shown in Figure D8.

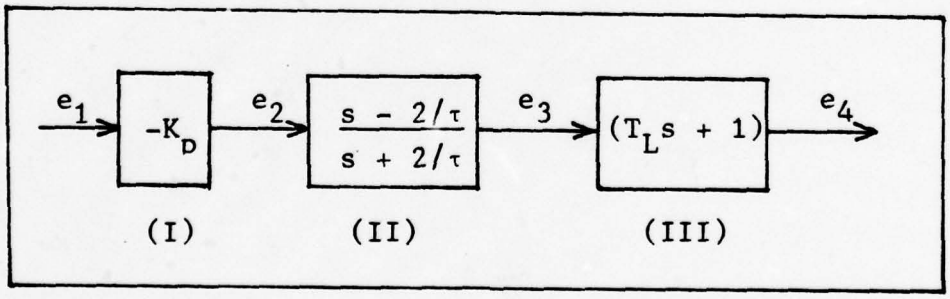

Figure D 8 Analog Pilot Model Block Diagram

The equation for the first block is

$$e_2 = -K_p e_1 \qquad (D15)$$

The analog computer circuit for block I in Figure D 9 is shown in Figure D9 .

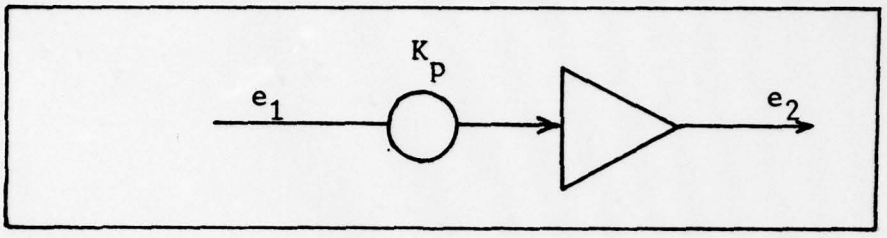

Figure D9 Circuit Diagram For Equation D15

The transfer function of the second block (Figure D10) is

$$\frac{e_3}{e_2} = \frac{s - 2/\tau}{s + 2/\tau} \tag{D16}$$

With τ chosen as 0.3 sec., Eqn. D16 may be rewritten as

$$-e_3 = -e_2 + \frac{6.667}{s}(e_2 + e_3) \tag{D17}$$

The computer simulation diagram of Eqn. D17 is shown in Fig. D10.

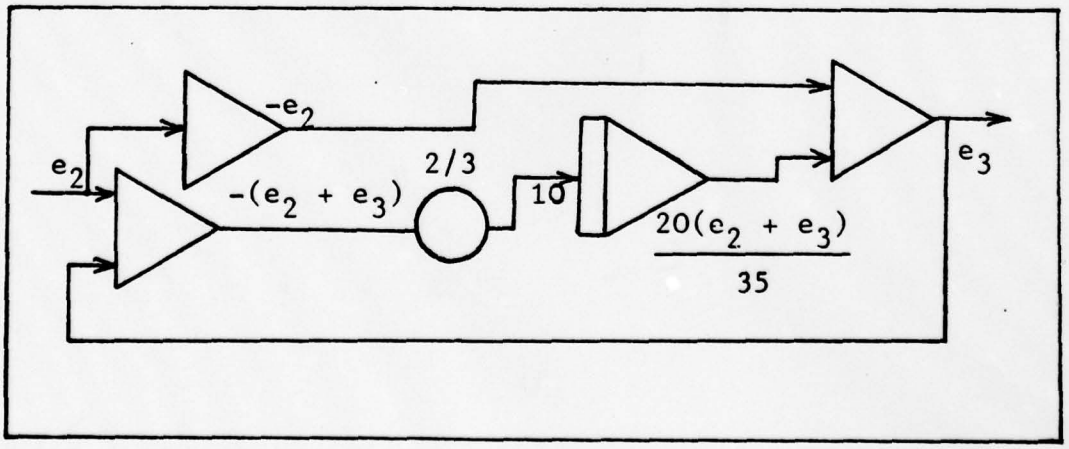

Figure D10 Circuit Diagram For Equation D17

The transfer function for the third block in Figure D10 is

$$\frac{e_4}{e_3} = T_L s + 1 \qquad \text{(D18)}$$

Eqn. D18 shows that the output e_4 consists of a sum of the input and its derivative. Simulation of derivatives of inputs is not desirable in analog computer programming. Since the value of T_L used was about 0.5 sec., Eqn. D18 was modified to include a pole at -20. A pole at -20 will not cause any significant changes and the errors are negligibly small. Therefore Eqn. D18 is modified as shown

$$\frac{e_4}{e_3} = \frac{(T_L s + 1)}{(s + 20)} = T_L - \frac{(20T_L - 1)}{(s + 20)} \qquad \text{(D19)}$$

The simulation diagram of Eqn. D19 is shown in Figure D11.

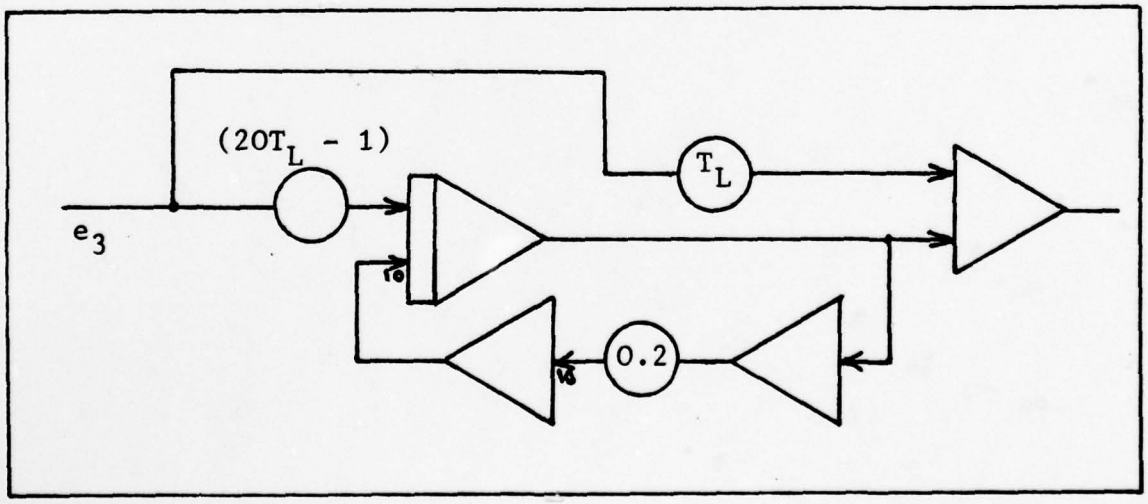

Figure D11 Circuit Diagram For Equation D19

Proportional Plus Integral Control

The proportional plus integral control was used in the two-loop closure study. In Figure D3, with the inner-loop closed, the system reduces to a Type-o System and therefore generates a steady-state error for a step γ-command. The proportional plus integral control makes the system Type 1, thus making it possible for the output to follow the input and driving e_γ, the error in 'γ', to zero.

The transfer function used for a proportional plus integral control is

$$\frac{y(s)}{x(s)} = 1 + \frac{a}{s} \qquad \text{(D20)}$$

where 'a' is a constant. The simulation diagram of Eqn. D20 is shown in Figure D12.

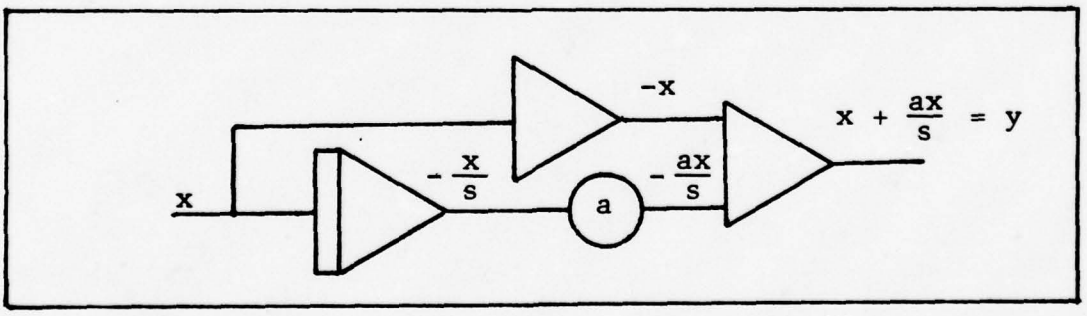

Figure D12 Circuit Diagram For Equation D20

Simulation of ISE

The ISE (integral of error squared) was used as the performance criterion for adjusting the value of any desired parameter. The simulation diagram for ISE is shown in Figure D13. Quarter square multipliers were used for squaring the

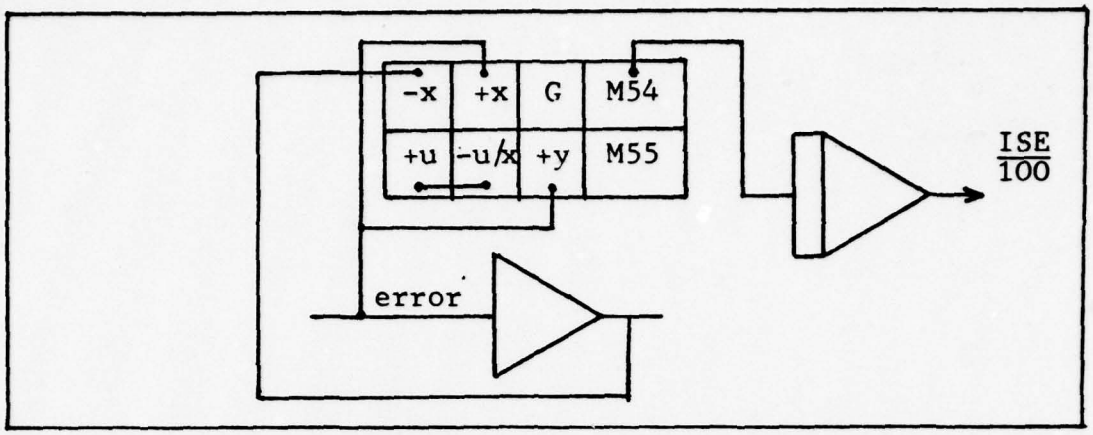

Figure D13 Quarter Square Multiplier Simulation Diagram

The analog simulation studies were thus conducted by patching the diagrams discussed above on one patching board. The appropriate blocks were cascaded to simulate systems shown in Figures D1 , D2 and D3 .

Appendix E

Open-Loop Frequency Response Plots of Pitch Angle Theta And Flight Path Angle (γ) For the Selected Aircraft-Control System Configurations Analyzed And Tables E1 thru E17

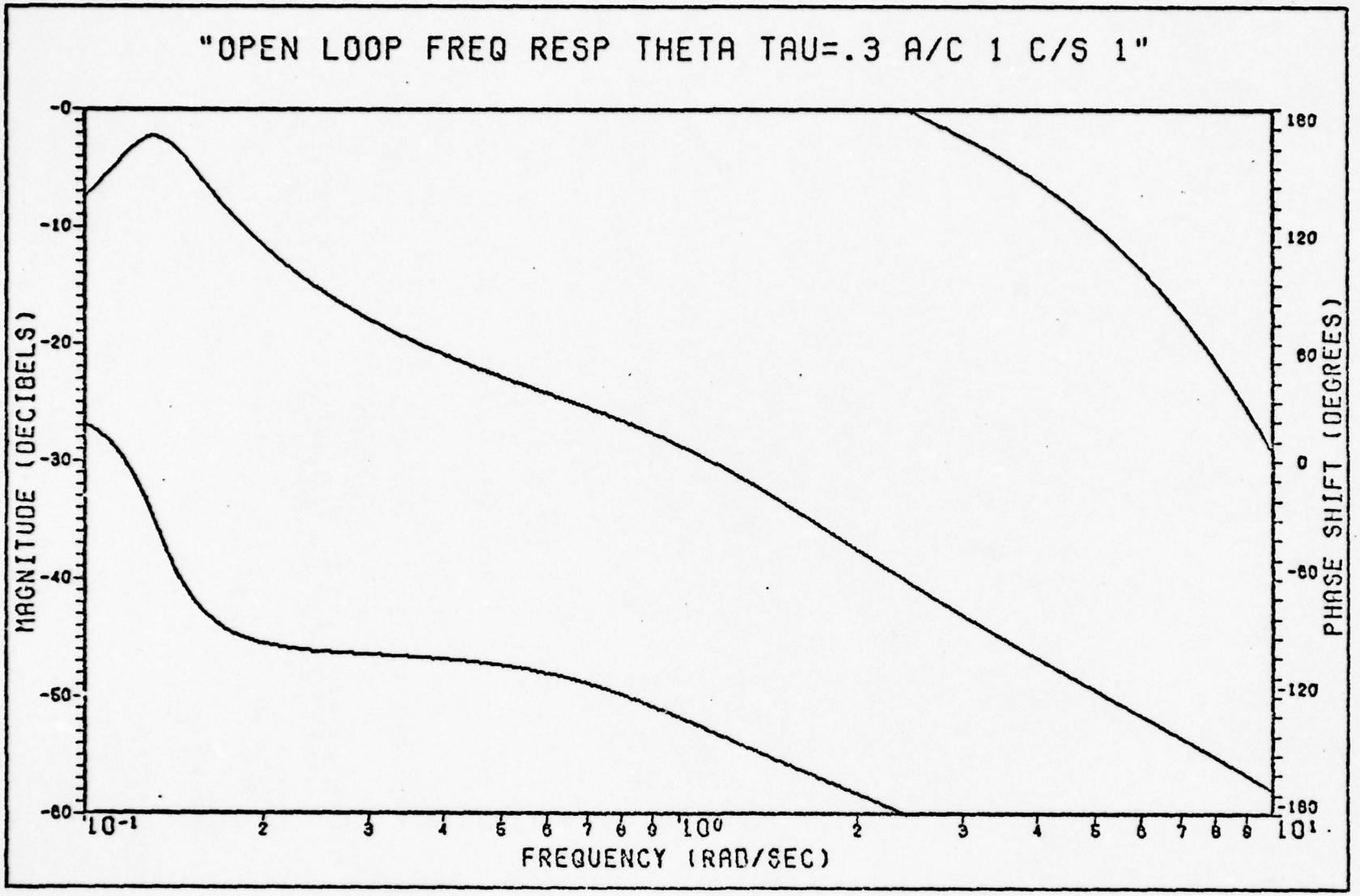

Fig. E1 Open-Loop Frequency Response θ For τ = 0.3 sec. A/C 1 C/S 1

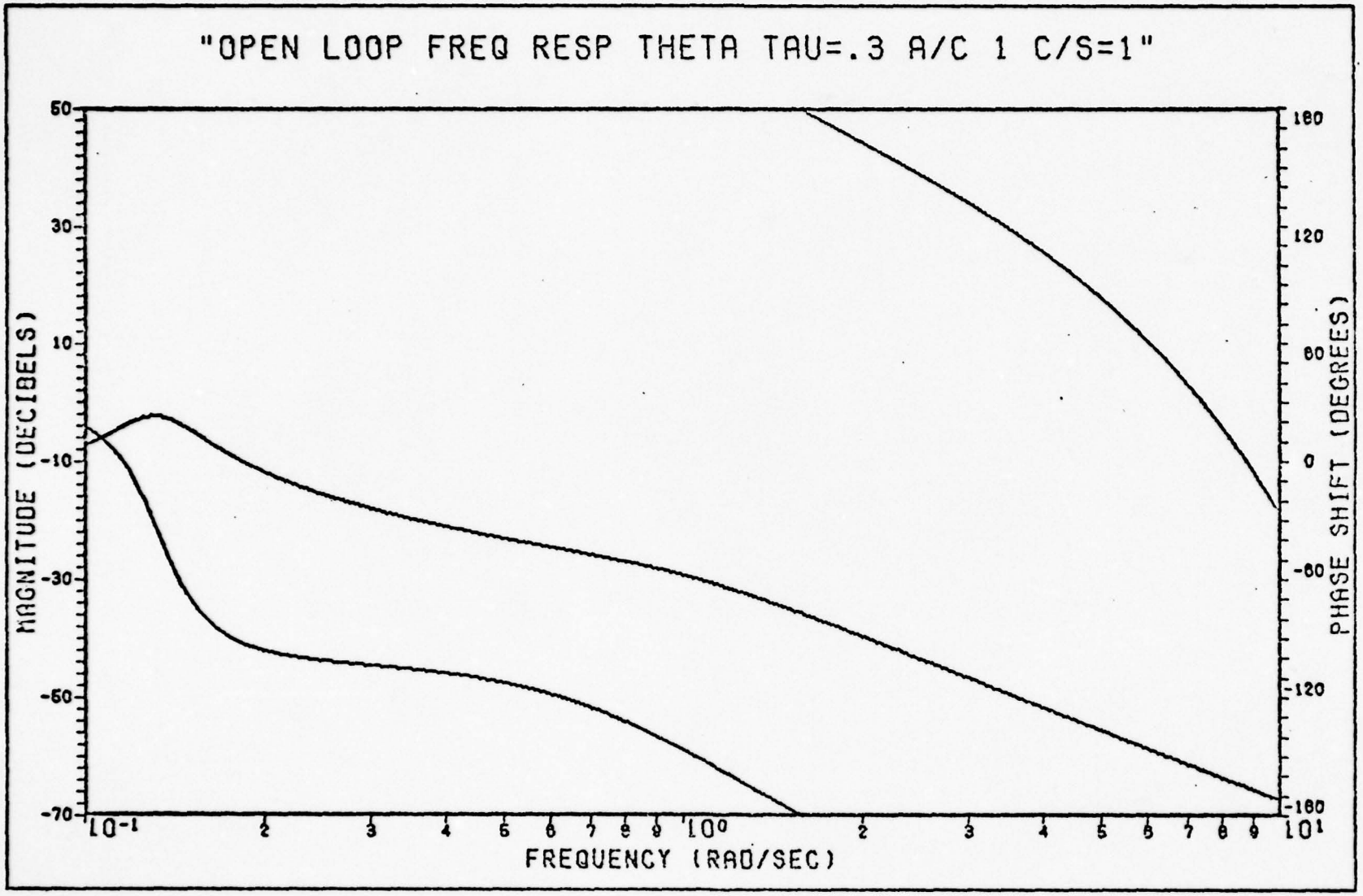

Fig. E2 Open-Loop Frequency Response θ For τ = 0.3 sec. A/C 1 C/S=1

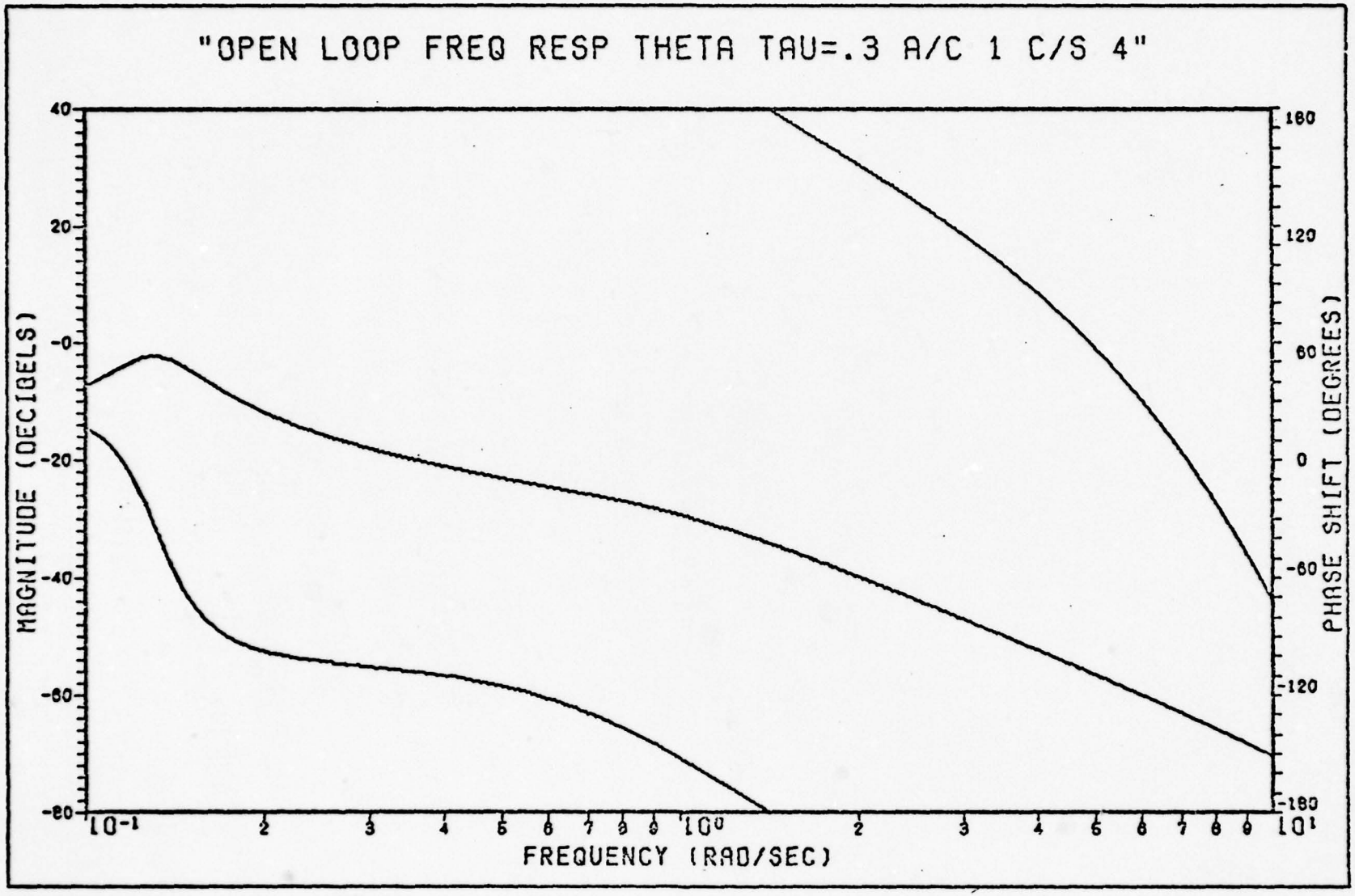

Fig. E3 Open-Loop Frequency Response θ For τ = 0.3 sec. A/C 1 C/S 4

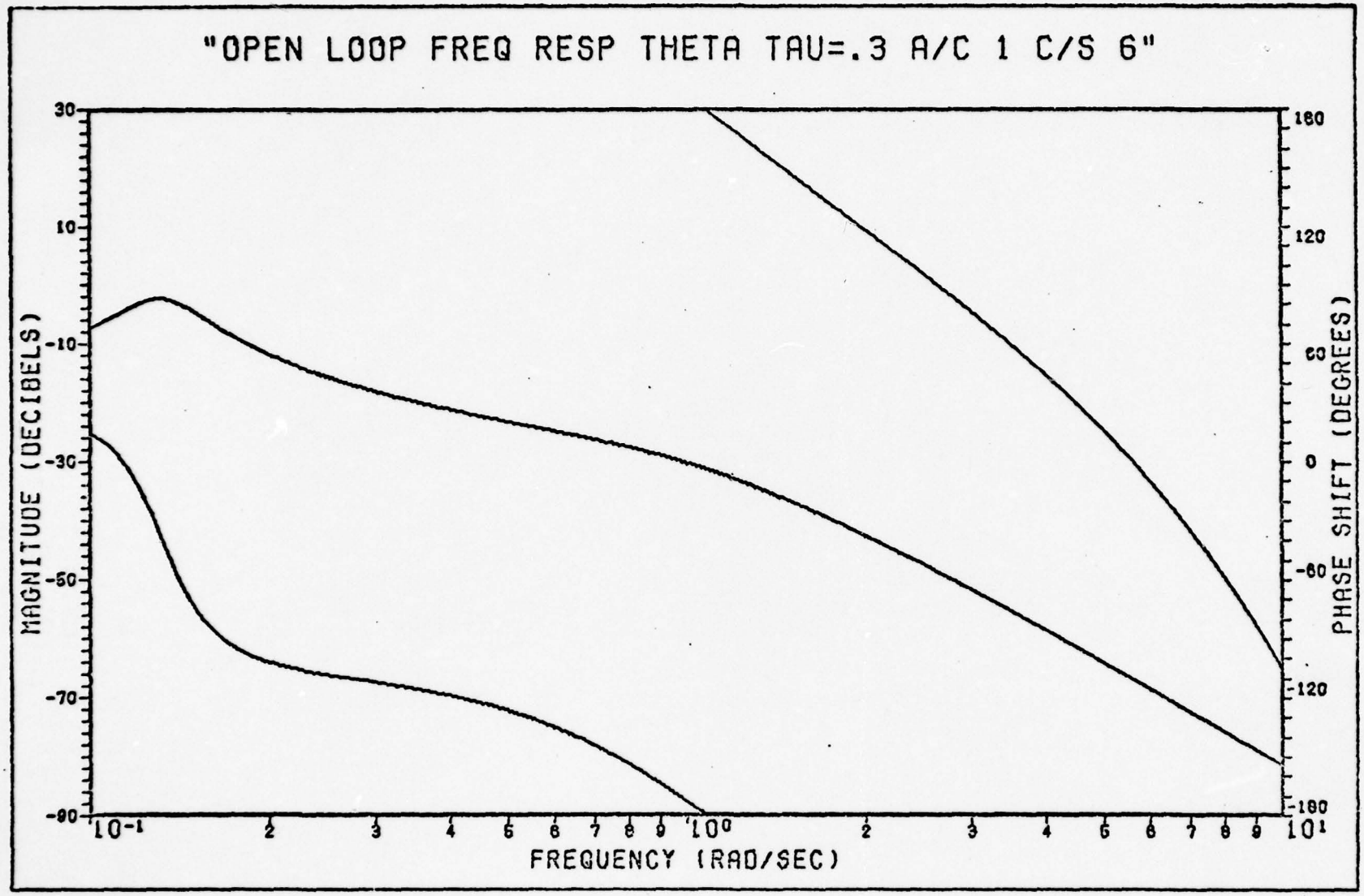

Fig. E4 Open-Loop Frequency Response θ For τ = 0.3 sec. A/C 1 C/S 6

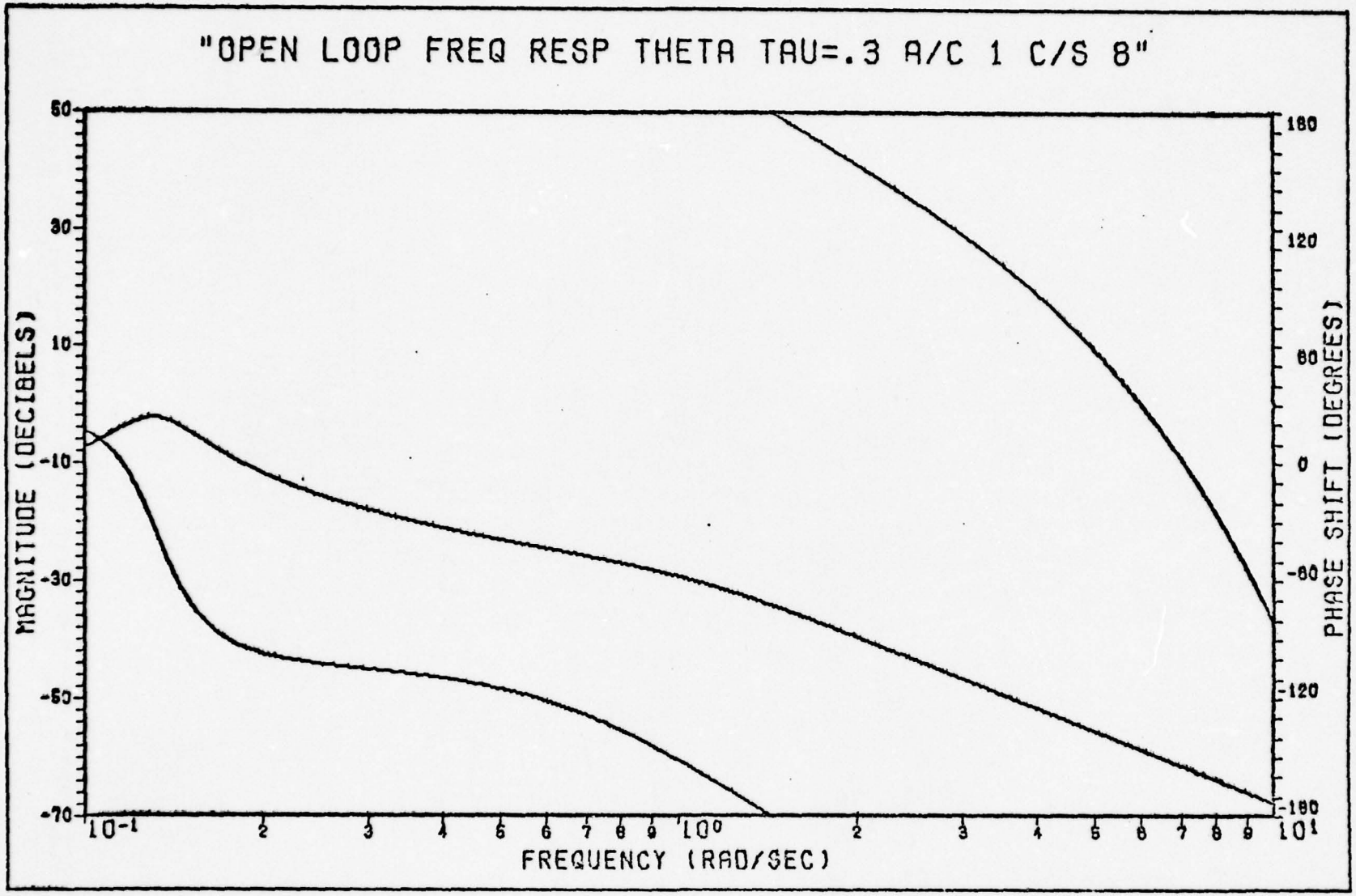

Fig. E5 Open-Loop Frequency Response θ For τ = 0.3 sec. A/C 1 C/S 8

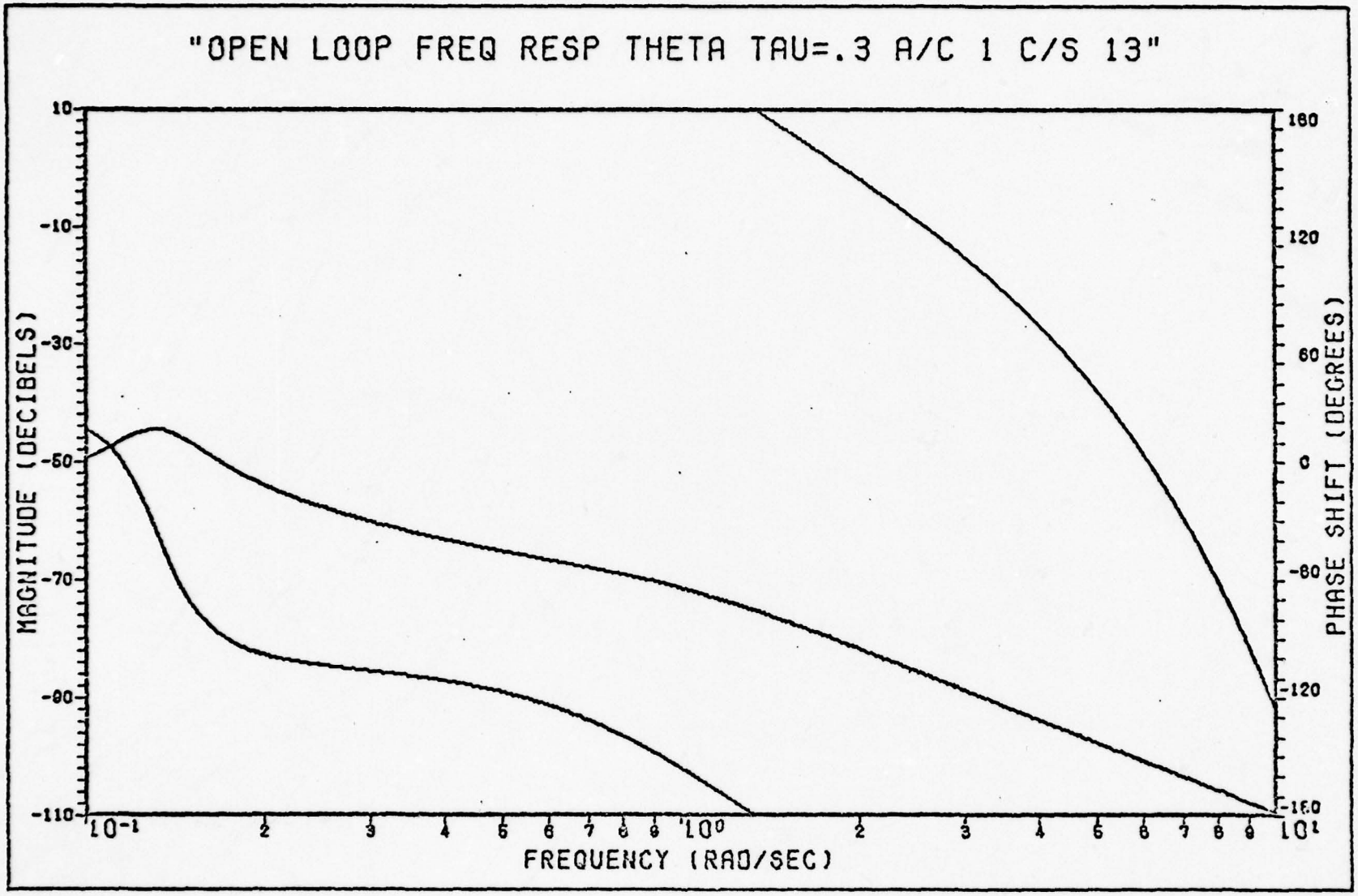

Fig. E6 Open-Loop Frequency Response θ For τ = 0.3 sec. A/C 1 C/S 13

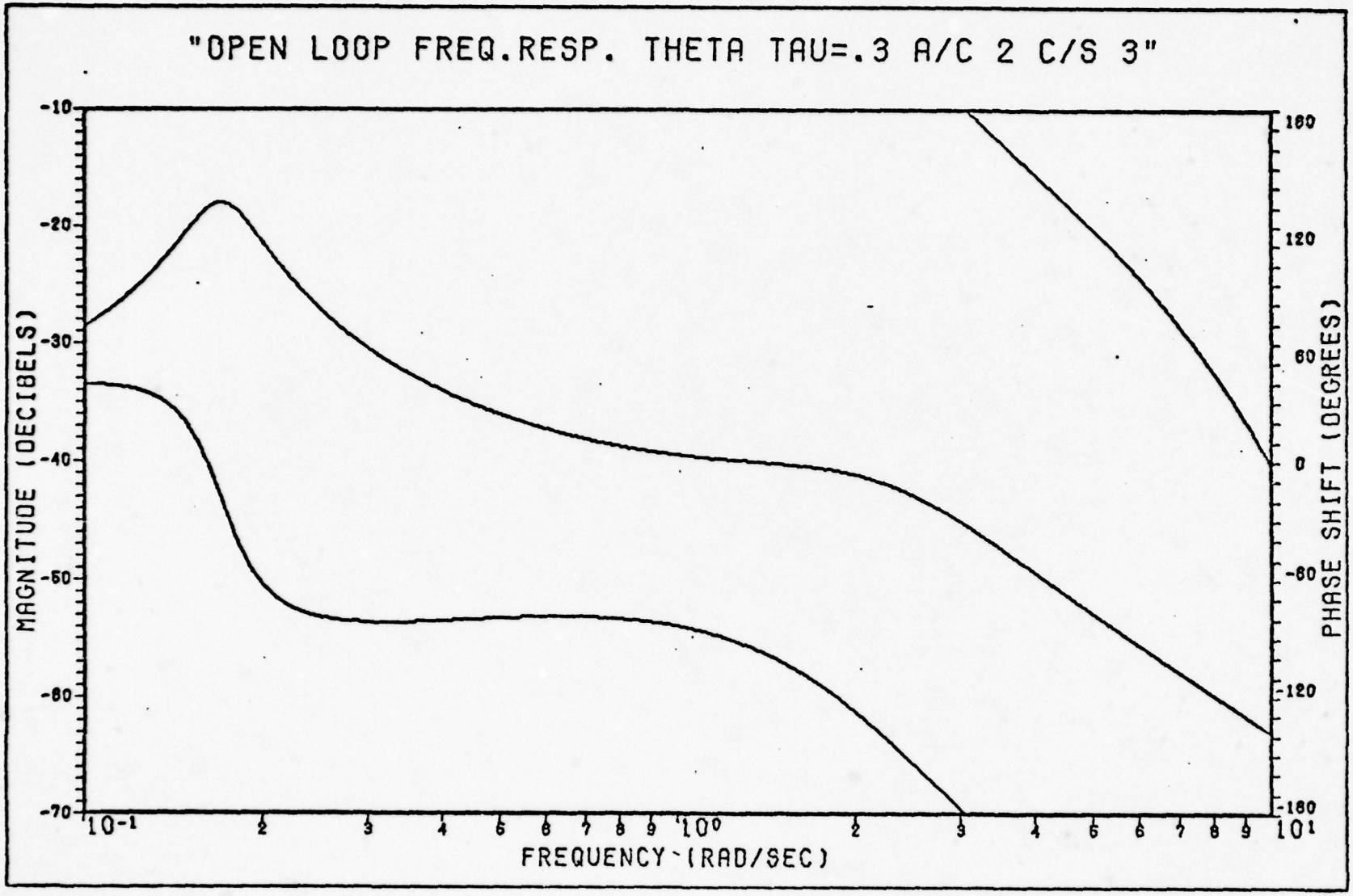

Fig. E7 Open-Loop Frequency Response θ For τ = 0.3 sec. A/C 2 C/S 3

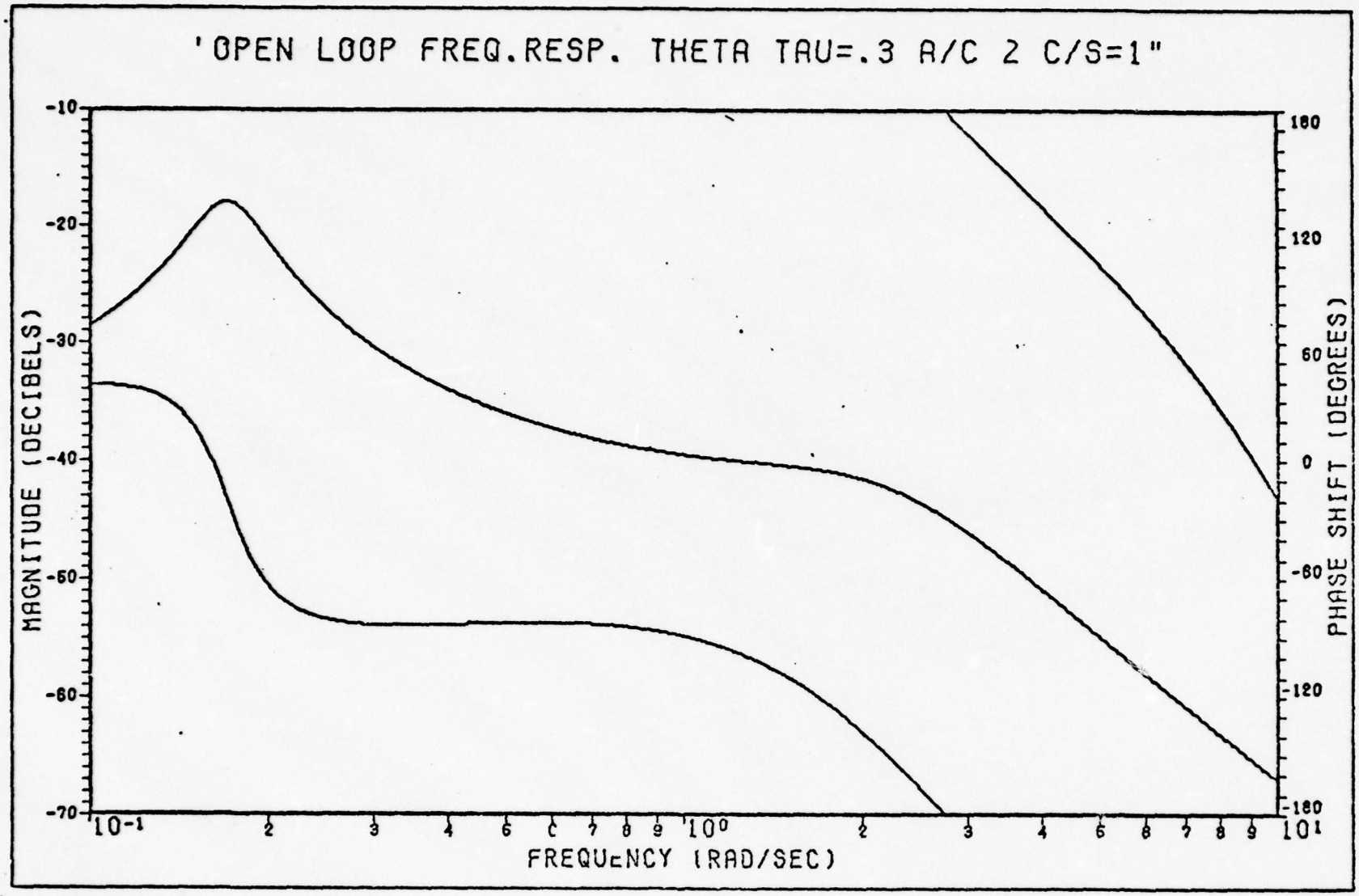

Fig. E8 Open-Loop Frequency Response θ For τ = 0.3 sec. A/C 2 C/S =1

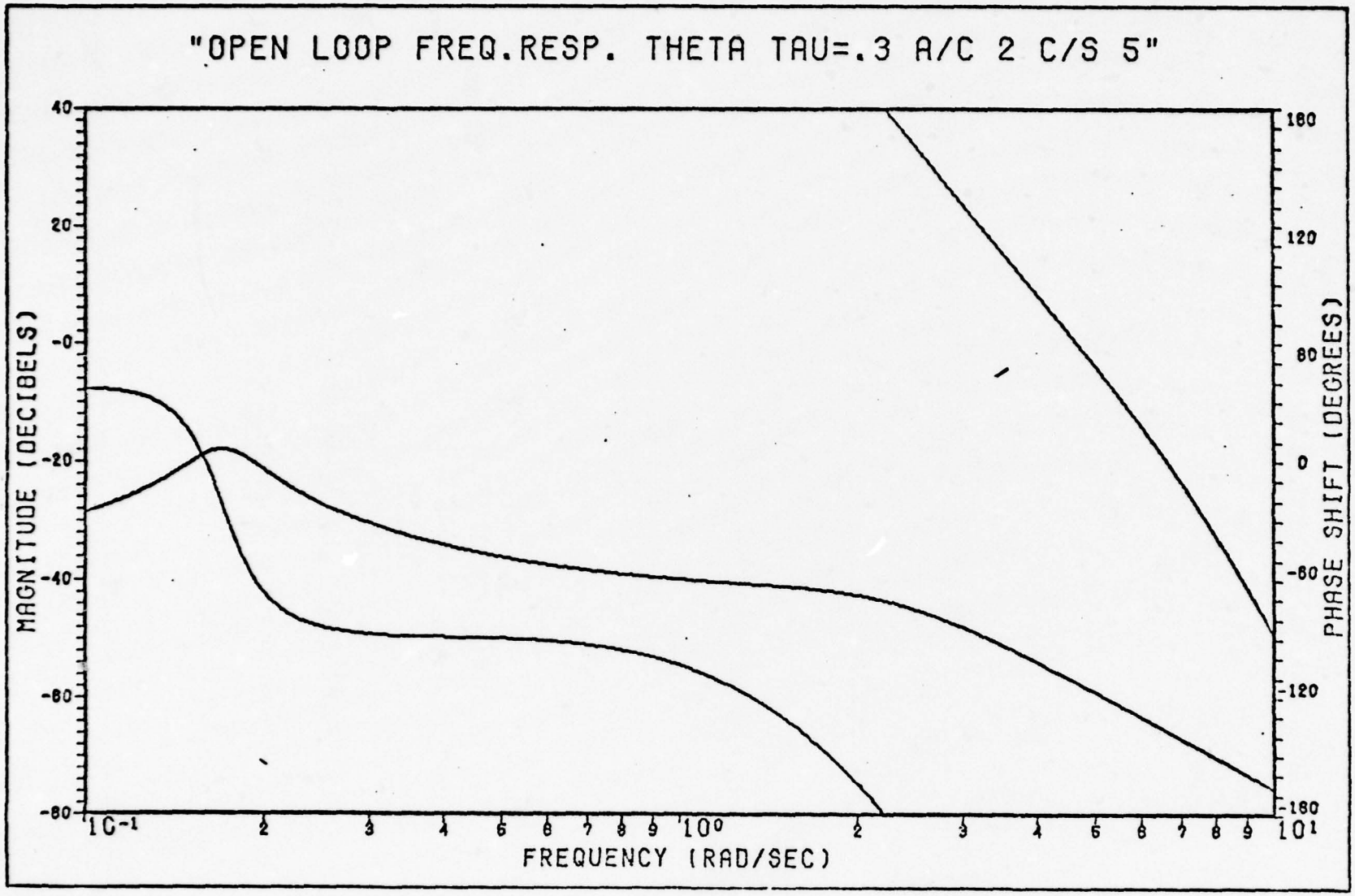

Fig. E9 Open-Loop Frequency Response θ For τ = 0.3 sec. A/C 2 C/S 5

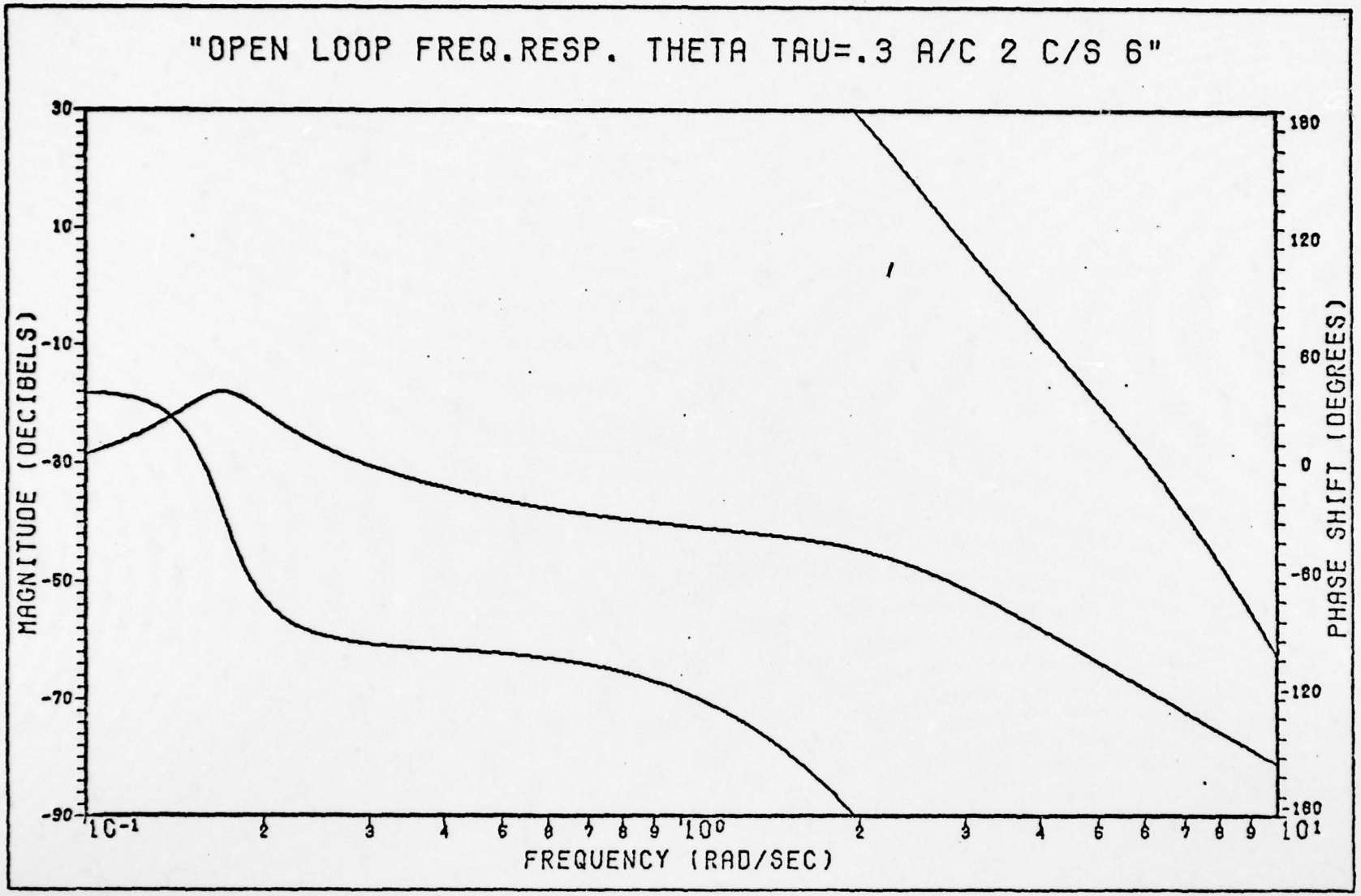

Fig. E10 Open-Loop Frequency Response θ For τ = 0.3 sec. A/C 2 C/S 6

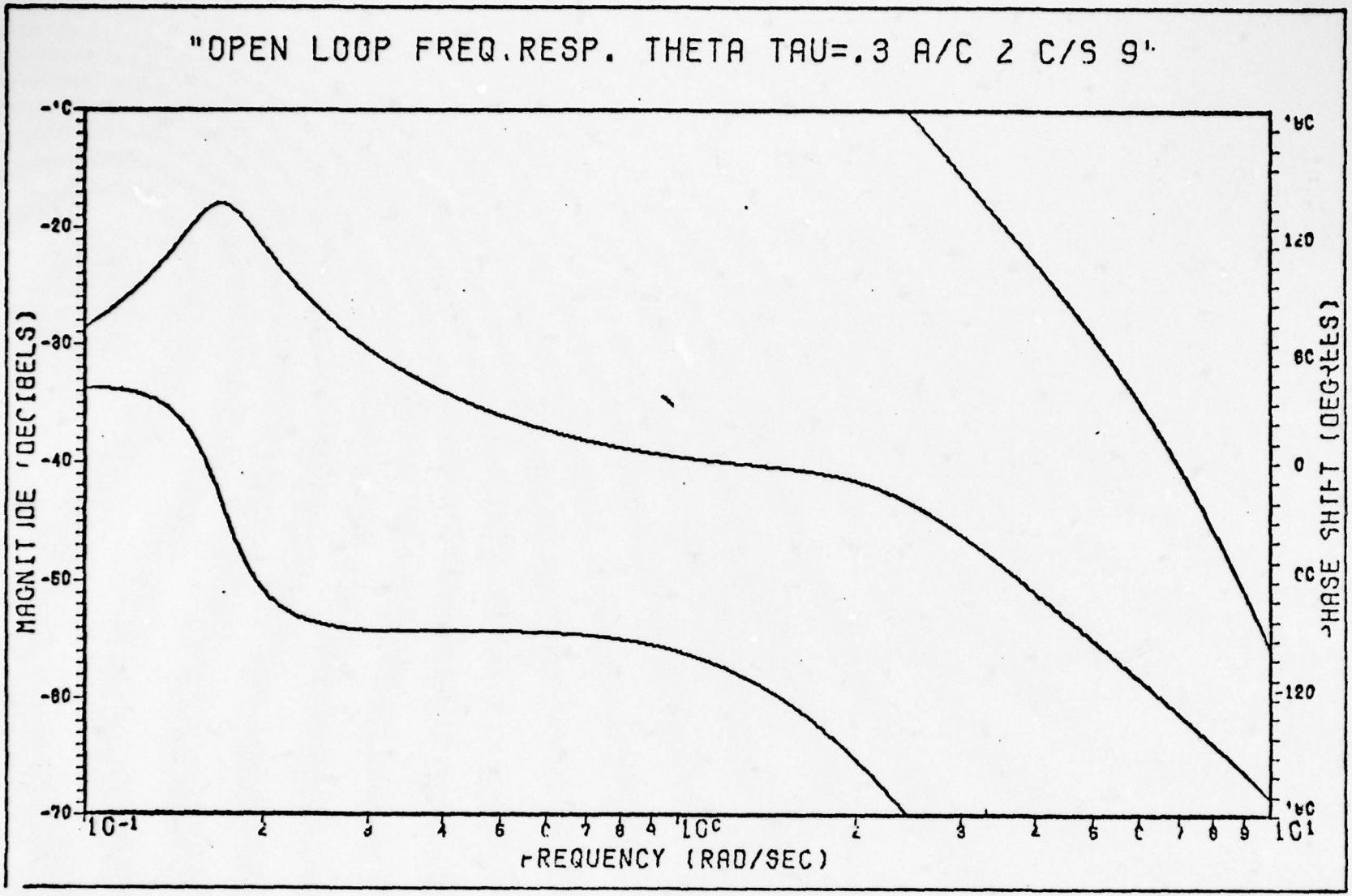

Fig. E11 Open-Loop Frequency Response θ For τ = 0.3 sec. A/C 2 C/S 9

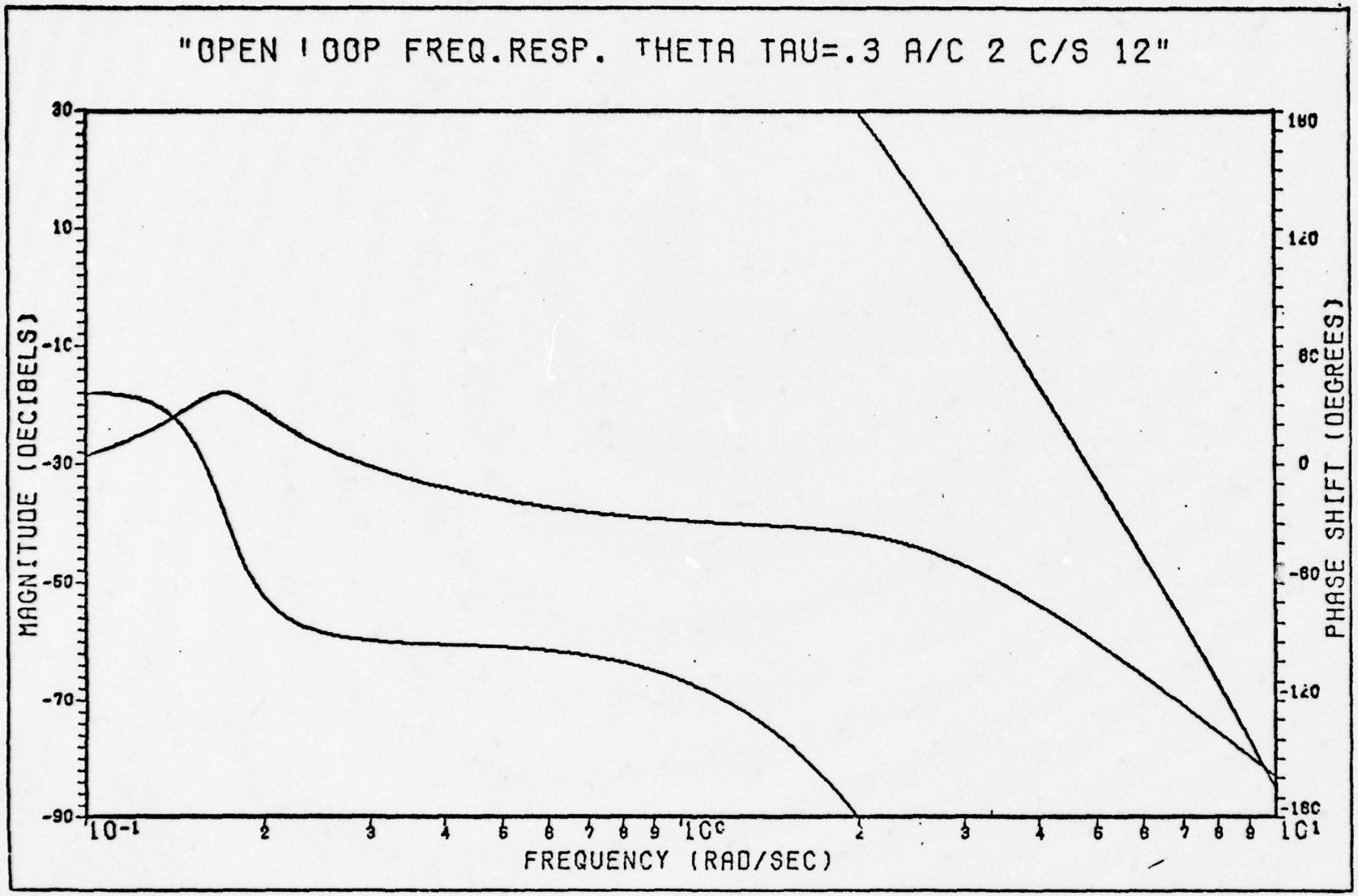

Fig. E12 Open-Loop Frequency Response θ For τ = 0.3 sec. A/C 2 C/S 12

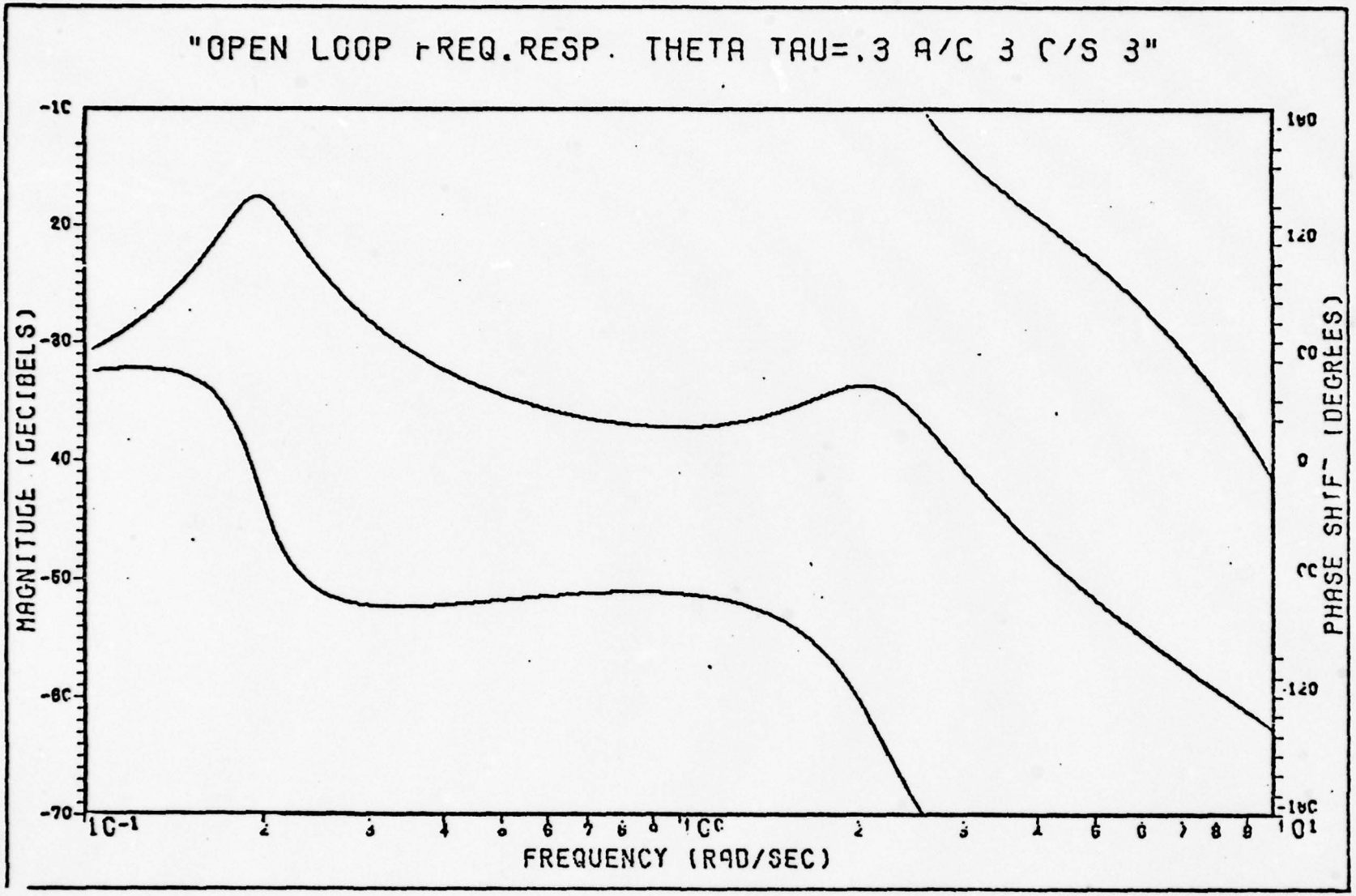

Fig. E13 Open-Loop Frequency Response θ For τ = 0.3 sec. A/C 1 C/S 1

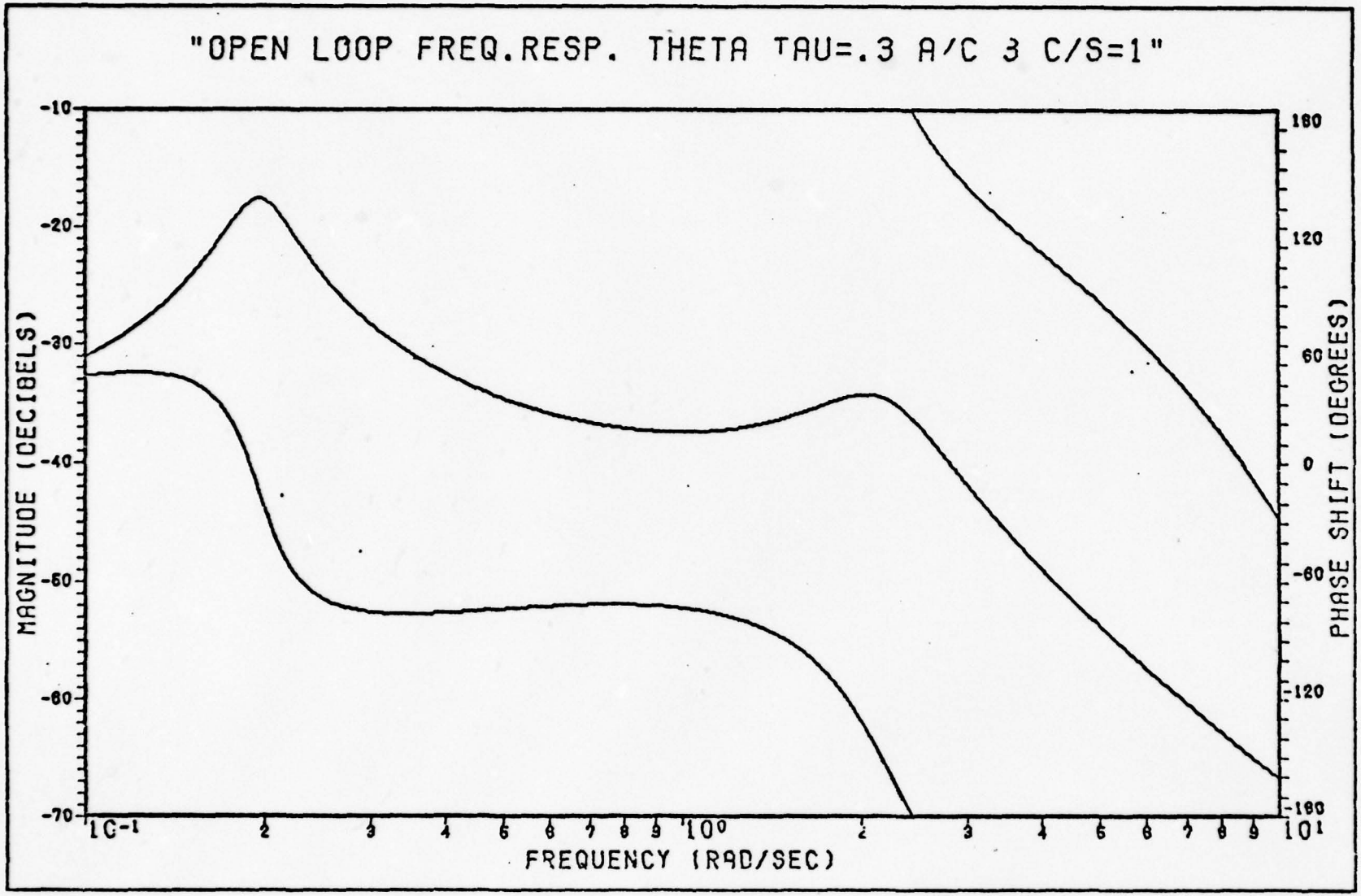

Fig. E14 Open-Loop Frequency Response θ For τ = 0.3 sec. A/C 3 C/S = 1

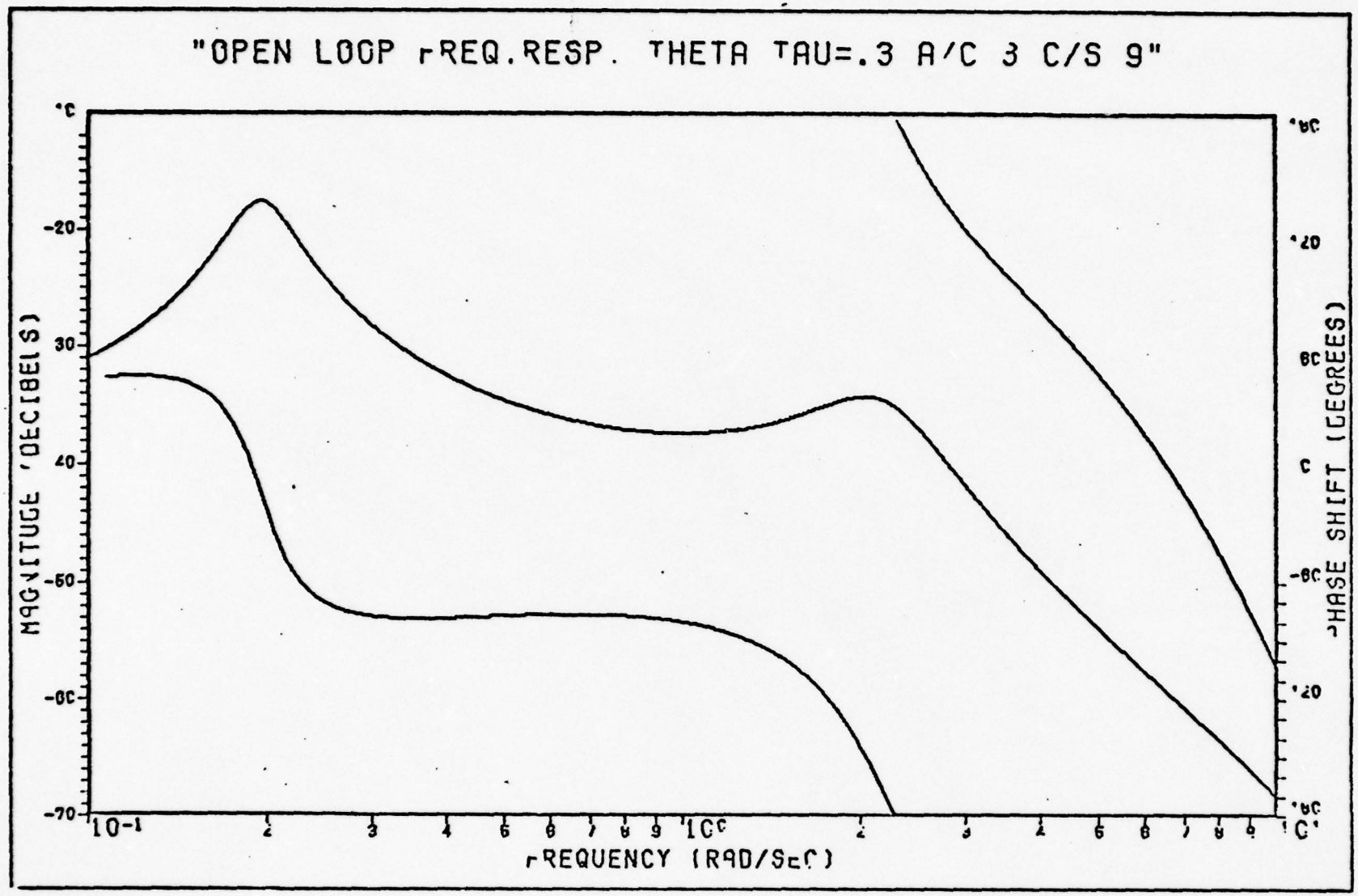

Fig. E15 Open-Loop Frequency Response θ For τ = 0.3 sec. A/C 3 C/S 9

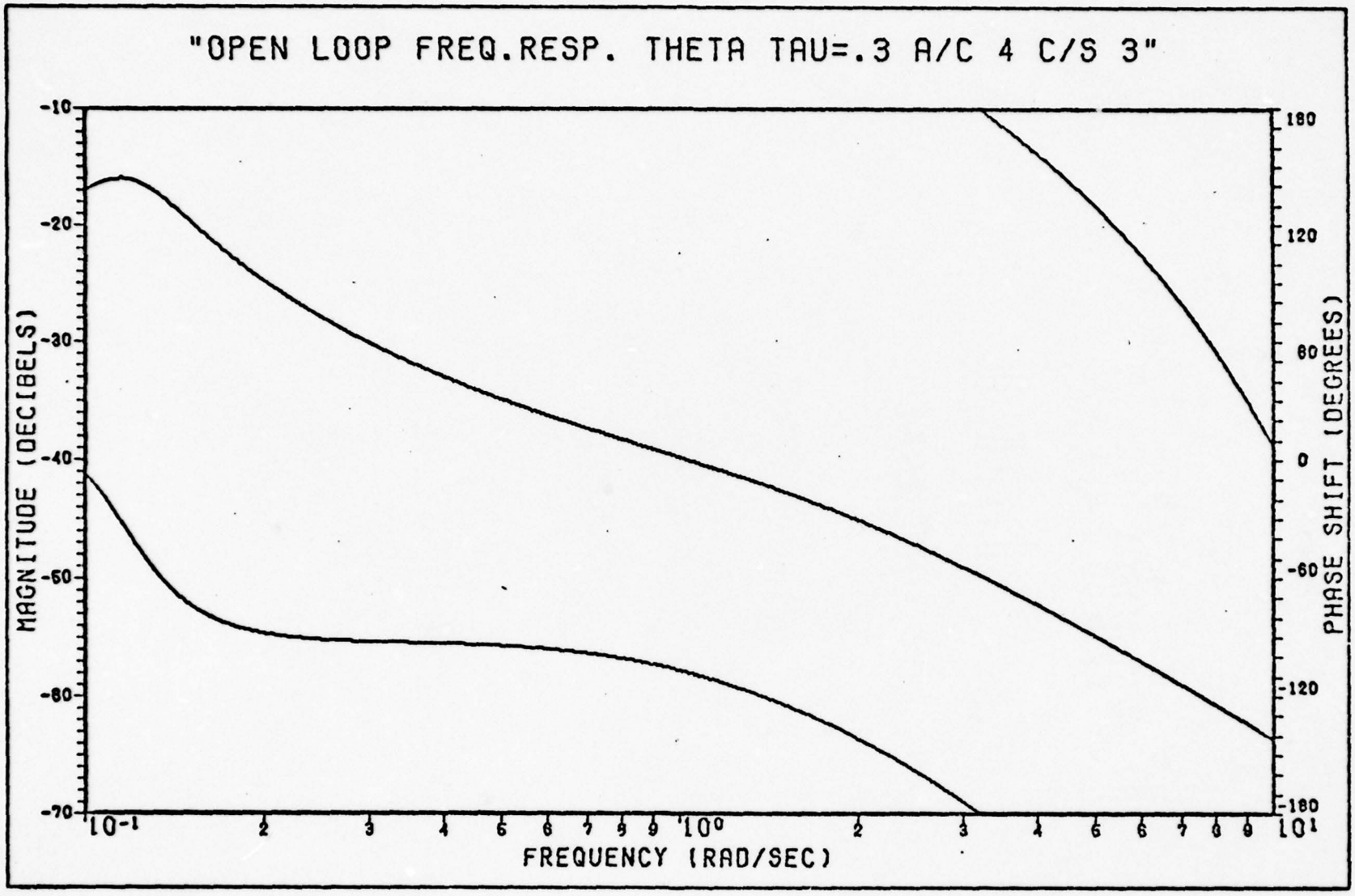

Fig. E16 Open-Loop Frequency Response θ For τ = 0.3 sec. A/C 4 C/S 3

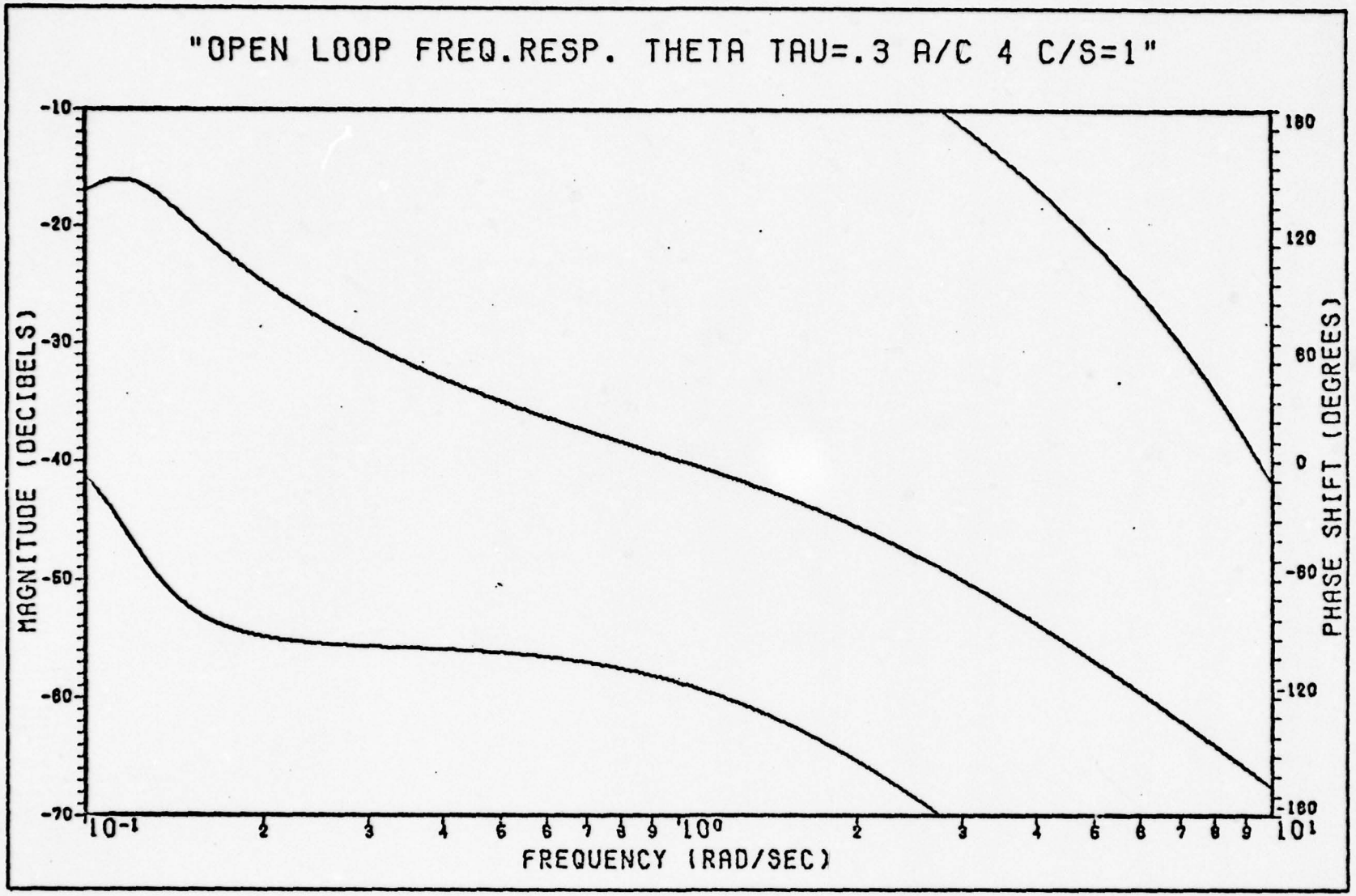

Fig. E17 Open-Loop Frequency Response θ For τ = 0.3 sec. A/C 4 C/S = 1

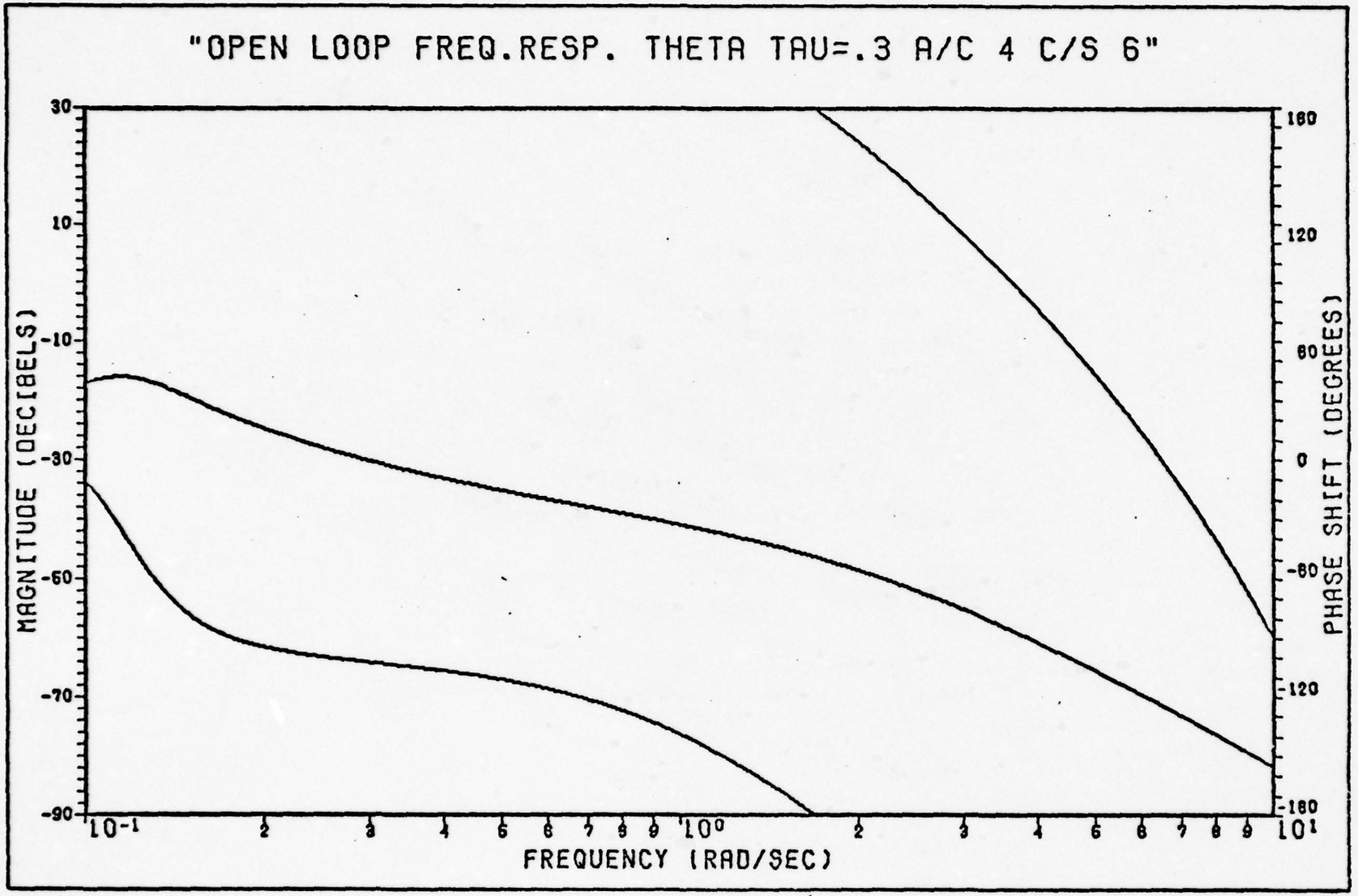

Fig. E18 Open-Loop Frequency Response θ For τ = 0.3 sec. A/C 4 C/S 6

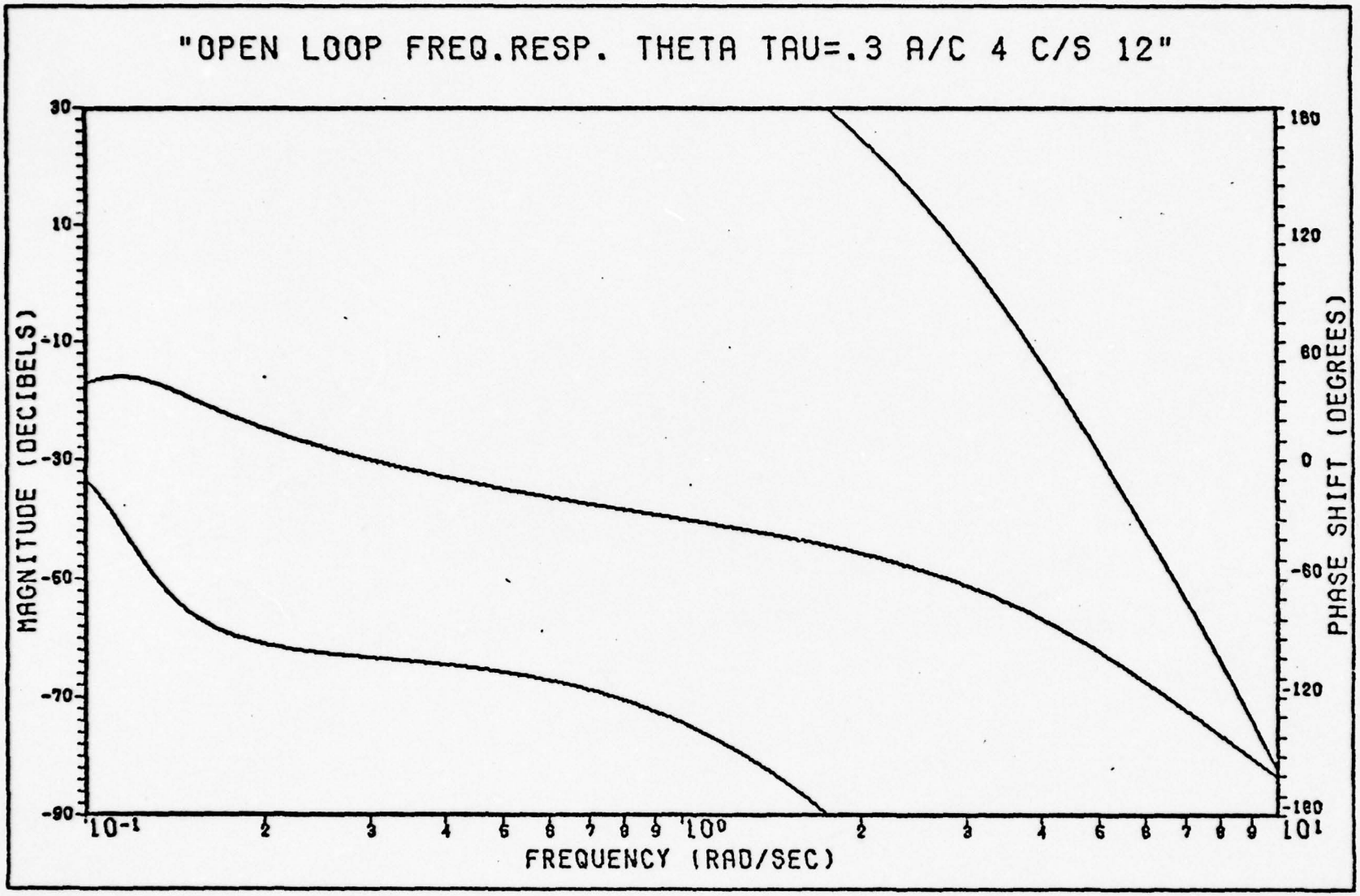

Fig. E19 Open-Loop Frequency Response θ For τ = 0.3 sec. A/C 4 C/S 12

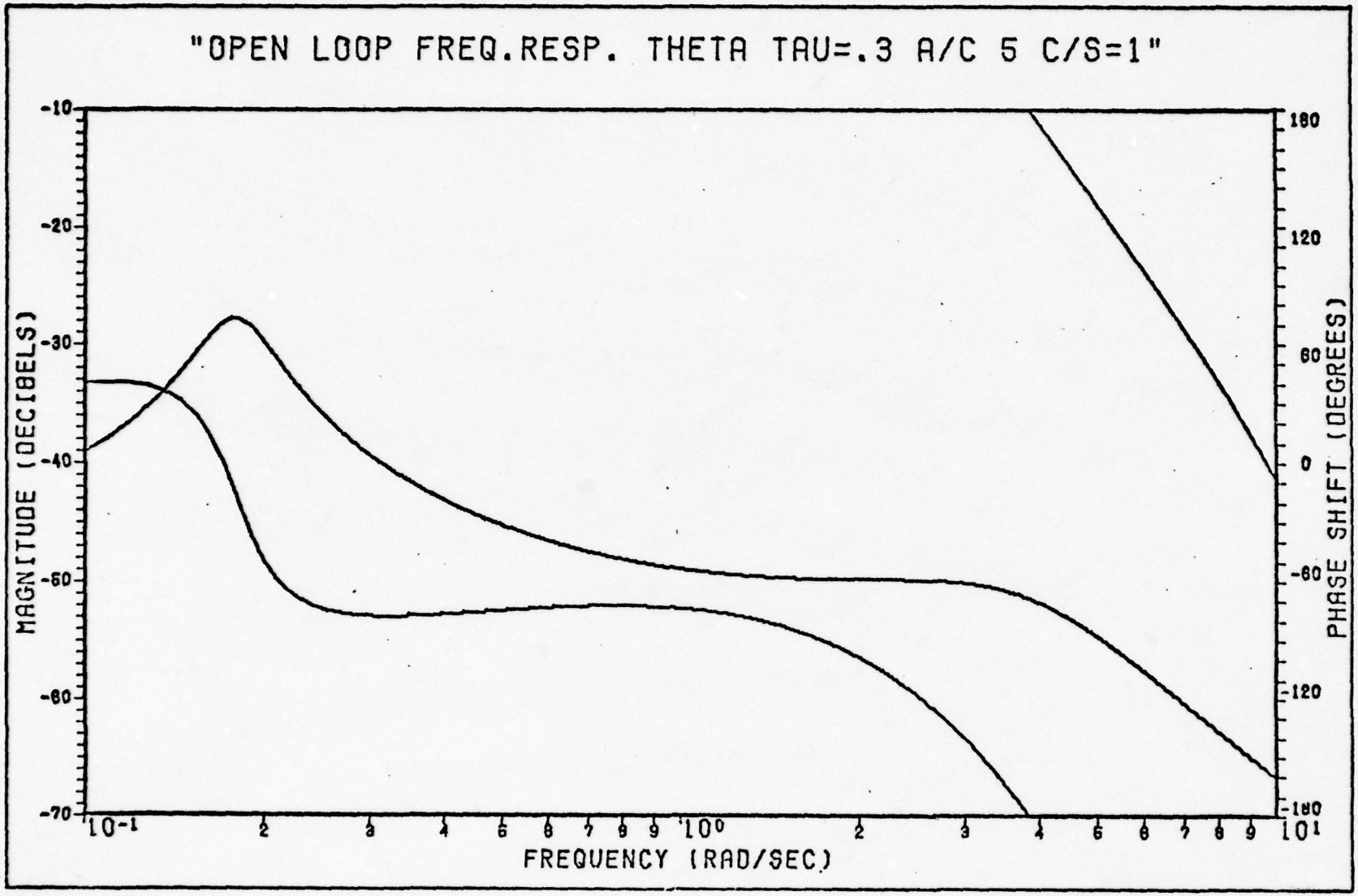

Fig. E20 Open-Loop Frequency Response θ For τ = 0.3 sec. A/C 5 C/S = 1

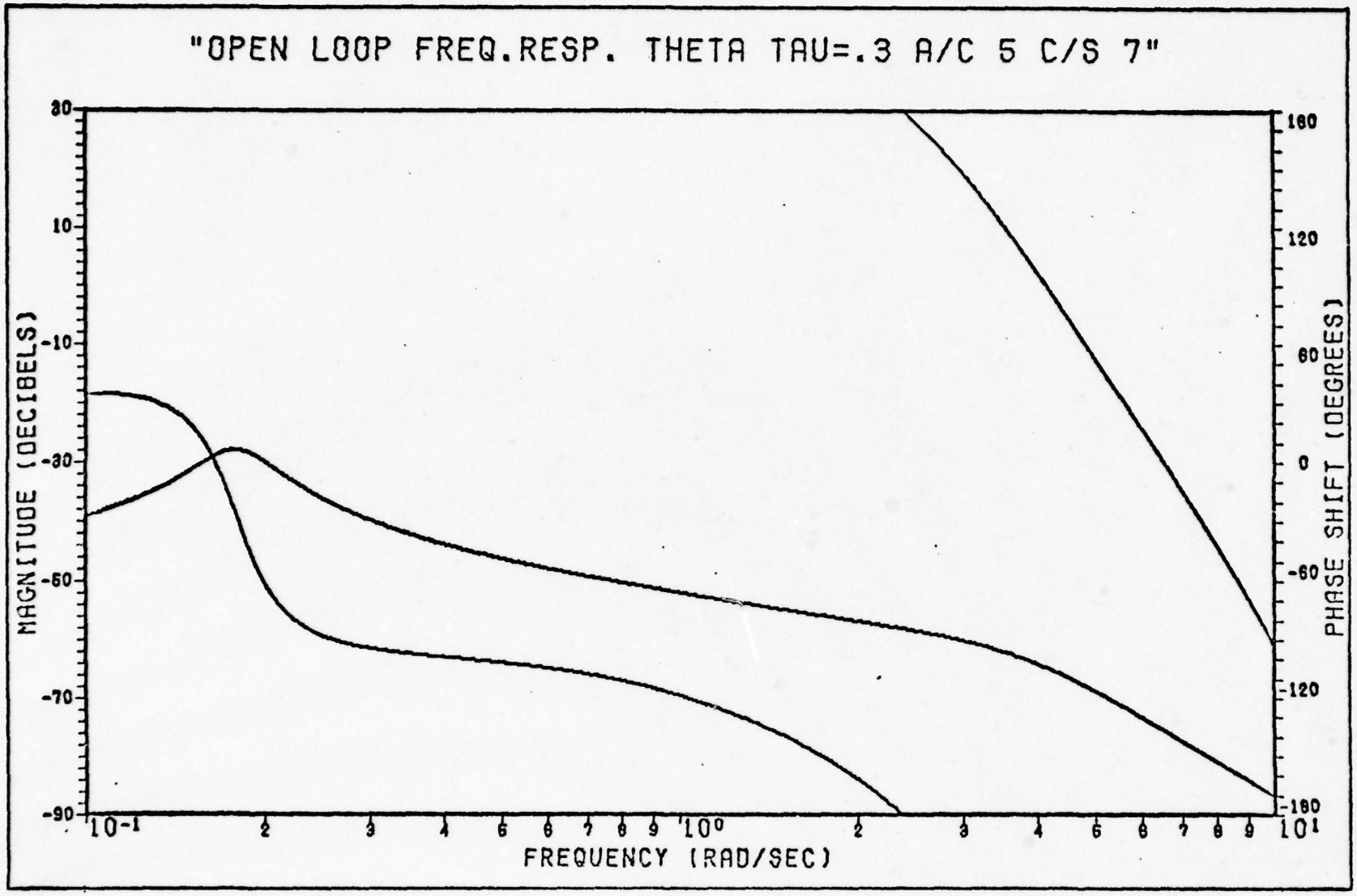

Fig. E21 Open-Loop Frequency Response θ For τ = 0.3 sec. A/C 5 C/S 7

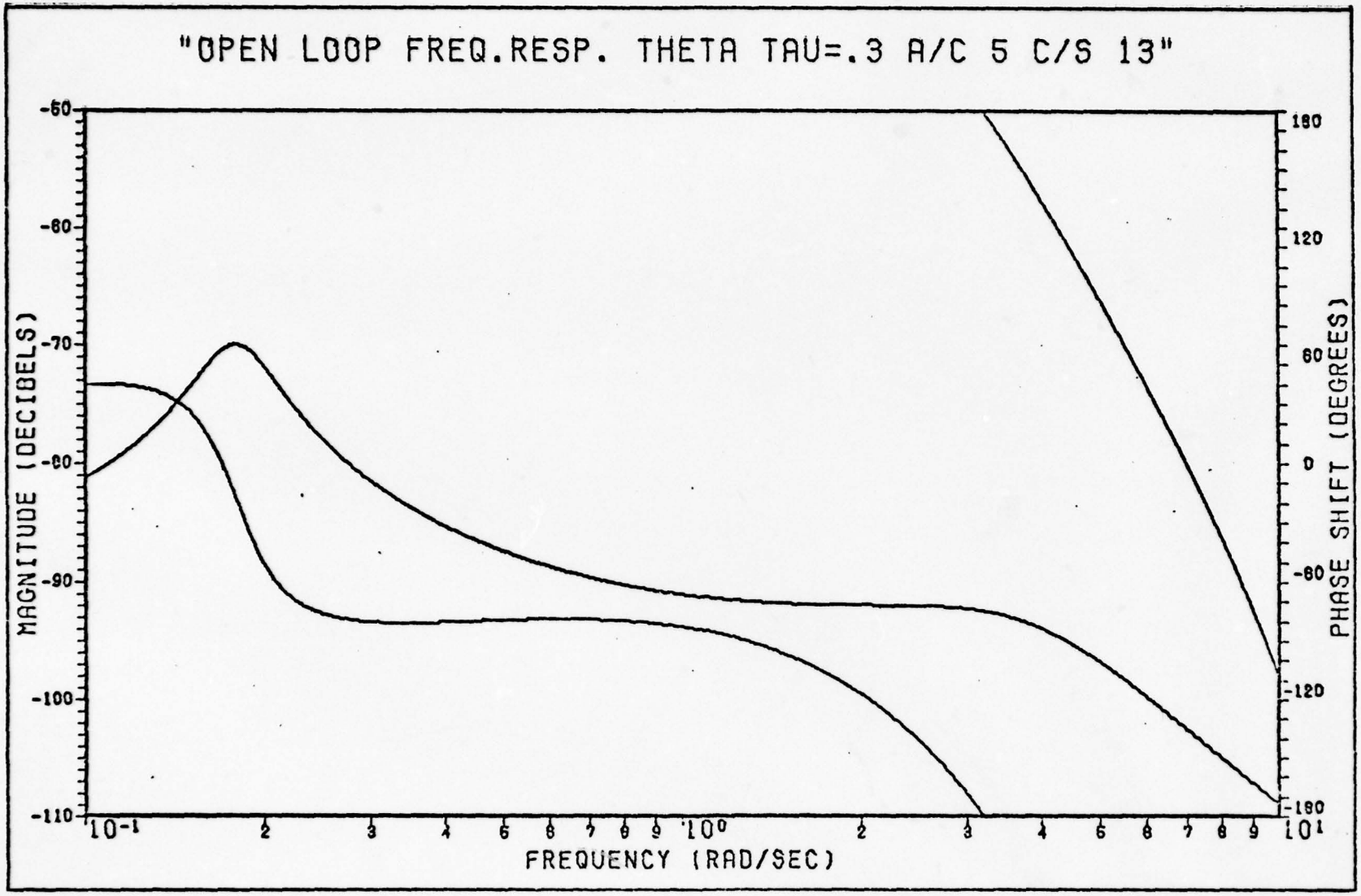

Fig. E22 Open-Loop Frequency Response θ For τ = 0.3 sec. A/C 5 C/S 13

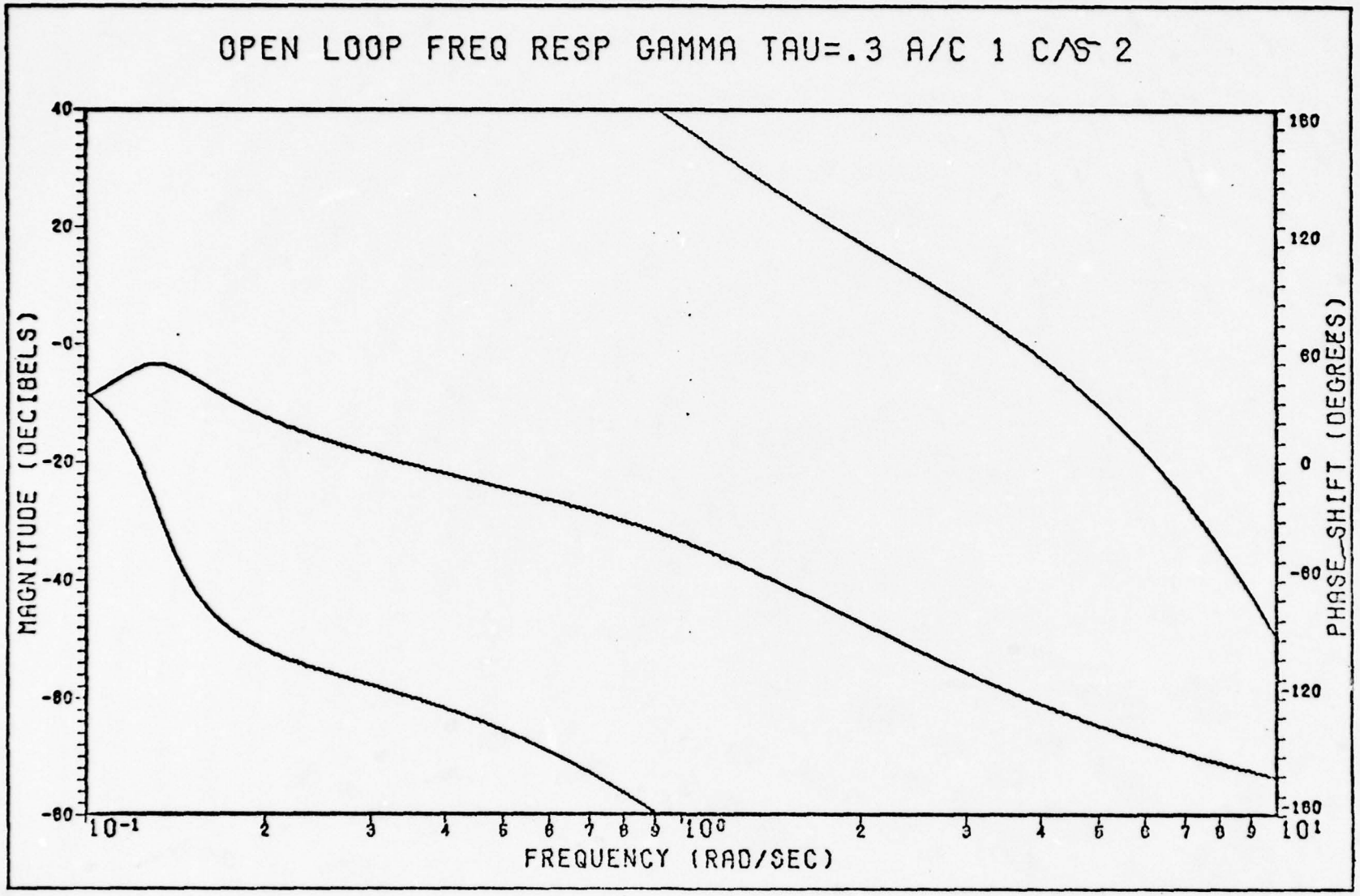

Fig. E23 Open-Loop Frequency Response γ For τ = 0.3 sec. A/C 1 C/S 2

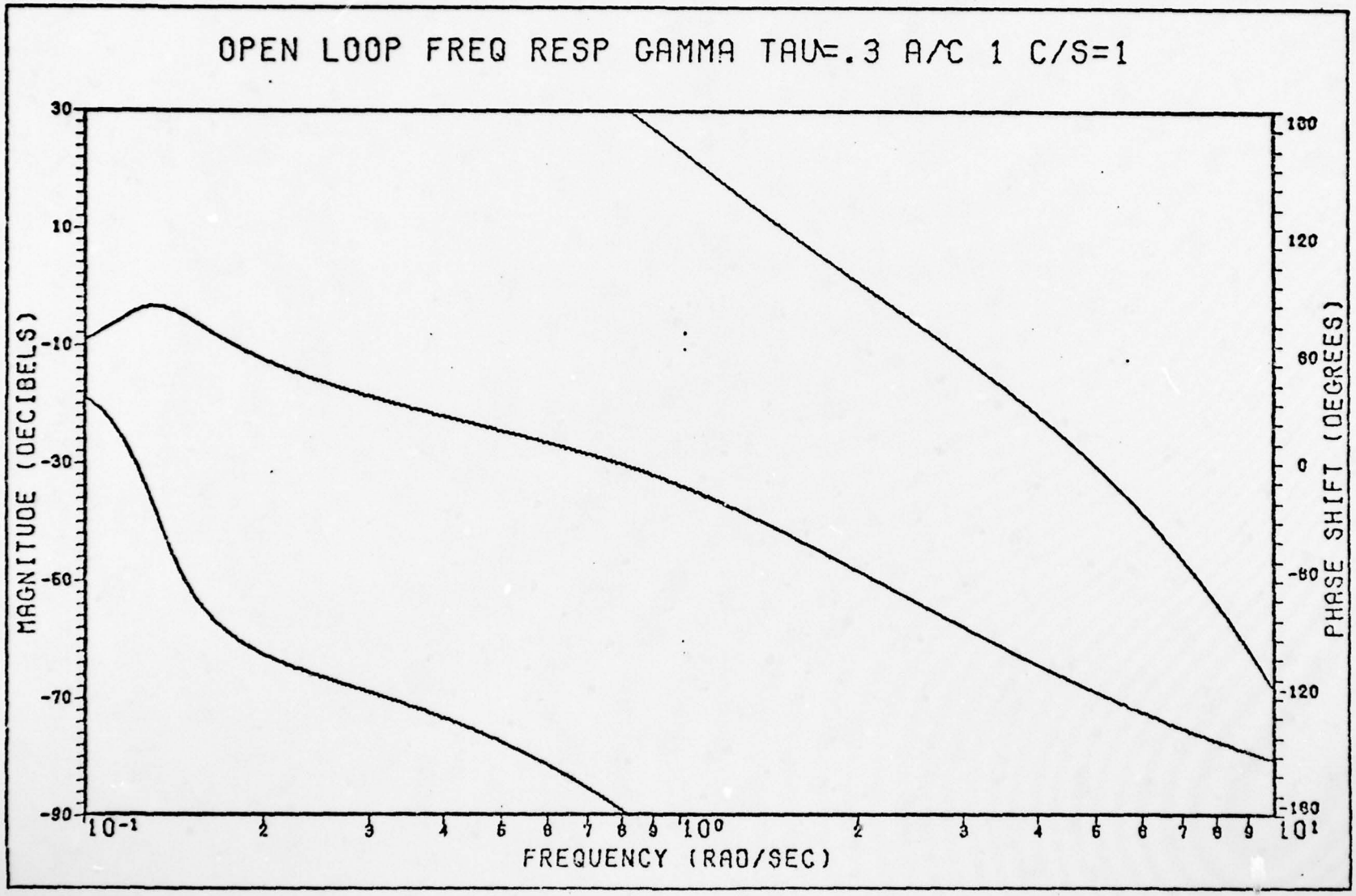

Fig. E24 Open-Loop Frequency Response γ For τ = 0.3 sec. A/C 1 C/S = 1

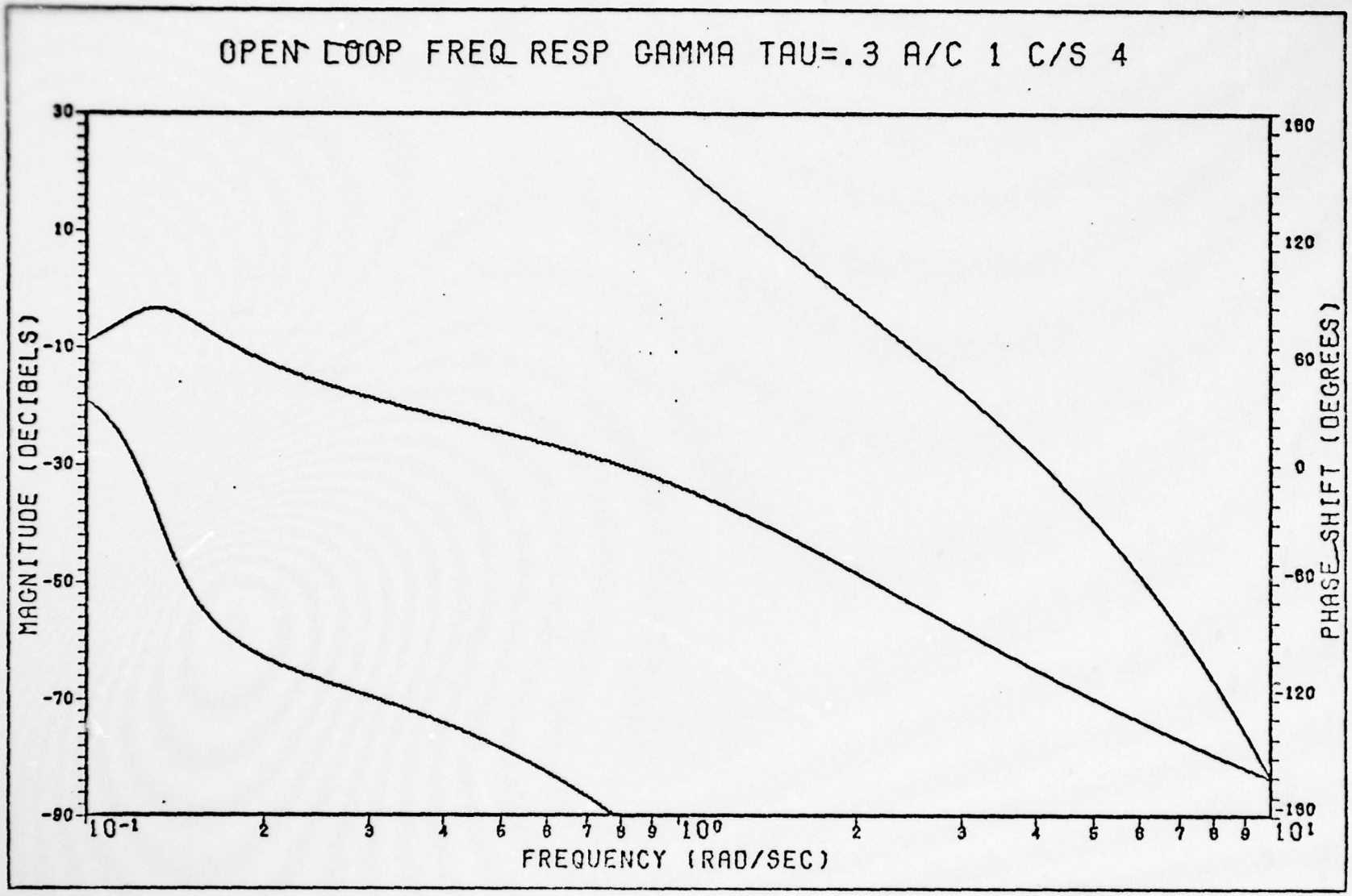

Fig. E25 Open-Loop Frequency Response γ For τ = 0.3 sec. A/C 1 C/S 4

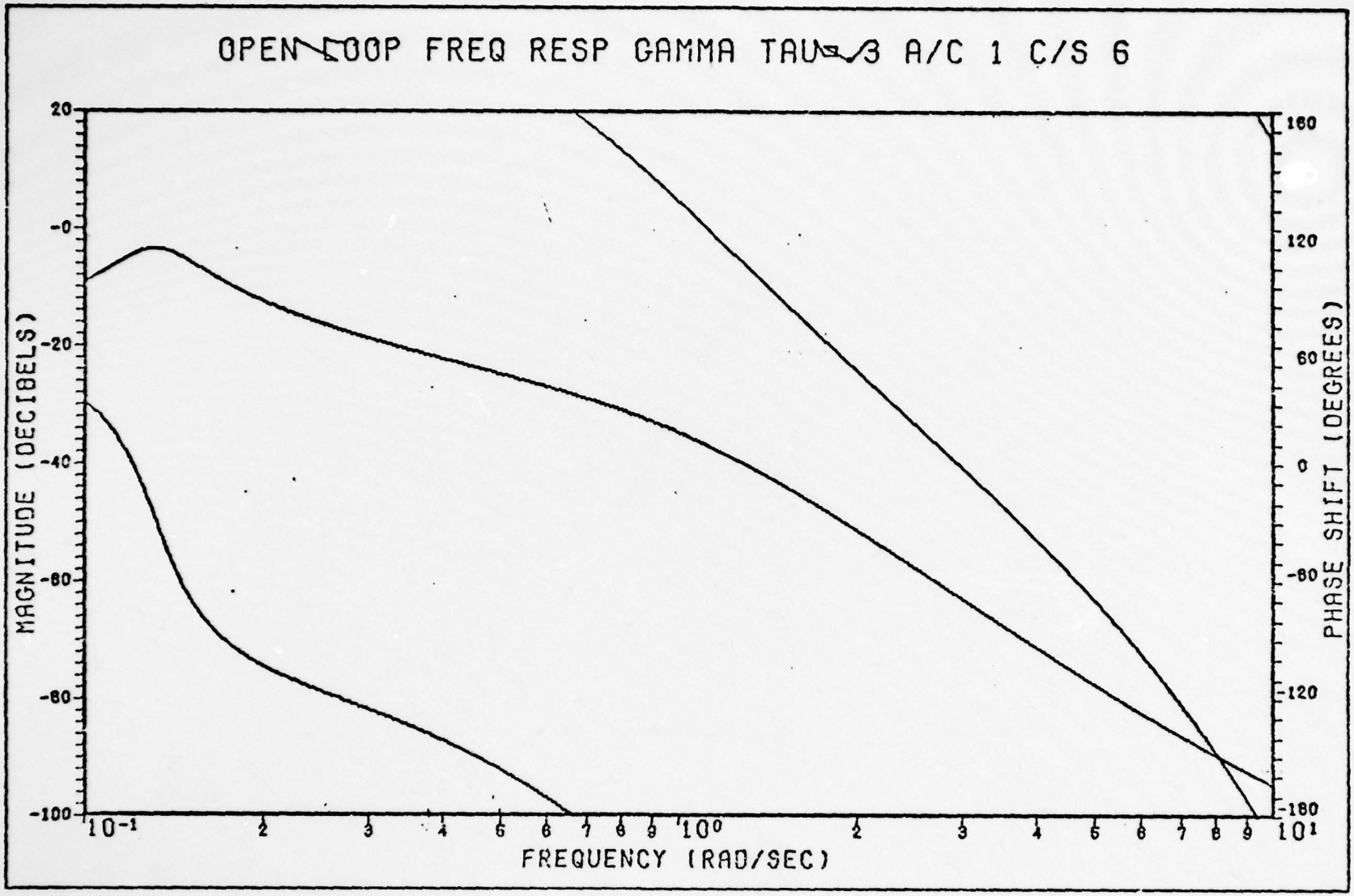

Fig. E26 Open-Loop Frequency Response γ For τ = 0.3 sec. A/C 1 C/S 6

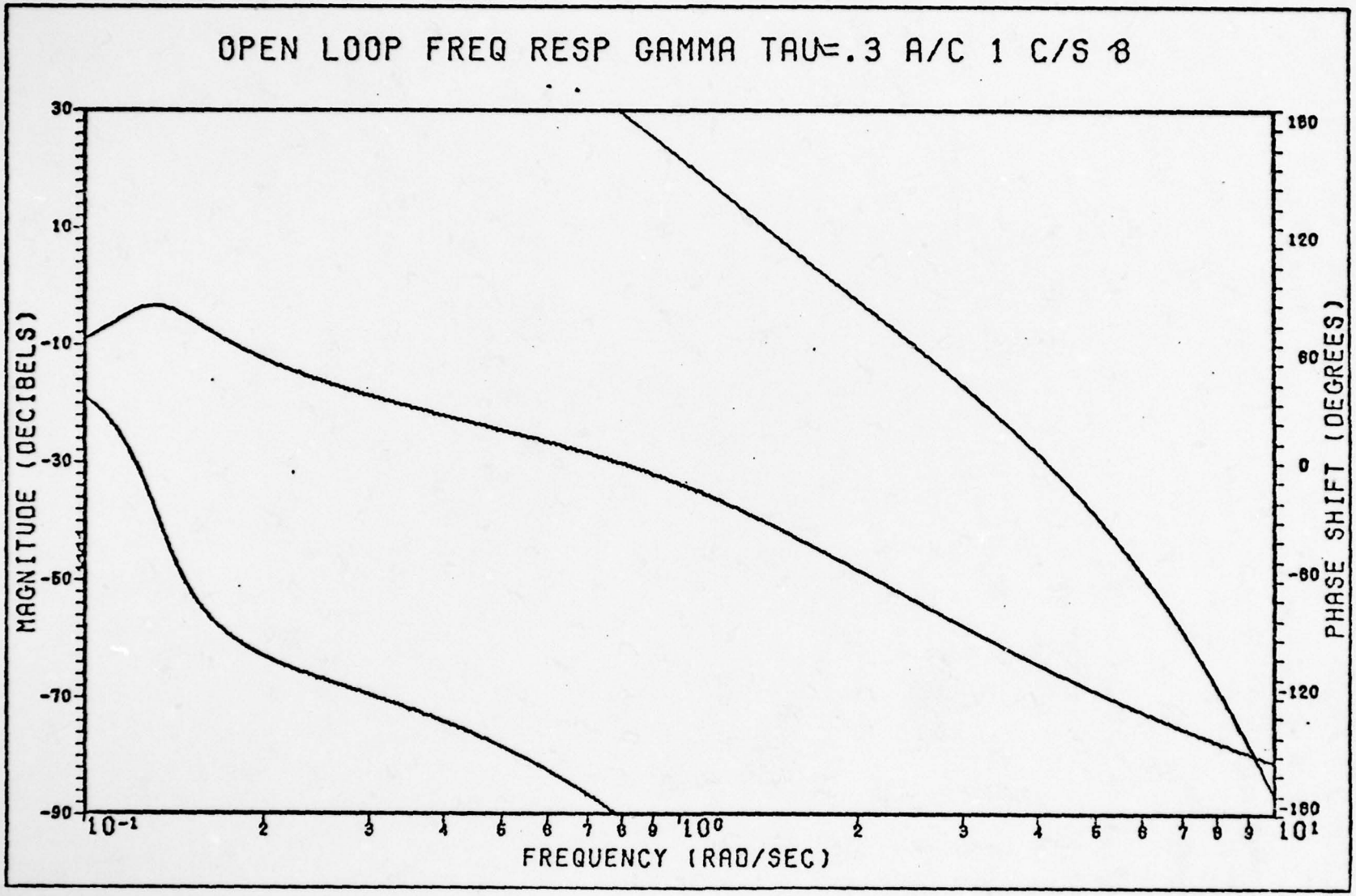

Fig. E27 Open-Loop Frequency Response γ For τ = 0.3 sec. A/C 1 C/S 8

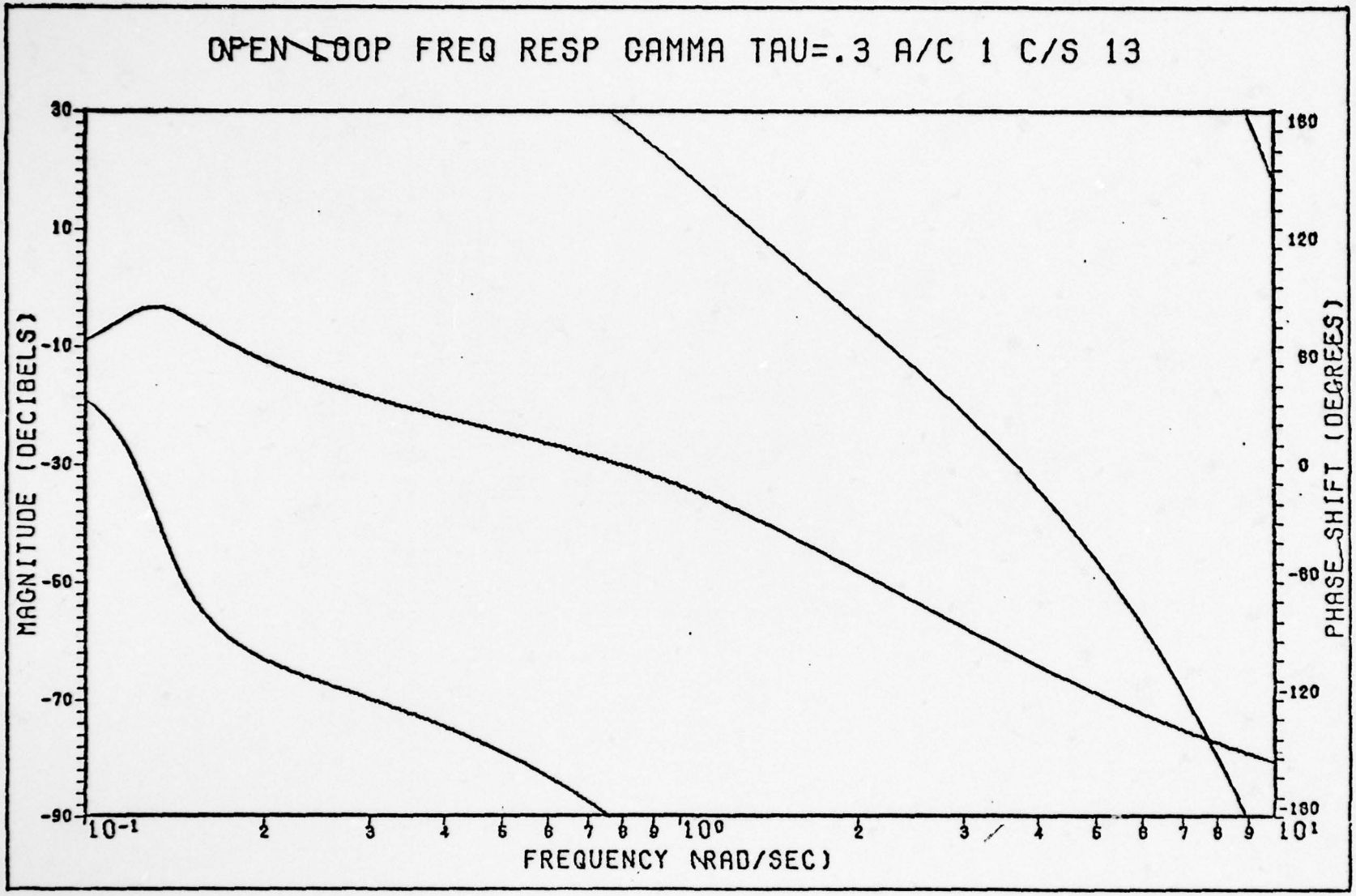

Fig. E28 Open-Loop Frequency Response γ For τ = 0.3 sec. A/C 1 C/S 13

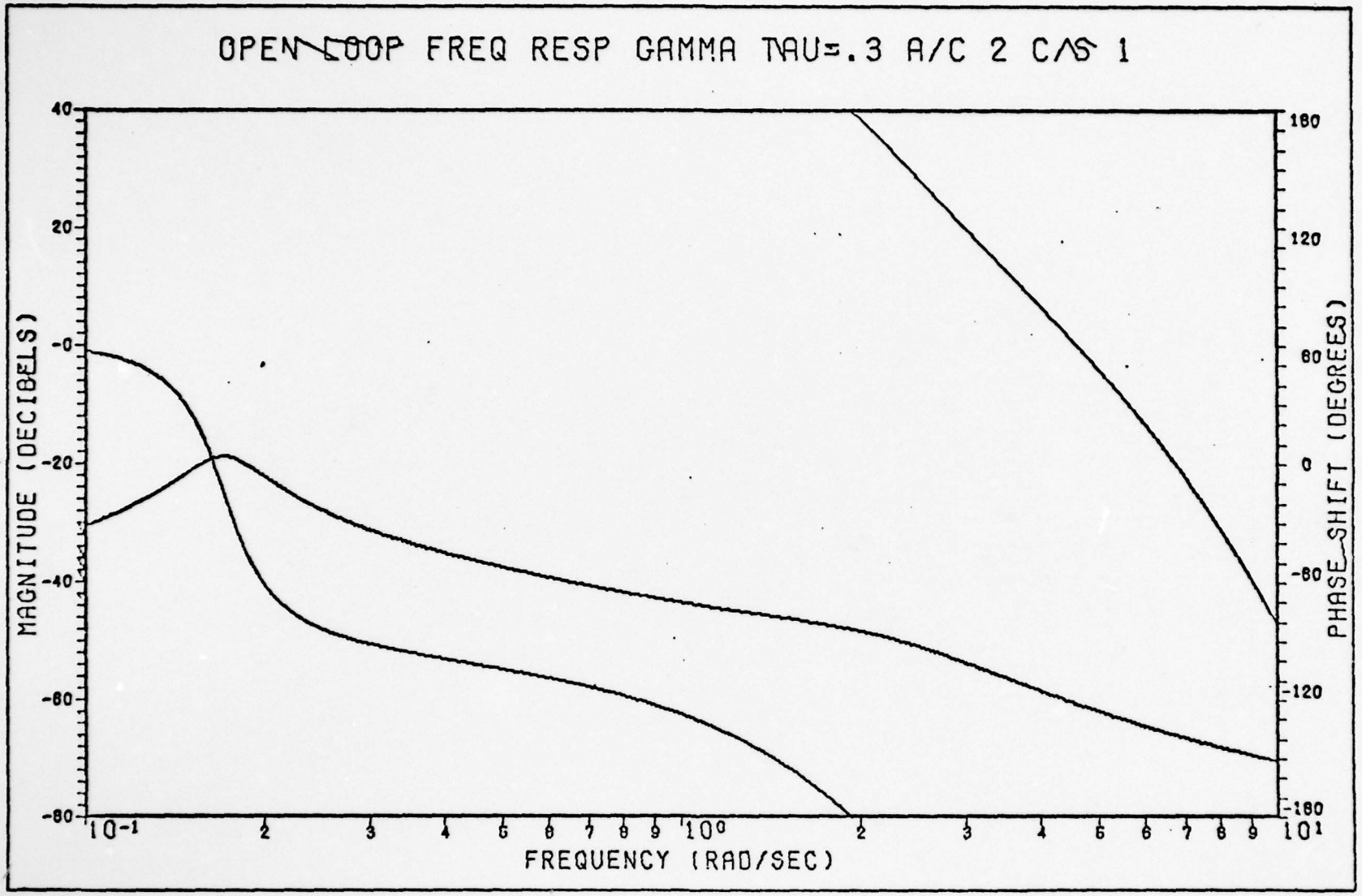

Fig. E29 Open-Loop Frequency Response γ For τ = 0.3 sec. A/C 2 C/S 1

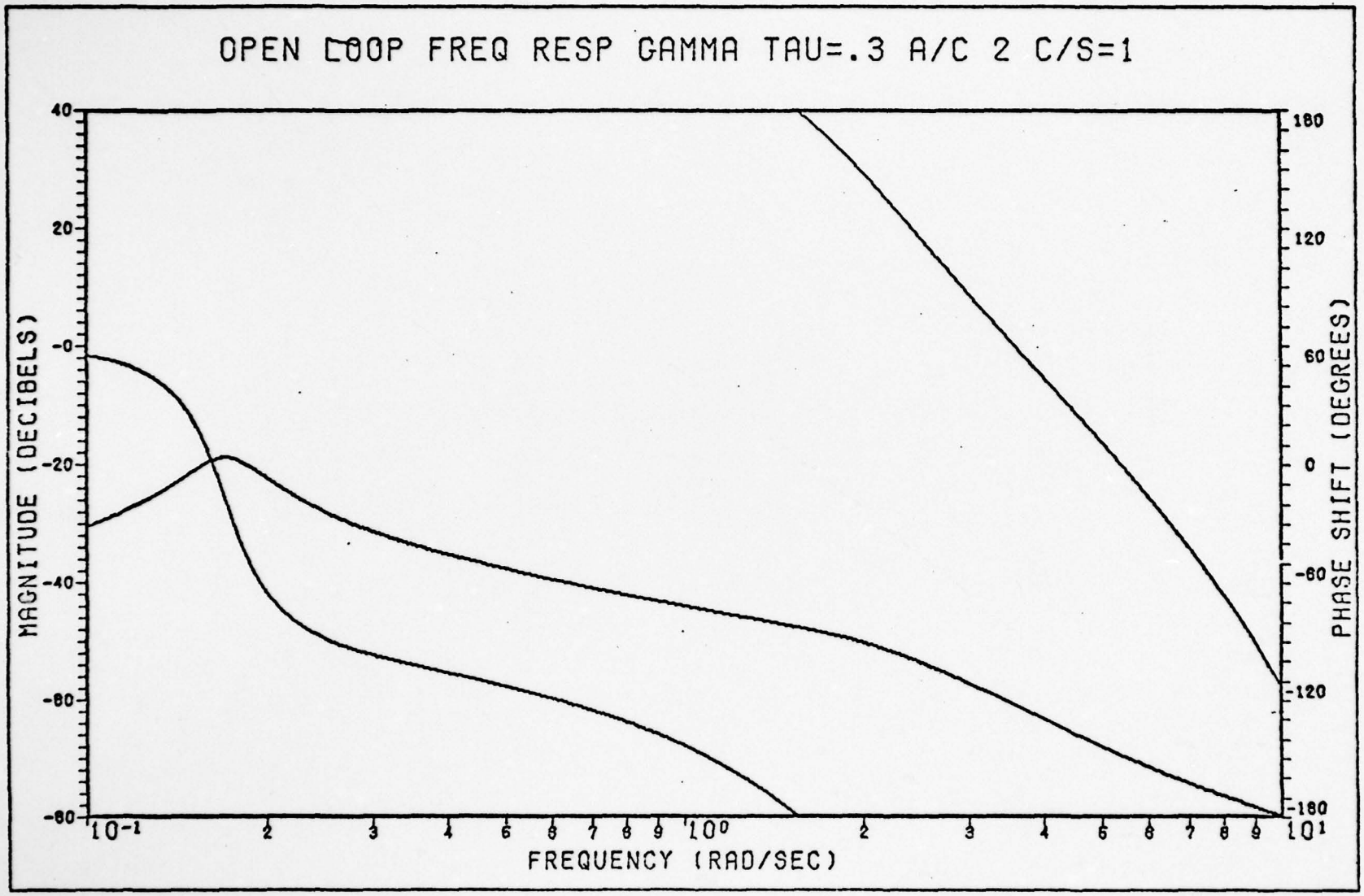

Fig. E30 Open-Loop Frequency Response γ For τ = 0.3 sec. A/C 2 C/S = 1

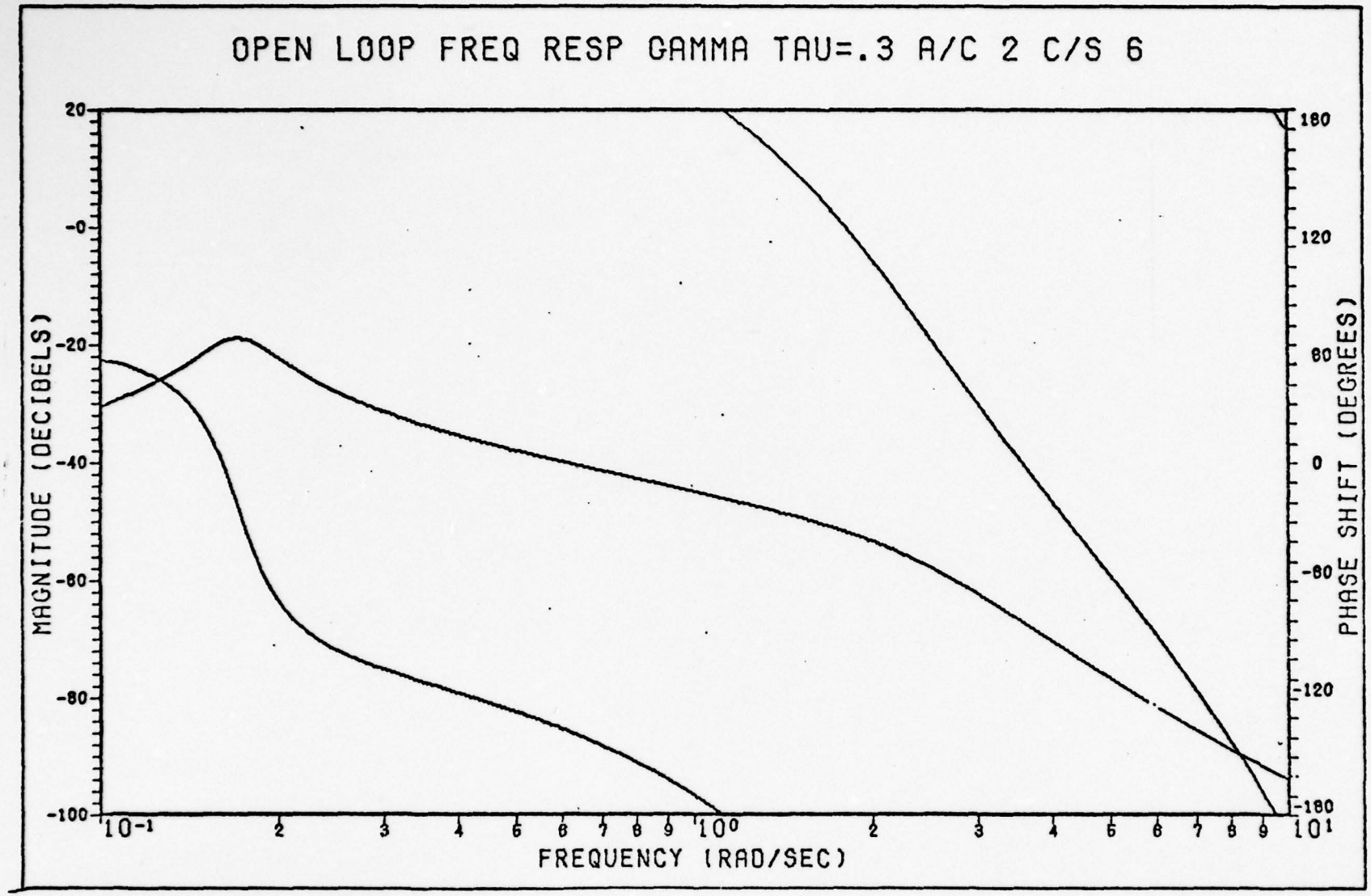

Fig. E31 Open-Loop Frequency Response γ For $\tau = 0.3$ sec. A/C 2 C/S 6

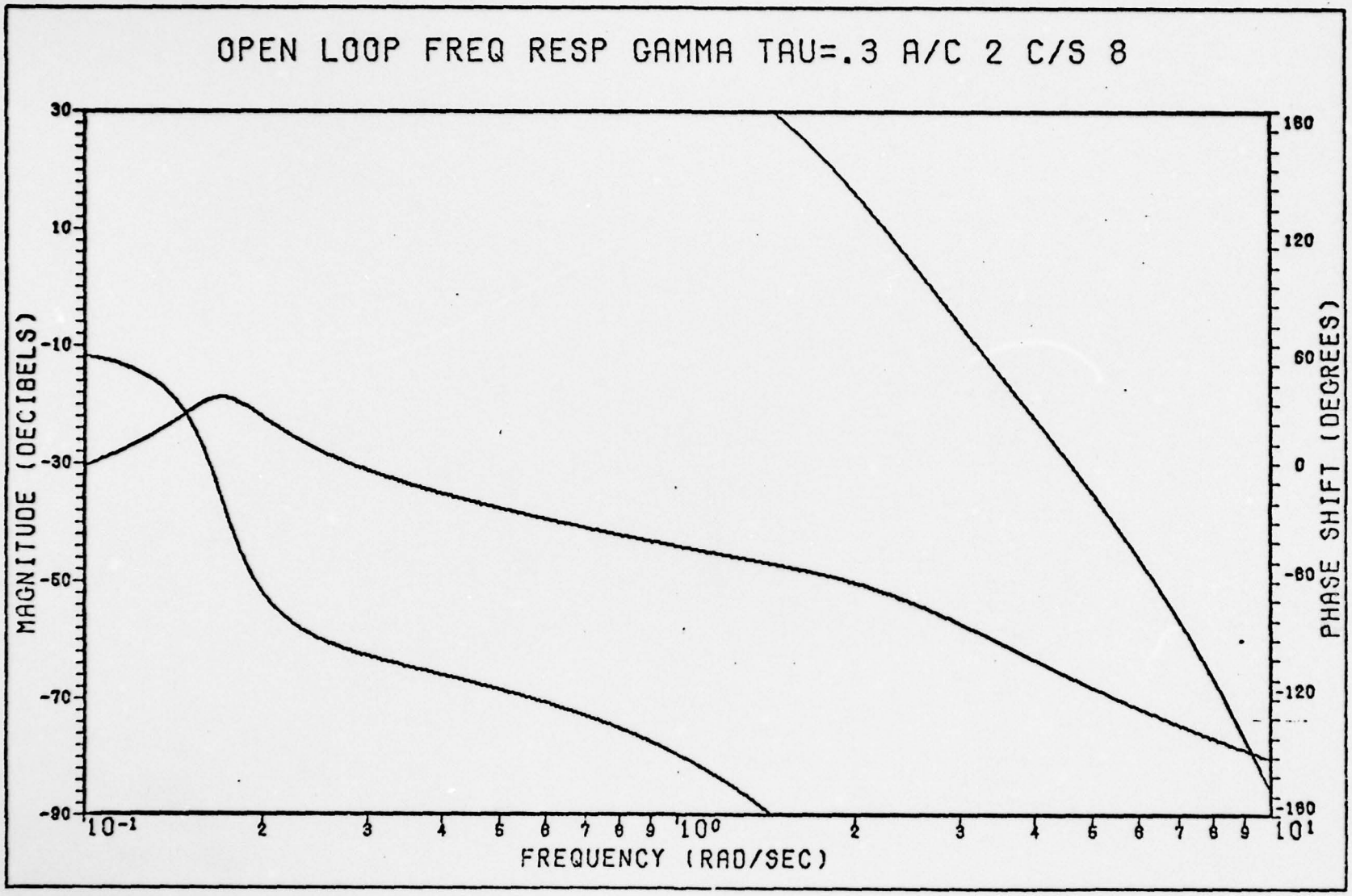

Fig. E32 Open-Loop Frequency Response γ For $\tau = 0.3$ sec. A/C 2 C/S 8

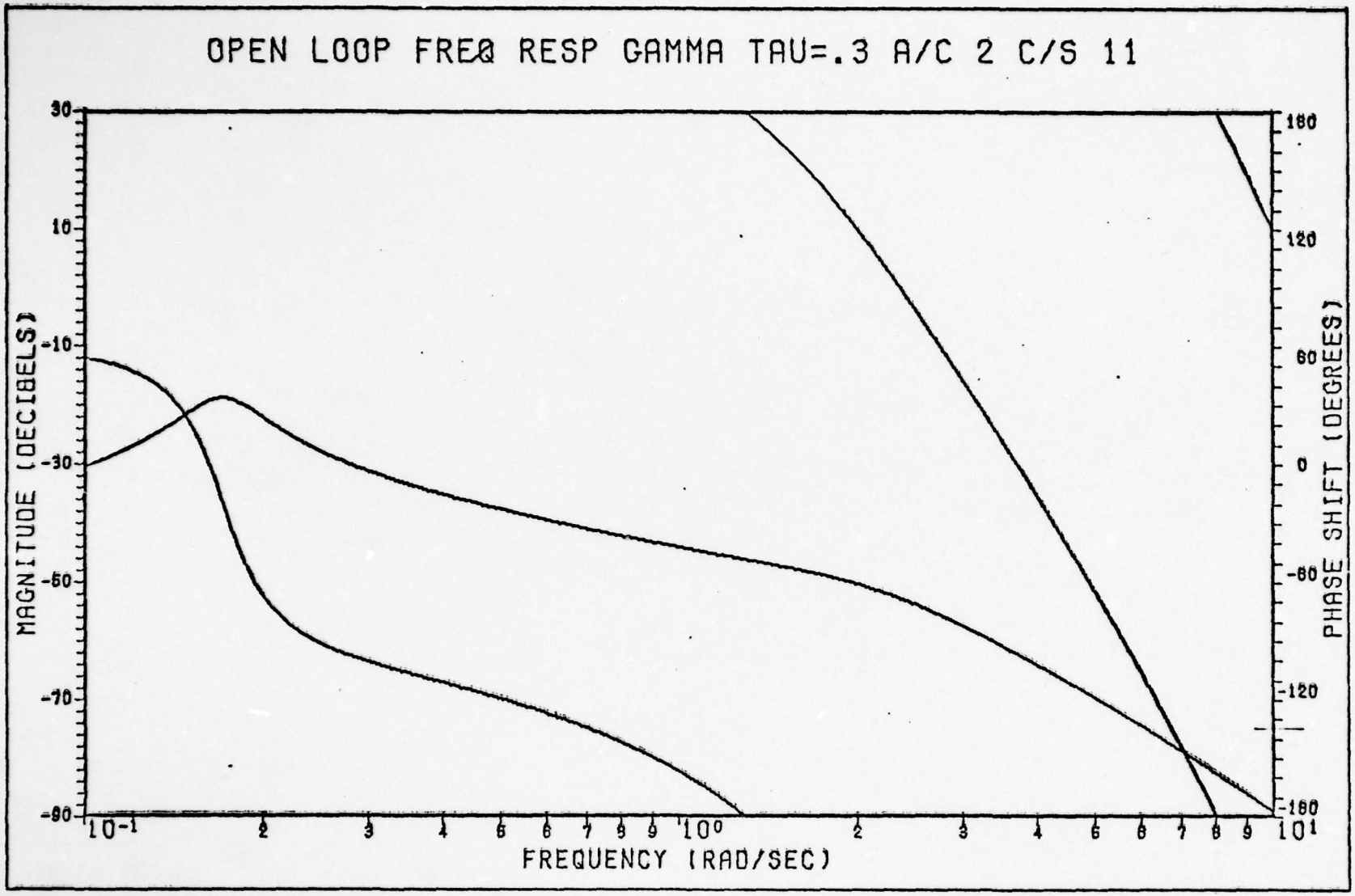

Fig. E33 Open-Loop frequency Response γ For $\tau = 0.3$ sec. A/C 2 C/S 11

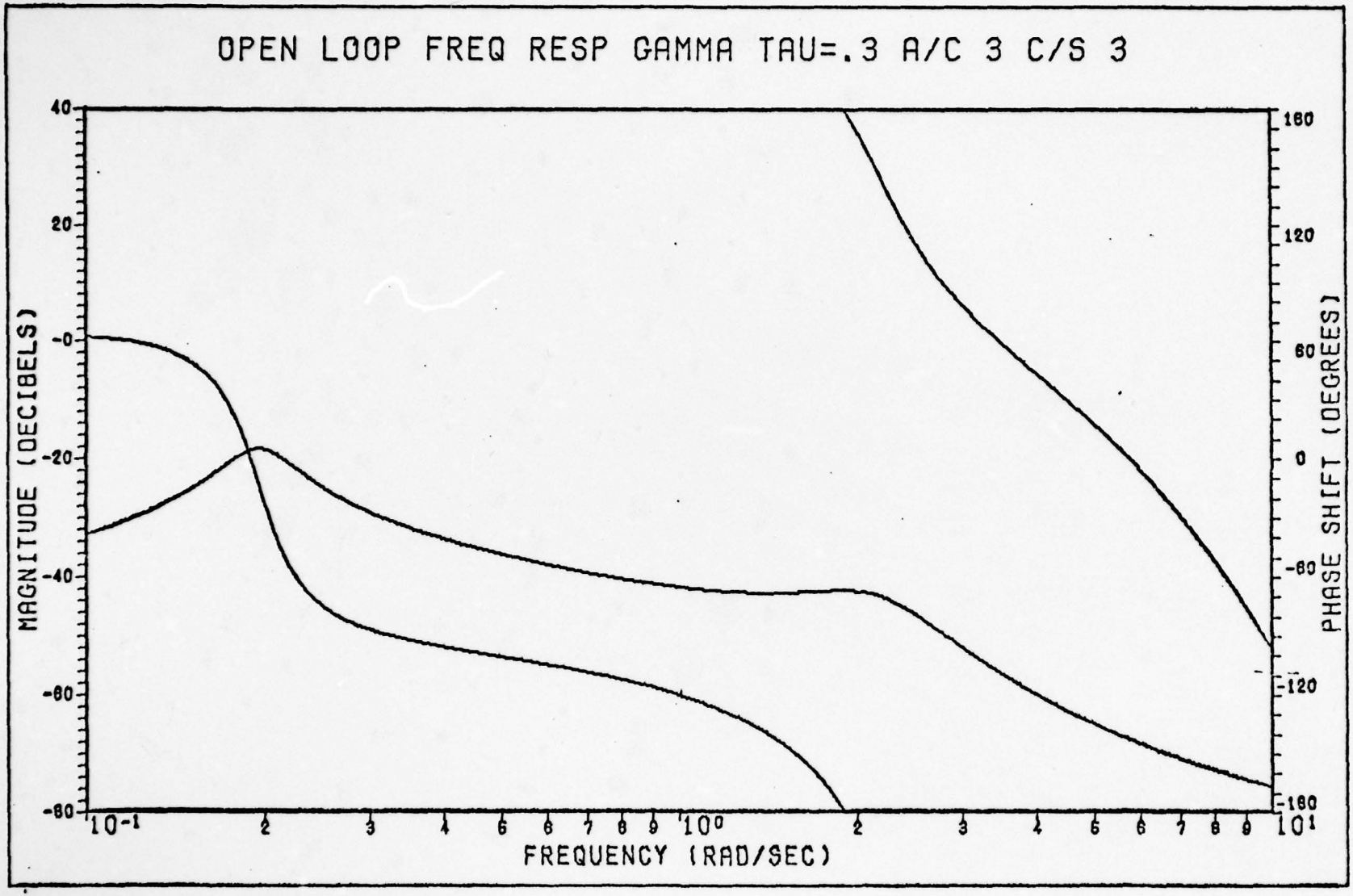

Fig. E34 Open-Loop Frequency γ For $\tau = 0.3$ sec. A/C 3 C/S 3

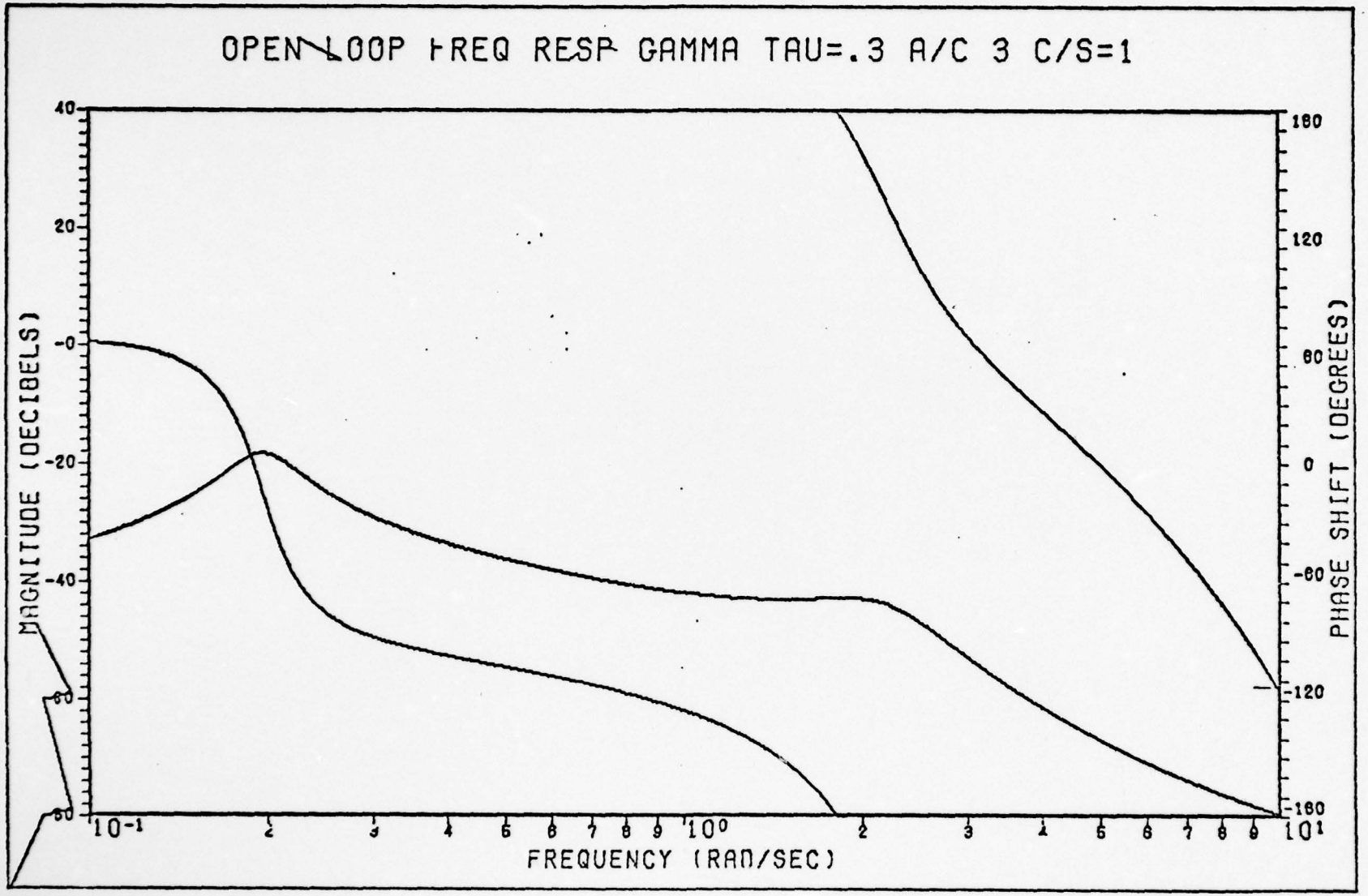

Fig. E35 Open-Loop Frequency Response γ For τ = 0.3 sec. A/C 3 C/S = 1

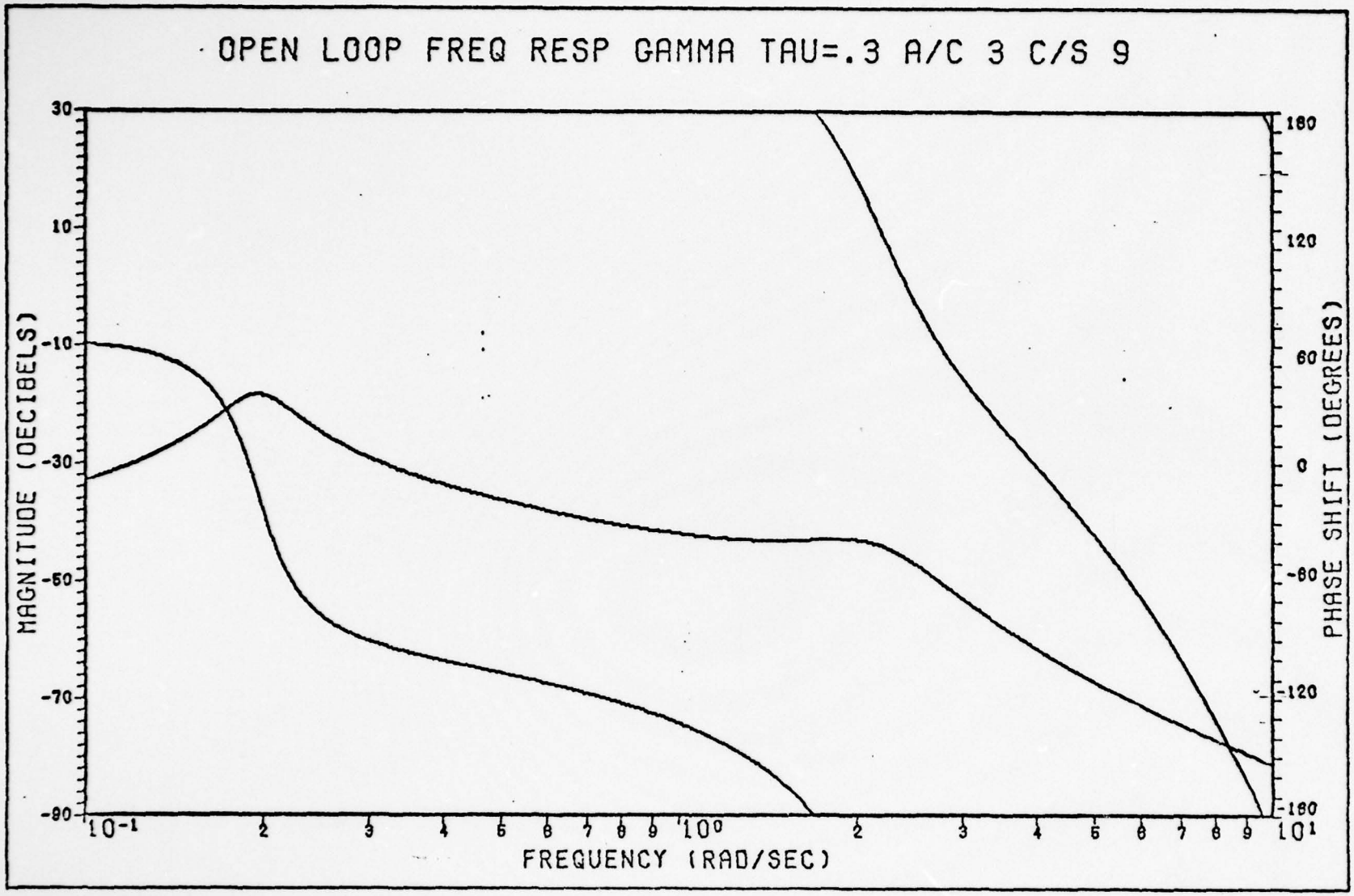

Fig. E36 Open-Loop Frequency Response γ For $\tau = 0.3$ sec. A/C 3 C/S 9

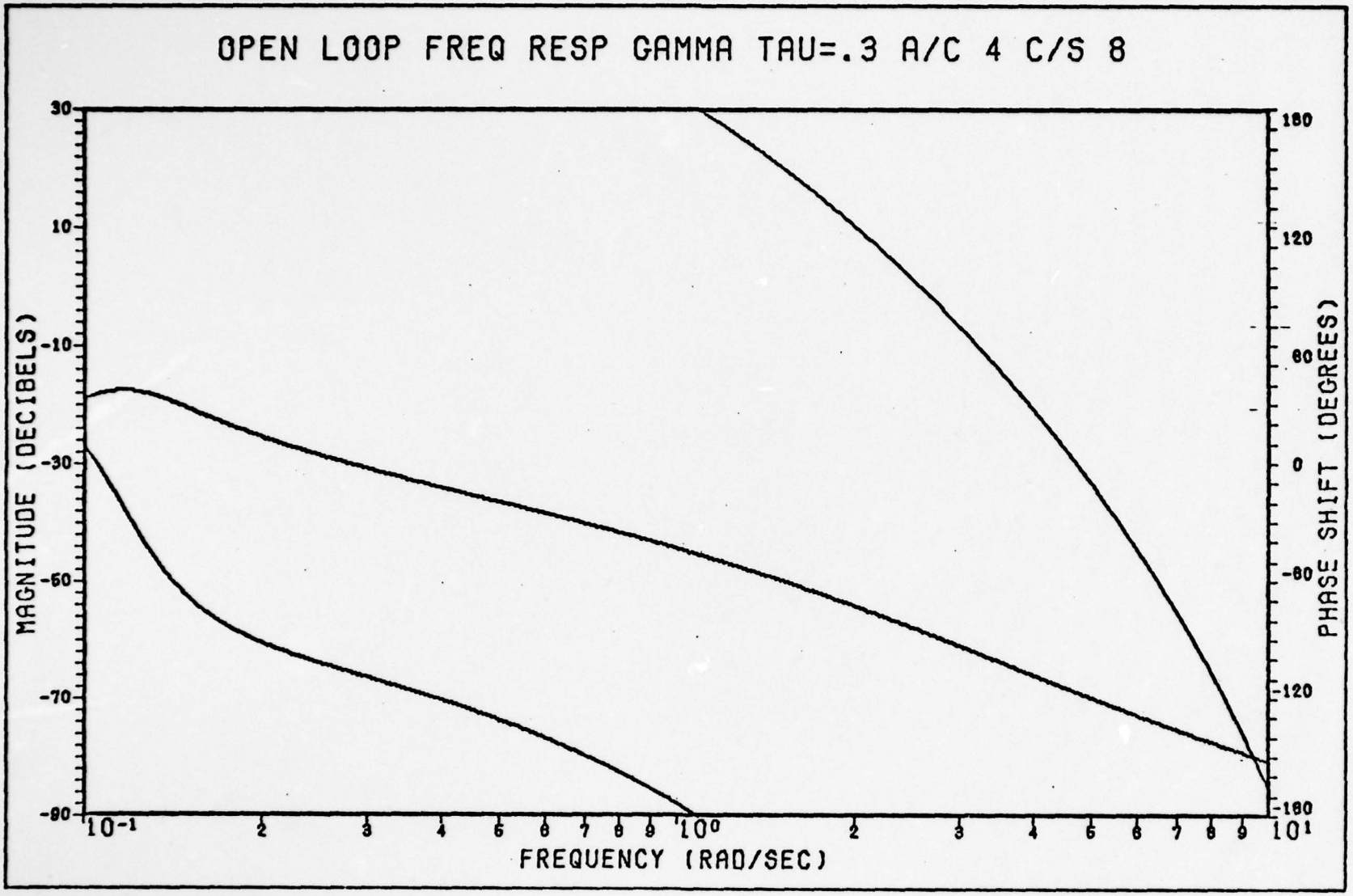

Fig. 37 Open-Loop Frequency Response γ For $\tau = 0.3$ sec. A/C 4 C/S 8

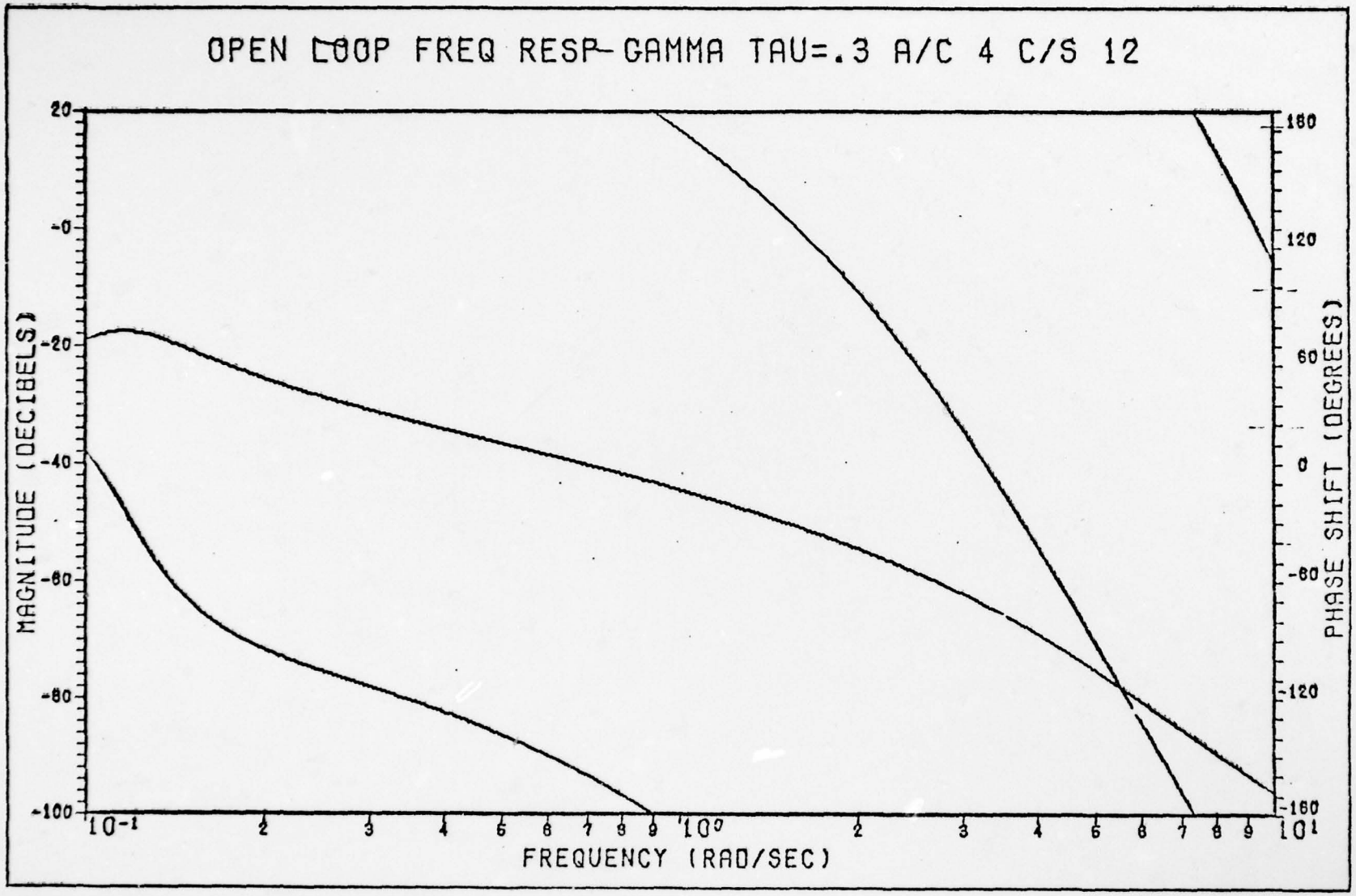

Fig. E38 Open-Loop Frequency Response γ For $\tau = 0.3$ sec. A/C 4 C/S 12

AD-A080 519 AIR FORCE INST OF TECH WRIGHT-PATTERSON AFB OH SCHOO--ETC F/G 5/8
ANALYSIS OF THE EFFECTS OF HIGHER ORDER CONTROL SYSTEMS ON AIRC--ETC(U)
DEC 79 M A PASHA

UNCLASSIFIED AFIT/GE/EE/79-27 NL

3 OF 3
AD A080519

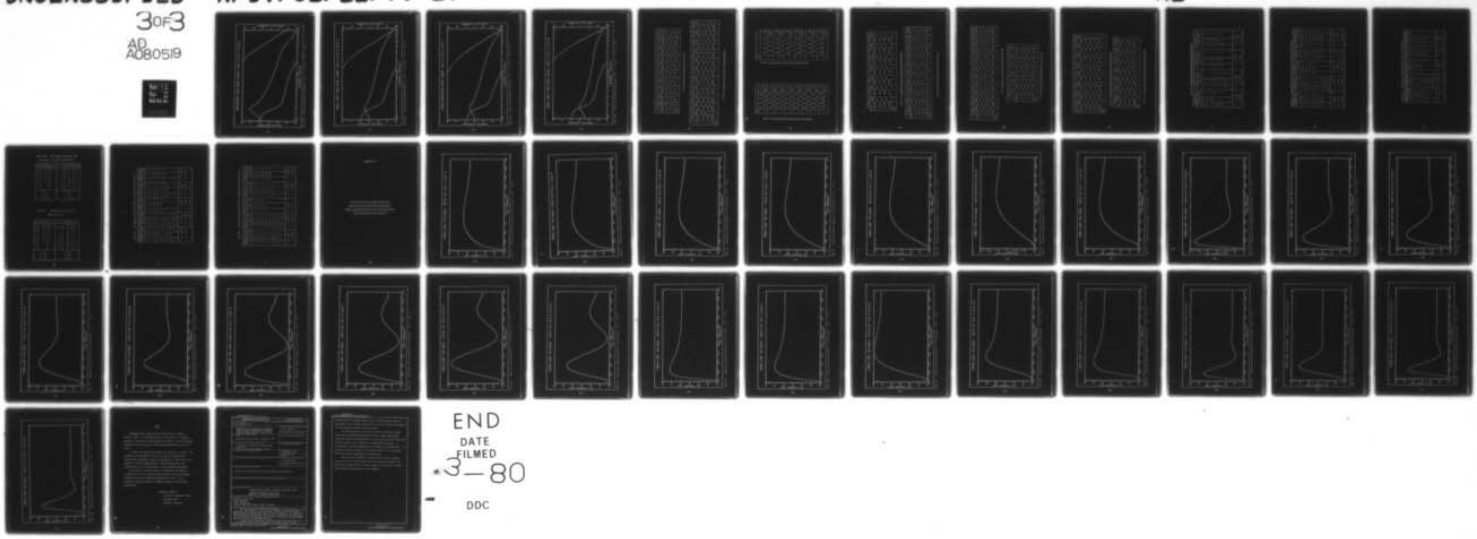

END
DATE FILMED
3-80
DDC

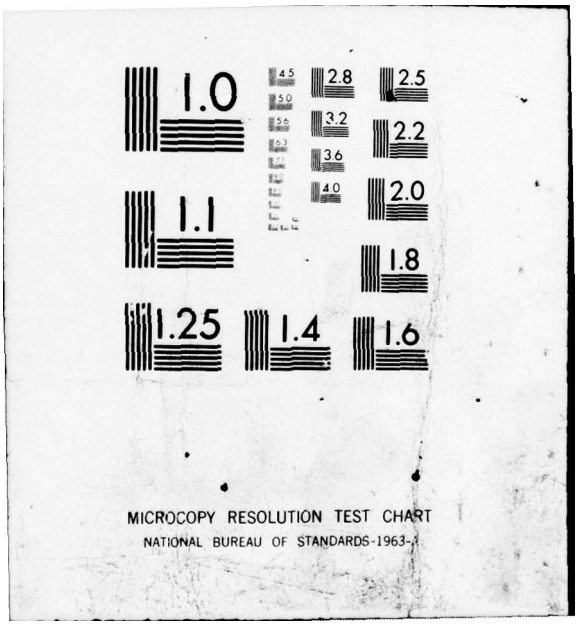
1.0
1.1
1.25
1.4
1.6
1.8
2.0
2.2
2.5
2.8
3.2
3.6
4.0
4.5
5.0
5.6
6.3
MICROCOPY RESOLUTION TEST CHART
NATIONAL BUREAU OF STANDARDS-1963-A

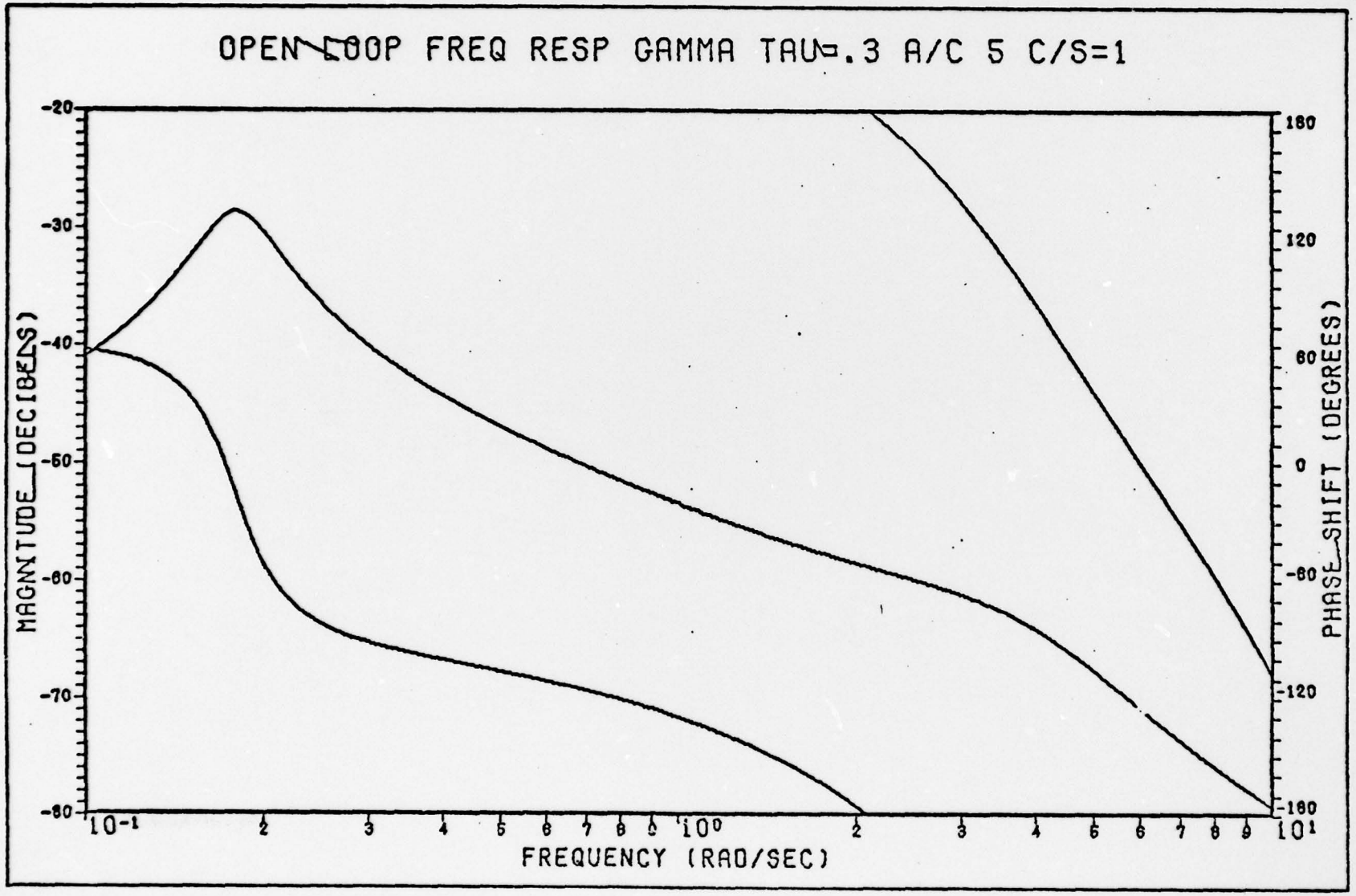

Fig. E39 Open-Loop Frequency Response γ For $\tau = 0.3$ sec. A/C 5 C/S = 1

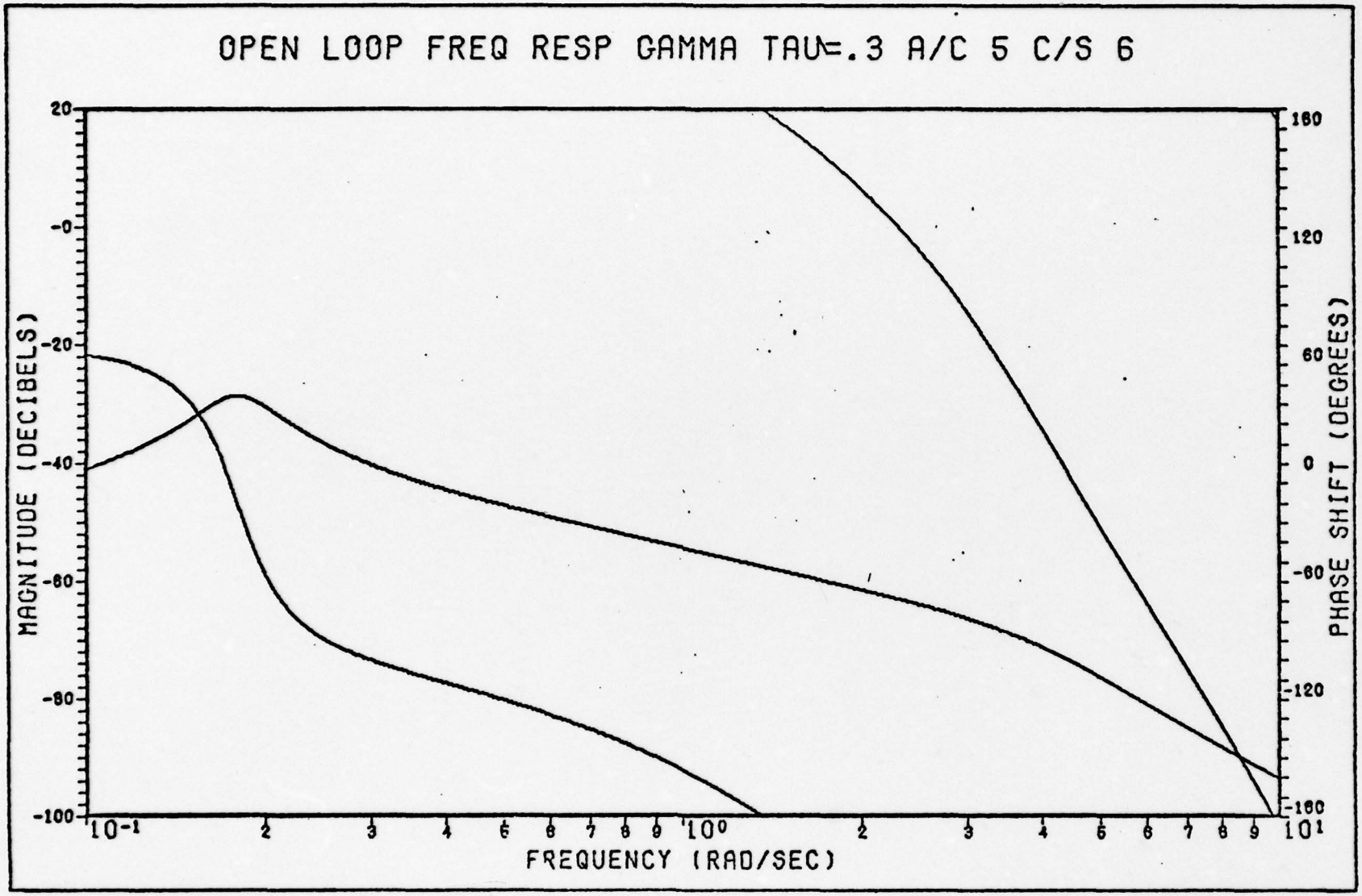

Fig. E40 Open-Loop Frequency Response γ For $\tau = 0.3$ sec. A/C 5 C/S 6

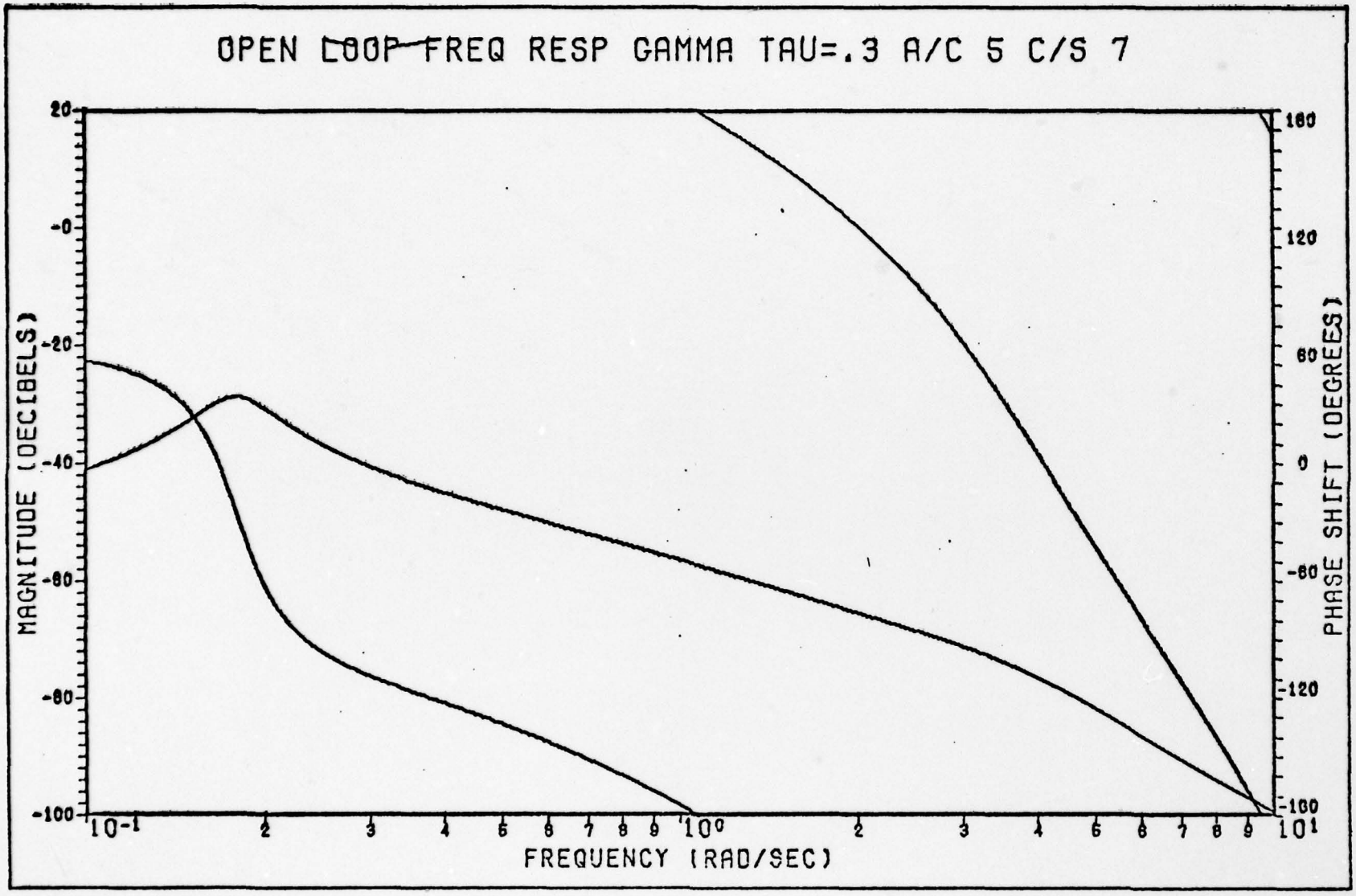

Fig. E41 Open-Loop Frequency Response γ For $\tau = 0.3$ sec. A/C 5 C/S 7

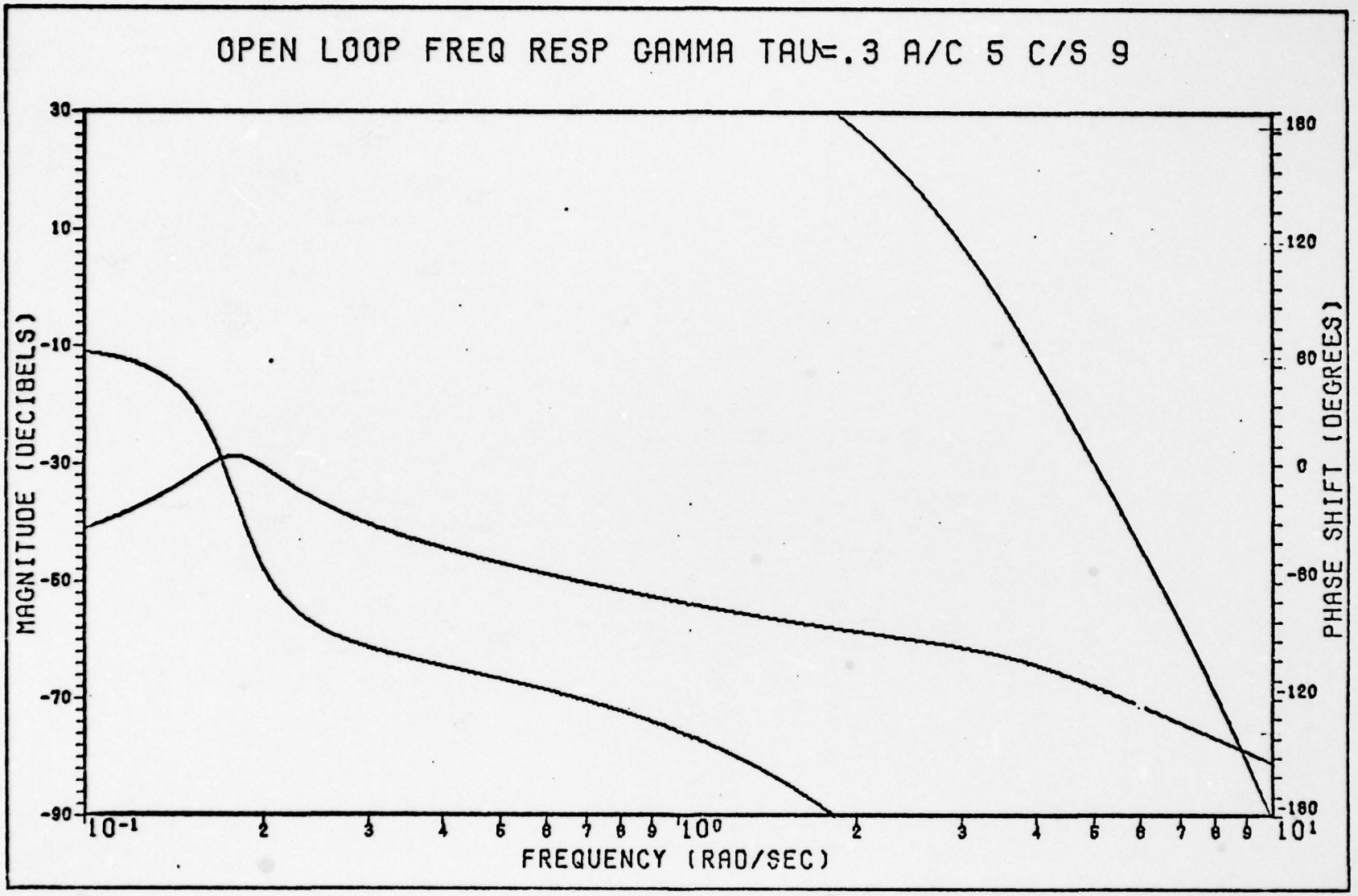

Fig. E42 Open-Loop Frequency Response γ For $\tau = 0.3$ sec. A/C 5 C/S 9

ω	c/S 1		c/S 2		c/S 3		c/S = 1		c/S 4		c/S 5		c/S 6		c/S 8		c/S 10		c/S 13	
	$\phi°$	$\frac{\delta\phi}{\delta\omega}$	$\phi°$	$\frac{\delta\phi}{\delta\omega}$	$\phi°$	$\frac{\delta\phi}{\delta\omega}$	$\phi°$	$\frac{\delta\phi}{\delta\omega}$	$\phi°$	$\frac{\delta\phi}{\delta\omega}$	$\phi°$	$\frac{\delta\phi}{\delta\omega}$	$\phi°$	$\frac{\delta\phi}{\delta\omega}$	$\phi°$	$\frac{\delta\phi}{\delta\omega}$	$\phi°$	$\frac{\delta\phi}{\delta\omega}$	$\phi°$	$\frac{\delta\phi}{\delta\omega}$
1	-130°		-135°		-140°		-146°		-152°		-160°		-172°		-150°		-157°		-166°	
		40		42		45		50		58		63		70		57		56		49
2	-170°		-177°		-185°		-196°		-210°		-223°		-242°		-207°		-213°		-215°	
		25		23		27		32		34		41		42		36		43		41
3	-195°		-200°		-202°		-228°		-244°		-264°		-284°		-243°		-256°		-256°	
		22		24		23		24		33		36		36		33		36		34
4	-217°		-224°		-235°		-252°		-277°		-300°		-320°		-276°		-252°		-290°	
PR	6		5		4		4		5		9		10		5		8		9	

Table E1 Aircraft No 1 Pitch Phase Angle and Slope Data

ω	c/S 1		c/S 3		c/S = 1		c/S 4		c/S 5		c/S 6		c/S 8		c/S 9		c/S 11		c/S 12		c/S 13	
	ϕ	$\frac{\delta\phi}{\delta\omega}$	$\phi°$	$\frac{\delta\phi}{\delta\omega}$	$\phi°$	$\frac{\delta\phi}{\delta\omega}$	$\phi°$	$\frac{\delta\phi}{\delta\omega}$	$\phi°$	$\frac{\delta\phi}{\delta\omega}$	$\phi°$	$\frac{\delta\phi}{\delta\omega}$	$\phi°$	$\frac{\delta\phi}{\delta\omega}$	$\phi°$	$\frac{\delta\phi}{\delta\omega}$	$\phi°$	$\frac{\delta\phi}{\delta\omega}$	$\phi°$	$\frac{\delta\phi}{\delta\omega}$	$\phi°$	$\frac{\delta\phi}{\delta\omega}$
1	-73°		-82°		-90°		-93°		-102°		-115°		-93°		-95°		-102°		-119°		-100°	
		37		46		48		55		60		69		54		55		63		61		56
2	-110°		-128°		-138°		-148°		-162°		-184°		-147°		-151°		-165°		-180°		-156°	
		49		52		54		62		68		66		63		60		73		82		64
3	-159°		-180°		-192°		-210°		-230°		-250°		-210°		-211°		-238°		-262°		-220°	
		41		38		42		45		50		46		43		48		53		60		50
4	-200°		-218°		-234°		-255°		-280°		-296°		-253°		-259°		-291°		-322°		-270°	
PR	5		3		2		4		6		9		5		7		10		10		8	

Table E2 Aircraft No. 2 Pitch Phase Angle and Slope Data

	c/S 3		c/S = 1		c/S 4		c/S 5		c/S 8		c/S 9	
ω	ϕ°	$\frac{\delta\phi}{\delta\omega}$	ϕ°	$\frac{\delta\phi}{\delta\omega}$	ϕ°	$\frac{\delta\phi}{\delta\omega}$	ϕ°	$\frac{\delta\phi}{\delta\omega}$	ϕ°	$\frac{\delta\phi}{\delta\omega}$	ϕ°	$\frac{\delta\phi}{\delta\omega}$
1	-70°		-72°		-78°		-87°		-78°		-80°	
		50		59		62		80		62		
2	-120°		-131°		-141°		-157°		-140°		-143°	
		84		89		95		98		92		
3	-204°		-220°		-236°		-255°		-232°		-238°	
		33		33		40		42		40		
4	-237°		-253°		-276°		-297°		-272°		-280°	
PR	5		4		7		10		7		8	

Table E3 Aircraft No 3 Pitch Phase Angle and Slope Data

	c/S 3		c/S = 1		c/S 5		c/S 6		c/S 8		c/S 9		c/S 12		c/S 13	
ω	ϕ°	$\frac{\delta\phi}{\delta\omega}$	ϕ°	$\frac{\delta\phi}{\delta\omega}$	ϕ°	$\frac{\delta\phi}{\delta\omega}$	ϕ°	$\frac{\delta\phi}{\delta\omega}$	ϕ°	$\frac{\delta\phi}{\delta\omega}$	ϕ°	$\frac{\delta\phi}{\delta\omega}$	ϕ°	$\frac{\delta\phi}{\delta\omega}$	ϕ°	$\frac{\delta\phi}{\delta\omega}$
1	-106°		-112°		-126°		-140°		-116°		-119°		-132°		-122°	
		34		40		54		57		45		46		64		46
2	-140°		-152°		-180°		-197°		-161°		-165°		-196°		-168°	
		32		36		46		48		41		45		61		50
3	-172°		-188°		-226°		-245°		-202°		-210°		-257°		-218°	
		30		38		38		38		38		39		53		41
4	-202°		-220°		-264°		-283°		-240°		-249°		-310°		-259°	
PR	3		2		6		7		4		3		9		8	

Table E4 Aircraft No 4 Pitch Phase Angle and Slope Data

ω ↓	c/S = 1 φ°	c/S = 1 δφ/δω	c/S 5 φ°	c/S 5 δφ/δω	c/S 6 φ°	c/S 6 δφ/δω	c/S 7 φ°	c/S 7 δφ/δω	c/S 8 φ°	c/S 8 δφ/δω	c/S 9 φ°	c/S 9 δφ/δω	c/S 13 φ°	c/S 13 δφ/δω
1	-73°	25	-88°	37	-100°	42	-119°	43	-78°	30	-80°	30	-81°	35
2	-98°	42	-125°	55	-142°	56	-162°	49	-108°	46	-110°	50	-116°	52
3	-140°	48	-180°	51	-198°	52	-211°	51	-154°	54	-160°	53	-168°	57
4	-188°		-231°		-250°		-262°		-208°		-213°		-225°	
PR	5		6		6		7		6		6		7	

Table E5 Aircraft No 5 Pitch Phase Angle and Slope Data

ω	c/S 1 φ°	c/S 1 δφ/δω	c/S 2 φ°	c/S 2 δφ/δω	c/S 3 φ°	c/S 3 δφ/δω	c/S=1 φ°	c/S=1 δφ/δω	c/S 4 φ°	c/S 4 δφ/δω	c/S 5 φ°	c/S 5 δφ/δω	c/S 6 φ°	c/S 6 δφ/δω	c/S 8 φ°	c/S 8 δφ/δω	c/S 10 φ°	c/S 10 δφ/δω	c/S 13 φ°	c/S 13 δφ/δω
0.5	-132°	51	-135°	54	-140°	53	-142°	58	-143°	60	-149°	63	-156°	72	-144°	58	-148°	60	-147°	63
1	-183°	57	-189°	61	-193°	65	-200°	70	-203°	77	-212°	82	-228°	84	-202°	78	-208°	77	-210°	75
2	-240°	33	-250°	31	-258°	32	-270°	36	-280°	42	-294°	48	-312°	53	-280°	42	-285°	51	-285°	50
3	-273°	25	-281°	21	-290°	28	-306°	30	-322°	36	-342°	41	-365°	37	-322°	35	-336°	36	-335°	38
4	-298°		-302°		-318°		-336°		-358°		-383°		-402°		-357°		-372°		-373°	
PR	6		5		4		4		5		9		10		5		8		9	

Table E6 Aircraft No 1 Flight Path Angle Phase and Slope Data

ω	C/S 1		C/S 3		C/S = 1		C/S 4		C/S 5		C/S 6		C/S 8		C/S 9		C/S 11		C/S 12		C/S 13	
	$\phi°$	$\frac{\delta\phi}{\delta\omega}$	$\phi°$	$\frac{\delta\phi}{\delta\omega}$	$\phi°$	$\frac{\delta\phi}{\delta\omega}$	$\phi°$	$\frac{\delta\phi}{\delta\omega}$	$\phi°$	$\frac{\delta\phi}{\delta\omega}$	$\phi°$	$\frac{\delta\phi}{\delta\omega}$	$\phi°$	$\frac{\delta\phi}{\delta\omega}$	$\phi°$	$\frac{\delta\phi}{\delta\omega}$	$\phi°$	$\frac{\delta\phi}{\delta\omega}$	$\phi°$	$\frac{\delta\phi}{\delta\omega}$	$\phi°$	$\frac{\delta\phi}{\delta\omega}$
0.7	-112°	13	-122°	16	-126°	16	-132°	18	-137°	21	-142°	28	-130°	18	-130°	20	-134°	23	-141°	21	-134°	18
1	-125°	58	-138°	62	-142°	68	-150°	73	-158°	82	-170°	88	-148°	75	-150°	78	-157°	83	-162°	95	-152°	88
2	-133°	57	-200°	60	-210°	65	-223°	67	-240°	72	-258°	72	-223°	67	-228°	66	-240°	77	-257°	85	-240°	64
3	-240°	50	-260°	40	-275°	42	-290°	50	-312°	48	-330°	50	-290°	47	-294°	50	-317°	59	-342°	67	-304°	50
4	-290°		-300°		-317°		-340°		-360°		-380°		-337°		-343°		-376°		-409°		-354°	
PR	5		4		2		4		6		9		5		7		10		10		8	

Table E7 Aircraft No. 2 Flight Path Angle Phase and Slope Data

ω	c/S 3		c/S-1		c/S 4		c/S 5		c/S 8		c/S 9	
	$\phi°$	$\frac{\delta\phi}{\delta\omega}$	$\phi°$	$\frac{\delta\phi}{\delta\omega}$	$\phi°$	$\frac{\delta\phi}{\delta\omega}$	$\phi°$	$\frac{\delta\phi}{\delta\omega}$	$\phi°$	$\frac{\delta\phi}{\delta\omega}$	$\phi°$	$\frac{\delta\phi}{\delta\omega}$
0.7	-109°	12	-112°	14	-118°	14	-123°	17	-118°	12	-119°	11
1	-121°	71	-126°	74	-132°	81	-140°	88	-130°	80	-130°	85
2	-192°	90	-200°	95	-213°	99	-228°	104	-210°	100	-215°	101
3	-282°	35	-295°	38	-312°	43	-332°	45	-310°	44	-316°	44
4	-317°		-333°		-355°		-377°		-356°		-360°	
PR	5		4		7		10		7		8	

Table E8 Aircraft No 3 Flight Path Angle Phase and Slope Data

	c/S 3		c/S = 1		c/S 5		c/S 6		c/S 8		c/S 9		c/S 12		c/S 13	
ω	ϕ°	$\frac{\delta\phi}{\delta\omega}$	ϕ°	$\frac{\delta\phi}{\delta\omega}$	ϕ°	$\frac{\delta\phi}{\delta\omega}$	ϕ°	$\frac{\delta\phi}{\delta\omega}$	ϕ°	$\frac{\delta\phi}{\delta\omega}$	ϕ°	$\frac{\delta\phi}{\delta\omega}$	ϕ°	$\frac{\delta\phi}{\delta\omega}$	ϕ°	$\frac{\delta\phi}{\delta\omega}$
0.7	-142°		-148°		-157°		-169°		-150°		-151°		-162°		-153°	
		24		22		26		29		23		25		28		25
1	-164°		-170°		-183°		-198°		-173°		-176°		-190°		-178°	
		55		60		72		75		65		66		82		71
2	-219°		-230°		-255°		-273°		-238°		-242°		-272°		-269°	
		41		43		57		58		52		54		70		54
3	-260°		-273°		-312°		-331°		-290°		-296°		-342°		-303°	
		35		40		48		47		42		44		60		47
4	-295°		-312°		-360°		-378°		-332°		-340°		-402°		-350°	
PR	3		2		6		7		4		3		9		8	

Table E9 Aircraft No 4 Flight Path Angle Phase and Slope Data

	c/S=1		c/S 5		c/S 6		c/S 7		c/S 8		c/S 9		c/S 13	
ω	ϕ°	$\frac{\delta\phi}{\delta\omega}$	ϕ°	$\frac{\delta\phi}{\delta\omega}$	ϕ°	$\frac{\delta\phi}{\delta\omega}$	ϕ°	$\frac{\delta\phi}{\delta\omega}$	ϕ°	$\frac{\delta\phi}{\delta\omega}$	ϕ°	$\frac{\delta\phi}{\delta\omega}$	ϕ°	$\frac{\delta\phi}{\delta\omega}$
1	-120°		-146°		-156°		-174°		-136°		-138°		-152°	
		54		56		64		65		51		52		42
2	-174°		-202°		-220°		-239°		-185°		-190°		-194°	
		53		63		62		59		57		58		60
3	-227°		-265°		-282°		-298°		-242°		-248°		-254°	
		53		59		61		58		57		58		63
4	-280°		-324°		-343°		-356°		-299°		-306°		-317°	
PR	5		6		6		7		6		6		7	

Table E10 Aircraft No 5 Flight Path Angle Phase and Slope Data

Table E11 Estimated and Actual PR Using Pitch Phase Data

Aircraft No:1			Aircraft No: 2			Aircraft No: 4			Aircraft No: 5		
c/S	Est. PR	Actual PR	c/S	Est. PR	Actual PR	c/S	Est. PR	Actual PR	a/S	Est. PR	Actual PR
=1	4.5	4	=1	5.8	2	=1	5	2	=1	5.3	5
4	6.5	5	4	6.5	4	5	5.6	7	5	6.4	6
5	8.2	9	5	7.2	6	6	5.6	7	6	6.7	6
6	7.6	10	6	6.9	9	8	5.3	4	7	6.5	7
8	7	5	8	6.4	5	9	5.6	3	8	5.8	6
10	9	8	9	6.5	7	12	7.8	9	9	6	6
13	8	9	11	7.6	10	13	6.2	8	13	6.4	7
			12	8.6	10						
			13	7	8						
$\alpha_1 = 0.041$			$\alpha_1 = -0.002$			$\alpha_1 = 0.006$			$\alpha_1 = -0.012$		
$\alpha_2 = 0.494$			$\alpha_2 = 0.116$			$\alpha_2 = 0.163$			$\alpha_2 = 0.079$		

Table E12 Estimated And Actual PR Using Eqn. 12 And Pitch Phase Data

Aircraft No 1			Aircraft No 2			Aircraft No 3			Aircraft No 4			Aircraft No 5		
c/S	Est. PR	Act. PR	c/S	Est. PR	Act. PR	c/S	Est. PR	Act. PR	c/S	Est. PR	Act. PR	c/S	Est. PR	Act. PR
=1	5.2	4	=1	5.5	2	=1	5.1	4	=1	1.5	2	=1	5.7	5
4	5.5	5	4	6.5	4	4	6.5	7	5	5.9	6	5	5.9	6
5	8	9	5	7.1	6	5	9.7	10	6	6.4	7	6	6.3	6
6	7.5	10	6	7	9	8	7.4	6	8	3.9	4	7	6.9	7
8	6.5	5	8	6.8	5	9	7.4	8	9	5.6	3	8	6.5	6
10	9.4	8	9	6	6				12	8.4	9	9	6.1	6
13	8.4	9	11	7.6	10				13	7.5	8	13	6.7	7
			12	8.5	10									
			13	6.4	8									
a_1 = 0.047			a_1 = -0.007			a_1 = 0.245			a_1 = 0.034			a_1 = -0.019		
a_2 = 0.48			a_2 = 0.143			a_2 = -0.614			a_2 = 0.567			a_2 = -0.077		
a_3 = 0.014			a_3 = -0.085			a_3 = 0.176			a_3 = -0.33			a_3 = 0.132		

Table E13 Estimated And Actual ΔPR Using Pitch Data And Eqn. 13

Aircraft No 1			Aircraft No 2			Aircraft No 3			Aircraft No 4			Aircraft No 5		
c/S	Est. ΔPR	Act. ΔPR	c/S	Est. ΔPR	Act. ΔPR	c/S	Est. ΔPR	Act. ΔPR	c/S	Est. ΔPR	Act. ΔPR	c/S	Est. ΔPR	Actual ΔPR
4	2.1	1	4	2.5	2	4	2.6	2	5	3.5	4	5	1.6	2
5	4.6	5	5	5.2	4	5	4.9	5	6	5	5	6	1.9	1
6	6.3	6	6	7	7	8	1.9	2	8	1.4	2	7	1.6	2
8	2.2	1	8	2.4	3	9	2.8	3	9	2.4	1	8	0.9	1
10	4	4	9	2.7	5				12	8.2	7	9	1.1	1
13	3.7	5	11	6.5	8				13	3.6	6	13	1.7	2
			12	9.9	8									
			13	3.9	6									
$\alpha_1 = 0.086$			$\alpha_1 = 0.107$			$\alpha_1 = 0.126$			$\alpha_1 = 0.07$			$\alpha_1 = 0.011$		
$\alpha_2 = 0.138$			$\alpha_2 = 0.102$			$\alpha_2 = 0.058$			$\alpha_2 = 0.169$			$\alpha_2 = 0.142$		

Table E15 Estimated And Actual ΔPR

Evaluated at ω_c Using Pitch Data

Aircraft No 1			Aircraft No 2		
c/S	Estimated ΔPR	Actual ΔPR	c/S	Estimated ΔPR	Actual ΔPR
4	2.2	1	4	2.3	2
5	4.2	5	5	4.9	4
6	7.3	6	6	7	7
8	1.7	1	8	2.2	3
10	2.6	4	9	2.8	5
13	3	5	11	6.5	8
			12	9.9	8
			13	4.3	6
a_1 = 0.17			a_1 = 0.124		
a_2 = -0.038			a_2 = 0.037		
ω_c = 2 rad/sec			ω_c = 3.3 rad/sec		

Table E14 Estimated And Actual PR

Using Eqn. 14

Aircraft No 1			Aircraft No 2		
c/S	Estimated PR	Actual PR	c/S	Estimated PR	Actual PR
4	1.1	1	4	3.6	2
5	4.8	5	5	5.5	4
6	6.3	6	6	6.8	7
8	1.5	1	8	3.6	3
10	4.7	4	9	3.7	5
13	3.7	5	11	6.4	8
			12	8.8	8
			13	4.6	6
a_0 = -2.61			a_0 = 1.87		
a_1 = 0.066			a_1 = 0.076		
a_2 = 0.474			a_2 = 0.07		

Table E16 Estimated And Actual PR Using γ Phase Angle Data And Eqn. 15

Aircraft No 1			Aircraft No 2			Aircraft No 3			Aircraft No 4			Aircraft No 5		
c/S	Est. PR	Act. PR	c/S	Est. PR	Act. PR	c/S	Est. PR	Act. PR	c/s	Est. PR	Act. PR	c/S	Est. PR	Act. PR
1	5.5	6	1	2.6	5	3	4.7	5	3	2	3	=1	5.1	5
2	5.9	5	3	2.8	3	=1	5.6	4	=1	2.5	2	5	6	6
3	5.7	4	=1	4.5	2	4	7.25	7	5	6.2	6	6	6.7	6
=1	6.3	4	4	4.8	4	5	9.7	10	6	6.3	7	7	7.42	7
4	6.6	5	5	7	6	8	6.42	7	8	4.1	4	8	5.6	6
5	7	9	6	9.1	9	9	8.4	8	9	5	3	9	5.7	6
6	8	10	8	5.6	5				12	9.2	9	13	6.1	7
8	6.3	5	9	6.7	7				13	6.2	8			
10	6.5	8	11	8	10									
13	7	9	12	9.9	10									
			13	8.5	8									
$\alpha_1 = -0.009$			$\alpha_1 = -0.135$			$\alpha_1 = -0.29$			$\alpha_1 = -0.162$			$\alpha_1 = 0.045$		
$\alpha_2 = 0.13$			$\alpha_2 = 0.152$			$\alpha_2 = 0.231$			$\alpha_2 = 0.273$			$\alpha_2 = -0.052$		
			$\alpha_3 = 0.267$			$\alpha_3 = 0.48$			$\alpha_3 = 0.3$					

Table E17 Estimated And Actual ΔPR Using γ Phase Angle Data And Eqn. 16

Aircraft No. 1			Aircraft No. 2			Aircraft No. 3			Aircraft No. 4			Aircraft No. 5		
c/S	Est. ΔPR	Act. ΔPR	c/S	Est. ΔPR	Act. ΔPR	c/s	Est. ΔPR	Act. ΔPR	c/S	Est. ΔPR	Act. ΔPR	c/S	Est. ΔPR	Act. ΔPR
1	4.2	2	1	3.9	3	3	1.6	1	3	0.7	1	5	0.6	1
2	2.9	1	3	2.7	1	4	1.7	2	5	4.2	4	6	1.1	1
3	0.9	0	4	0.4	2	5	4.6	5	6	4.9	5	7	2.6	2
4	0.5	1	5	4.1	4	8	3.1	2	8	1.7	2	8	0.64	1
5	3	5	6	8.8	7	9	3	3	9	2.8	1	9	0.76	1
6	6	5	8	1.4	3				12	7.4	7	13	0.82	2
8	0.8	1	9	4.5	5				13	4	6			
10	2.5	4	11	5.9	8									
13	2.2	5	12	7.8	8									
			13	5	6									
$\alpha_1 = 0.411$			$\alpha_1 = -0.175$			$\alpha_1 = 0.111$			$\alpha_1 = -0.125$			$\alpha_1 = 0.068$		
$\alpha_2 = 0.019$			$\alpha_2 = 0.69$			$\alpha_2 = 0.3$			$\alpha_2 = 0.584$			$\alpha_2 = -0.215$		

Appendix F

Selected Open-Loop Impulse Response Plots of Pitch Angle Theta Using Short Period Approximation For The Aircraft-Control System Configurations Analyzed

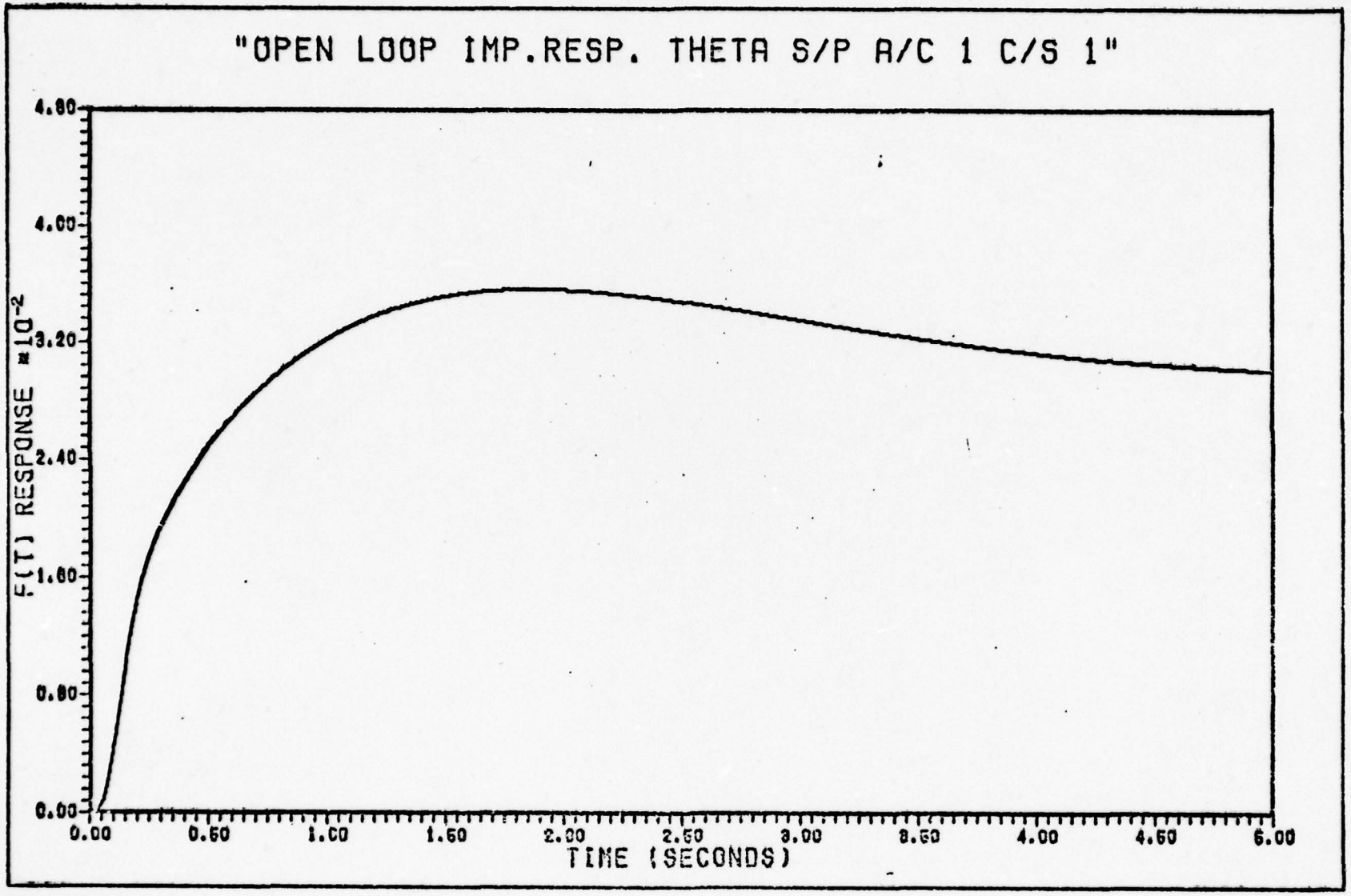

Fig. F1 Open-Loop Impulse Response of Pitch Angle A/C 1 C/S 1

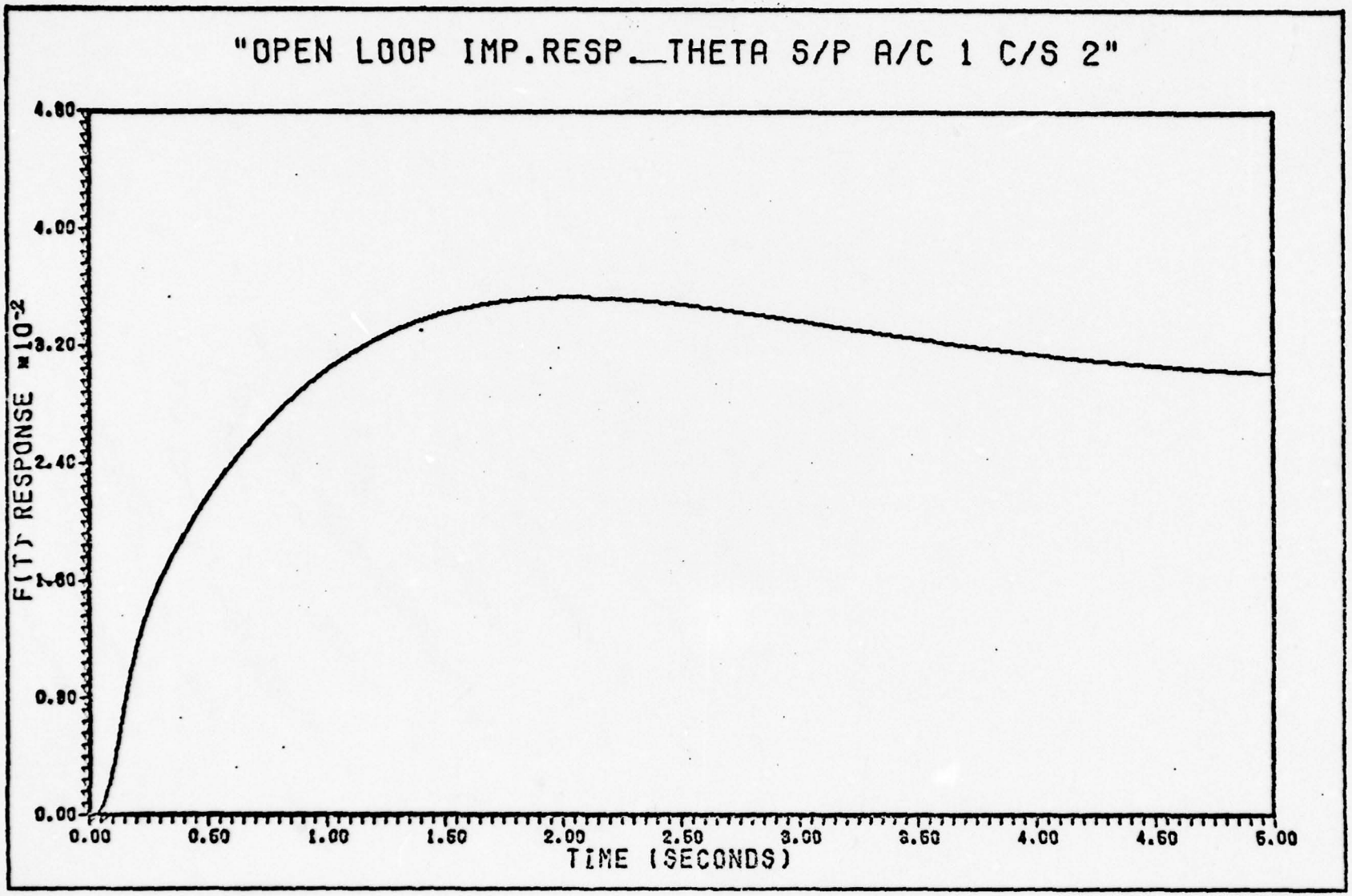

Fig. F2 Open-Loop Impulse Response of Pitch Angle A/C 1 C/S 2

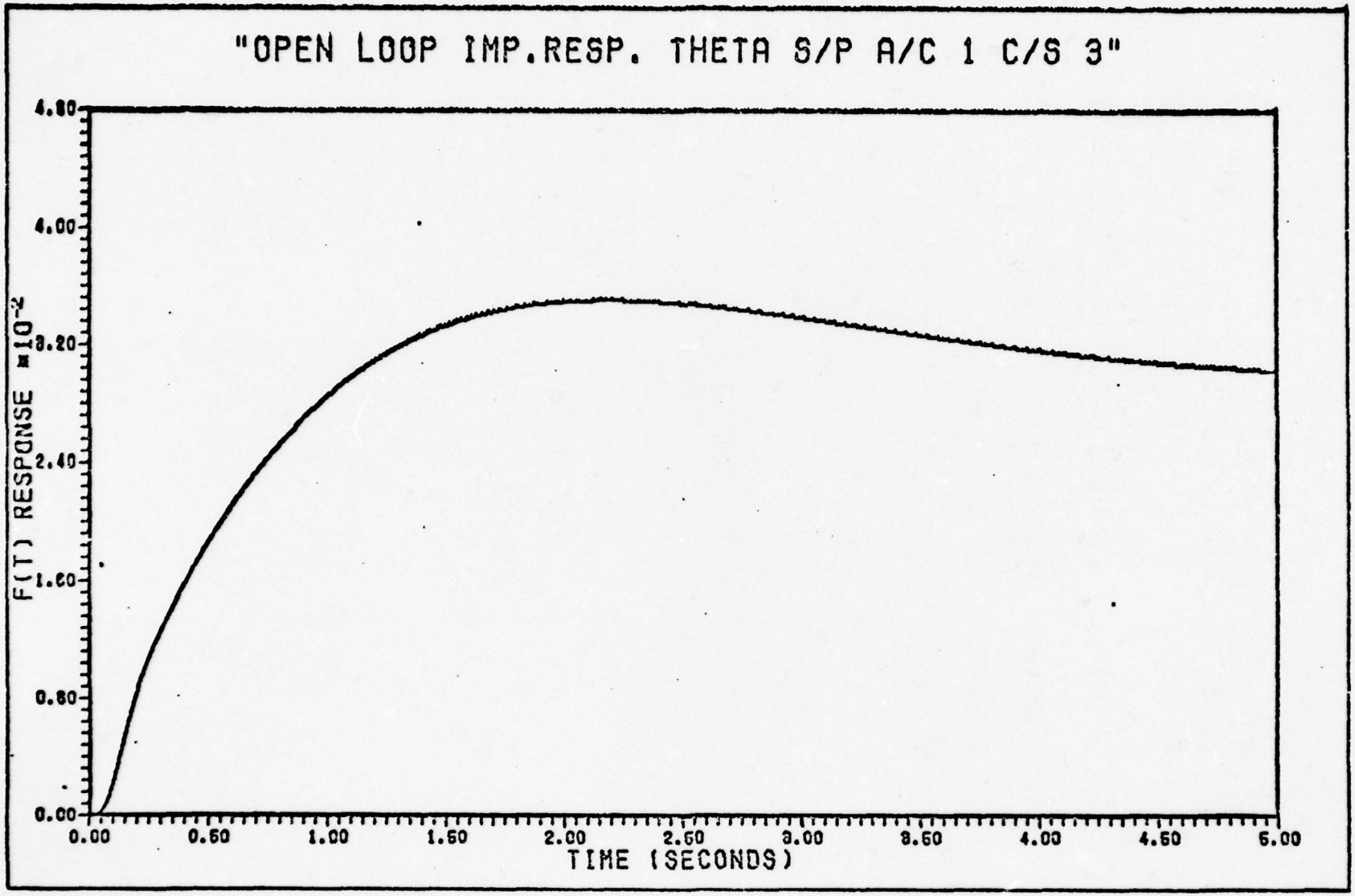

Fig. F3 Open-Loop Impulse Response of Pitch Angle A/C 1 C/S 3

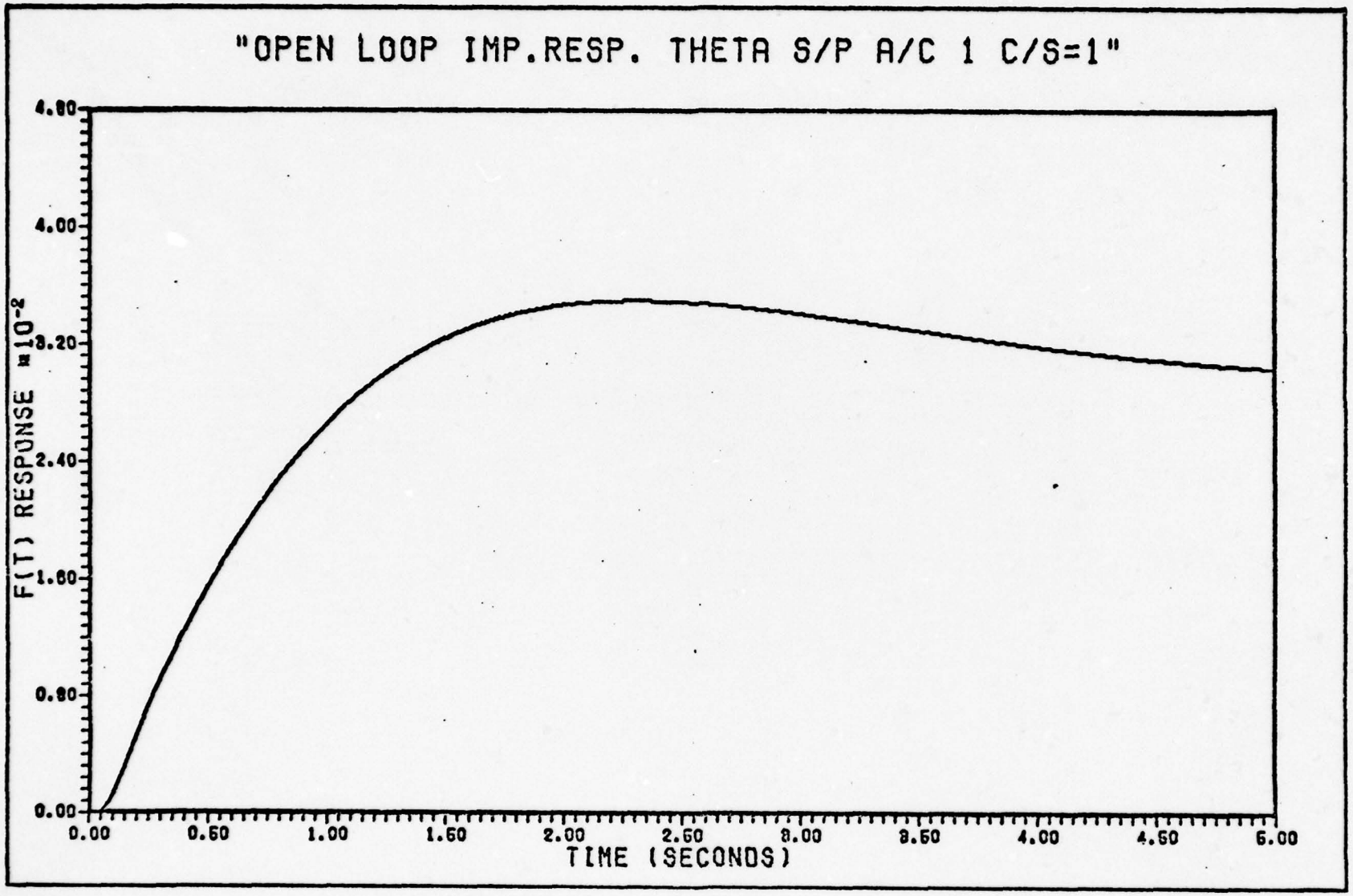

Fig. F4 Open-Loop Impulse Response of Pitch Angle A/C 1 C/S = 1

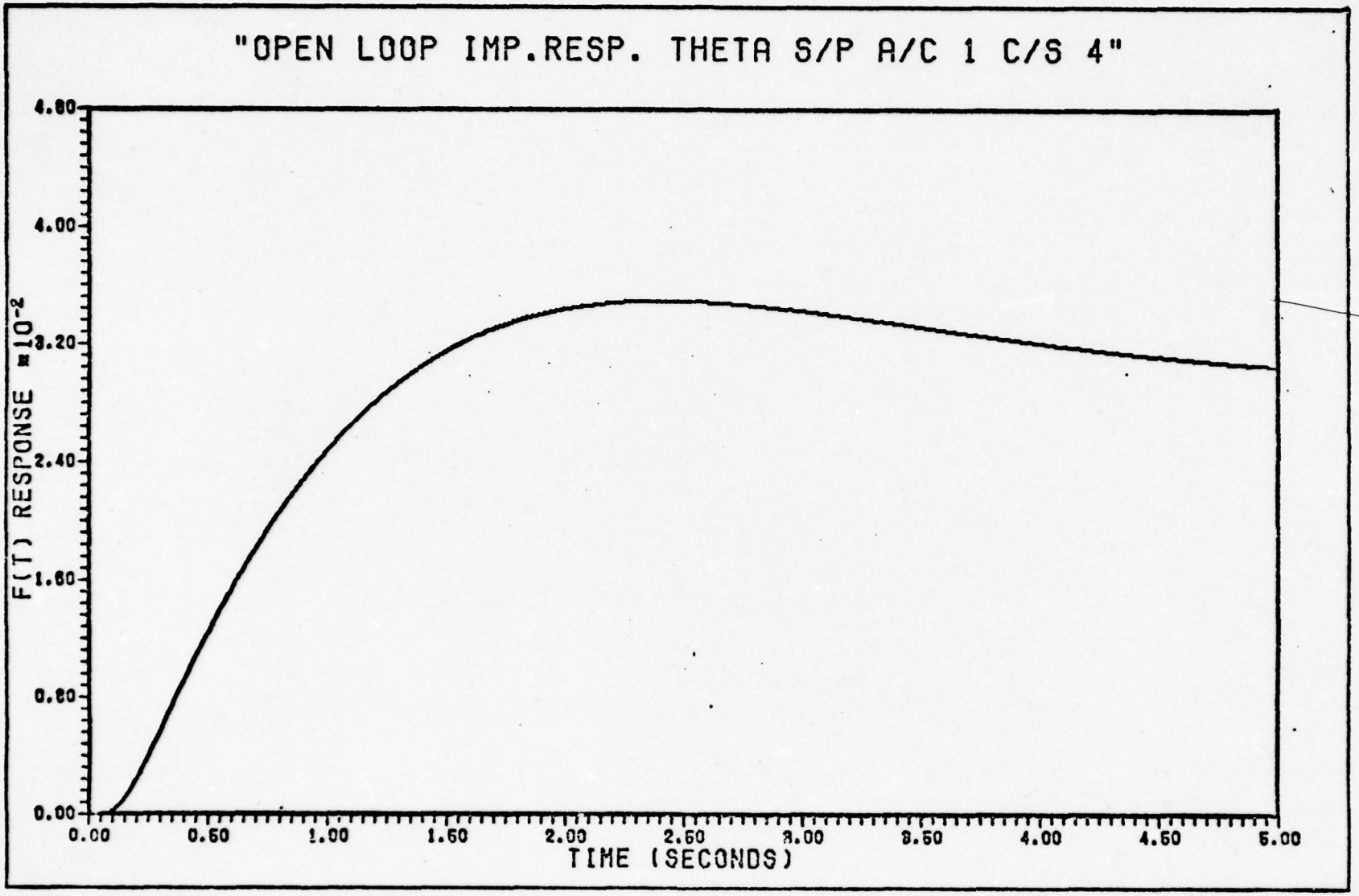

Fig. F5 Open-Loop Impulse Response of Pitch Angle A/C 1 C/S 4

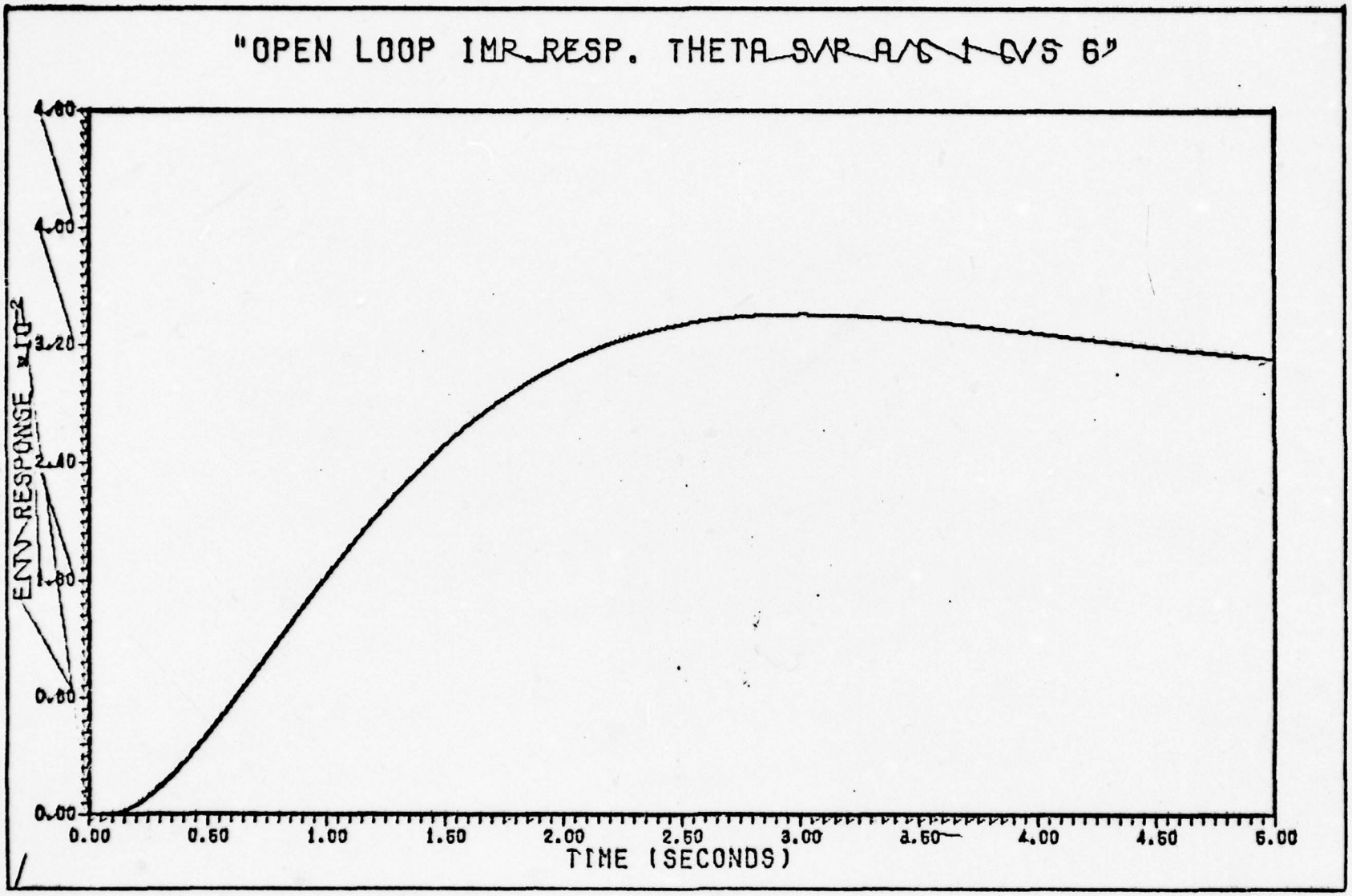

Fig F6 Open-Loop Impulse Response of Pitch Angle A/C 1 C/S 6

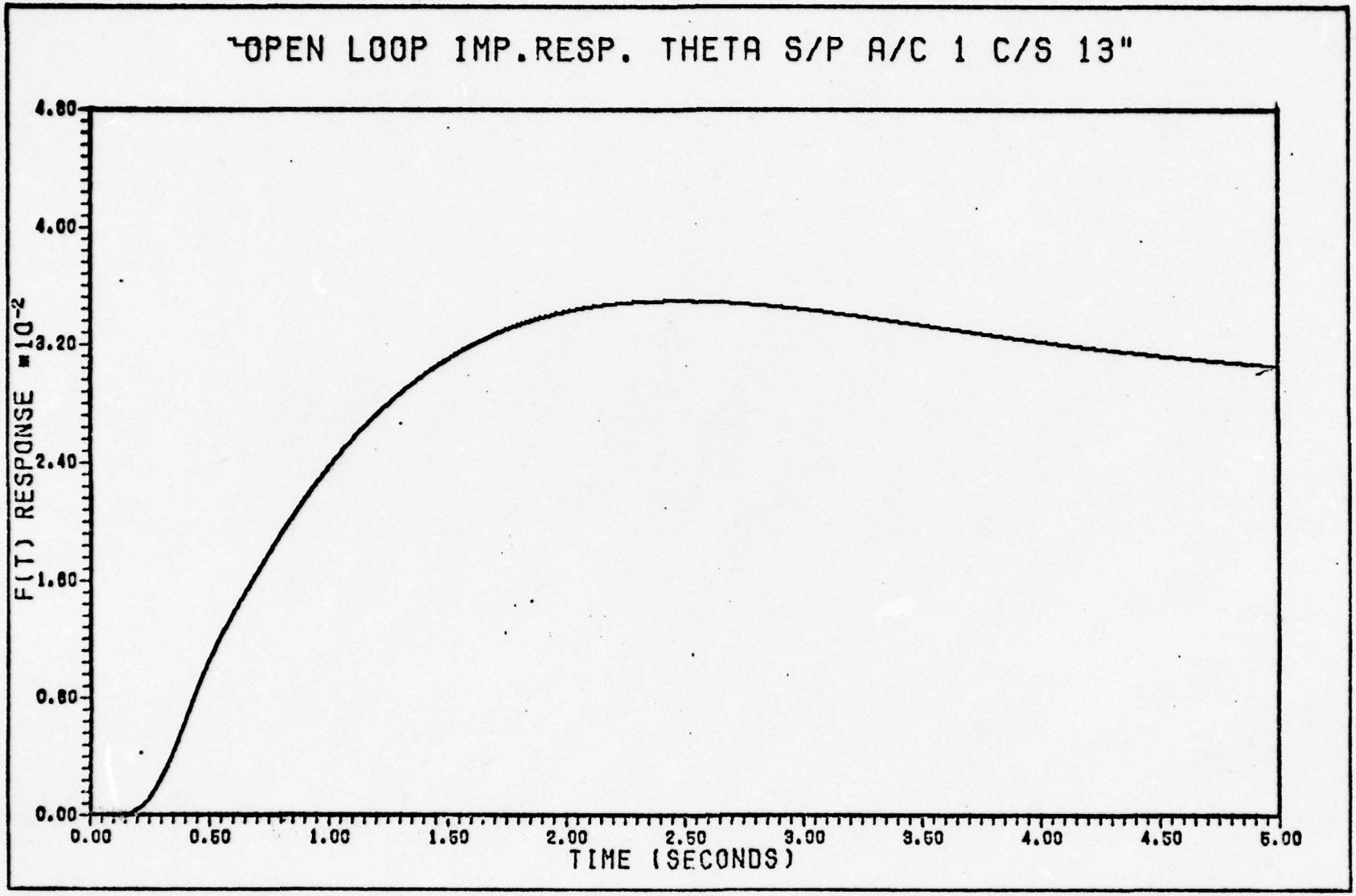

Fig. F7 Open-Loop Impulse Response of Pitch Angle A/C 1 C/S 13

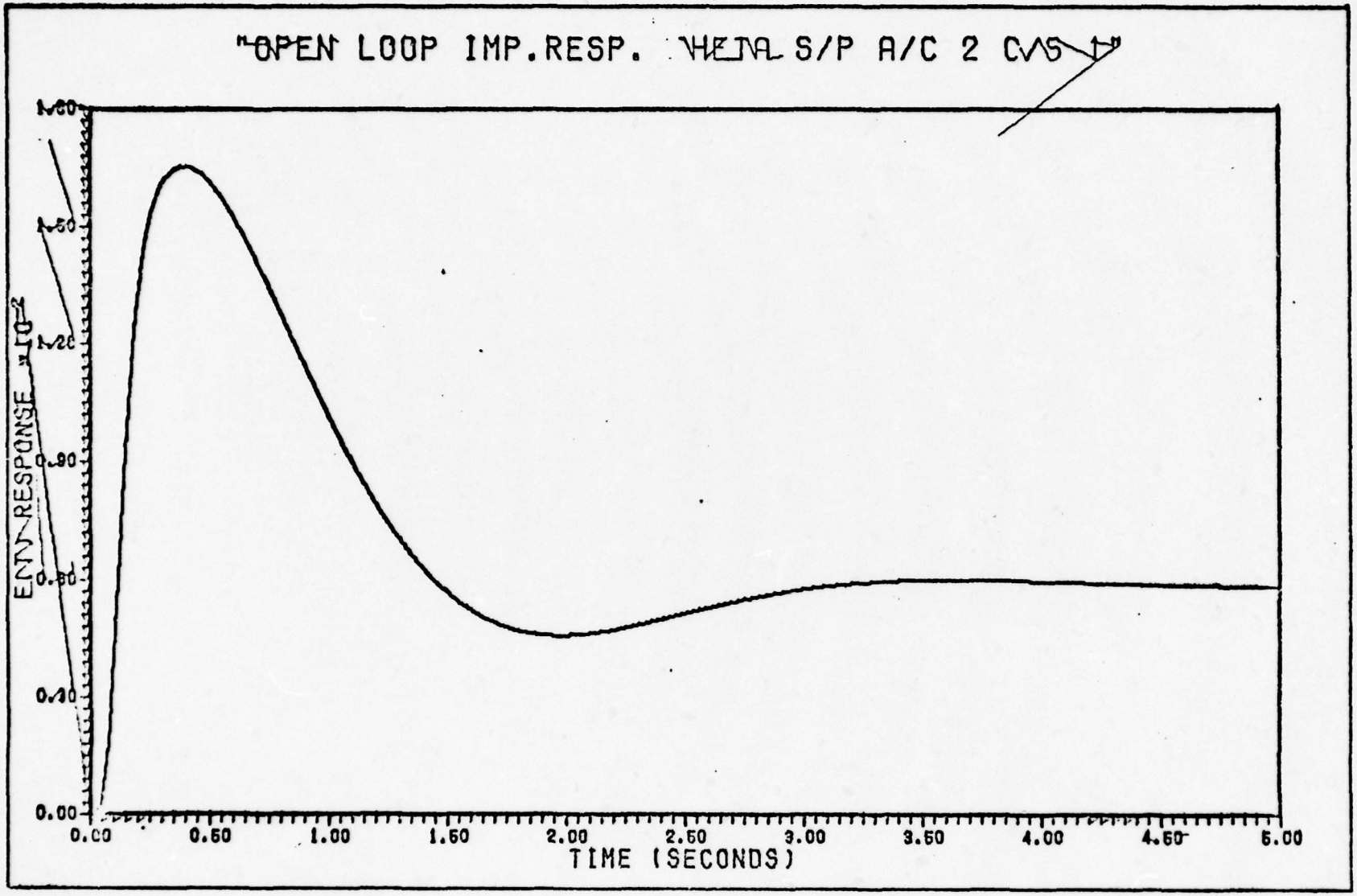

Fig. F8 Open-Loop Impulse Response of Pitch Angle A/C 2 C/S 1

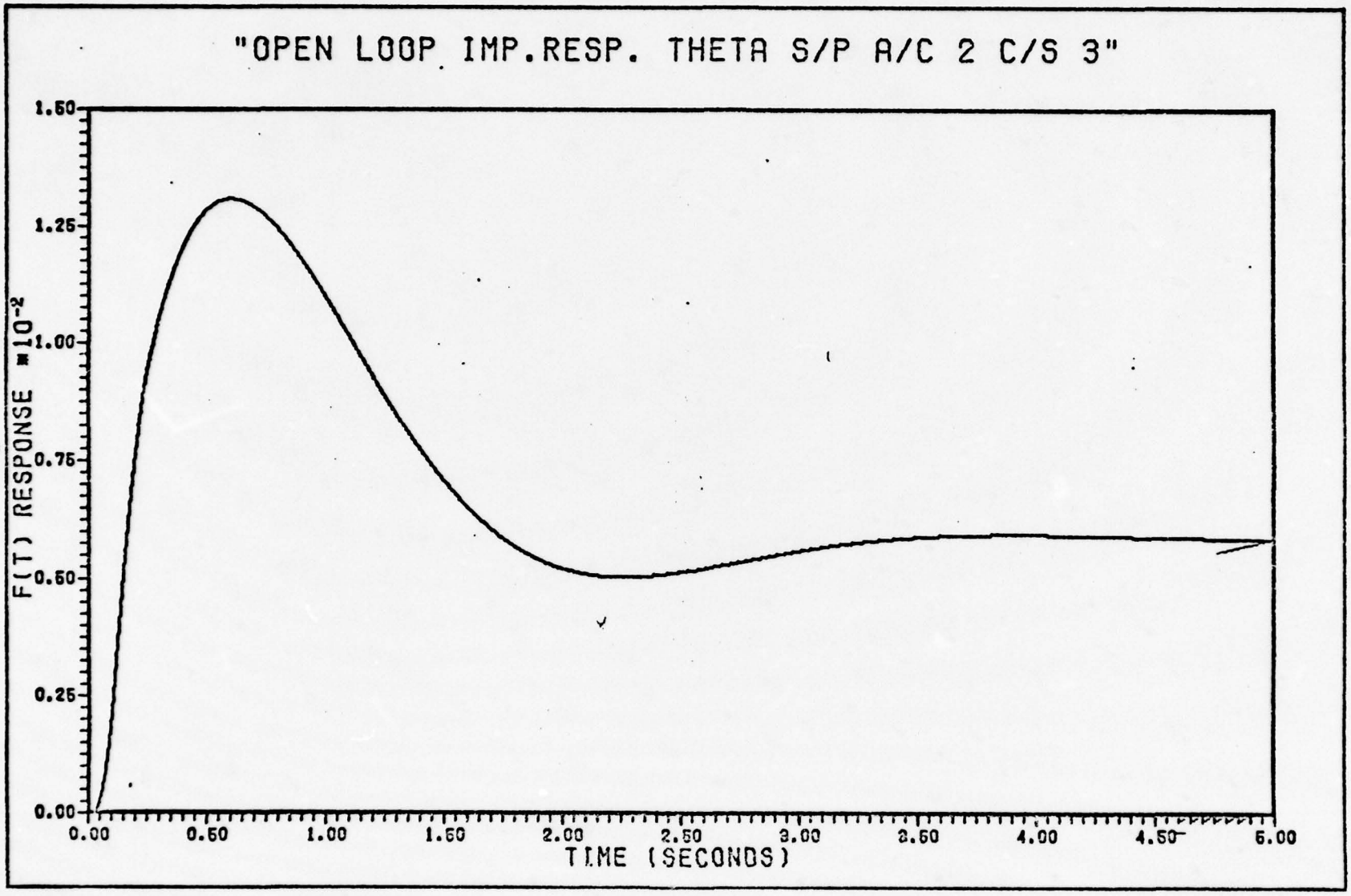

Fig. F9 Open-Loop Impulse Response of Pitch Angle A/C 2 C/S 3

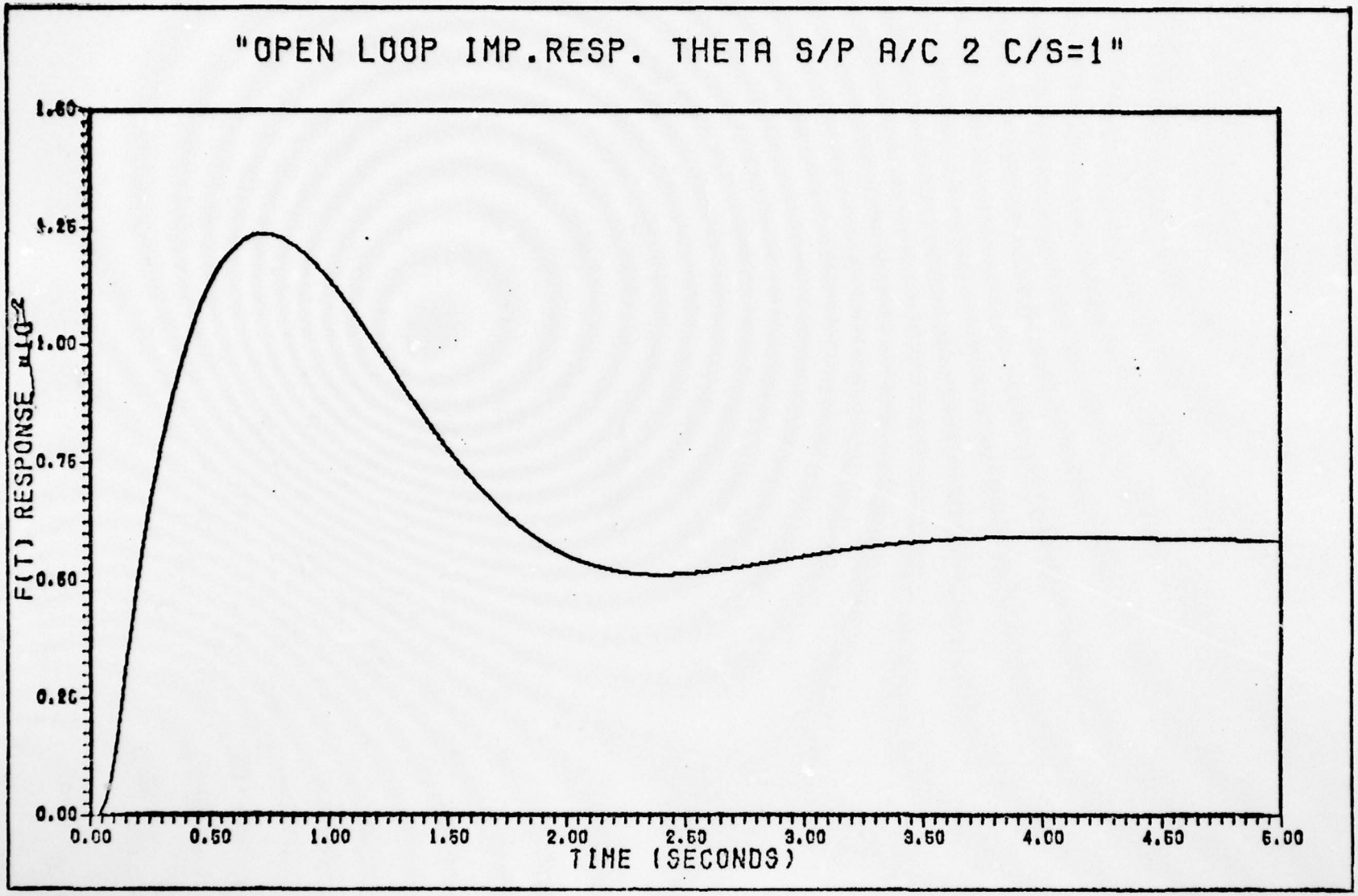

Fig. F10 Open-Loop Impulse Response of Pitch Angle A/C 2 C/S = 1

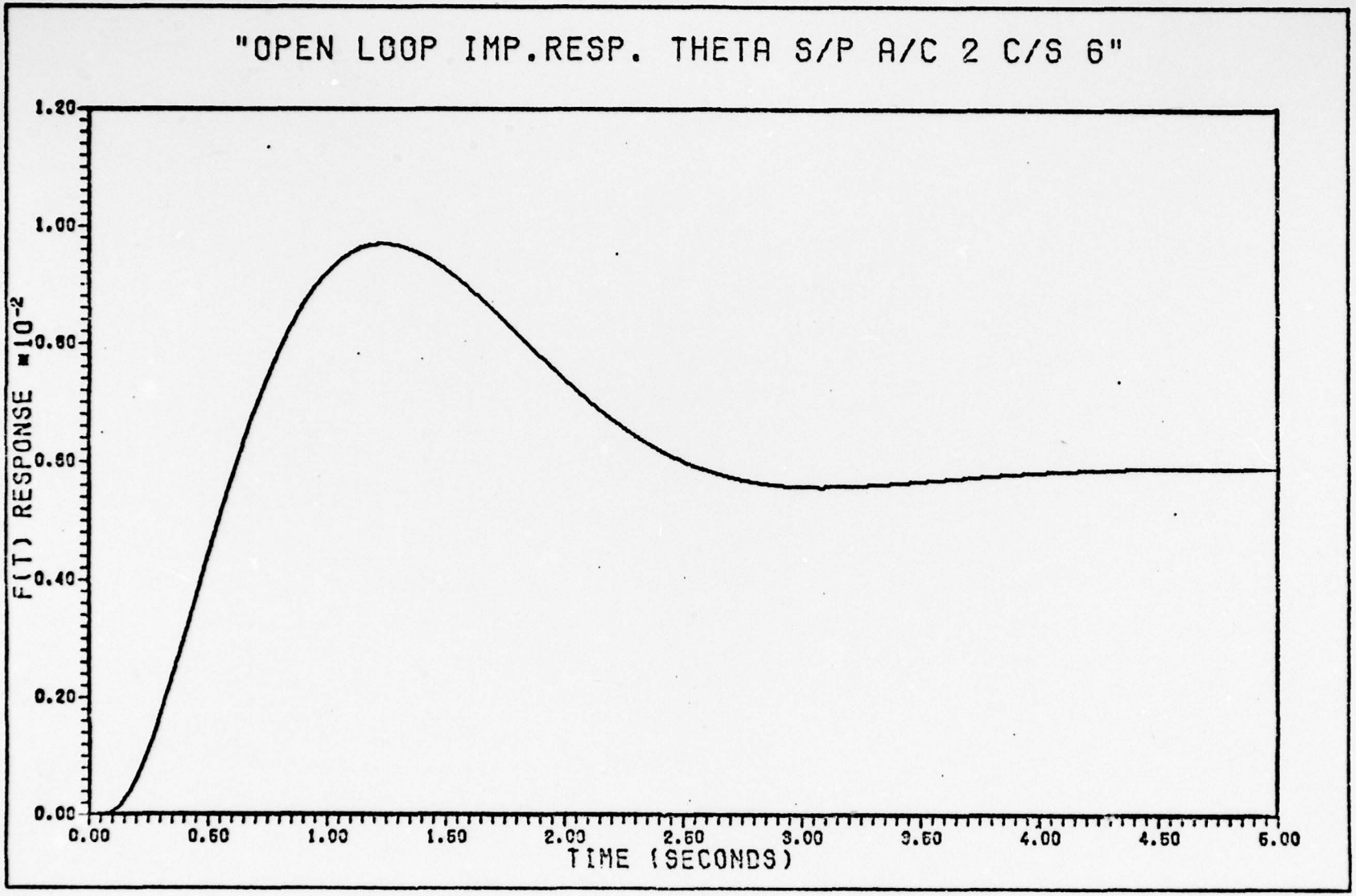

Fig. F11 Open-Loop Impulse Response of Pitch Angle A/C 2 C/S 6

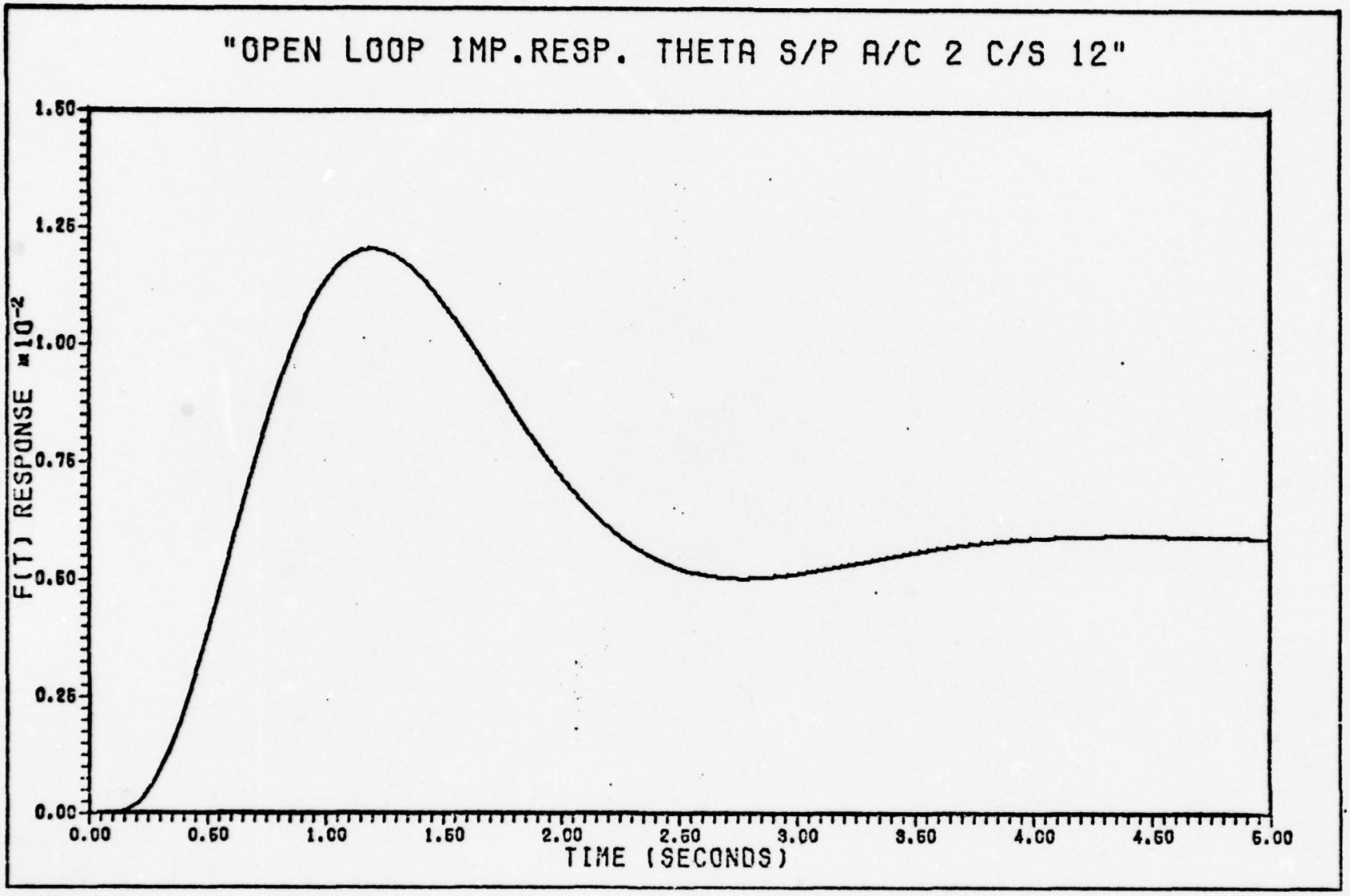

Fig. 12 Open-Loop Impulse Response of Pitch Angle A/C 2 C/S 12

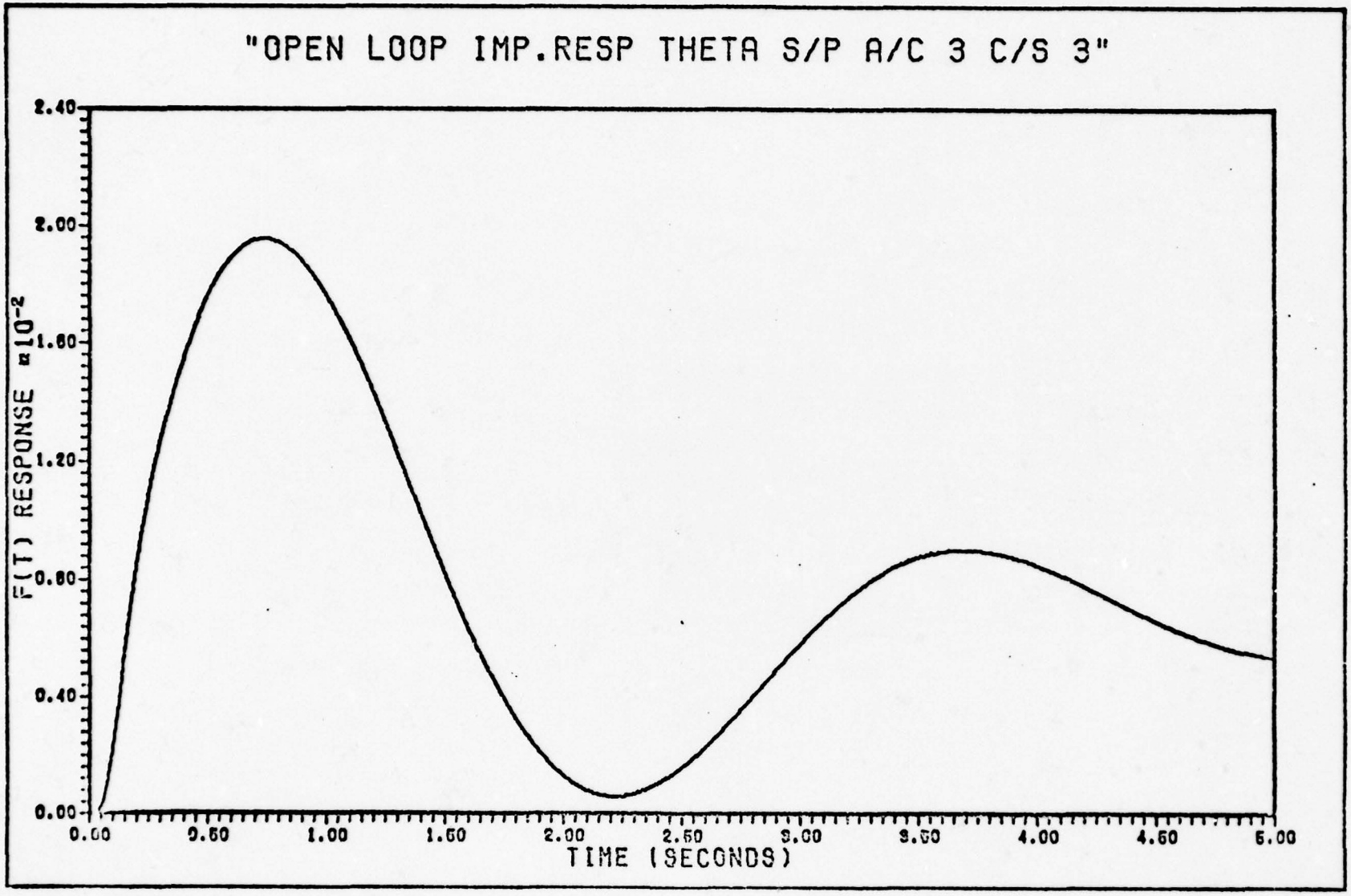

Fig. F13 Open-Loop Impulse Response of Pitch Angle A/C 3 C/S 3

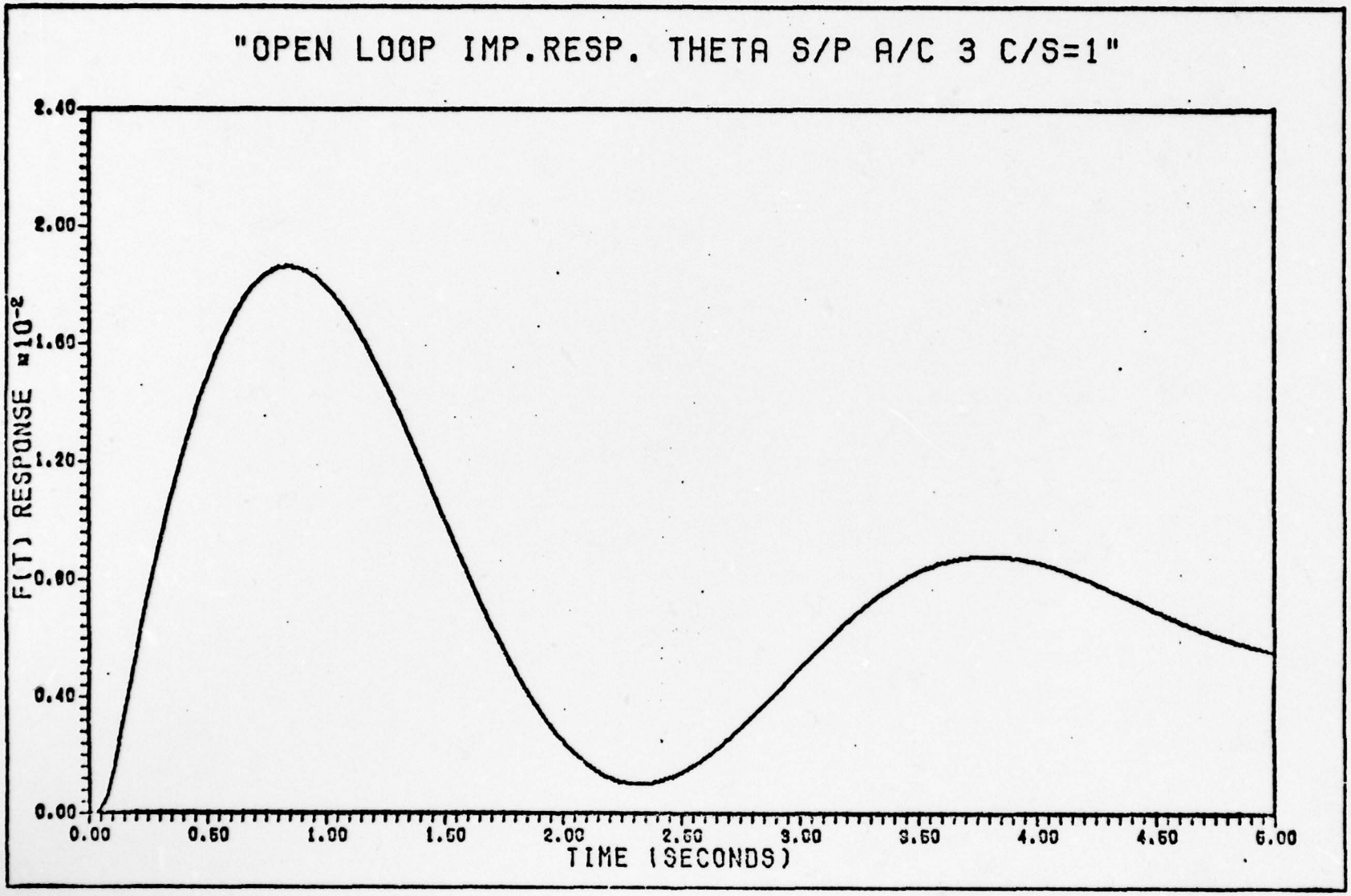

Fig. F14 Open-Loop Impulse Response of Pitch Angle A/C 3 C/S = 1

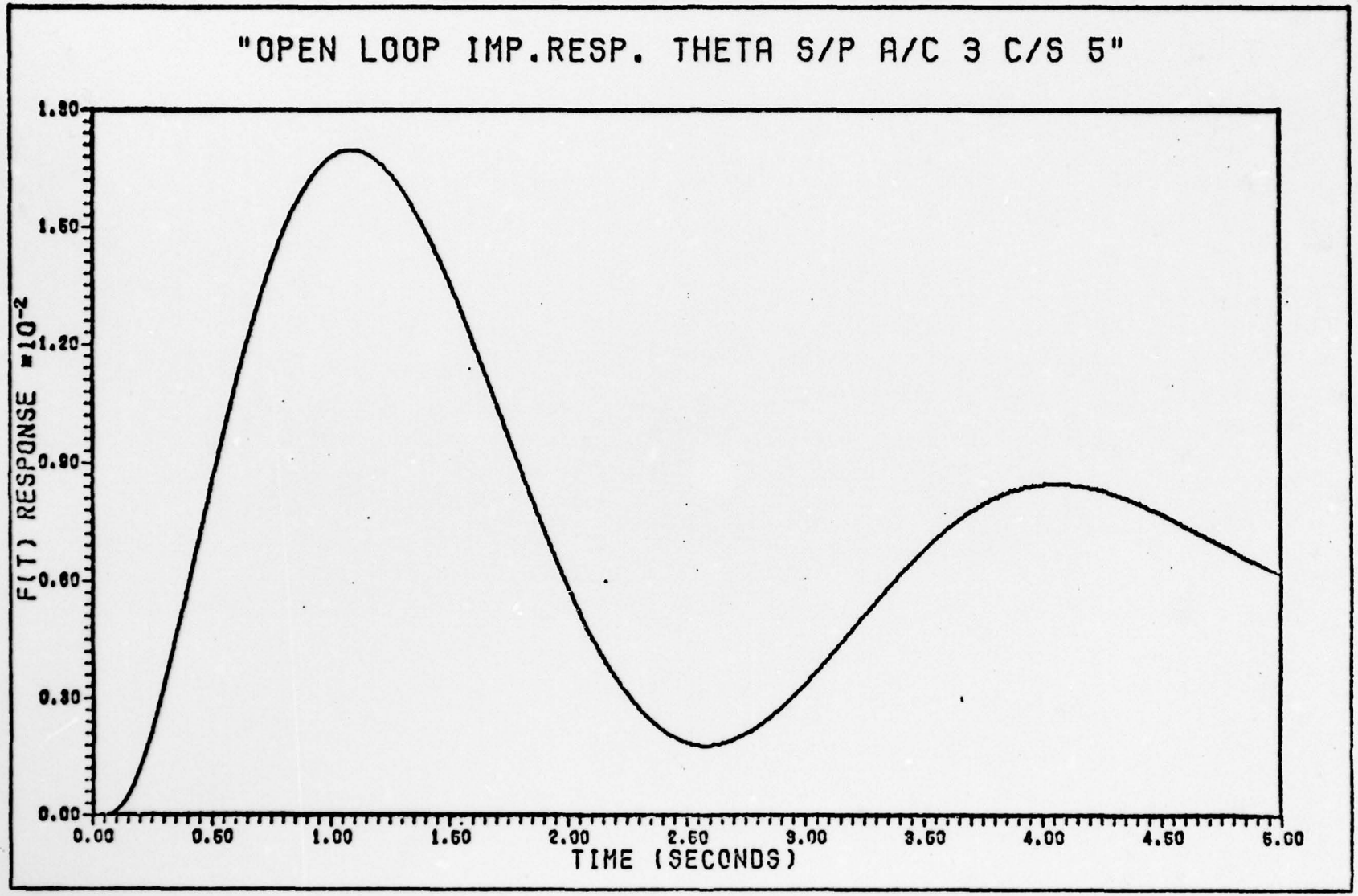

Fig. F15 Open-Loop Impulse Response of Pitch Angle A/C 3 C/S 5

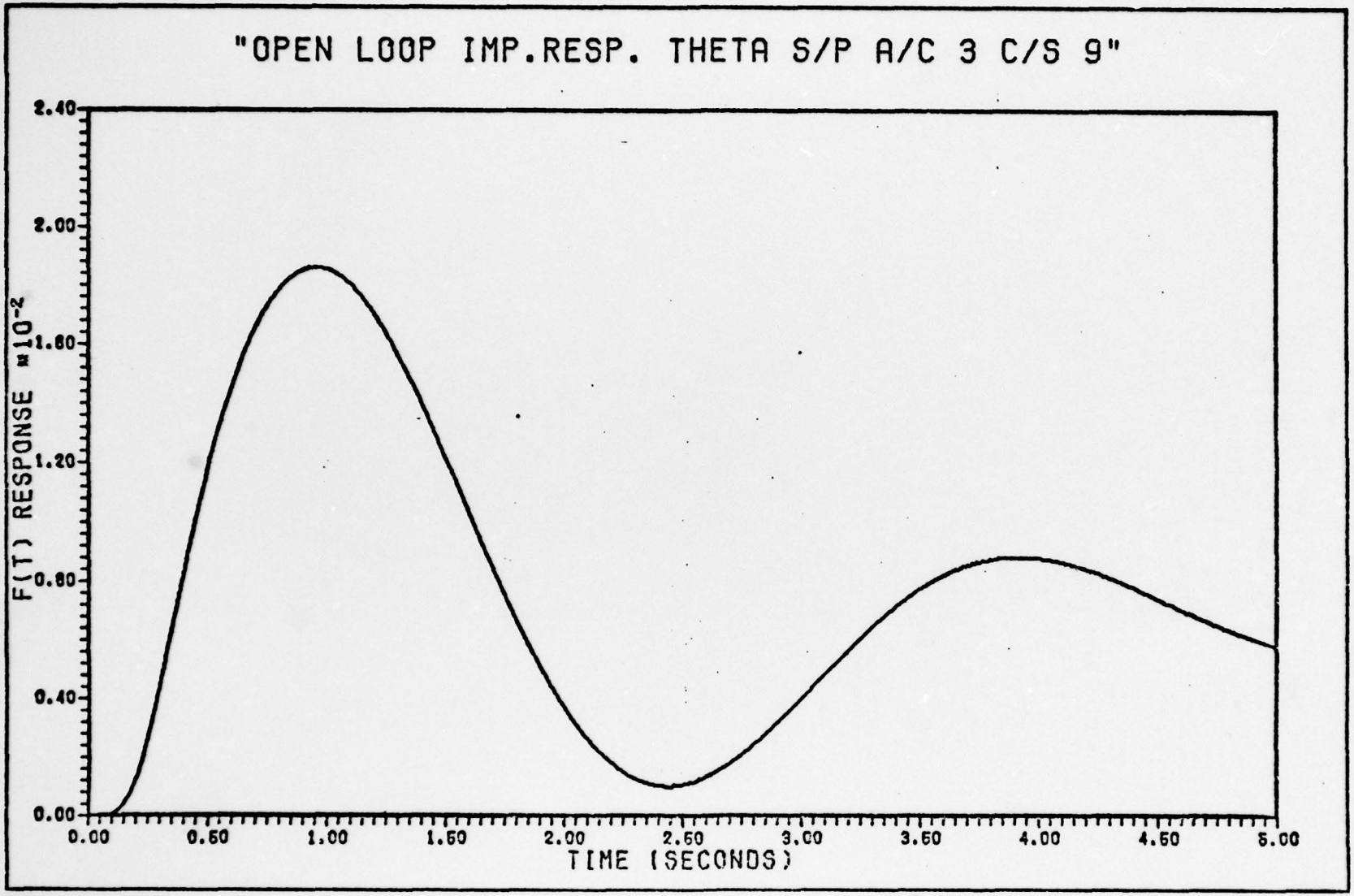

Fig. F16 Open-Loop Impulse Response of Pitch Angle A/C 3 C/S 9

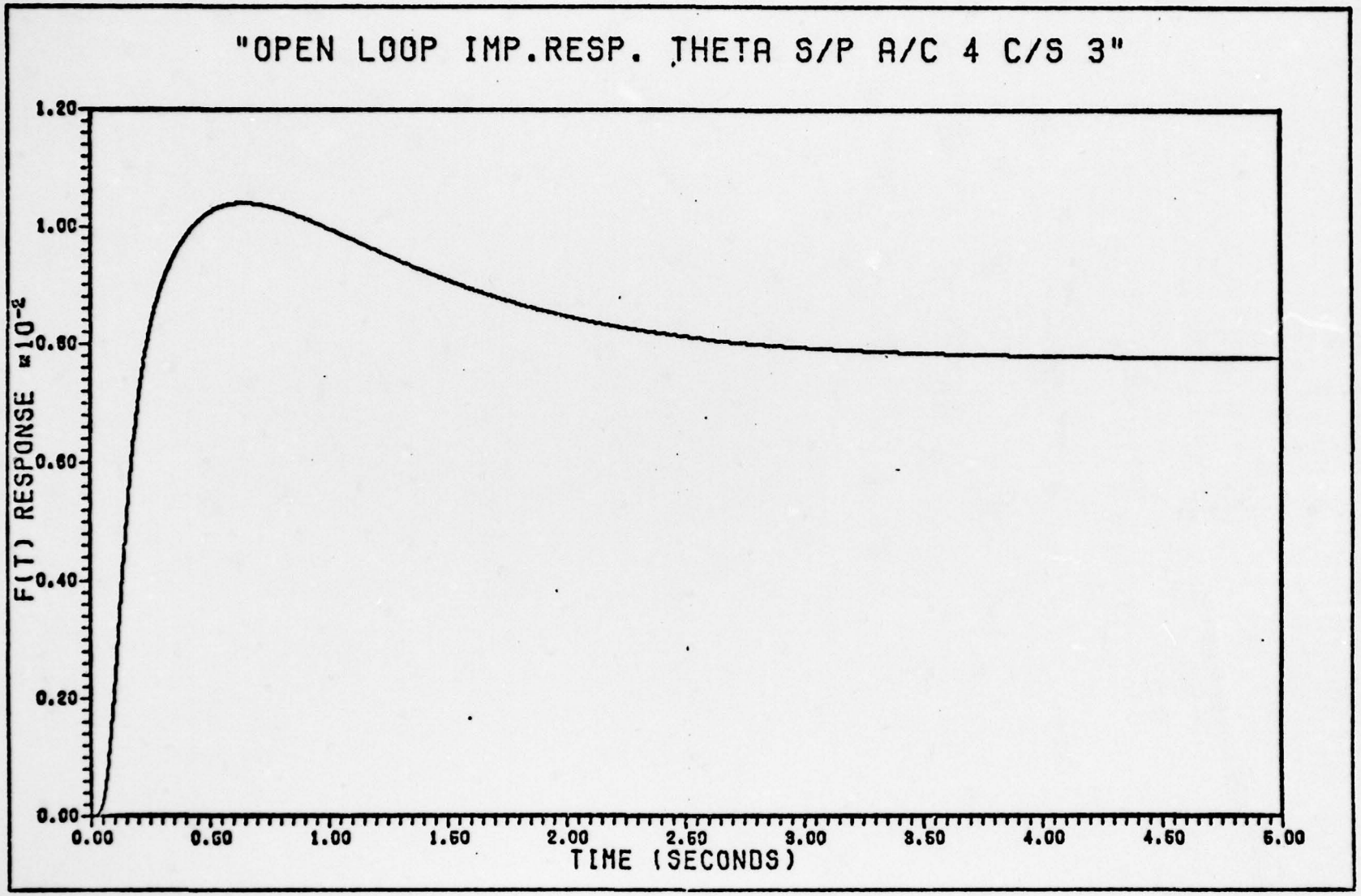

Fig. F17 Open-Loop Impulse Response of Pitch Angle A/C 4 C/S 3

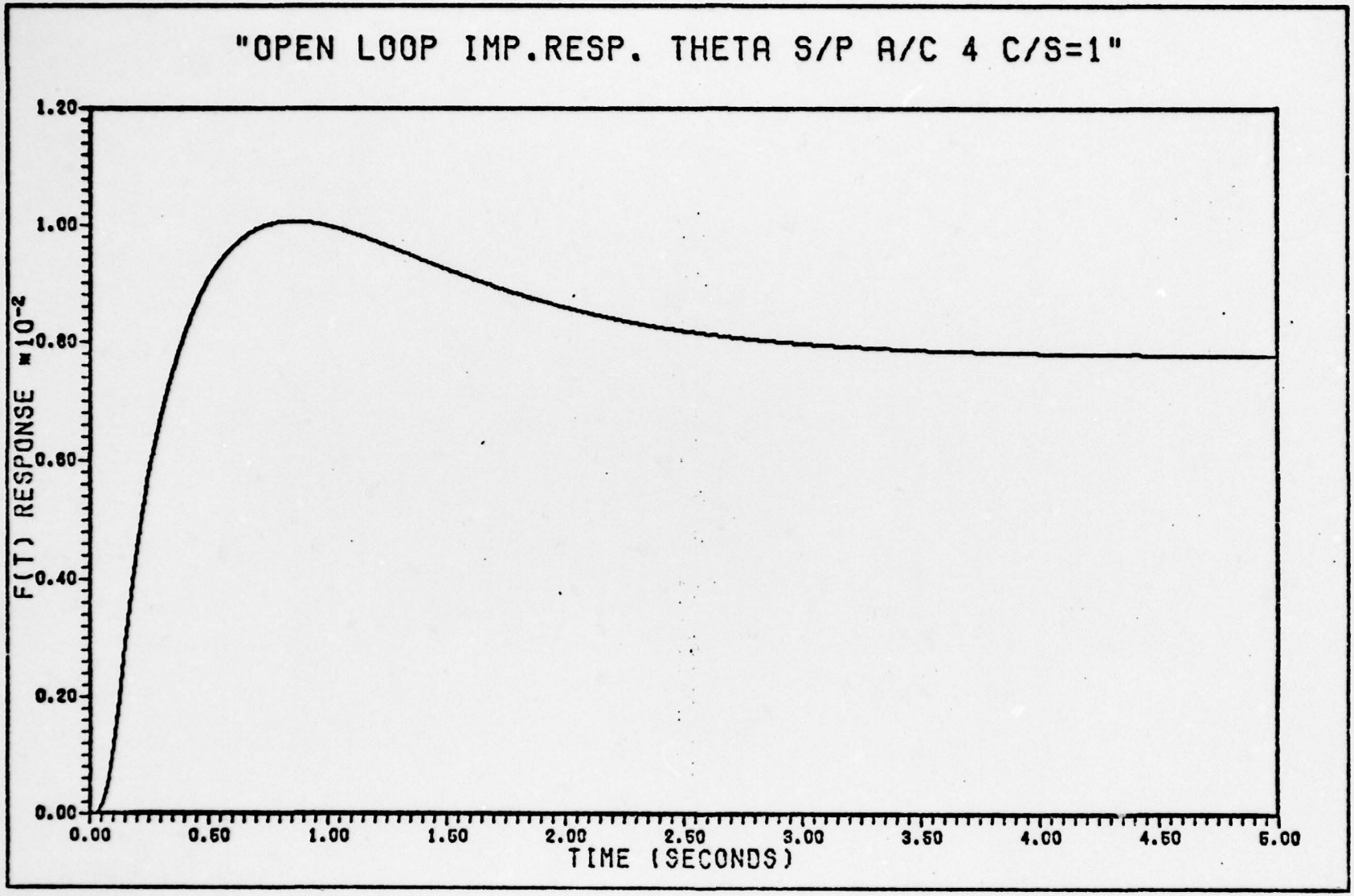

Fig. F18 Open-Loop Impulse Response of Pitch Angle A/C 4 C/S = 1

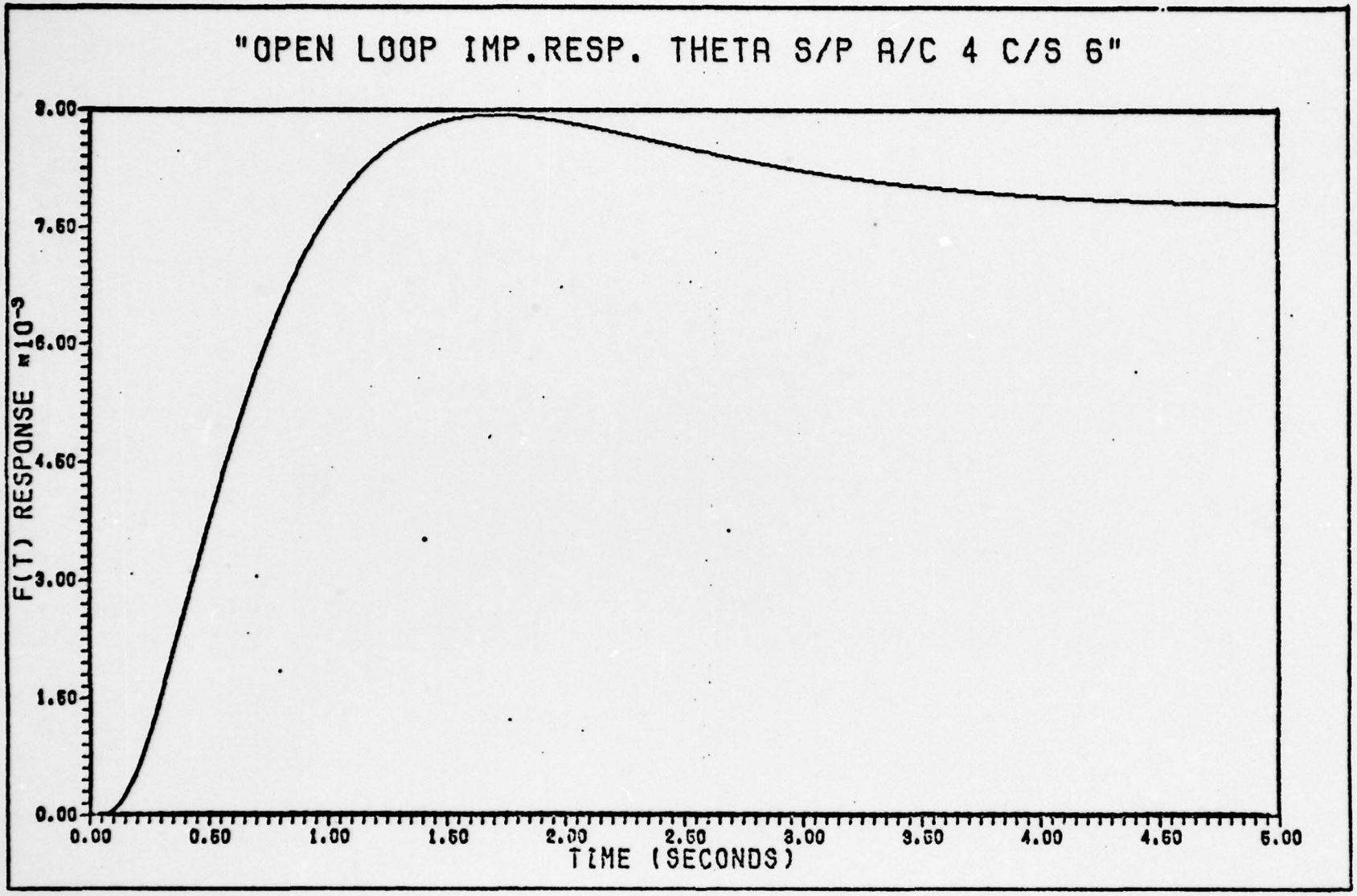

Fig. F19 Open-Loop Impulse Response of Pitch Angle A/C 4 C/S 6

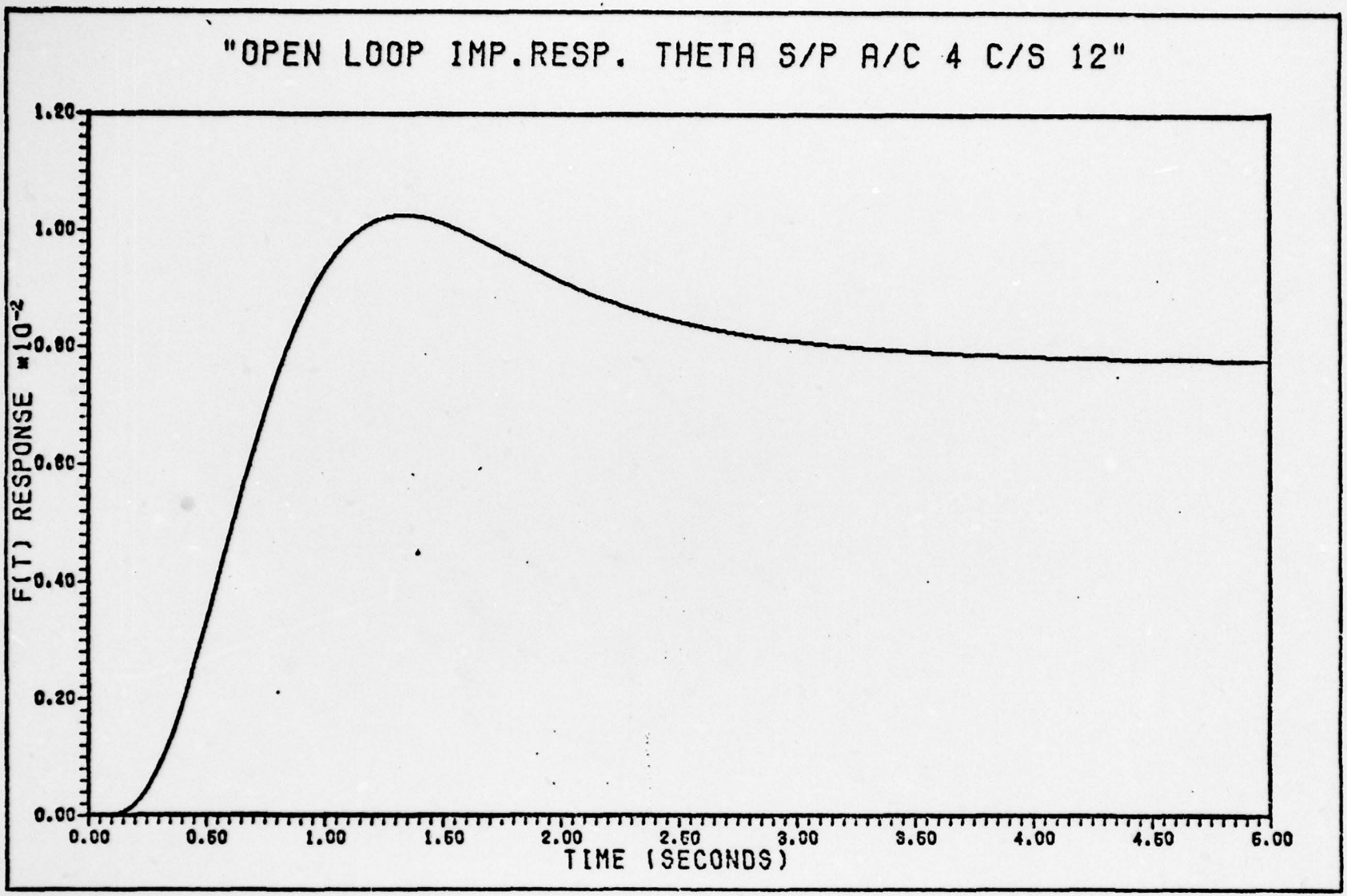

Fig. F20 Open-Loop Impulse Response of Pitch Angle A/C 4 C/S 12

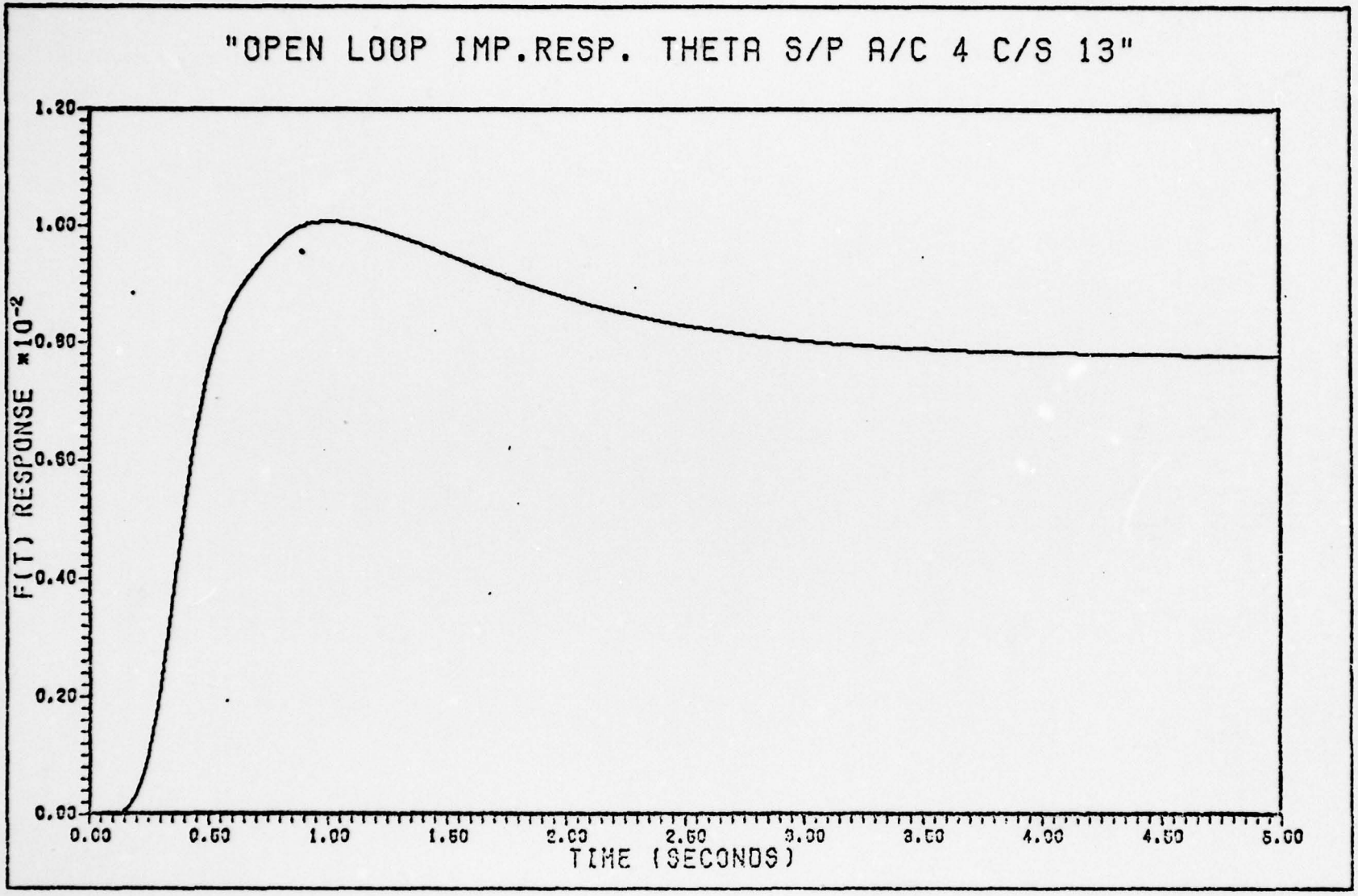

Fig. F21 Open-Loop Impulse Response of Pitch Angle A/C 4 C/S 13

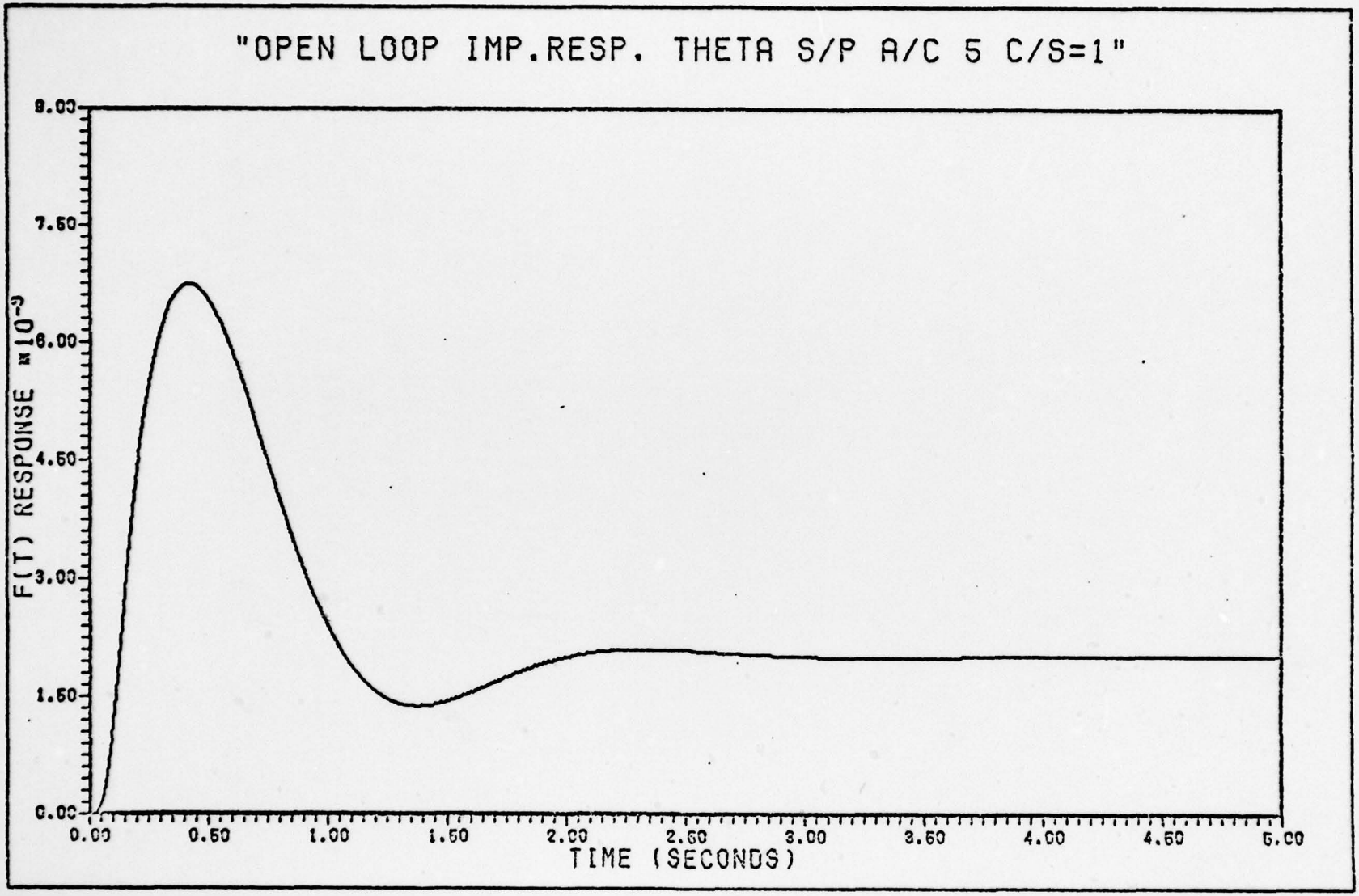

Fig. F22 Open-Loop Impulse Response of Pitch Angle A/C 5 C/S = 1

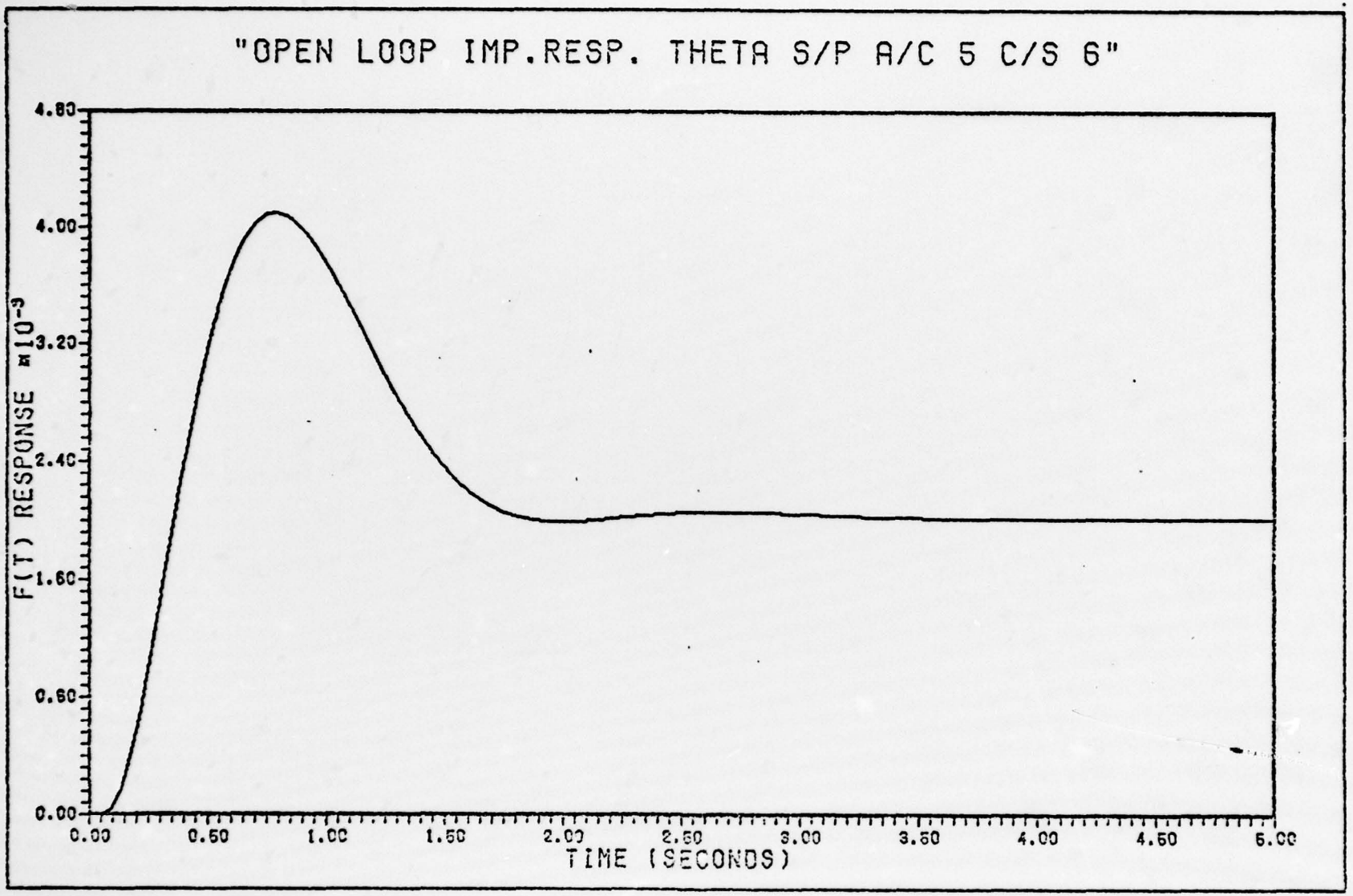

Fig. F23 Open-Loop Impulse Response of Pitch Angle A/C 5 C/S 6

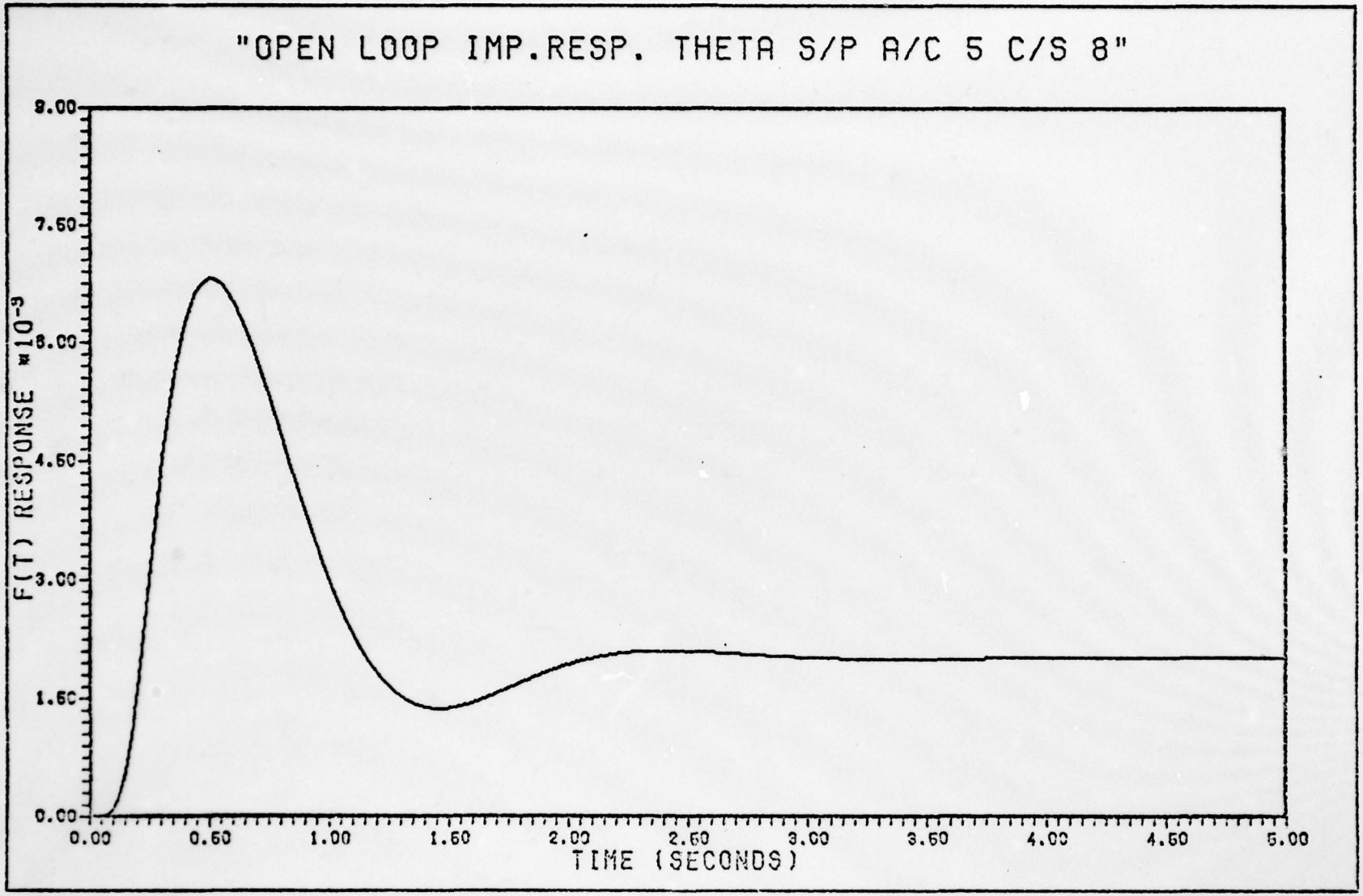

Fig. F24 Open-Loop Impulse Response of Pitch Angle A/C 5 C/S 8

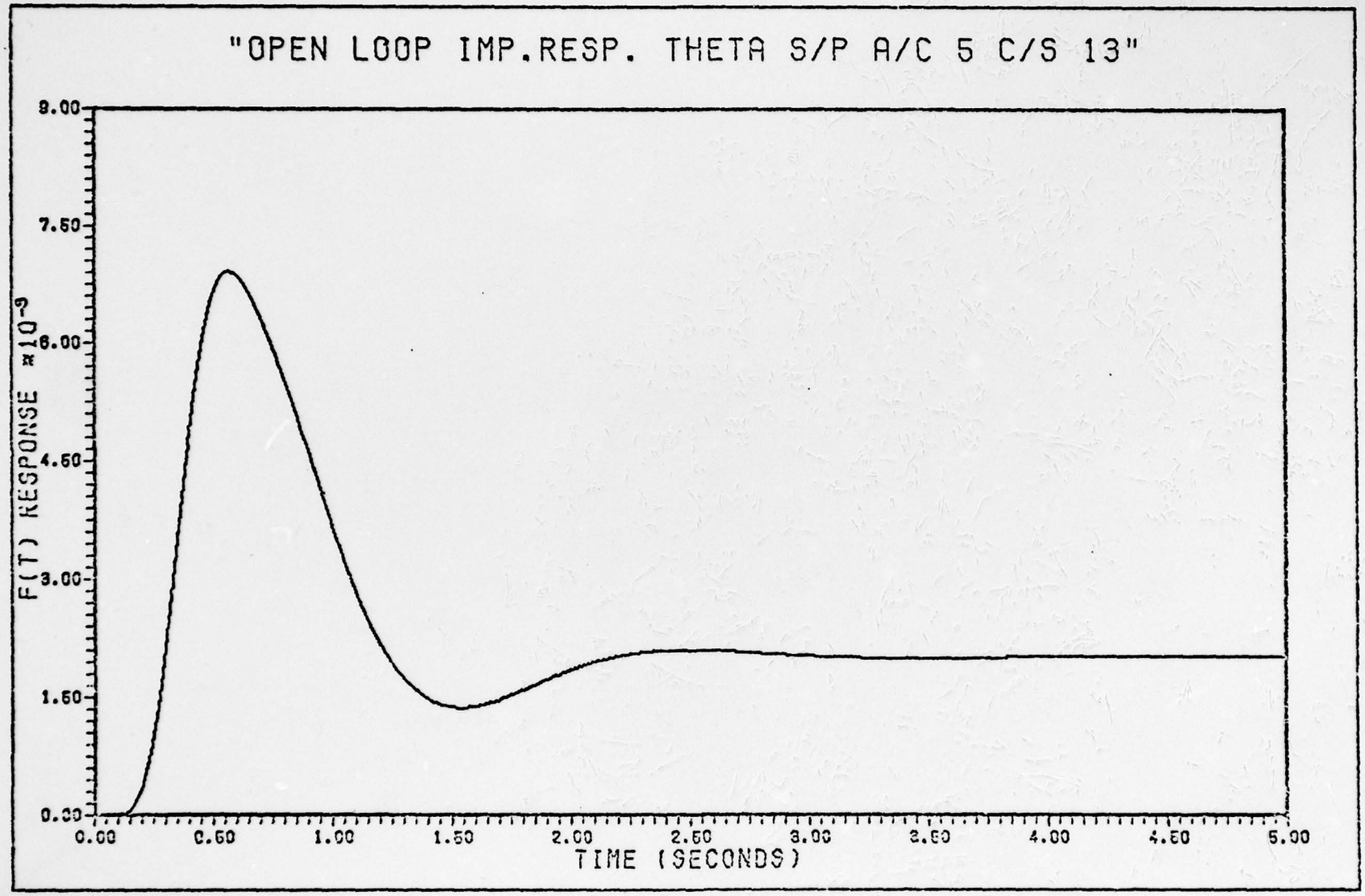

Fig. F25 Open-Loop Impulse Response of Pitch Angle A/C 5 C/S 13

Vita

Muhammad Anwar Pasha was born February 10, 1948 at Madras, India. He attended Marie Colaco School at Karachi, Pakistan, getting his matriculation in 1963. He then attended Adamjee Sciençe College at Karachi and obtained his F.Sc. in 1965.

In 1966, he joined the Pakistan Air Force as a cadet. He attended the Pakistan Air Force College of Aeronautical Engineering at Karachi, where he graduated in 1969 with a B.E. degree in Avionics Engineering. Upon graduation he was commissioned as a Flying Officer in the Engineering Branch.

He served on various duties at different maintenance assignments in P.A.F. before being selected for the resident Graduate Electrical Engineering program at AFIT. He is currently undergoing the M.S. degree program in Electrical Engineering.

Permanent address:

c/o P.A.F. Officer's Mess
Korangi Creek
Karachi, Pakistan

UNCLASSIFIED
SECURITY CLASSIFICATION OF THIS PAGE (When Data Entered)

REPORT DOCUMENTATION PAGE		READ INSTRUCTIONS BEFORE COMPLETING FORM
1. REPORT NUMBER AFIT/GE/EE/79-27	2. GOVT ACCESSION NO.	3. RECIPIENT'S CATALOG NUMBER
4. TITLE (and Subtitle) ANALYSIS OF THE EFFECTS OF HIGHER ORDER CONTROL SYSTEMS ON AIRCRAFT APPROACH AND LANDING LONGITUDINAL HANDLING QUALITIES		5. TYPE OF REPORT & PERIOD COVERED M.S. Thesis 6. PERFORMING ORG. REPORT NUMBER
7. AUTHOR(s) Muhammad Anwar Pasha Sqn/Ldr PAF		8. CONTRACT OR GRANT NUMBER(s)
9. PERFORMING ORGANIZATION NAME AND ADDRESS Air Force Institute of Technology (AFIT/EN) Wright Patterson AFB, OH 45433		10. PROGRAM ELEMENT, PROJECT, TASK AREA & WORK UNIT NUMBERS
11. CONTROLLING OFFICE NAME AND ADDRESS		12. REPORT DATE December 1979 13. NUMBER OF PAGES 214
14. MONITORING AGENCY NAME & ADDRESS(if different from Controlling Office)		15. SECURITY CLASS. (of this report) Unclassified 15a. DECLASSIFICATION/DOWNGRADING SCHEDULE

16. DISTRIBUTION STATEMENT (of this Report)

Approved for public release; distribution unlimited.

17. DISTRIBUTION STATEMENT (of the abstract entered in Block 20, if different from Report)

18. SUPPLEMENTARY NOTES

Approved for public release; IAW AFR 109-17

Joseph P. Hipps, Major USAF
Director of Public Relations

19. KEY WORDS (Continue on reverse side if necessary and identify by block number)

Handling Qualities
Pilot Rating
Pilot Modelling
Landing Approach Higher Order Systems

20. ABSTRACT (Continue on reverse side if necessary and identify by block number)

The approach and landing longitudinal flying qualities data generated by Calspan using variable stability NT-33 aircraft combined with significant control system dynamics was analyzed. Three different approaches were used to determine the relationship between pilot ratings and the pilot workload, system sensitivity, and the system performance.

An open-loop frequency response analysis showed that for a particular cross over frequency and phase margin (fixed

DD FORM 1 JAN 73 1473 EDITION OF 1 NOV 65 IS OBSOLETE

UNCLASSIFIED
SECURITY CLASSIFICATION OF THIS PAGE (When Data Entered)

performance), the phase angle (pilot workload) and slope of the phase curve (system sensitivity) at the crossover frequency correlated well with the pilot ratings.

An optimum pilot lead time for pitch tracking, flight path angle tracking, and both pitch and flight path angle tracking tasks is determined by a closed-loop analog simulation using integral error squared as a performance measure. A correlation is found between pilot ratings and performance. An attempt is made to explain the landing task as a closed-loop pitch and flight path angle tracking task.

The open-loop impulse response of the pitch attitude showed that the initial delay and the transient behavior of the pitch response have a direct impact on the pilot ratings, pilot induced oscillations, and comments.